UNIVERSITÀ POLITECNICA DELLE MARCHE

Doctoral school in Science

Civil and Environmental Protection – XIV cycle

FROM REGIONAL TO LOCAL CLIMATE SCENARIO: TOWARD AN INTEGRATED STRATEGY FOR CLIMATE IMPACTS REDUCTION

PhD candidate:

Lorenzo Sangelantoni

Tutor:

Prof. Aniello Russo

Abstract

Lying at the center of Mediterranean basin, identified as one of the most sensitive area to anthropogenic climate change, Italy is expected to be particularly susceptible to global climate change. Italian peninsula represents an interesting example of challenging climate-change scenario definition case of study. Given the significant latitudinal extension, its climate results heterogeneous, covering a transitional zone where both semi-arid and temperate climate dynamics interact. Complex topography, high mountain chains and diverse coastline make difficult defining a comprehensive climate scenario able to characterize local climate response. Moreover, considerable climate change related impacts are expected on agriculture, tourism, water resources and geo-hydrological hazard, pillars of the socio-economic national structure. These considerations encase the importance of providing usable future climate information to society and decision makers to further climate impacts mitigation and adaptation measures on both national and local scale.

Climate scenario is a plausible characterization of future climate conditions, constructed for explicit use in investigating potential consequences of anthropogenic climate change. Climate scenario generally relies on numerical simulations performed by climate models that describe the response of the climate system to a different greenhouse gas and aerosol atmospheric concentrations. Climate projections alone rarely provide sufficient information to estimate future impacts of climate change. Climate models feature systematic errors and have to be manipulated and combined with observed climate data before to be used as inputs for impact models. According to these main pillars of climate change research, doctoral work is articulated in three consequential phases aiming to provide a solid basis for climate change impacts research. First part, provides a comprehensive assessment of the projected Climate Change Signal (CCS i.e. long-term statistics difference between a future and a past climate simulation), over a study area roughly covering the Italian peninsula. In this phase, analysis regard mean and distribution tails changes of key climate variables, expected changes over inter-annual variability and finally robustness of climate projections is inferred evaluating climate models agreement over resulting CCS. Moreover, an introductive model performances evaluation is proposed. Considering the employment of climate projections in climate impacts research, second research phase, is dedicated to a quality-evaluation and error reduction of climate simulations, through an empirical-statistical bias correction

method (Quantile Mapping (QM)). This phase is devoted to provide for the first time a climate scenario over Italian peninsula reporting both original and bias corrected simulations. Moreover, specific analysis on the effect of the QM over the original CCS was brought out. Third part (referred as "local experiment"), takes a step further, using QM on a particular configuration allowing for simulations error reduction and resolution increase at the same time. This latter research pillar focuses on the definition of local-scale climate scenario over representative stations of Marche region (one of the 20 administrative division of Italy). Conceptually, this phase aims to bridge the gap between the resolution of climate models and local scale where climate impacts act and have to be characterized. Finally, the research provides a quality improved regional to local scale climate information directly usable in climate impacts modeling.

Besides, doctoral research has enjoyed a collaboration with Canadian research institute «Ouranos», whose activities are mainly focused on regional climatology and adaptation to climate change. Collaboration has enabled the production of a scientific publication (Gennaretti et al. 2015). In this work, two two-dimensional bias correction methods are tested and applied in the context of a Canadian Arctic coastal zones daily climate scenario aiming to properly simulate observed inter-variable interdependence. In fact, in artic-climate context temperature-precipitation interdependence are strong and play relevant role in determining important physical characteristic as extreme events and extension and duration of snow cover.

Contents

Introduction

Why climate changes – short global warming history and principles

«Humanity is carrying out a wide-scale geophysical experiment never happened in the past and that cannot be reproduced in the future». This famous sentence formulated by Roger Revelle (1909-1991), published on «Tellus» journal, condensed in the half of 20th century, the essence of global warming issue. Revelle was not first scientist to postulate a potential atmosphere warming related to human activities. Greenhouse effect is being discussed since the half of 19th century, when Irish physicist John Tyndall (1820-1893) noted H_2O and CO_2 infrared absorption property and thus potentially important for climate in the 1861. Even, J. B. Fourier (1768-1830) theorized the analogy between warming effect of the atmosphere and a greenhouse in the 1827. However, one of the most relevant personality about theorization of global warming threat is represented by the Swedish chemist and physicist Svante August Arrhenius (1859-1927), which in the 1896 postulated the relation between climate change and CO_2 as result of fossil fuels burning (at that time mainly coal). He provided a quantitative description of the CO_2 and water vapor in the thermal balance of the atmosphere, estimating that a doubling of the CO_2 concentration could lead to an increase of the global temperature of roughly 4 °C (close to the results of modern climate model simulations). During the 20th century and especially in the last thirty years new technologies including satellites, radar, telecommunication and supercomputing helped scientists to dramatically increase their understanding of climate system dynamics. In the 1988, was founded the Intergovernmental Panel on Climate Change (IPCC) as the result of concerted effort made by climate scientists to summarize the current state of knowledge. From then, IPCC reports represent recognized "center of gravity" concerning current climate science understanding. IPCC reports have the relevant role of making available to worldwide societies and policy makers best estimates of how global warming and related outcomes may evolve. The ability of producing improved climate information of the last three decades matched to a rising attention on making knowledge usable for all level society and on identifying best practices to do it. At this regard, «The Global Framework for Climate Services» implemented by the World Meteorological Organization in the 2009, attempts to identify a structure to support more informed decisions for saving lives, protecting the environment and assists economic

development coping with current and expected climatic changes (Vaughan and Dessai 2014). Climate services is a term come into favor fairly recent but it condenses thirty-years scientific effort for producing a flux of usable and tailored climate information for sectors as diverse as agriculture, health, water management and disaster risk reduction and for all the contexts that require climate information for their specific operations.

Climate change consists on “changes in climate conditions identified by statistical significant shifts on mean and/or variability of its properties, persisting for an extended period of decades or longer” (World Meteorological Organization (WMO); Intergovernmental Panel on Climate Change (IPCC), 2007). The United Nation Framework Convention on Climate change (UNFCCC, 2011) provides another definition of climate change: "a change of climate which is attributed directly or indirectly to human activity that alters the composition of the global atmosphere and which is in addition to natural climate variability observed over comparable time periods”. In the latter definition is present the key distinction between natural climate variability interacting (sharpening or dampening) with alteration ascribable to human activities.

Climate system is feed by the incoming solar radiation. This energy interacts with the Earth’s surface and with the atmosphere in order to achieve energetic equilibrium. The mean state of the atmosphere can be altered through internal processes and/or external forcing. Internal processes generate the intrinsic natural climate system variability present at all the time scale. Atmospheric processes relying internal variability operate on time scales ranging from instantaneous (condensation of water vapor in the clouds) to longer time scales involving complex interactions between climate components (atmosphere-hydrosphere-cryosphere-biosphere-land surface).

External influences, contributing to the climate variability, consist on processes influencing the level of *solar radiation input* (solar activity or Earth’s orbit configuration), and *radiative processes* which distribute solar energy between Earth and atmosphere. Solar radiation input is function of solar activity that, excluding paleoclimate variability, effects of are considered modest in recent climate changes and Earth’s orbit configuration. The latter, is estimated playing a relevant role on determining ice-age cycle. According to the M. Milankovitch (1879-1958) theory, incoming solar radiation would be influenced by orbital parameters such Earth’s orbit eccentricity, Earth’s axes inclination and the equinox precession cycles. However, only the former factor is considered relevant on influencing the

quantity of incoming solar radiation. Orbit eccentricity determines the level of seasonal variation regarding solar energy input (up to 30% during maximum eccentricity) varying on 100000 and 400000-year time scale.

The second external influence, involving radiative processes, is represented by natural phenomena such volcanism. These events consistently alter atmospheric reflectivity and consequently climate system energetic balance. Another source of radiative processes alteration is not natural and it is being taken place, since industrial revolution, strictly connected to anthropogenic activities (Hegerl et al. 2007).

Alterations regards the atmospheric chemical composition, through anthropogenic emission of radiatively important gasses (Greenhouse Gasses, GHGs), aerosols and by changing land surface properties. Longwave (or infrared) radiation, emitted from the Earth's surface to balance solar radiation input, is consistently absorbed by atmospheric constituent GHGs (i.e. water vapor, carbon dioxide, methane, nitrous dioxide and other gasses) and clouds, which themselves emit longwave radiation in all directions. The downward component of this radiative emission increase heat in the lower layers of the atmosphere (Troposphere) and to the Earth's surface. Additional warming of the surface determines higher upward infrared emission provoking further warming of the atmosphere. In this way recursive cycle has triggered, according to Stefan-Boltzmann low asserting that the energy released by a body (Hearth's surface and atmosphere) is function of its temperature ($E = \sigma T^4$; where σ is the Stefan-Boltzmann constant). This is the greenhouse effect. In addition to GHGs concentration, Earth's radiative balance is altered by aerosols. Depending on their chemical composition, concentration and lifetime can increase atmospheric reflectivity (enhancing albedo effect, indeed cooling effect) or conversely can act as strong solar radiation absorbers with a warming effect. Moreover, aerosols serve as clouds condensation. Clouds play a double role in climate system, increasing the albedo (cooling effect) but also warming through infrared downward emission. It depends on their altitude, physical properties and the chemical composition of cloud condensation nuclei. In general, cold clouds (cirrus) located roughly at 6000 m of altitude strength surface infrared emission blocking with a warming effect. Low-level clouds, with liquid content (stratus), reflect incoming solar radiation provoking cooling effect. Hence, it is of large interest identify which kind of clouds will be fostered by future climatic alterations. Human's activities are not only altering atmospheric composition. Energy and water budgets are being altered as well by the changes of land surface properties. Conversion or burning forests to obtain

cultivable areas deeply affect carbon storage in the vegetation, adds CO_2 and decreases atmospheric CO_2 extraction, reflectivity of land surface, and finally atmospheric water vapor supply. All these factors, produce a radiative forcing, that represents a measure of the net change in the energy balance in response to an external perturbation. Once a forcing is applied, complex internal feedbacks determine the response of climate system general differing from a simple linear one. There are many mechanisms (feedback) in the climate system that can either amplify ('positive feedbacks') or diminish ('negative feedbacks') the effect of a certain change in climate forcing. An example of positive feedback is the reduction of ice albedo, where a decrease in the snow cover exposes darker underneath surface to absorb more solar radiation. Another positive feedback consists on methane release by several Earth's surface or seafloor. Due to an increase of temperature, large Tundra and Arctic ecosystems of Asia and North-America are subjected to permafrost degradation. In such contexts, anaerobic decomposition of organic matter release massive methane emissions in to the atmosphere. The same happens in the oceans, where the increase of temperature produces release of seafloor-methane hydrates. An example of negative feedback could be represented by the increase in concentration of atmospheric aerosols with high level of reflectivity that enhance the atmospheric albedo effect.

These processes and many other alterations regarding fundamental aspects of biogeochemical cycles (e.g. Nitrogen cycle) and biological processes, are concurring on determining current shifts in global climate conditions.

How to predict future climate conditions - Climate projections

The current increase in GHGs concentration is considered virtually certain linked with observed alterations of the climate system (Myhre et al. 2013). Moreover, human influence on climate system is almost certain to continue in the near future (Hegerl et al. 2007). These evidences make societies increasingly demanding reliable projections of future climate change. Climate projections represent the basis for analyzing adaptation strategies, exploring mitigation measures and to support political decisions (Cubasch et al. 2013). Meanwhile knowledge of past and current climate variations is based on the statistical treatment of climate observations; future climate conditions description relies on the projections provided by climate models. World Meteorological Organization defines climate projections as the probability that certain climatic variation will take place in the next decades according to possible global socio-economic scenarios. In particular, to these scenarios correspond

particular future evolution of atmospheric GHGs concentration that affect future climate conditions. IPCC (2013) provides an updated climate projection definition consisting on an estimate of future climate conditions provided by climate models.

Basis for projections of future climate change are provided by climate models, describing the response of climate system to different radiative forcing from seasonal to decadal time scales (Stocker et al. 2010). Climate models are complex systems relying on a set of mathematical equations that are discretized on a grid and numerically solved on large computers (Knutti 2008). Mathematical equations describe the well-known physical principles (e.g. conservation of mass, energy, momentum, equation of state) that govern time derivative air masses motion and relation amongst variables at a given moment. Other processes occurring at scales smaller than the grid cell must be simplified and parameterized. For example, sub-grid processes that require parameterizations are the growing of trees, that modifying Earth's surface can influence climate, or the treatment of moist convection and radiative transfer. For the part of the model governed by the fundamental physical lows computational capacity and thus higher resolution will improve the simulations. The term resolution is widespread used to describe the degree of refinement of a climate model grid. The increase of model resolution coupled to the increase of representation of smaller scale phenomena is roughly proportional to the computational time (and costs). Doubling the horizontal resolution of a climate models we double the operations that must be performed in calculating each term of each of the equation for each variable in each grid box. When horizontal resolution is increased, it is also necessary to proportionally reduce the time step to properly represent flux exchanges between one cell and the others. Conversely, for the part of the model solving empirical relation where no fundamental underlying lows exist the limiting factor are represented by human understanding of phenomena instead computational limits. Climate modeling has benefited from a variety of approaches to constructing climate models. In particular, benefits come from models that aim to simulate particular aspects of climate system, without attempting to include the full climate system complexity. A variety of climate models exists, guided by the different questions of interest developed to study different aspects of climate system components. Not always the most complicated model represent the best solution for that particular investigation being for instance not easy to interpret and too computational challenging (Knutti 2008). Indeed, it is possible to classify climate models in order of increasing complexity. Earth System Models are the current state-of-art models and they expand the Atmospheric-Ocean General Circulation Models

including description of various biogeochemical cycles such as Nitrogen cycle, Carbon cycle, Sulphur cycle, or Ozone (Flato et al. 2013). These represent the most comprehensive tools for simulating past and future response of climate system to various external forcing. Atmospheric-Ocean General Circulation Models (AOGCM) are considered standard climate models in climate change research. AOGCMs aim to represent physical component dynamics of climate system (atmosphere, ocean, land and sea-ice) and their response to future GHGs and aerosols forcing.

Regional Climate Models (RCMs) (Giorgi 1990), provide climate system representation comparable to that provided by AOGCMs, though generally run without interactive ocean and sea-ice. They are extensively used in climate for seasonal predictions to decadal climate projections. RCMs are characterized by higher resolution (10-50 km) and are the most common tool employed in regional climate research. Essentially, regional climate models simulate how global-scale climate change might affect individual region, reproducing effects of local topography over temperature and precipitation distribution patterns. Such models generate its small-scale climate response in function of the large-scale changes specified by the driving AOGCMs.

The RCMs higher resolution has obtained downscaling information belonging from the GCM. Since the 1990s RCMs have been constantly employed and improved, setting the basis to the tremendous development undergone by regional climate change studies in the last decade (Giorgi 2006a).

Producing regional climate projections

The remarkable development of regional climate change studies relies on a recognized evidence: is regional-to-local the spatial scale at which climate impacts act and have to be characterized. In climate change research, the term “regional” has a broad sense, indicating the entire range of spatial scale below the ≈ 10000 km^2. Climate is globally changing but with highly heterogeneous temporal rate, spatial patterns and magnitude (Bindoff et al. 2013). Impacts of climate change are being observed to non-linearly respond to increase in temperature being function of particular ecological, cultural and socio-economic frame of human societies (Burke et al. 2015). In this context, regional climate information is necessary for assessing the impacts of climate changes over human and natural systems and develop mitigations and adaptation measures according to the different national level contexts (Giorgi et al. 2009). By the capability of providing solid and valuable regional-to-local scale

climate projections depends the tendency of end-user and policy makers to undertake mitigating and adaptive actions. Until the IPCC IV Assessment Report (2007), AOGCMs represented the main source of future climate information at global and sub-continental scale. Also with improved representation of many physical atmospheric and Earth surface processes, AOGCMs cannot capture effects of local forcing in function of the particular physiography and land-cover that deeply affect climate dynamics at the finer scales. AOGCMs coarse resolution is believed particularly limited on describing extreme events that are crucial information for the regional and local end-users (Giorgi et al. 2009). RCMs are indeed devoted to properly modulate the large-planetary-scale structure changes at regional (and in the best case local) scale according to the diversified local level (morphology, coastline physiography land-cover etc.) forcing.

To "regionalize" climate simulations provided by AOGCMs two principal methodologies (one dynamical and one statistical) exist. Concerning dynamical method, it could be discerned in two approaches. One approach, described by Giorgi (1990), implies different physical parameterizations in the nested (RCM) and driving model (GCM). Each parameterization is developed and optimized for the respective model resolution. This concept is known as one way nesting (Giorgi 1990). In the second approach (Laprise et al. 1998), the full physics of a GCM is implemented within a regional dynamical framework, and the regional model thus obtained is mostly run using driving conditions from the donor GCM. However, for regional climate modeling, basic point is the quality of forcing fields; good quality of these fields generally lead to improved quality of regional model experiment, regardless the means of these fields are obtained.

The second approach to downscale global climate information to more impact-suitable regional or local scale is represented by statistical downscaling. Statistical downscaling methodologies relying on the perfect prognosis principle (perfect prog. Wilks, 2011) have been considered for long time indicated technic tools for resolving the scale discrepancies between climate simulations and the resolution required for impact assessment (Maraun et al. 2010). Statistical downscaling establishes that local climate could be represented through a statistical model (transfer function) between large-scale observation/reanalysis data and local observation over present-day climate (Maraun et al. 2010; Themeßl et al. 2011b; Maraun et al. 2015). Applied directly to GCMs or RCMs for providing local climate scenarios, these statistical methods do not act on the correction of model outputs but only on refining spatial resolution. (Murphy 1999; Themeßl et al. 2011b). As seen for the dynamical

downscaling techniques, it could represent a drawback since systematic errors characterizing coarse-scale simulations could be passively inherit on the regional domain. This last concept let us introducing a relevant aspect connected with climate projections assessment referred as “climate projection uncertainties”.

Choice of downscaling method represents only one source concurring on the level of the intrinsic uncertainties affecting climate projections. Coherent interpretation and communication of climate projections uncertainties represent embedded processes in every future projections assessment, allowing end-users to evaluate consistencies of projected changes (Huard et al. 2014). In addition to downscaling approach, one of the most relevant uncertainty source regards “model configuration”. It is directly connected to the level of understanding of the physical processes which climate models are expected to reproduce. This kind of error can be directly propagate, if not amplified, from global to regional models (Giorgi et al. 2009). Other source of regional climate projection uncertainties is represented by the climate internal variability reproduction, mostly important in the short-term projection since could hide the presence of significant climate change signal (Hawkins and Sutton 2011). Frequently in climate change research multi-model ensemble approach, where several simulations averaged (arithmetically or weighted), is preferred. This approach leads to the production of a probabilistic climate change information (according to the number of ensemble member that produce same projection). Spread within of the multi-model ensemble could be used as explorative method of uncertainties. Finally, another source of uncertainty refers to the choice of future emission scenario providing radiative forcing boundary conditions to the climate simulations. It has been noted that the configuration of the driving AOGCM and the emission scenario uncertainties represent the two most relevant sources of uncertainty pertaining to regional climate projections, particularly at longer time-scale (Giorgi et al. 2009).

At European level, the most comprehensive research works based on regional-scale climate projections assessment are presented in PRUDENCE (Christensen and Christensen 2007), ENSEMBLES (van der Lindend and Mitchell 2009) and EURO-CORDEX (Jacob et al. 2013) projects. They are the reference European projects where a massive number of multi-RCM simulations and are produced, and employed in climate-impacts research. PRUDENCE project represents the first example where a wide number of climate projections have been employed in climate impacts studies as economy, agriculture and hydrology to depict a future impact scenario over these spheres (Déqué et al. 2005; Beniston et al. 2007;

Leander and Buishand 2007; Christensen and Christensen 2007). ENSEMBLES (van der Lindend and Mitchell 2009) represents a milestone of European climate change research. The research core of the project consists on providing multiple climate model runs ("ensembles") providing a wide range of future projections assessed to define which more probable. This probabilistic information represents essential tool to assist society and policy makers in defining future measures to face climate change. Members of the project the most renowned European climate research centers (plus Canadian scientific consortium Ouranos). Each research institution contributed with its own simulations of the 20th and 21st century climate. CORDEX project has two-fold purpose, firstly providing a set of new high-resolution ensemble simulations for impact assessment and secondly to establish shared metrics for evaluating and benchmarking model performances (Giorgi et al. 2009; 2011; Vautard et al. 2013; Jacob et al. 2013; Kotlarski et al. 2014).

Italy, an interesting and challenging regional climate change case of study

As previously stated, climate is globally changing but with highly heterogeneous rate, spatial patterns and magnitude (Bindoff et al. 2013). Impacts of climate change are being observed to non-linearly respond to increase in temperature being function of particular ecological, cultural and socio-economic frame of human societies (Burke et al. 2015). For these reasons, changes in climate dynamics should be characterized as whole with exposure, vulnerability and adaptive-capacity characterizing each individual community. At this regard, Mediterranean basin, laying in unique geographical and transitional climate context has been identified as one of the world climate change Hot-Spot (Giorgi 2006b). Conceptually, a climate change Hot Spot, represents a region where coexist potential high impacts over the human-natural systems and a highly responsive climate to global change. (Giorgi 2006b). Lying at the center of Mediterranean basin, Italian peninsula, it is expected to be particularly susceptible to global climate change (Coppola and Giorgi 2010). Semi-arid conditions characterize southernmost regions, temperate conditions the central/northern sectors and cold climate characterizes Alpine area. Climate dynamics are deeply affected by the presence of the two major mountain chains Alps and Appennines respectively west-east and north-south oriented. Moreover, complex topography, high mountain and diverse coastline physiography make challenging to interpret local climate dynamics in response to the expected north-hemisphere major atmospheric modes alteration (Xoplaki et al. 2003; Xoplaki et al. 2004; Gaetani et al. 2011; Xoplaki et al. 2012; Bucchignani et al. 2015). For

these characteristics, Italian peninsula represents an interesting example of challenging climate-change case of study. Despite, comprehensive assessment of climate projections over Italia peninsula are still relatively sparse (Coppola and Giorgi 2010; Bucchignani et al. 2015; ISPRA 2015). According to expected changes affecting Mediterranean basin during the 21st century, Italian peninsula are expected to be affected by an exacerbation of the current warming and drying trends (Gao et al. 2006; Diffenbaugh et al. 2007; Hertig et al. 2010; Efthymiadis et al. 2011; Planton et al. 2012; Gualdi et al. 2013; Drobinski et al. 2014; Lionello et al. 2014). However, according to its high climate heterogeneity, relevant distinctions should be emphasized. As expected, change signal is in function of temporal horizon and the emission scenario considered but evident seasonal and latitudinal patterns also resulted (Giorgi 2006; Coppola and Giorgi 2010; Lionello 2012; Lionello et al. 2012). Moreover, several studies highlighted an asymmetry of temperature and precipitation distribution changes where extreme events are expected vary differently from the average. (Diffenbaugh et al. 2007; Fischer et al. 2007; Haarsma et al. 2009; Tolika et al. 2009; Hertig et al. 2010; Efthymiadis et al. 2011; Heinrich and Gobiet 2012). However, regarding future extreme events trend, many authors underline relevant uncertainties over magnitude and distribution patterns of expected changes. An example could be represented by the well-known climate models misrepresentation of complex dry-soil atmosphere feedbacks (Seneviratne et al. 2010; Orlowsky and Seneviratne 2011; Boberg and Christensen 2012) playing relevant role on determining length and magnitude of heat waves. At this regard, projected changes in inter-annual variability (oscillation of climate condition year-by-year) represent a good indicator on interpreting future temperature extreme trends. In Schär et al. (2004), was noted as future European summer climate might experience an increase in year-to-year variability, deeply affecting the incidence of heatwaves and drought. For precipitation, following thermodynamic and dynamic principles a generalized decrease of mean precipitation and an increase of extreme precipitation could be expected (Emori 2005; Palmer 2013; Coumou et al. 2014). However, especially for precipitation, identifying future dynamics and establishing a direct connection between increase in atmosphere temperature and extremes is anything but trivial (Frei and Schär 2001). Conversely, studies as Mariotti et al. (2008) and Senatore et al. (2011) highlight relevant consistency over expected changes in hydrologic cycle. Strong reduction of land-surface moisture availability is expected, where a significant decrease of main precipitation is coupled to an increase of winter evaporation (mainly over north-Italy) and a decrease of evaporation during summer (due to lower soil

moisture) over land. Concerning the Mediterranean Sea, precipitation reduction lower river run-off, warming-enhanced evaporation lead to a consistent loss in fresh water (Mariotti et al. 2008). These change patterns would be in agreement with the expected changes in the large-scale atmospheric modes with a north-ward expansion of the Hadley cell (Seidel et al. 2008; Planton et al. 2012) and increased positive phases of North Atlantic Oscillation (NAO) (Giorgi and Lionello 2008). The latter, substantially affects Atlantic storm track northward steering and cyclogenesis activity that regulate precipitation distribution in the whole Mediterranean region mainly in winter season (Giorgi and Lionello 2008; Xoplaki et al. 2012). For Italian peninsula, NAO positive phase means negative anomalies affecting winter precipitation. During this phase, compactness of polar vortex implicates higher-latitude Atlantic storm track. In turn, different studies stress how north-hemisphere large-scale circulation mode phases, are in turn influenced by the sea-ice extension and subsequently to the rate of its decline (Deser et al. 2010; Overland and Wang 2010). At this regard, Grassi et al. (2013) found evidences of increased NAO negative phase correlated to the reduction of winter sea-ice in correspondence of Barents-Kara sea region. NAO negative phase determines rippled sub-polar jet stream fostering low-pressure systems at the Mediterranean latitude. The same authors, referring to the Mediterranean region, indicate that even in the presence of general consistent increase of temperature cold spell will not disappear. Results indicated a tendency of increasing cold-rainy spells of winter precipitation over Italy with particular mention to the intense precipitation over the southern part of the Italian peninsula during winter season connected to a reduced extension of north-west Russian Arctic sea-ice. These highly diversified evidences stress the complexity of the large-scale dynamics interacting on defining Italian peninsula climate response to the anthropogenic forcing.

Bridging climate projections to climate impacts assessment

Intergovernmental Panel on Climate Change (IPCC) defines climate scenario as a "plausible representation of future climate that has been constructed for explicit use in investigating the potential impacts of anthropogenic climate change" (Mearns et al. 2001). Climate projections provided by climate models represent essential source of information for investigating the climate impacts for specific guesses about future human activities. However, alone, climate models projections do not provide sufficient information for defining future climate scenarios and related impacts to human and natural systems. Climate projections have to be properly managed and post-processed making them usable by climate

vulnerability, impacts and adaptation specialists. At this regard, the science of climate scenario provides the essential connection between climate simulations, produced by climate modelers and climate impact science. Several studies demonstrated that even newest generation of RCMs are still affected by systematic errors (Christensen et al. 2008; Boberg and Christensen 2012; Kotlarski et al. 2014). It complicates and deeply affects the capability of simulating and analyzing future climate impacts (Fowler et al. 2007). Hence, has been commonly established that some form of prior climate model outputs post-processing are strongly recommended before to use climate model outputs as inputs in impact modelling (Christensen et al. 2008).

Connection between climate model projections and climate impact research is particular delicate when local scale processes are considered (Smith et al. 2014). Local climate dynamics are the result of complex interactions between synoptic scale air mass motion, local morphology and orography. Even very high-resolution climate models (≈ 12 km) are limited in representing local climatology in complex physiography contexts. To be properly used in local impacts definition climate model outputs should be subjected to a double process devoted on the one hand to reduce model error (e.g. reduce discrepancies between meteorological observation and simulation over a common time segment) and on the other downscaled in order to include local climatology. As previously stated, statistical downscaling methodologies relying on the perfect prognosis principle (perfect prog. Wilks, 2011), have been considered for long time indicated technic tools for resolving the scale discrepancies between climate scenario and the resolution required for impact assessment (Maraun et al. 2010). Statistical downscaling establishes that local climate could be represent through a statistical model (transfer function) between large-scale observation/reanalysis data and local observation over present-day climate (Maraun et al. 2010; Themeßl et al. 2011b; Maraun et al. 2015). However, applied directly to GCMs or RCMs for providing local climate scenarios, these statistical methods do not act on the reduction of model output errors but only on refining spatial resolution. (Murphy 1999; Themeßl et al. 2011b).

Statistical post-processing bias correction according to the principle of Model Output Statistics (MOS; Wilks, 2011) may help to overcome this problem. In particular configurations, statistical bias correction techniques, couple RCM errors reduction to an improvement of the resolution at the same time (Themeßl et al. 2011b; Themeßl et al. 2011a; Casati et al. 2013; Smith et al. 2014). Statistical bias correction methods are indeed designed

to bridge the gap between climate model simulations and the climate data needed for quantitative assessment of climate impacts projections (Hempel et al. 2013).

Conceptually, bias correction methodologies aiming to reduce model errors could be discerned in two groups (Casati et al. 2013):

- Change factor methods that directly apply an average RCMs simulated climate change signal from future and present simulations to present climate observations. This method is widely called delta-change approach (Lenderink et al. 2007).
- Bias correction methods that rely on the relationship between present period observations and simulations to correct future model projections. In this context, the simplest approach corrects future climate simulation through a constant mean bias value characterizing simulations and observations during a present period. A drawback of this simple method is that error is considered constant over the whole statistical distribution consequently errors in variability are not corrected. Considering the future changes will differently affect mean values from high percentiles these technique could be considered too simplistic (Hagemann et al. 2011). Furthermore, given the high susceptibility of infrastructural and ecological systems to future extreme climatic events, it is suggestable to correct the entire statistical spectrum of climate model simulations. This could be performed through *parametric* (Piani et al. 2009; Piani et al. 2010) and *non-parametric* (empirical) bias correction methods (Boé et al. 2007; Deque 2007; Themeßl et al. 2011b; Themeßl et al. 2011a). A complete overview of statistical methodologies of bias correction is presented in Themeßl et al. (2011b), Berg et al. (2012) and Teutschbein and Seibert (2012) reporting comparison studies.

Amongst different approaches, empirical quantile mapping has been demonstrated to successfully remove systematic model errors due to high flexibility and high performance at high quantiles (Boé et al. 2007; Deque 2007; Themeßl et al. 2011b; Dosio and Paruolo 2011; Gudmundsson et al. 2012; Casati et al. 2013). In some particular configuration, such as employing in the correction finer grid or point scale observations, quantile mapping could help to bridge the gap between climate simulations and impact models resolution. In this case, bias correction performs error reduction and increase of simulation resolution (downscaling) at the same time also accounting for representativeness error (Casati et al. 2013). In fact, employing point-scale observations the discrepancies between observations

and simulations could result not only from intrinsic model error, but also from the spatial scale mismatch between model grid box and point-scale observations (Maraun et al. 2015).

However, in climate change studies, it is not sufficient to prove bias correction efficacy on correcting recent or present climatology; of primary importance is also to characterize the effects of bias correction over the climate change signal (i.e. statistics difference between a future and past climate simulation). The influence of bias correction on future simulations and over climate change signal is only recently considered. (Scherrer et al. 2005; Dosio et al. 2012; Maurer and Pierce 2014; Gobiet et al. 2015). In Hagemann et al. (2011) and Haerter et al. (2011) has been observed that quantile mapping stretches the original climate change signal of a factor consistent with the ratio of observed and simulated standard deviation. Such modification of the original climate change signal is being strongly discussed and generally considered as deficiency of bias correction methods (Hempel et al. 2013). However, Maurer and Pierce (2014) argued that quantile mapping do not deteriorate the quality of climate change signal resulting from a multi-model ensemble experiment. Only recently has been provide an analytical demonstration (Gobiet et al. 2015) that regards this modification no more as a deficiency of bias correction but rather as an improvement of climate change signal. Analytical demonstration of Gobiet and colleagues (2015), relies on an intensity-dependence of model errors observed in several studies (Christensen et al. 2008; Themeßl et al. 2011a; Boberg and Christensen 2012). In these studies, has been noted a relationship between monthly mean temperature simulation errors and the observed monthly mean temperature with larger biases in warmer months than in colder months. Follows that where an error intensity-dependence exists climate change signal referred to warm months would be exaggerated. The effect of quantile mapping on climate change signal is mainly caused by the correction of the intensity-dependence of model error. That is, the effect should be seen as an improvement instead a drawback on the bias correction application in future climate change studies. However, considerations on improvement provided by quantile mapping relies on the postulate of a time-invariant model error characteristic. This means that the same processes misrepresented in present climate would be misrepresented even in the future climate simulation with similar bias associated to similar temperature. Since the correction function accounts for temperature-dependent biases, the future projections associated with those processes can be improved by quantile mapping. On the other hand quantile mapping cannot correct model errors generated by new physical processes that could occur in the future climate and not present in current dynamics (Casati et al. 2013). Maraun

(2012) in an experiment over Europe and employing ENSEMBLES project simulations found that in a transient climate change study biases are quite stable and bias correction on average improves the quality of climate scenario for climate impact studies.

Research pillars

Present work, according to different methodological approaches followed, could be discerned in three main pillars. First, a comprehensive regional climate projections assessment, roughly covering Italian peninsula is provided. In the second pillar, the same climate model outputs have been post-processed according to an empirical statistical bias correction. This second section is devoted to reduce the multi-model ensemble simulations error but without effects over the resolution of climate simulations since the correction function is built using equal resolution observed datasets. Third pillar takes a step further, shifting from regional to local-scale future climate scenario over representative Marche region (one of the 20 administrative divisions of Italy). Here same post-processing method was employed but built considering higher resolution ensemble simulations and point-scale observations. This configuration allows obtaining simulations error reduction coupled to spatial resolution increase.

In the first pillar, a preliminary evaluation of the employed climate models through three statistical tests was performed. This section deals with the capability of the individual ensemble member to reproduce observed climatology of representative observational stations. Secondly, temperature and precipitation end-21st century climate change signal was analyzed. More in detail, considered variables are daily mean, minimum and maximum temperature and daily-cumulated precipitation. These key climate variable are the most used in climate change impact assessment studies (Giorgi et al. 2004). By definition, climate change signal is detected by comparing long-term statistics between a future (scenario) and past (reference) climate simulation (Mearns et al. 2001). Since changes are expected to differently affect mean value from high percentiles, different statistics signal have been considered. Furthermore, seasonal inter-annual temperature and precipitation variability response to increased radiative forcing was analyzed. Finally, operating with a multi-model ensemble approach, according to two different metrics, climate projections robustness and uncertainties were inspected.

In the subsequent two pillars, two different spatial scale climate scenarios (one roughly covering Italian peninsula and the second focused over representative stations of Marche region) are built. In these sections, the focus is over the effect of the statistical bias correction on the climate change signal performed with original simulations. Indeed, discrepancies between original and bias-corrected results were assessed. While the statistical correction methodology is unvaried in the two experiments, substantial difference lies on the horizontal resolution of the simulations and observations employed. The first experiment (regional experiment) involves a regional dimension roughly covering Italian peninsula. Here, a multi-model ensemble (van der Lindend and Mitchell 2009), having a horizontal resolution of 25 km, is corrected employing an observational gridded dataset with the same horizontal resolution (Haylock et al. 2008). Given no spatial scale mismatch between simulation and observation, bias correction is expected to reduce simulation error with no effect on the resolution of climate simulations. This configuration has been chosen to avoid problems related to the representativeness error problems occurring where spatial scale mismatch between simulation and reference observation exists. Indeed, it is possible to isolate climate model errors generated by systematic model biases coupled to internal variability misrepresentation. Third pillar reports an experiment (local experiment) relying on higher resolution (12.5 km) multi model ensemble (Jacob et al. 2013) corrected with point-scale observational data. The observation are point-scale climatological time series provided by the observational network of Marche region Civil Protection. Given the spatial scale mismatch between simulations and observations, quantile mapping couples error reduction to the increase of climate projection resolution at the same time. Observational stations have been selected to represent the two main climatological sector of Marche region. A valley/coastal band belonging to “temperate sub-coastal” (pertaining to type “C” Koppen climate classification) climate classification characterized by temperature annual average between 10 °C and 14.4 °C. Rainfall are all year long distributed with a maximum in autumn (end-October - December) and a second relative maximum in spring (March – April). The overall annual precipitation are between 550-700 mm in the southern part (south of Ancona) and 700-800 (north of Ancona). The second climate sector considered corresponds to the hill-mountain regional areas. Here, the climate is defined “temperate-sub continental” with annual mean temperature enclosed between 10 °C and 14.4°C. The difference is in the minimum temperature of cold months (from -1 °C to +3.9 °C against from 4 °C to 5.9 °C).

Moreover, the periods characterized by mean temperature >= 20 °C are from 1 to 3 months against 3 months in sub-coastal bend. Annual precipitation between 750 to 1000 mm.

Finally, in the perspective of future climate change, Marche region, according to what observed by Giorgi and Coppola (2007) and Mariotti et al. (2008), is located on a particular transitional latitude. Concerning future winter precipitation climate change signal, the 2-degrees (from 42° N to 45° N) latitudinal band would be characterized by uncertain change sign (negative signal south of 42° N and a positive signal north of 45° N).

Bibliography

Beniston M, Stephenson DB, Christensen OB, Ferro C a T, Frei C, Goyette S, Halsnaes K, Holt T, Jylhä K, Koffi B, Palutikof J, Schöll R, Semmler T, Woth K (2007) Future extreme events in European climate: An exploration of regional climate model projections. Climatic Change 81:71–95. doi: 10.1007/s10584-006-9226-z

Berg P, Feldmann H, Panitz H-J (2012) Bias correction of high resolution regional climate model data. Journal of Hydrology 448-449:80–92. doi: 10.1016/j.jhydrol.2012.04.026

Bindoff N, Stott P, AchutaRao K, Allen M, Gillett N, Gutzler D, Hansingo K, Hegerl G, Hu Y, Jain S, Mokhov I, Overland J, Perlwitz J, Sebbari R, Zhang X (2013) Detection and Attribution of Climate Change: from Global to Regional. Climate Change 2013: The Physical Science Basis Contribution of Working Group I to the Fifth Assessment Report of the Intergovenermnetal Panel on Climate Change 867–952.

Boberg F, Christensen JH (2012) Overestimation of Mediterranean summer temperature projections due to model deficiencies. Nature Climate Change 2:433–436. doi: 10.1038/nclimate1454

Boé J, Terray L, Habets F, Martin E (2007) Statistical and dynamical downscaling of the Seine basin climate for hydro-meteorological studies. 1655:1643–1655. doi: 10.1002/joc

Bucchignani E, Montesarchio M, Zollo AL, Mercogliano P (2015) High-resolution climate simulations with COSMO-CLM over Italy: performance evaluation and climate projections for the 21st century. International Journal of Climatology. doi: 10.1002/joc.4379

Burke M, Hsiang SM, Miguel E (2015) Global non-linear effect of temperature on Economic Production. Nature. doi: 10.1038/nature15725

Casati B, Yagouti A, Chaumont D (2013) Regional climate projections of extreme heat events in nine pilot Canadian communities for public health planning. Journal of Applied Meteorology and Climatology 52:2669–2698. doi: 10.1175/JAMC-D-12-0341.1

Christensen J, Kjellström E, Giorgi F, Lenderink G, Rummukainen M (2010) Weight assignment in regional climate models. Climate Research 44:179–194. doi: 10.3354/cr00916

Christensen JH, Boberg F, Christensen OB, Lucas-Picher P (2008) On the need for bias correction of regional climate change projections of temperature and precipitation. Geophysical Research Letters 35:L20709. doi: 10.1029/2008GL035694

Christensen JH, Christensen OB (2007) A summary of the PRUDENCE model projections of changes in European climate by the end of this century. Climatic Change 81:7–30. doi: 10.1007/s10584-006-9210-7

Coppola E, Giorgi F (2010) An assessment of temperature and precipitation change projections over Italy from recent global and regional climate model simulations. International Journal of Climatology 32:11–32. doi: 10.1002/joc

Coumou D, Petoukhov V, Rahmstorf S, Petri S, Schellnhuber HJ (2014) Quasi-resonant circulation regimes and hemispheric synchronization of extreme weather in boreal summer. Proceedings of the National Academy of Sciences. doi: 10.1073/pnas.1412797111

Cubasch U, Wuebbles D, Chen D, Facchini MC, Frame D, Mahowald N, Winther J-G (2013) Introduction In: Climate Change 2013: The Physical Science Basis. Contribution of Working Group I to the Fifth Assessment Report of the Intergovernmental Panel on Climate Change. Climate Change 2013: The Physical Science Basis Contribution of Working Group I to the Fifth Assessment Report of the Intergovernmental Panel on Climate Change 119–158. doi: 10.1017/CBO9781107415324.007

Deque M (2007) Frequency of precipitation and temperature extremes over France in an anthropogenic scenario: Model results and statistical correction according to observed values. Global and Planetary Change 57:16–26. doi: 10.1016/j.gloplacha.2006.11.030

Déqué M, Jones RG, Wild M, Giorgi F, Christensen JH, Hassell DC, Vidale PL, Rockel B, Jacob D, Kjellström E, de Castro M, Kucharski F, van den Hurk B (2005) Global high resolution versus Limited Area Model climate change projections over Europe: Quantifying confidence level from PRUDENCE results. Climate Dynamics 25:653–670. doi: 10.1007/s00382-005-0052-1

Deser C, Tomas R, Alexander M, Lawrence D (2010) The seasonal atmospheric response to projected Arctic sea ice loss in the late twenty-first century. Journal of Climate 23:333–351. doi: 10.1175/2009JCLI3053.1

Diffenbaugh NS, Pal JS, Giorgi F, Gao X (2007) Heat stress intensification in the Mediterranean climate change hotspot. Geophysical Research Letters 34:1–6. doi: 10.1029/2007GL030000

Dosio a., Paruolo P (2011) Bias correction of the ENSEMBLES high-resolution climate change projections for use by impact models: Evaluation on the present climate. Journal of Geophysical Research 116:D16106. doi: 10.1029/2011JD015934

Dosio a., Paruolo P, Rojas R (2012) Bias correction of the ENSEMBLES high resolution climate change projections for use by impact models: Analysis of the climate change signal. Journal of Geophysical Research: Atmospheres 117:1–24. doi: 10.1029/2012JD017968

Drobinski P, Ducrocq V, Alpert P, Anagnostou E, Béranger K, Borga M, Braud I, Chanzy a., Davolio S, Delrieu G, Estournel C, Boubrahmi NF, Font J, Grubišić V, Gualdi S, Homar V, Ivančan-Picek B, Kottmeier C, Kotroni V, Lagouvardos K, Lionello P, Llasat MC, Ludwig W, Lutoff C, Mariotti a., Richard E, Romero R, Rotunno R, Roussot O, Ruin I, Somot S, Taupier-Letage I, Tintore J, Uijlenhoet R, Wernli H (2014) HyMeX: A 10-Year Multidisciplinary Program on the Mediterranean Water Cycle. Bulletin of the American Meteorological Society 95:1063–1082. doi: 10.1175/BAMS-D-12-00242.1

Efthymiadis D, Goodess CM, Jones PD (2011) Trends in Mediterranean gridded temperature extremes and large-scale circulation influences. Natural Hazards and Earth System Science 11:2199–2214. doi: 10.5194/nhess-11-2199-2011

Emori S (2005) Dynamic and thermodynamic changes in mean and extreme precipitation under changed climate. Geophysical Research Letters 32:L17706. doi: 10.1029/2005GL023272

Fischer EM, Seneviratne SI, Vidale PL, Lüthi D, Schär C (2007) Soil moisture-atmosphere interactions during the 2003 European summer heat wave. Journal of Climate 20:5081–5099. doi: 10.1175/JCLI4288.1

Flato G, Marotzke J, Abiodun B, Braconnot P, Chou SC, Collins W, Cox P, Driouech F, Emori S, Eyring V, Forest C, Gleckler P, Guilyardi E, Jakob C, Kattsov V, Reason C, Rummukainen M (2013) Evaluation of Climate Models. Climate Change 2013: The Physical Science Basis Contribution of Working Group I to the Fifth Assessment Report of the Intergovernmental Panel on Climate Change 741–866. doi: 10.1017/CBO9781107415324

Fowler HJ, Blenkinsop S, Tebaldi C (2007) Linking climate change modelling to impacts studies : recent advances in downscaling techniques for hydrological. International Journal of Climatology 1578:1547–1578. doi: 10.1002/joc

Frei C, Schär C (2001) Detection Probability of Trends in Rare Events: Theory and Application to Heavy Precipitation in the Alpine Region. Journal of Climate 14:1568–1584. doi: 10.1175/1520-0442

Gaetani M, Baldi M, Dalu G a., Maracchi G (2011) Jetstream and rainfall distribution in the Mediterranean region. Natural Hazards and Earth System Sciences 11:2469–2481. doi: 10.5194/nhess-11-2469-2011

Gao X, Pal JS, Giorgi F (2006) Projected changes in mean and extreme precipitation over the Mediterranean region from a high resolution double nested RCM simulation. Geophysical Research Letters 33:2–5. doi: 10.1029/2005GL024954

Gennaretti F, Sangelantoni L, Grenier P (2015) Toward daily climate scenarios for Canadian Arctic coastal zones with more realistic temperature-precipitation interdependence. Journal of Geophysical Research: Atmospheres 120, doi: 10.1002/2015JD023890

Giorgi F (2006a) Regional climate modeling: Status and perspectives. Journal de Physique IV (Proceedings) 139:101–118. doi: 10.1051/jp4:2006139008

Giorgi F (2006b) Climate change hot-spots. Geophysical Research Letters 33:1–4. doi: 10.1029/2006GL025734

Giorgi F (1990) Simulation of regional climate using a limited area model nested in a general circulation model. Journal of Climate 3:941–963.

Giorgi F, Bi X, Pal J (2004) Mean, interannual variability and trends in a regional climate change experiment over Europe. II: Climate change scenarios (2071-2100). Climate Dynamics 23:839–858. doi: 10.1007/s00382-004-0467-0

Giorgi F, Jones C, Asrar GR (2009) Addressing climate information needs at the regional level : the CORDEX framework. WMO bulletin 58:175–183.

Giorgi F, Lionello P (2008) Climate change projections for the Mediterranean region. Global and Planetary Change 63:90–104. doi: 10.1016/j.gloplacha.2007.09.005

Gobiet a., Suklitsch M, Heinrich G (2015) The effect of empirical-statistical correction of intensity-dependent model errors on the climate change signal. Hydrology and Earth System Sciences Discussions 12:5671–5701. doi: 10.5194/hessd-12-5671-2015

Grassi B, Redaelli G, Visconti G (2013) Arctic sea ice reduction and extreme climate events over the mediterranean region. Journal of Climate 26:10101–10110. doi: 10.1175/JCLI-D-12-00697.1

Gualdi S, Somot S, Li L, Artale V, Adani M, Bellucci a., Braun a., Calmanti S, Carillo a., Dell'Aquila a., Déqué M, Dubois C, Elizalde a., Harzallah a., Jacob D, L'Hévéder B,

May W, Oddo P, Ruti P, Sanna a., Sannino G, Scoccimarro E, Sevault F, Navarra a. (2013) The CIRCE Simulations: Regional Climate Change Projections with Realistic Representation of the Mediterranean Sea. Bulletin of the American Meteorological Society 94:65–81. doi: 10.1175/BAMS-D-11-00136.1

Gudmundsson L, Bremnes JB, Haugen JE, Engen-Skaugen T (2012) Technical Note: Downscaling RCM precipitation to the station scale using statistical transformations - a comparison of methods. Hydrology and Earth System Sciences 16:3383–3390. doi: 10.5194/hess-16-3383-2012

Haarsma RJ, Selten F, Hurk B Vd, Hazeleger W, Wang X (2009) Drier Mediterranean soils due to greenhouse warming bring easterly winds over summertime central Europe. Geophysical Research Letters 36:1–7. doi: 10.1029/2008GL036617

Haerter JO, Hagemann S, Moseley C, Piani C (2011) Climate model bias correction and the role of timescales. Hydrology and Earth System Sciences 15:1065–1079. doi: 10.5194/hess-15-1065-2011

Hagemann S, Chen C, Haerter JO, Heinke J, Gerten D, Piani C (2011) Impact of a Statistical Bias Correction on the Projected Hydrological Changes Obtained from Three GCMs and Two Hydrology Models. Journal of Hydrometeorology 12:556–578. doi: 10.1175/2011JHM1336.1

Hawkins E, Sutton R (2011) The potential to narrow uncertainty in projections of regional precipitation change. Climate Dynamics 37:407–418. doi: 10.1007/s00382-010-0810-6

Haylock MR, Hofstra N, Klein Tank a. MG, Klok EJ, Jones PD, New M (2008) A European daily high-resolution gridded data set of surface temperature and precipitation for 1950-2006. Journal of Geophysical Research: Atmospheres. doi: 10.1029/2008JD010201

Hegerl GC, Zwiers FW, Braconnot P, Gillett NP, Luo Y, Orsini JAM, Nicholls N, Penner JE, Stott P a (2007) Understanding and Attributing Climate Change. Climate Change 2007: The Physical Science Basis. Contribution of Working Group I to the Fourth Assessment Report of the Intergovernmental Panel on Climate Change. Cambridge University Press, Cambridge, United Kingdom and New York, NY, USA

Heinrich G, Gobiet A (2012) The future of dry and wet spells in Europe: A comprehensive study based on the ENSEMBLES regional climate models. International Journal of Climatology 32:1951–1970. doi: 10.1002/joc.2421

Hempel S, Frieler K, Warszawski L, Schewe J, Piontek F (2013) A trend-preserving bias

correction – The ISI-MIP approach. Earth System Dynamics 4:219–236. doi: 10.5194/esd-4-219-2013

Hertig E, Seubert S, Jacobeit J (2010) Temperature extremes in the Mediterranean area: Trends in the past and assessments for the future. Natural Hazards and Earth System Science 10:2039–2050. doi: 10.5194/nhess-10-2039-2010

Huard D, Chaumont D, Logan T, Sottile M-F, Brown RD, St-Denis BG, Grenier P, Braun M (2014) A Decade of Climate Scenarios – The Ouranos Consortium Modus Operandi. Bulletin of the American Meteorological Society 140116121450005. doi: 10.1175/BAMS-D-12-00163.1

ISPRA - Istituto Superiore per la Protezione e la Ricerca Ambientale (2015) Il clima futuro in Italia: analisi delle proiezioni dei modelli regionali

Jacob D, Petersen J, Eggert B, Alias A, Christensen OB, Bouwer LM, Braun A, Colette A, Déqué M, Georgievski G, Georgopoulou E, Gobiet A, Menut L, Nikulin G, Haensler A, Hempelmann N, Jones C, Keuler K, Kovats S, Kröner N, Kotlarski S, Kriegsmann A, Martin E, Meijgaard E, Moseley C, Pfeifer S, Preuschmann S, Radermacher C, Radtke K, Rechid D, Rounsevell M, Samuelsson P, Somot S, Soussana J-F, Teichmann C, Valentini R, Vautard R, Weber B, Yiou P (2013) EURO-CORDEX: new high-resolution climate change projections for European impact research. Regional Environmental Change 14:563–578. doi: 10.1007/s10113-013-0499-2

Knutti R (2008) Should we believe model predictions of future climate change? Philosophical transactions Series A, Mathematical, physical, and engineering sciences 366:4647–4664. doi: 10.1098/rsta.2008.0169

Kotlarski S, Keuler K, Christensen OB, Colette a., Déqué M, Gobiet a., Goergen K, Jacob D, Lüthi D, Van Meijgaard E, Nikulin G, Schär C, Teichmann C, Vautard R, Warrach-Sagi K, Wulfmeyer V (2014) Regional climate modeling on European scales: A joint standard evaluation of the EURO-CORDEX RCM ensemble. Geoscientific Model Development 7:1297–1333. doi: 10.5194/gmd-7-1297-2014

Laprise R, Caya D, Giguere M, Bergeron G, Côté H, Blanchet J, Boer GJ, McFarlane N a. (1998) Climate and climate change in western canada as simulated by the Canadian regional climate model. Atmosphere-Ocean 36:119–167. doi: 10.1080/07055900.1998.9649609

Leander R, Buishand TA (2007) Resampling of regional climate model output for the simulation of extreme river flows. Journal of Hydrology 332:487–496. doi:

10.1016/j.jhydrol.2006.08.006

Lenderink G, Buishand a., van Deursen W (2007) Estimates of future discharges of the river Rhine using two scenario methodologies: direct versus delta approach. Hydrology and Earth System Sciences 11:1145–1159. doi: 10.5194/hess-11-1145-2007

Lionello, P., Malanotte-Rizzoli, P., & Boscolo, R. (Eds.). (2006) Mediterranean climate variability (Vol. 4). Elsevier

Lionello P (2012) The Climate of the Mediterranean Region From the Past to the Future, 1st edn. Elsevier

Lionello P, Abrantes F, Congedi L, Dulac F, Gacic M, Gomis D, Goodess C, Hoff H, Kutiel H, Luterbacher J, Planton S, Reale M, Schröder K, Vittoria Struglia M, Toreti A, Tsimplis M, Ulbrich U, Xoplaki E (2012) Introduction: Mediterranean Climate—Background Information. The Climate of the Mediterranean Region xxxv–xc. doi: 10.1016/B978-0-12-416042-2.00012-4

Lionello P, Abrantes F, Gacic M, Planton S, Trigo R, Ulbrich U (2014) The climate of the Mediterranean region: research progress and climate change impacts. Regional Environmental Change. doi: 10.1007/s10113-014-0666-0

Maraun D (2012) Nonstationarities of regional climate model biases in European seasonal mean temperature and precipitation sums. Geophysical Research Letters 39:1–5. doi: 10.1029/2012GL051210

Maraun D, Wetterhall F, Ireson AM, Chandler RE, Kendon JE, Widmann M, Brienen S, Rust HW, Sauter T, Themeßl M, Venema VKC, Chun KP (2010) Precipitation Downscaling Under Climate Change : Recent Developments To Bridge the Gap Between Dynamical Models and the End User. Review of Geophysics 48:1–34. doi: 10.1029/2009RG000314.1

Maraun D, Widmann M, Gutierrez JM, Kotlarski S, Chandler RE, Hertig E, Wibig J, Huth R, Wilcke R a I (2015) VALUE: A framework to validate downscaling approaches for climate change studies. Earth's Future 3:1–14. doi: 10.1002/2014EF000259

Mariotti A, Zeng N, Yoon J-H, Artale V, Navarra A, Alpert P, Li LZX (2008) Mediterranean water cycle changes: transition to drier 21st century conditions in observations and CMIP3 simulations. Environmental Research Letters 3:044001. doi: 10.1088/1748-9326/3/4/044001

Maurer EP, Pierce DW (2014) Bias correction can modify climate model simulated precipitation changes without adverse effect on the ensemble mean. Hydrology and

Earth System Sciences 18:915–925. doi: 10.5194/hess-18-915-2014

Mearns, L. O., M. Hulme, T. R. Carter, R. Leemans, M. Lal, and P. Whetton (2001)Climate Scenario Development. Climate Change 2001: The Scientific Basis, 739–768

Murphy J (1999) An evaluation of statistical and dynamical techniques for downscaling local climate. Journal of Climate 12:2256–2284. doi: 10.1175/1520-0442(1999)012<2256:AEOSAD>2.0.CO;2

Myhre G, Shindell D, Bréon F-M, Collins W, Fuglestvedt J, Huang J, Koch D, Lamarque J-F, Lee D, Mendoza B, Nakajima T, Robock a., Stephens G, Takemura T, Zhan H (2013) 2013: Anthropogenic and Natural Radiative Forcing. Climate Change 2013: The Physical Science Basis Contribution of Working Group I to the Fifth Assessment Report of the Intergovernmental Panel on Climate Change 659–740. doi: 10.1017/CBO9781107415324.018

Orlowsky B, Seneviratne SI (2011) Global changes in extreme events: regional and seasonal dimension. Climatic Change 110:669–696. doi: 10.1007/s10584-011-0122-9

Overland JE, Wang M (2010) Large-scale atmospheric circulation changes are associated with the recent loss of Arctic sea ice. Tellus, Series A: Dynamic Meteorology and Oceanography 62:1–9. doi: 10.1111/j.1600-0870.2009.00421.x

Palmer TN (2013) Climate extremes and the role of dynamics. Proceedings of the National Academy of Sciences of the United States of America 110:5281–2. doi: 10.1073/pnas.1303295110

Piani C, Haerter JO, Coppola E (2009) Statistical bias correction for daily precipitation in regional climate models over Europe. Theoretical and Applied Climatology 99:187–192. doi: 10.1007/s00704-009-0134-9

Piani C, Weedon GP, Best M, Gomes SM, Viterbo P, Hagemann S, Haerter JO (2010) Statistical bias correction of global simulated daily precipitation and temperature for the application of hydrological models. Journal of Hydrology 395:199–215. doi: 10.1016/j.jhydrol.2010.10.024

Planton S, Lionello P, Artale V, Aznar R, Carrillo A, Colin J, Congedi L, Dubois C, Elizalde A, Gualdi S, Hertig E, Jacobeit J, JordÃ G, Li L, Mariotti A, Piani C, Ruti P, Sanchez-Gomez E, Sannino G, Sevault F, Somot S, Tsimplis M (2012) The Climate of the Mediterranean Region in Future Climate Projections.

Schär C, Vidale PL, Lüthi D, Frei C, Häberli C, Liniger M a, Appenzeller C (2004) The role of increasing temperature variability in European summer heatwaves. Nature 427:332–

336. doi: 10.1038/nature02300

Scherrer SC, Christof A, A. LM, Schar Christof (2005) European temperature distribution changes in observations and climate change scenarios. Geophysical Research Letters. doi: 10.1029/2005GL024108

Seidel D, Fu Q, Randel W, Reichler T (2008) Widening of the tropical belt in a changing climate. Nature Geoscience 1:21–24. doi: 10.1038/ngeo.2007.38

Senatore A, Mendicino G, Smiatek G, Kunstmann H (2011) Regional climate change projections and hydrological impact analysis for a Mediterranean basin in Southern Italy. Journal of Hydrology 399:70–92. doi: 10.1016/j.jhydrol.2010.12.035

Seneviratne SI, Corti T, Davin EL, Hirschi M, Jaeger EB, Lehner I, Orlowsky B, Teuling AJ (2010) Investigating soil moisture-climate interactions in a changing climate: A review. Earth-Science Reviews 99:125–161. doi: 10.1016/j.earscirev.2010.02.004

Smith PC, Heinrich G, Suklitsch M, Gobiet A, Stoffel M, Fuhrer J (2014) Station-scale bias correction and uncertainty analysis for the estimation of irrigation water requirements in the Swiss Rhone catchment under climate change. Climatic Change 127:521–534. doi: 10.1007/s10584-014-1263-4

Stocker T, Dahe Q, Plattner G-K, Tignor M, Midgley P (2010) IPCC Expert Meeting on Assessing and Combining Multi Model Climate Projections - Meeting Report.

Tang Q, Zhang X, Yang X, Francis J a (2013) Cold winter extremes in northern continents linked to Arctic sea ice loss. Environmental Research Letters 8:014036. doi: 10.1088/1748-9326/8/1/014036

Teutschbein C, Seibert J (2012) Bias correction of regional climate model simulations for hydrological climate-change impact studies: Review and evaluation of different methods. Journal of Hydrology 456-457:12–29. doi: 10.1016/j.jhydrol.2012.05.052

Themeßl MJ, Gobiet A, Heinrich G (2011a) Empirical-statistical downscaling and error correction of regional climate models and its impact on the climate change signal. Climatic Change 112:449–468. doi: 10.1007/s10584-011-0224-4

Themeßl MJ, Gobiet A, Leuprecht A (2011b) Empirical-statistical downscaling and error correction of daily precipitation from regional climate models. International Journal of Climatology 1544:1530–1544. doi: 10.1002/joc.2168

Tolika K, Maheras P, Tegoulias I (2009) Extreme temperatures in Greece during 2007: Could this be a “return to the future”? Geophysical Research Letters 36:1–5. doi: 10.1029/2009GL038538

Van der Linden, P., & Mitchell, J. E. (2009) ENSEMBLES: Climate Change and its Impacts: Summary of research and results from the ENSEMBLES project. Met Office Hadley Centre

Vaughan C, Dessai S (2014) Climate services for society: origins, institutional arrangements, and design elements for an evaluation framework. Wiley Interdisciplinary Reviews: Climate Change 5:587–603. doi: 10.1002/wcc.290

Vautard R, Gobiet A, Jacob D, Belda M, Colette A, Déqué M, Fernández J, García-Díez M, Goergen K, Güttler I, Halenka T, Karacostas T, Katragkou E, Keuler K, Kotlarski S, Mayer S, Meijgaard E, Nikulin G, Patarčić M, Scinocca J, Sobolowski S, Suklitsch M, Teichmann C, Warrach-Sagi K, Wulfmeyer V, Yiou P (2013) The simulation of European heat waves from an ensemble of regional climate models within the EURO-CORDEX project. Climate Dynamics 41:2555–2575. doi: 10.1007/s00382-013-1714-z

Wilks, D. S. (2011). Statistical methods in the atmospheric sciences (Vol. 100). Academic press.

Xoplaki E, Gonzalez-Rouco JF, Luterbacher J, Wanner H (2003) Mediterranean summer air temperature variability and its connection to the large-scale atmospheric circulation and SSTs. Climate Dynamics 20:723–739. doi: 10.1007/s00382-003-0304-x

Xoplaki E, González-Rouco JF, Luterbacher J, Wanner H (2004) Wet season Mediterranean precipitation variability: Influence of large-scale dynamics and trends. Climate Dynamics 23:63–78. doi: 10.1007/s00382-004-0422-0

Xoplaki E, Trigo RM, García-Herrera R, Barriopedro D, D'Andrea F, Fischer EM, Gimeno L, Gouveia C, Hernández E, Kuglitsch FG, Mariotti A, Nieto R, Pinto JG, Pozo-Vázquez D, Saaroni H, Toreti A, Trigo IF, Vicente-Serrano SM, Yiou P, Ziv B (2012) Large-scale atmospheric circulation driving extreme climate events in the mediterranean and its related impacts. In: The Climate of the Mediterranean Region. pp 347–417

Even if not directly cited in the text, essential knowledge and cues for the introductive chapter have been found in:

Neelin, J. D. (2010) Climate change and climate modeling. Cambridge University Press.

Mercalli, L. (2009) Che tempo che farà: breve storia del clima con uno sguardo al futuro. Rizzoli.

1. An assessment of temperature and precipitation projections over Italian peninsula from regional climate model ensemble simulations

1.1 Datasets and methodology

1.1.1 Simulation Datasets

In this chapter, high resolution climate simulations from regional climate models (RCMs), run in the context of ENSEMBLES European project (http://ensembles-eu.metoffice.com, van der Lindend & Mitchell 2009), are assessed. Due to limited computational resources, only a small sub-set of the possible GCM-RCM combinations was considered (Table 1).

Institute	RCM	Driving GCM	Resolution	Period	SRES	Variable
DMI	HIRHAM5	ECHAM5-r3	25 km	1961- 2090	A1B	tas; pr
KNMI	RACMO2.1	ECHAM5-r3	25 km	1961-2090	A1B	tas; pr
MPI	REMO5.7	ECHAM5-r3	25 km	1961-2090	A1B	tas; pr
SMHI	RCA3.0	ECHAM5-r3	25 km	1961-2090	A1B	tas; pr
CNRM	Aladin	ARPEGE_RM5.1	25 km	1961-2090	A1B	tas; pr
ICTP	RegCM3	ECHAM5-r3	25 km	1961-2090	A1B	tas; pr

Table 1.1. List of climate models providing climate simulations.

All RCMs are driven by the same GCM (ECHAM5-r3) except the Aladin driven by ARPEGE_RM5.1 GCM. Climate variables assessed in this study consist on daily mean, minimum, maximum surface temperature (respectively tas, tmin and tmax) and daily cumulated precipitation (pr) from 1961 to 2090. Simulations present a common horizontal resolution of 25 km and an intermediate atmospheric greenhouse gasses concentration scenario A1B (CO_2 concentration of about 700 ppm by 2100, Nakicenovic Nebojsa 2000), reported in figure 1.1 in comparison with other emission scenarios.

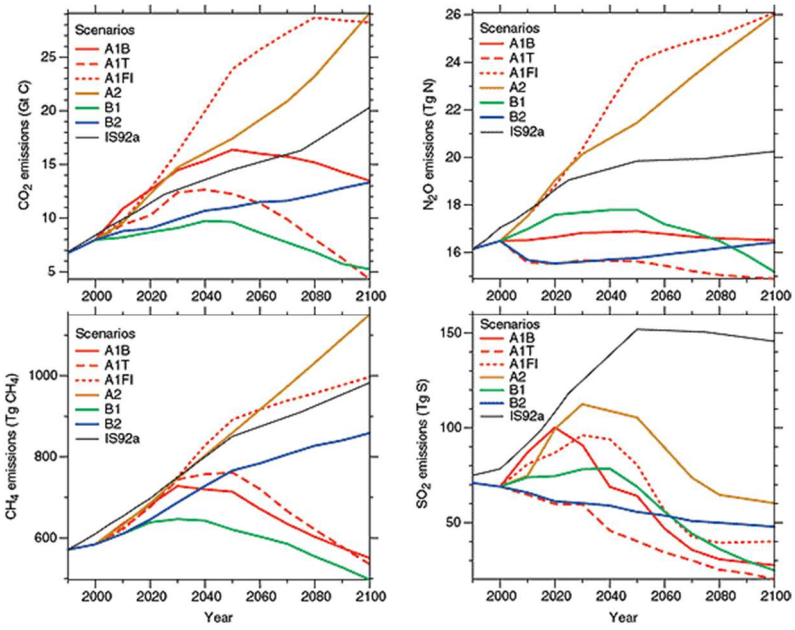

Figure 1.1. Anthropogenic emissions of CO_2, CH_4, N_2O and Sulphur dioxide for the six illustrative SRES scenarios, A1B, A2, B1 and B2, A1FI and A1T. [IPCC Special Report on Emissions Scenarios].

Simulations spatial domain covers a longitudinal range from 6 °E to 18.5 °E and a latitude going from 40 °N to 48 °N. All Italian peninsula has represented except for Calabria region, Sicily Island and south Sardinia. Considering computational limits, we preferred to include Alpine region, even beyond Italian borders, than the southernmost part. This choice follows a rationale connected to current and expected climate change dynamics. Given its particular morphological, climatic, ecological, and hydrological features, Alpine region is already presenting more than average sensitivity to current climate change (Gobiet et al. 2014). Moreover, for what concerns temperature and precipitation, Alpine region acts as hinge of the latitudinal/seasonal climate oscillation identified by Giorgi & Coppola 2007. Another source of scientific interest is that Alps latitude is expected to represent the transition zone (positive-negative) of projected winter precipitation change. From scientific literature current and projected climate change involving southernmost part of Italy (Sicily and Calabria region, not represented in the study area) is not dissimilar to those affecting southernmost part of the study area (Giorgi and Lionello 2008). Study area is reported in figure 1.2.

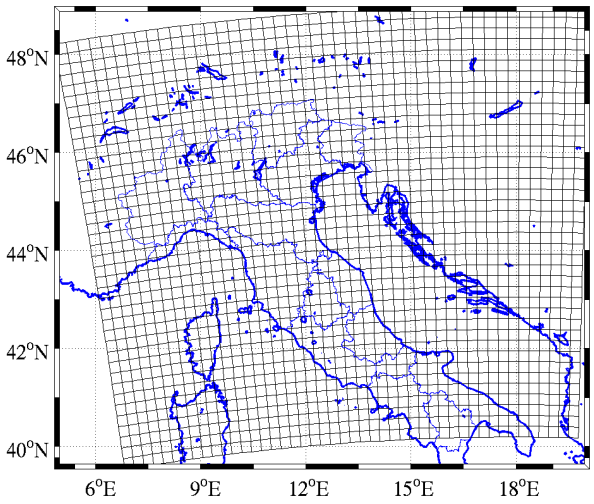

Figure 1.2. Numerical climate models grid and geographical domain of the study area.

1.1.2 Climate model simulations setup

The response of the climate system to an increasing of GHGs and aerosol concentrations is assessed through an ensemble of six regional climate model simulations. In a variety of applications, not only limited to the weather and climate prediction/projection problems, was demonstrated that combining different models generally skill, reliability and consistency of model predictions or projections result improved (Tebaldi and Knutti 2007). Ensemble of climate models could be interpreted as a combination of climate model simulations. Multi-model ensemble averages provide one commonly used way to condense information from many climate models running the same experiment. The ensemble average tend to provide a smoother representation of climate evolution compared to the interpretation belonging to the individual ensemble member. This is because if one single simulation produces a strong localized feature, such strong drought, it is improbable that all the other members will reproduce in the same place the same magnitude drought; events amplitude is indeed reduced in the average (J. D. Neelin, 2010). In the recent years, two principal approaches to combine climate simulations have been mainly employed. One is the *"Perturbed-physics ensemble"* (Collins et al. 2011). This approach involves perturbing physical parameters within a single model structure with different choice and range of perturbation. A key strength of this approach is the ability to produce a large numbers of ensemble members in relatively easy way (Collins et al. 2011). This study relies on a second approach of combining multiple climate simulations, named *"Multi-model ensemble"* (Palmer et al. 2004). Multi-model ensemble is defined as a set of model simulations from structurally different models, where one (in this study) or more initial conditions (e.g. GHGs concentration future paths) are available from each model (if more initial conditions for each model are available the experiments are often said to make up a super-ensemble) (Tebaldi and Knutti 2007). Belonging from different models, developed by different institutional research center, multi-model ensemble projections account for a wider spectrum of modelling choices and the inherent deficiency of each member. Within multi-model ensemble approach, different ways to combine model simulations exists. One, based on *weighted averages*, where models are weighted in function of demonstrated capability on reproducing real world observed time series (Christensen et al. 2010). Intuitively, it makes perfect sense to trust, but the difficulty lays to identify model that systematically outperform in each context (i.e. over different variable, season, orographic context and statistical momentum) and shared metrics to evaluate performances. Weighted averages approach is found to better perform in cases

where sufficient information is available to correctly determine the weight of the individual ensemble member (Knutti et al. 2010). In our case, previous statistical assessment of models performance did not highlight clear hierarchy of models skill. It makes potentially controversial to assign a fixed weight to each of the ensemble members. For this reason, climate projections presented here rely on *equally weighted*, namely arithmetically averaged following the concept of "one model, one vote". Other concern refers to the optimal number of ensemble members. Knutti et al. (2010) demonstrated considerable improvement is only seen for up to about 5 models, and after 10 models the biases are almost stable. Indeed, considering large ensembles are computationally expensive, a six-member multi-model ensemble was chosen. Finally, six simulations were linearly interpolated on a common 25 km resolution grid and then averaged grid point by grid point. This procedure repeated for each climate variables considered. The result could be imagine as a single climate simulation representing all the ensemble members' average.

1.1.3 Analysis: climate change signal, climate models evaluation and inter-model agreement

Climate change signal is defined as the difference of a selected climate statistic in the scenario (2061-2090) and reference (1961-1990) simulations. Different statistics was selected to derive changes over both mean and extremes (corresponding to the tails of the variable statistical distribution). Climate change signal has been derived grid-point wise for four climate variables (tmean, tmin, tmax and pr). This allows analyzing climatic change spatial pattern, highlighting most sensitive areas to future changes.

Specific section investigates the response of the inter-seasonal climate variability to the increase of atmospheric anthropogenic GHG and aerosols concentration. Inter-seasonal variability was measured comparing future and reference period seasonal standard deviation for temperature and coefficient of variance for precipitation. Inter-seasonal variability change signal was obtained by first calculating the standard deviation at each grid point of the multi-model ensemble for both periods, successively performing a percentage difference. For precipitation, the same procedure was followed but computing coefficient of variation given by the ratio between standard deviation and average (σ/μ). Use of coefficient of variation removes the well-known dependency of the precipitation standard deviation on the mean (Giorgi and Lionello 2008).

Another methodological section assesses the agreement of the different models over the change signal outlined. Adopting multi-model ensemble approach, quantifying the agreement of ensemble members over a certain projection means characterizing its consistency and uncertainty. This is general addressed analyzing inter-model spread where high deviation suggests higher uncertainty projection. Here a step further was undertaken studying not merely inter-model spread but the agreement of the ensemble members over the sign and statistical significance of change signal. Hence, two metrics were adopted: first metric has been employed in the *4th Assessment Report of the Intergovernmental Panel on Climate Change* (Solomon et al. 2007) and is based on inter-model agreement on the sign of change, stippling areas where at least the majority of models (66%) shows the same sign of change. Second metric (Tebaldi et al. 2011), maps models agreement on signal statistical significance, stippling areas where the majority of models report significant change signal. Addressing statistical significance means that models produced changes outside the boundary of natural climate variability (Tebaldi et al. 2011). Statistical significance has been tested (t-test) for each ensemble member, grid point by grid point for daily mean temperature and daily-cumulated precipitation climate change signal.

Before presenting climate projections assessment, ensemble members have been tested against observed time series belonging to three reference stations of Marche region (one of the 20 administrative divisions of Italy) located in the Adriatic coast of central Italy. Even if not comprehensive for entire Italian peninsula climatology it is important to assess the capability of climate models of reproducing past-observed temperature and precipitation climatology. The observational datasets are provided by the observational network of Marche region Civil Protection chosen in function of temporal homogeneity over the segment 1971-2000 and for representing three different climate conditions. For temperature, one station (Ancona) is located along the coast and is characterized by a maritime-Mediterranean climate with warm summer and temperate winters. A second station (Fabriano) is located far away from the sea (60 km) at an elevation of 320 m. Surrounded by complex morphology, local climate is only slightly affected by the presence of Adriatic sea. A third station (Montemonaco 990 m a.s.l.) was chosen for representing mountain climate. For precipitation coast, hill and mountain sectors are respectively represented by Pesaro (sea level), Jesi (96 m a.s.l.) and Bolognola (1000 m a.s.l.). This phase aimed to test the capability of climate models of reproducing past climate features over diversified morphology. Employed statistical tests consider simulated and observed daily time series gathered in

monthly basis in order to evaluate entire annual cycle bias distribution. Three widely adopted indices for performance evaluation were employed, namely Mean Bias (MB), Mean Absolute Error (MAE) and Root-Mean-Square error (Bucchignani et al. 2015).

$$MB = \frac{1}{N}\sum_{i=1}^{N}(S_i - O_i)$$

$$MAE = \frac{1}{N}\sum_{i=1}^{N}|S_i - O_i|$$

$$RMSE = \sqrt{\frac{1}{N}\sum_{i=1}^{N}(S_i - O_i)^2}$$

Where S_i and O_i are respectively simulated and observed daily values considering i-th month. Through a dedicated function, simulated time series are extracted from the nearest grid point to the observational station. MB represents the discrepancies between the simulated and observed monthly means during the time segment considered (1971-2000). MAE represent the same operation but the monthly bias absolute value is considered. The root of the square of the mean absolute bias gives the RMSE. This simple arithmetic manipulation allows higher sensitivity to very high model bias (outliers) and to maintain the original physical value of the variable (D. S. Wilks, 2011). The evaluation phase wants to investigate the capability of single ensemble member on reproducing the mean temperature and precipitation characterizing the reference period month by month. However, simulations capability on reproducing temporal correlation with past observed variability has not considered since expected to be very low. This is because, forced by GCMs, RCMs are not "synchronized" (this was in the case boundary conditions were provided by observations or reanalysis) with the observed temporal succession of weather states. In this GCMs-driven RCMs configuration, trends and variability changes are simulated in function of variation in radiative forcing in turn linked to the alteration of GHGs concentration. For these reasons, only comparison of the reference period monthly mean reproduction has been studied.

1.2 Results

1.2.1 Climate models evaluation

Temperature

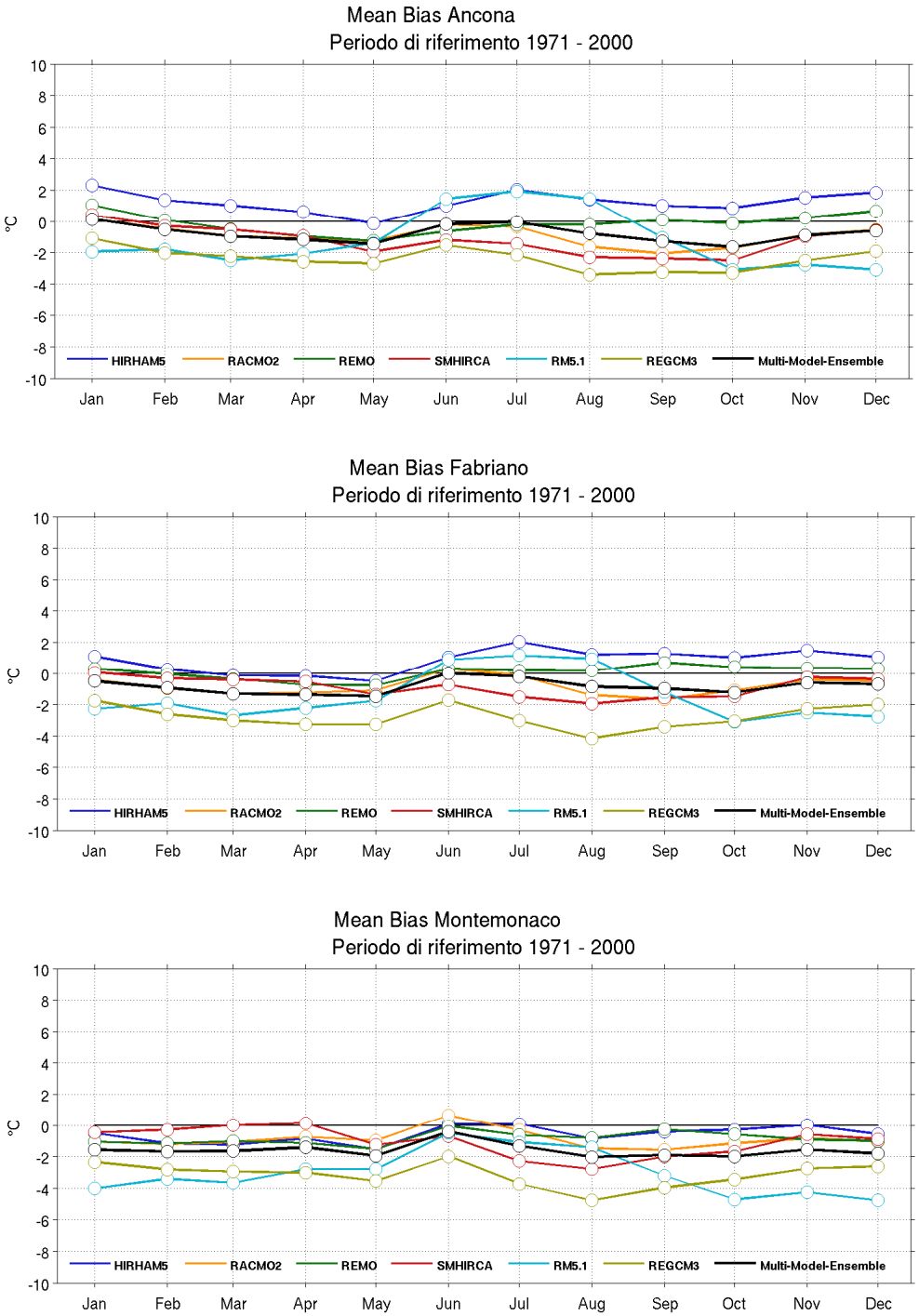

Figure 1.3. Monthly temperature Mean Bias (MB) for the three representative stations of Ancona (upper panel), Fabriano (central panel) and Montemonaco (lower panel) respectively representing coast, hill and mountain Marche region climatology.

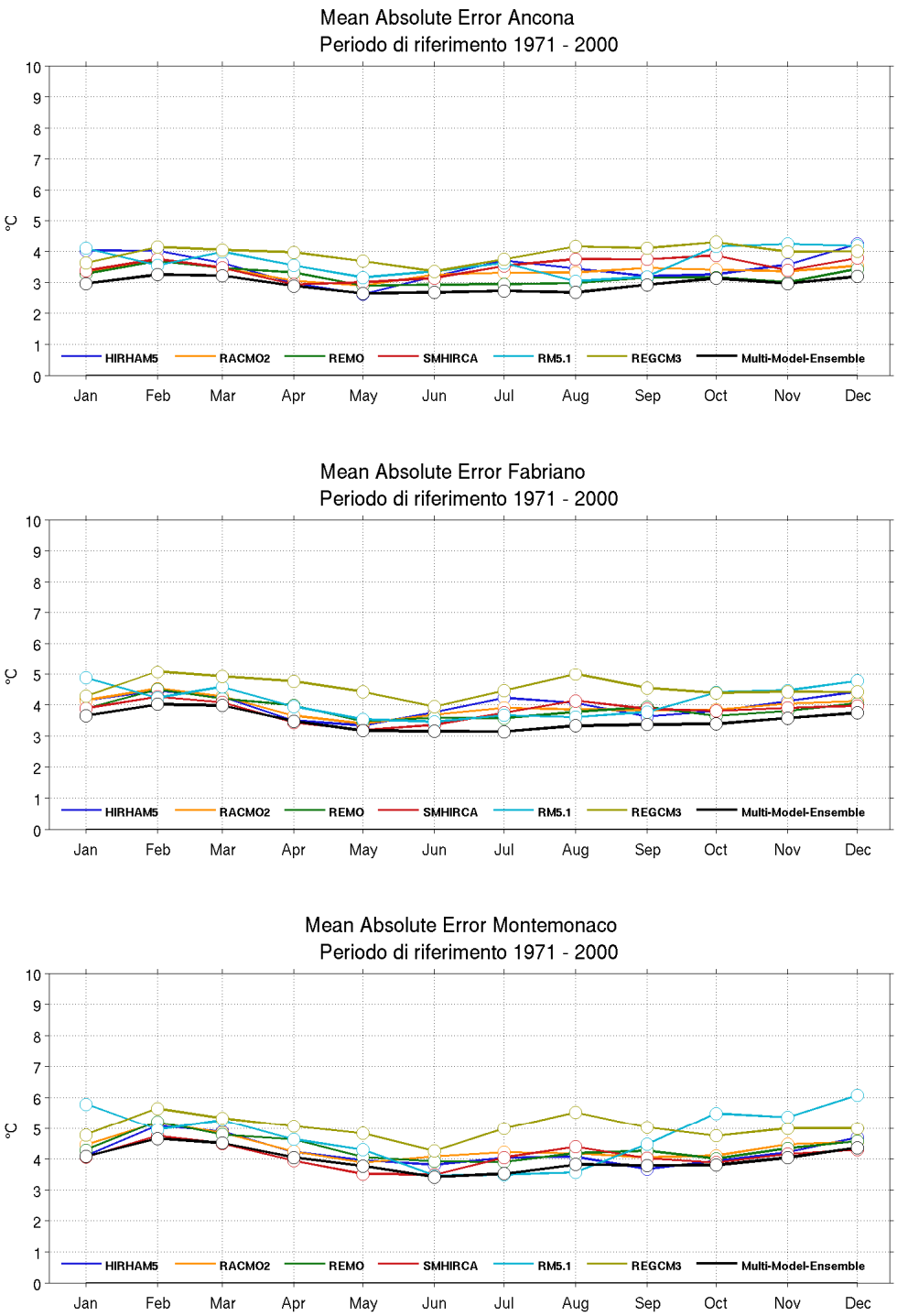

Figure 1.4. Monthly temperature Mean Absolute Error (MAE) for the three representative stations of Ancona (upper panel), Fabriano (central panel) and Montemonaco (lower panel) respectively representing coast, hill and mountain Marche region climatology.

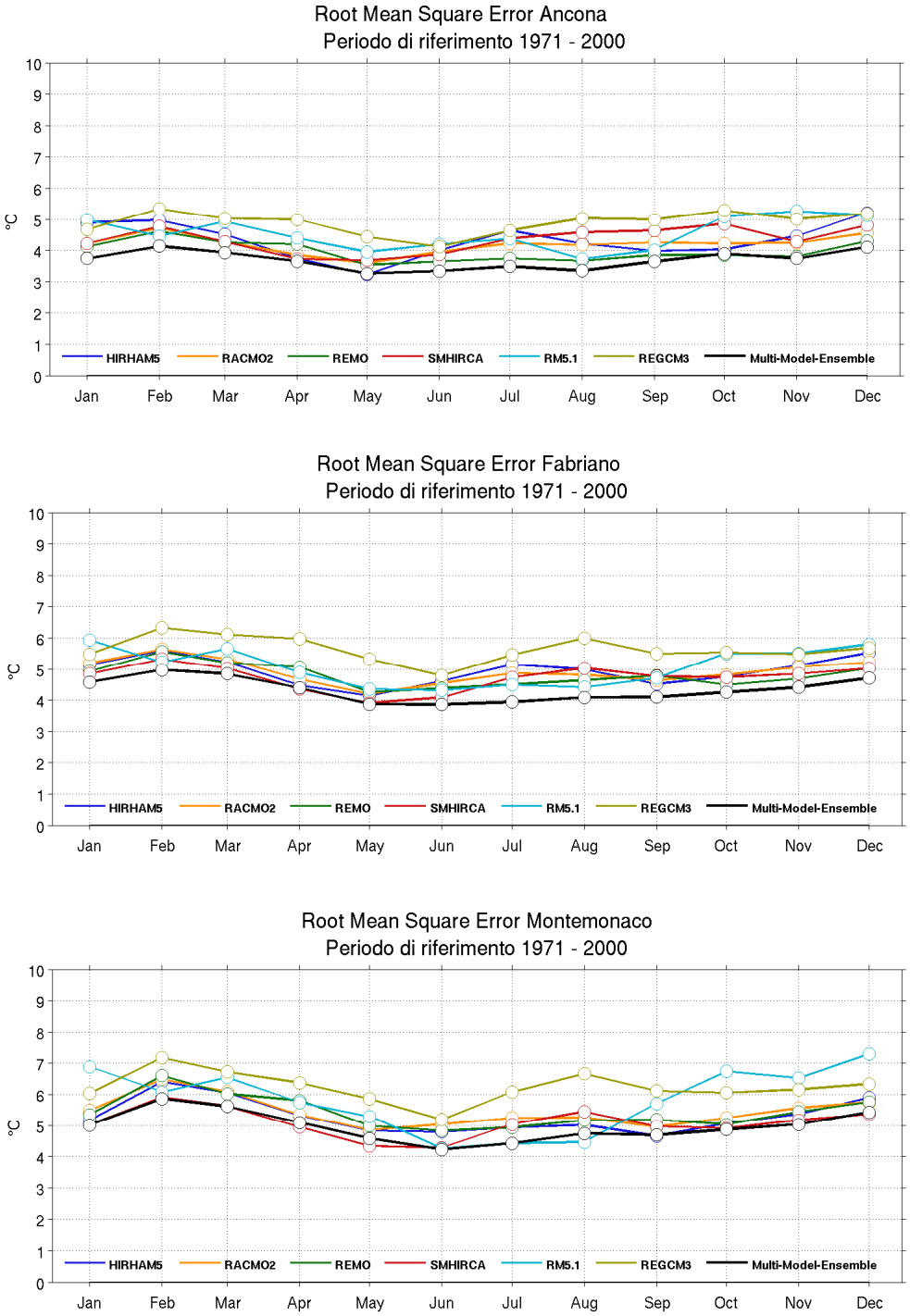

Figure 1.5. Monthly temperature Root Mean Square Error (RMSE) for the three representative stations of Ancona (upper panel), Fabriano (central panel) and Montemonaco (lower panel) respectively representing coast, hill and mountain Marche region climatology.

Figures from 1.3 to 1.5 report validation results corresponding respectively to MB, MAE and RMSE applied on daily temperature monthly averages for the period 1971-2000. For all the three tests, simulation monthly biases are reported in the y-axes in Celsius Degrees. Statistical tests are devoted to assess the capability of simulating temperature annual cycle over the past time segment over three representative morphological contexts (coast, hill and mountain). The three statistical tests underline two principal characteristic of temperature annual cycle bias. Firstly, it is noteworthy how the multi-model ensemble (black line) guaranties the nearest simulated value to the observation. This confirms the add value of using an ensemble approach in climate simulations. Secondly, how the simulation discrepancies follow the complexity of the territory. Minor biases resulted in simulation of valley-coast station temperature with increasing biases over hill and mountain stations. Concerning the annual cycle, higher biases resulted over intermediate season spring and autumn with an underestimation up to 2 °C (considering the MB). In the coast and hill stations summer-months temperature are almost perfectly simulated with MB close to zero.

Figures from 1.6 to 1.8 report evaluation of simulated monthly precipitation for three Marche region stations representing coast hill and mountain sectors. Biases are indicated in millimeter on the y-axes. Results show two interesting aspects: first climate simulations more than expected well reproduce hill and coast stations precipitation annual cycle. This also considering the effect of representativeness error that must be taken in account when an area-averaged value (simulation) is compared versus a point-scale observation. Precipitation MB for Pesaro and Jesi stations reports biases close to zero peaking to -1 mm for June and December months. Secondly, it is observable how performance of climate models decreases over mountain station of Bolognola (1000 m a.s.l.). It is noticeable how larger bias (negative bias, meaning an underestimation of precipitation over complex orography) affects spring and autumn months (up to 7 mm/month considering the MAE of the multi-model ensemble; black line). Reporting error physical values (mm) this fact is quite obvious since higher precipitation along these months are generally concentrated.

Precipitation

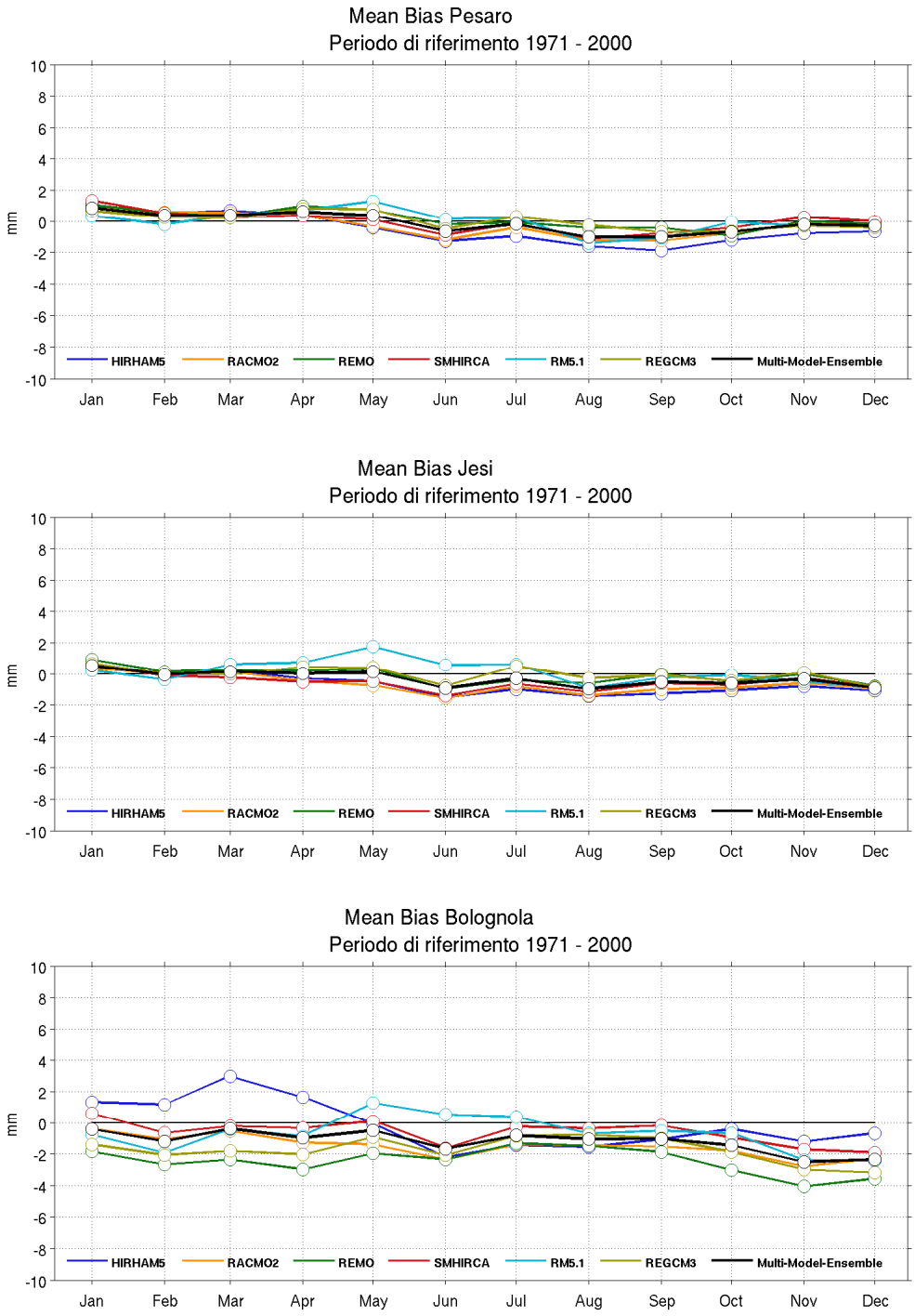

Figure 1.6. Monthly precipitation Mean Bias (MB) for the three representative stations of Pesaro (upper panel), Jesi (central panel) and Bolognola (lower panel) respectively representing coast, hill and mountain Marche region climatology.

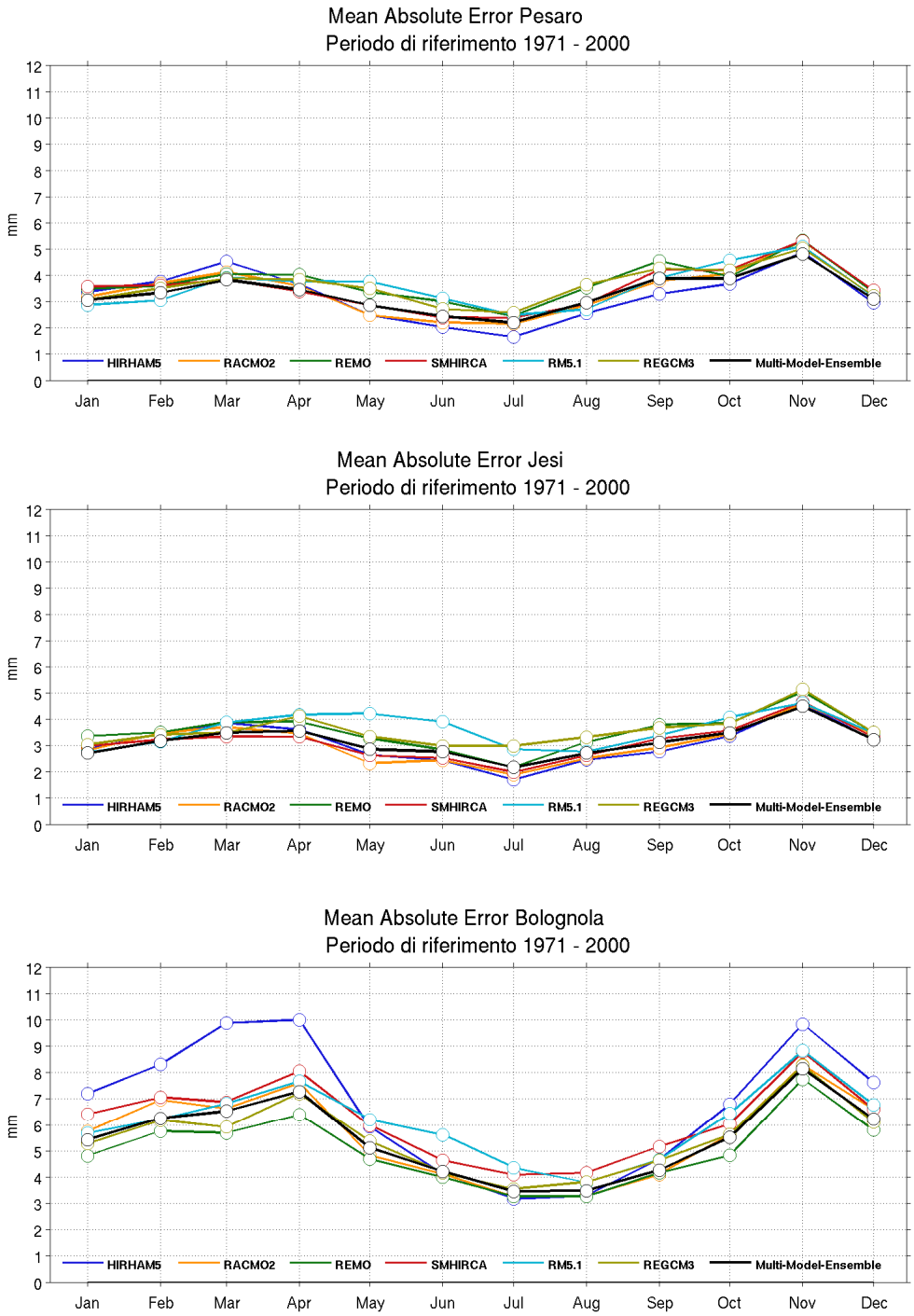

Figure 1.7. Monthly precipitation Mean Absolute Error (MAE) for the three representative stations of Pesaro (upper panel), Jesi (central panel) and Bolognola (lower panel) respectively representing coast, hill and mountain Marche region climatology.

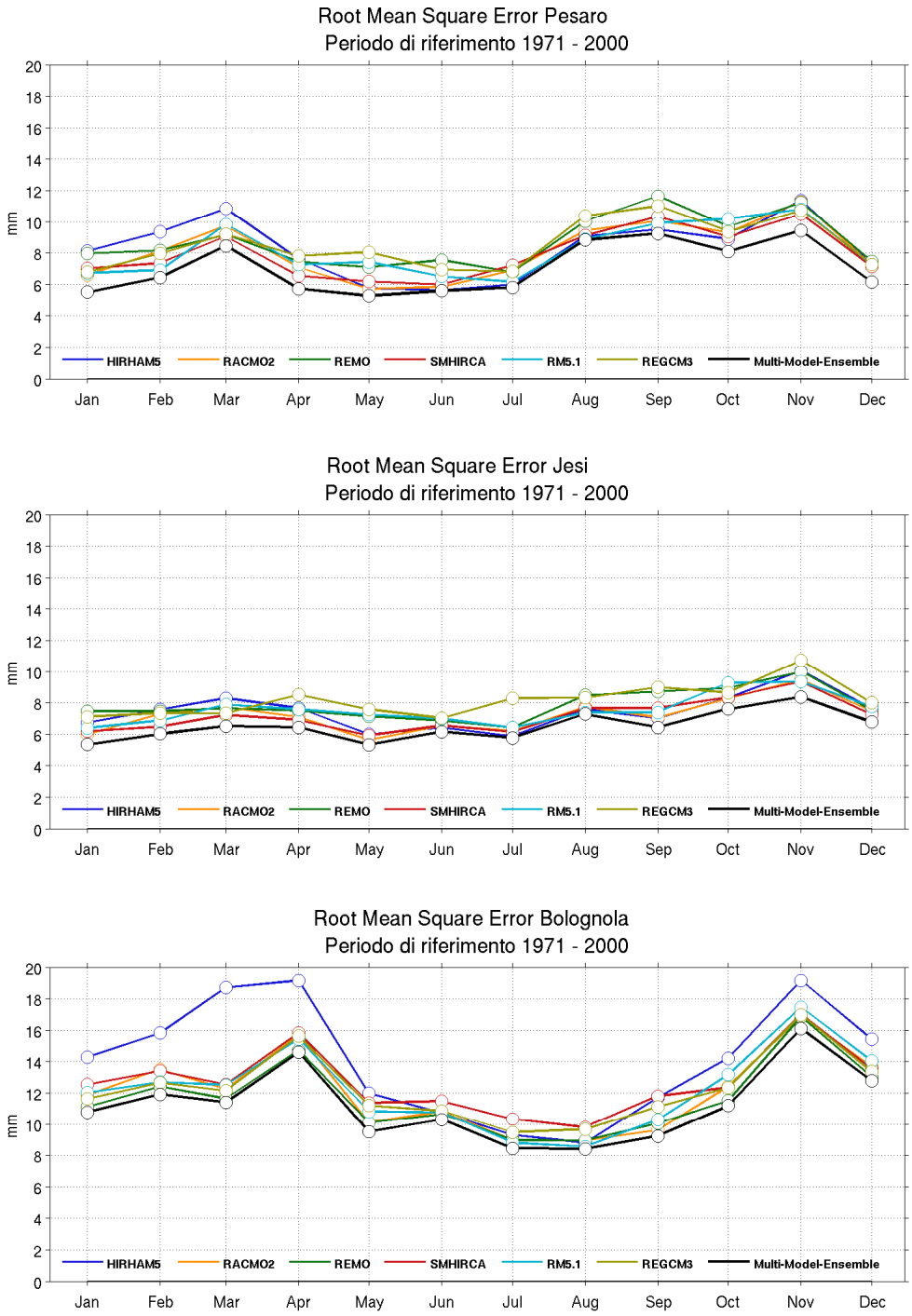

Figure 1.8. Monthly precipitation Root Mean Square Error (RMSE) for the three representative stations of Pesaro (upper panel), Jesi (central panel) and Bolognola (lower panel) respectively representing coast, hill and mountain Marche region climatology.

1.2.2 Climate Change Signal Assessment

Mean temperature

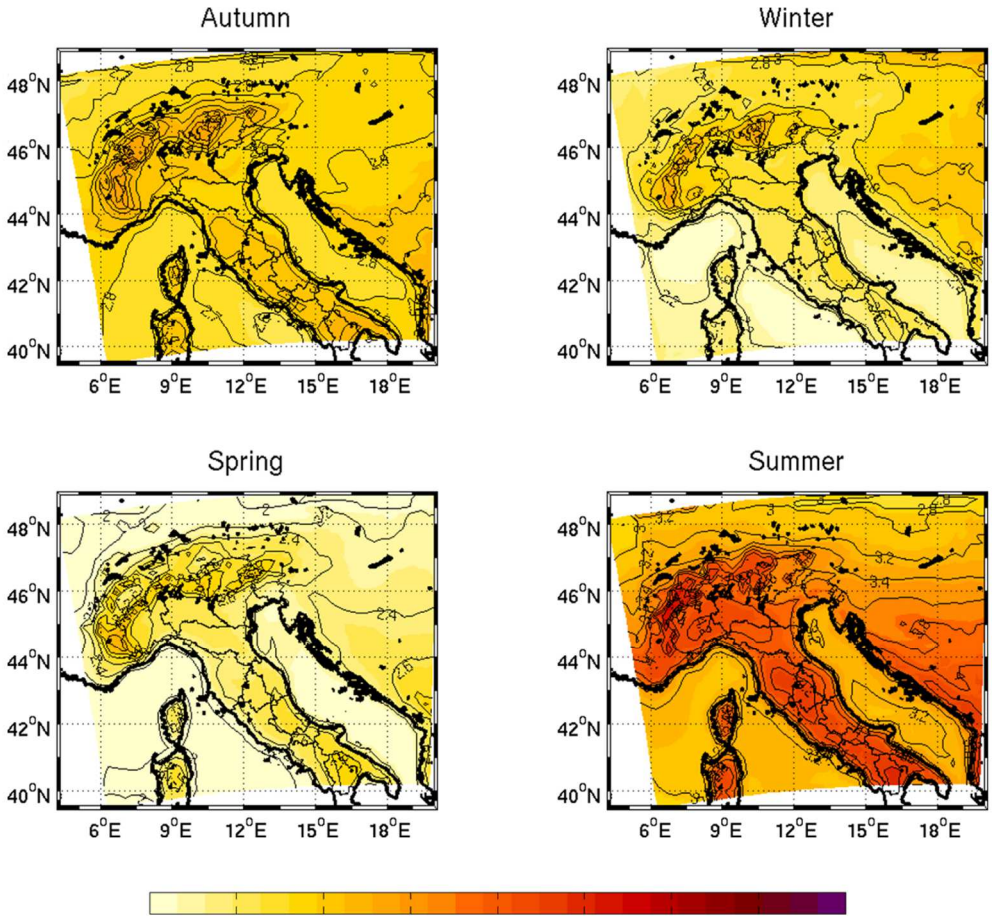

Figure 1.9. Multi-model ensemble seasonal mean temperature change (2061-2090 minus 1961-1990). Units are °C.

Figure 1.9 shows multi-model ensemble projections of seasonal mean temperature (tas hereafter) change over study area. Change signal consists on a projected anomaly computed for a future period (2061-2090) over the reference period (1961-1990). Seasonal change signal plots are built in order to characterize expected magnitude, seasonal cycle and spatial pattern of the expected changes. All the four seasons result affected by a warming signal ranging from ≈ 2.5 to 5 °C. Summer season signal stands out with higher increase up to 4 / 5 °C followed by autumn season (≈ 2.5 - 3 °C). Spatial patterns highlight Alpine region as the most affected by higher signal. Anomaly gap is mainly about +0.5 °C against surrounding areas in all seasons. Coastal areas in summer season show slight dampened signal down to

+4°C. Unsurprisingly higher seawater thermal capacity establish a sea-inland signal gradient. Conversely, a latitudinal gradient characterizes continental-climate part of the study area.

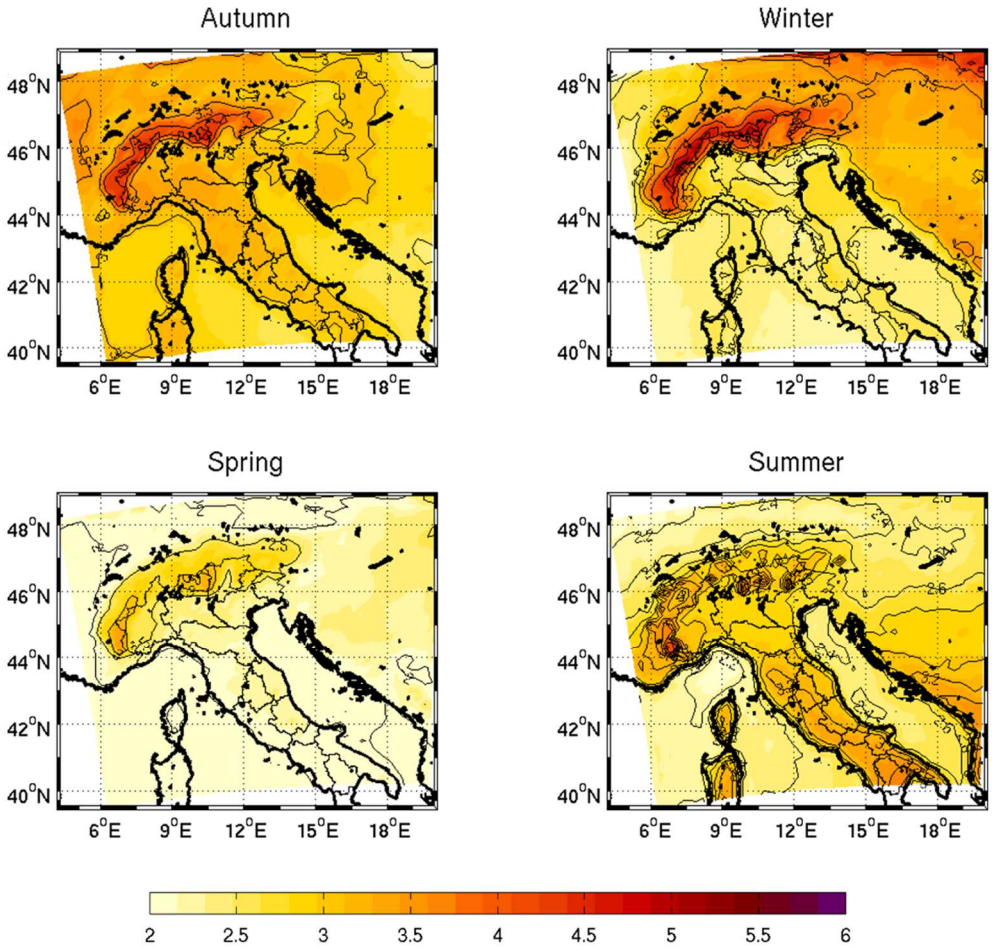

Figure 1.10. Multi-model ensemble seasonal mean temperature 5th percentile (tas05P) change (2061-2090 minus 1961-1990). Units are °C

Figure 1.10 reports signal referred to the left tail (5th percentile) of daily mean temperature distribution (tas05P hereafter). This analysis involves low frequency cold-day changes. As seen for the mean values, summer and autumn seasons result affected by major temperature increase (≈ 3-5.5 °C). Lower signal projected in spring and winter seasons ≈ +2 °C, only Alps stand out with higher signal (≈ +3 °C). Interestingly Alps show higher signal absolute value coupled to a relevant gap against surrounding lowlands mainly in autumn and spring seasons. This elevation-dependent warming signal confirms results from previous studies (Giorgi et al. 1997; Hall 2004; Kotlarski et al. 2012; Scherrer et al. 2012) where a decrease of the lapse-rate in a warmer climate was detected. The elevation-dependence of temperature

signal could be interpreted by means of two relevant mechanisms: (i) large-scale changes of environmental lapse rate and (ii) to more regional effects related to changes in snow cover. Regarding the former, theoretical considerations suggest that climate change will lead to a decrease of free-tropospheric lapse rates, i.e., the upper troposphere will warm stronger than the lower, ultimately because the moist adiabatic lapse rate decreases with temperature. Second mechanism, involves surface-atmosphere exchange processes consisting in the snow-albedo feedback: a shortening of the snow season will result in a lower surface albedo would potentially amplify a large-scale warming signal (Hall 2004; Scherrer et al. 2012; Kotlarski et al. 2012).

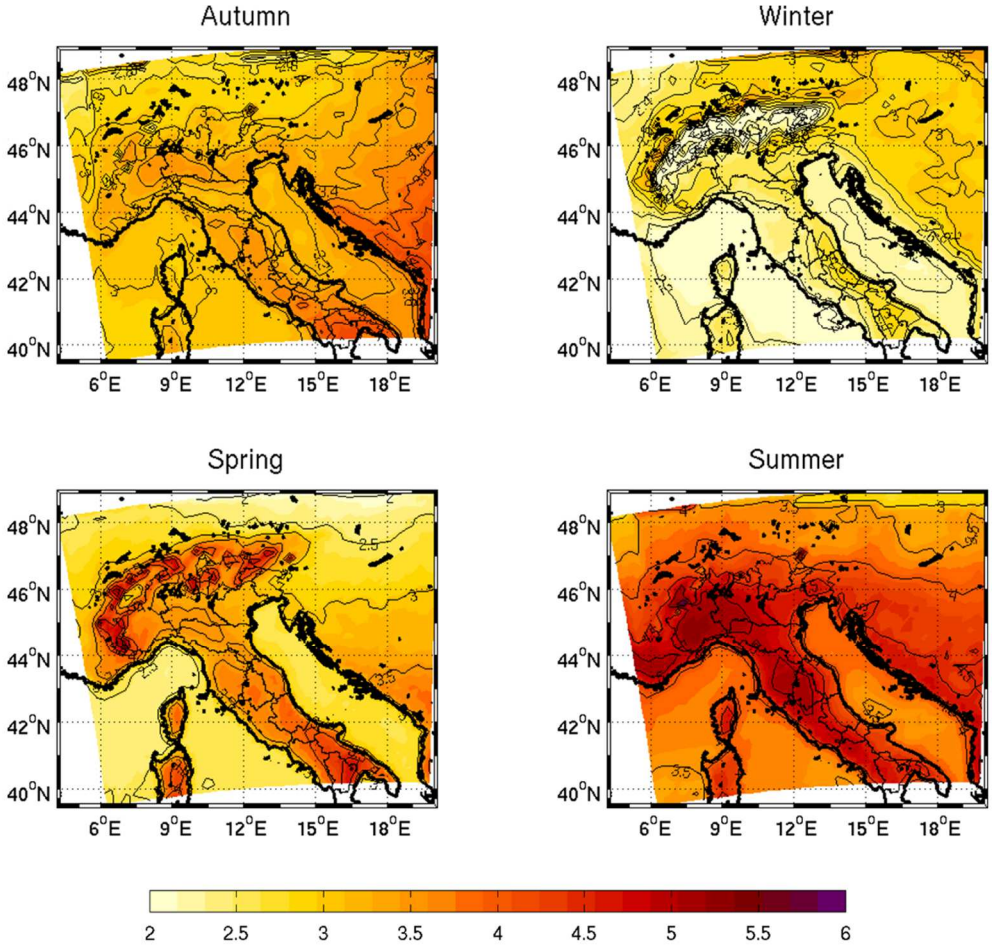

Figure 1.11. Multi-model ensemble seasonal mean temperature 95th percentile (tas95P) change (2061-2090 minus 1961-1990). Units are °C.

Changes over the right tail of daily mean temperature (tas95P hereafter) distribution in figure 1.9 are displayed. Signal over this distribution portion corresponds to changes over low frequency high daily mean temperature. Seasonal patterns of change indicates once

again summer season affected by higher positive temperature change (≈ 3.5-5.5 °C) followed by spring (≈ 3-5 °C), autumn (≈ 3-4 °C) and winter seasons (≈ 2-3 °C). Seasonal oscillation of tas95P signal roughly resembles what seen for daily mean temperature change, but with a higher magnitude of spring and summer signals. In these seasons, warming overcomes at least 1 °C mean values signal. Latitudinal gradient characterizes signal spatial patterns during autumn, spring and summer seasons, whit higher positive changes (≈ 1 °C) over southern part of domain. Moderate spatial heterogeneity involves winter season. Alpine region presents signal up to 1 °C lesser in winter and higher, coupled to the southern Italy, in spring. The limited temperature signal over Alps is plausible considering soil-atmosphere feedback, coupling temperature with precipitation change signal (see next section). Detected higher winter precipitation over Alps would lead to wetter soils, which in turn increase moisture flux due to evapotranspiration into the atmosphere. This results in increased humidity and potentially to cloud formation creating a positive feedback loop (Gobiet et al. 2014).

Minimum temperature

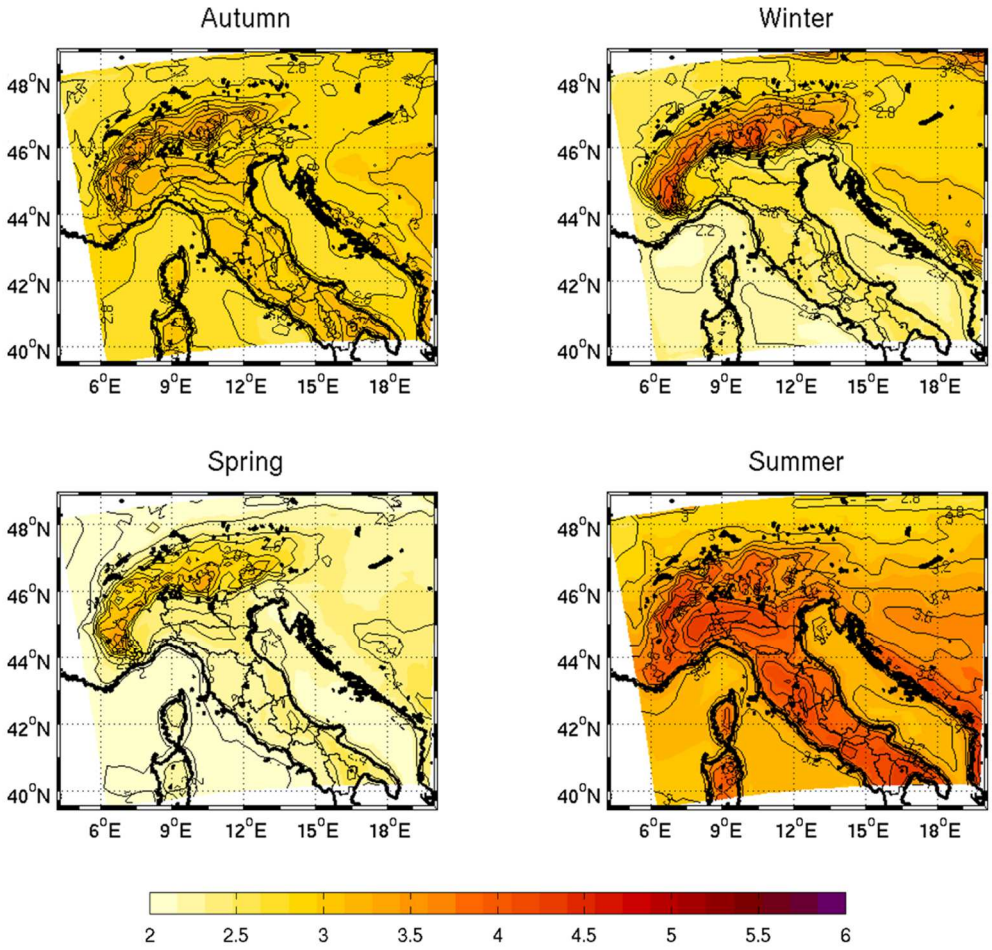

Figure 1.12. Multi-model ensemble seasonal minimum temperature (tmin) change (2061-2090 minus 1961-1990). Units are °C.

As expected, projected changes of minimum daily temperature (tmin hereafter, figure 1.12) resulted connected with mean temperature having similar magnitude, seasonal and spatial patterns (figure 1.9). Summer is confirmed the most affected season by stronger warming signal (≈ 4 °C), followed by autumn and winter seasons (≈ 2.5-3 °C). It is worth noting an even larger elevation-dependence of change signal compared to mean temperature signal. Elevation-dependency is relevant in winter and spring seasons and particularly evident over the left tail of the variable distribution (tmin05P hereafter), as shown in figure 1.13.

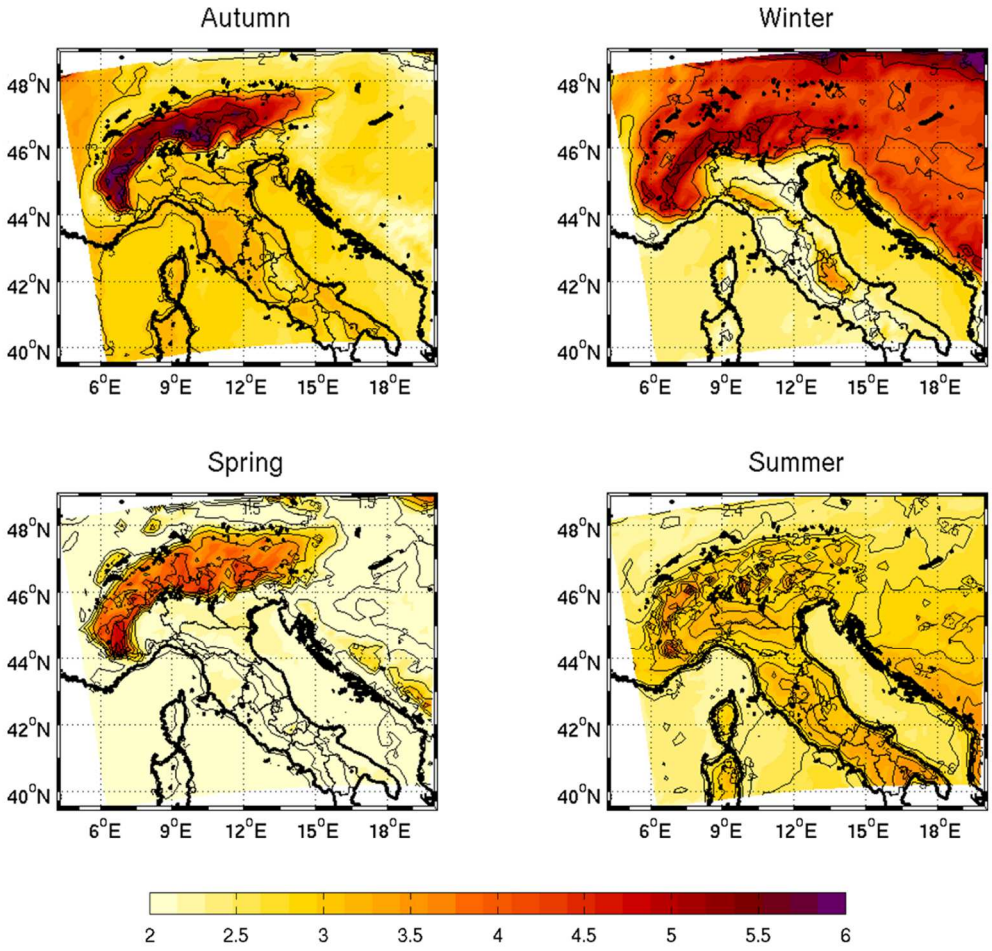

Figure 1.13. . Multi-model ensemble seasonal minimum temperature 5th percentile (tmin05P) change (2061-2090 minus 1961-1990). Units are °C.

Tmin05P could be considered as the change signature of cold-temperature extreme. In this particular assessment, an exacerbation of the aforementioned signal elevation-dependence can be noted. Seasonal analysis reports autumn season warming signal affecting particularly Alps (≈ 5.5-6 °C). The rest of Italy displays positive anomalies between ≈ 3 and 3.5 °C. In winter, at least twice as warming signal is present in correspondence of mountainous areas of Alps, Appennines and continental areas (up to 5.5 °C). In these areas, characterized by a winter lasting snow cover, the lack of albedo effect consistently dampens cold-extremes. Similar spatial pattern results for spring season but with lower signal magnitude. Here, signal does not exceed +2.5 °C except over Alpine region affected by a signal of +4 °C. Coherently, summer is the only season to present spatial homogeneous signal distribution, ranging from ≈ 2.5-3.5 °C.

Maximum temperature

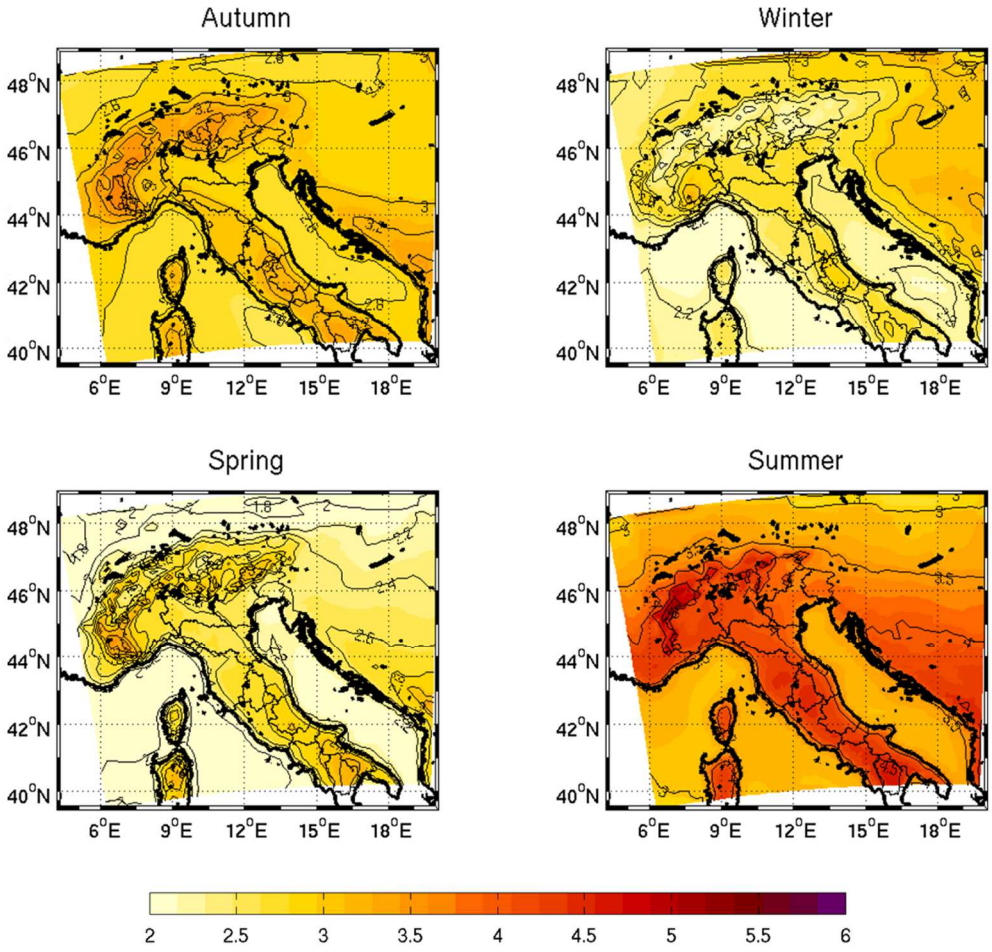

Figure 1.14. Multi-model ensemble seasonal mean maximum temperature (tmax) change (2061-2090 minus 1961-1990). Units are °C.

In figure 1.14 results for mean seasonal maximum temperature (tmax hereafter) are reported. As shown for the mean temperature (figure 1.7), tmax changes result ranging from ≈ 2.5 to 3.5 °C during autumn, winter and spring season. Summer season shows a higher warming signal up to ≈ 4.5 °C. Alpine region stands slightly out in winter and springtime while in summer season shows warming signal dipole, where Alps and inner-southern area show higher warming signal up to 4.5 °C. Some decimal degrees less is the warming signal characterizing the center and northern part of Italy. As noted in Goubanova and Li (2007) and Beniston et al (2007), we can further observe that changes in seasonal mean tmax and tmin have similar magnitudes. However, the signal of tmax results slightly higher than relative tmin signal during spring and summer seasons.

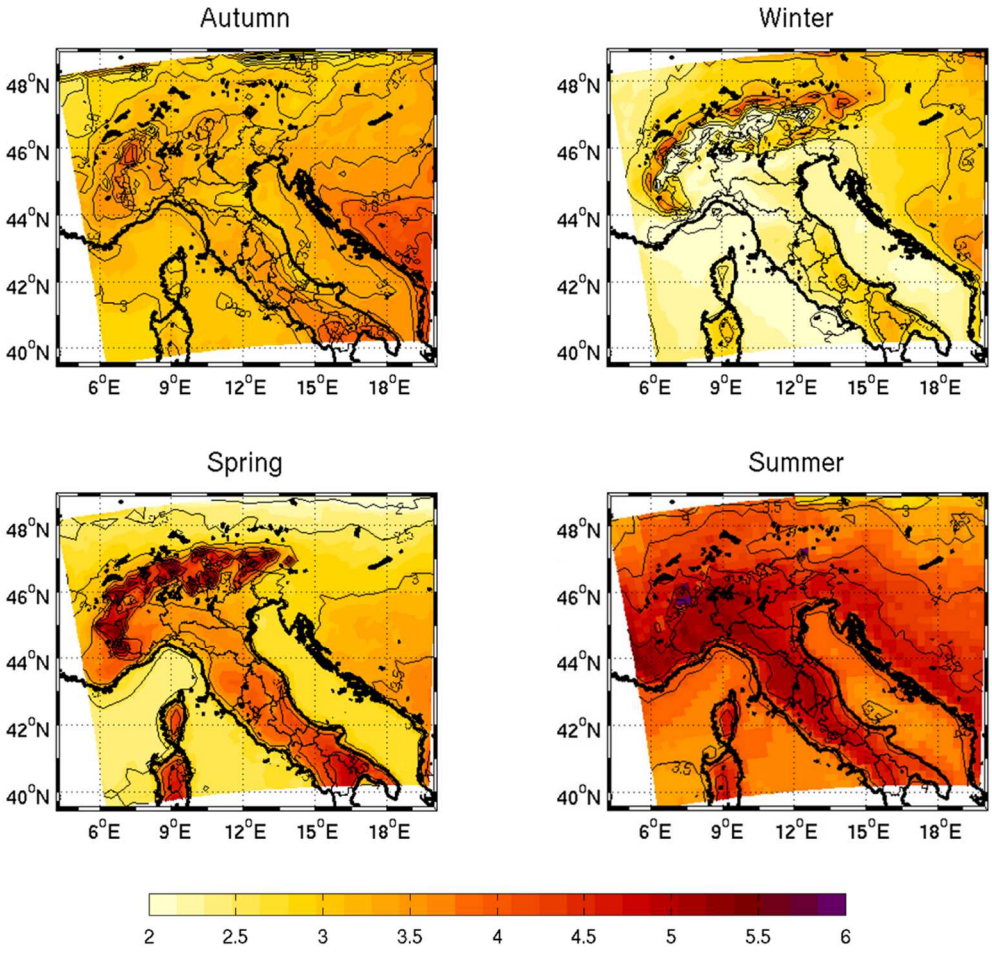

Figure 1.15. Multi-model ensemble seasonal maximum temperature 95th percentile (tmax95P) change (2061-2090 minus 1961-1990). Units are °C.

In Mediterranean climate context, one of the most interesting and high-impacting aspect of future climate regards extreme high temperature. Anomalous warm months or seasons in the last 1-2 decades of the observational record have prompted in many publications to explore and explain these events (Schär et al. 2004; Beniston et al. 2007; Gobiet et al. 2014). Feedbacks between soil-moisture deficits and heat-waves have recently attracted much interest as an explanatory causal mechanism (Vautard et al. 2013). It has been observed the northward shift of drought that originate in the Mediterranean during winter, yields preconditions capable of triggering intense and persistent heat waves in Europe (Gobiet et al. 2014) as already experienced in 2003 and 2007 droughts (Ciais et al. 2005; Tolika et al. 2009). In this study, extreme high temperature expected changes were inspected considering the seasonal 95th percentile of daily maximum temperature (tmax95P hereafter) future change. Changes tmax95P well agree with changes in tmax but showing greater absolute value. As reported for mean and minimum temperature the right tail distribution exhibits a

higher signal compared to mean value excluding winter season. Spring and summer seasons confirm strong signal ranging from 3.5 to more than 5.5 °C. In summer season hot-extremes signal shows higher values over inner-central part and north-western Italy. Longitudinal gradient characterizes eastern Italy with lower positive anomalies of ≈ 1 °C than the western part. Winter season shows least increasing in tmax95P. In Padana valley and south side of Alps a signal lower than 2 °C is projected.

Mean precipitation

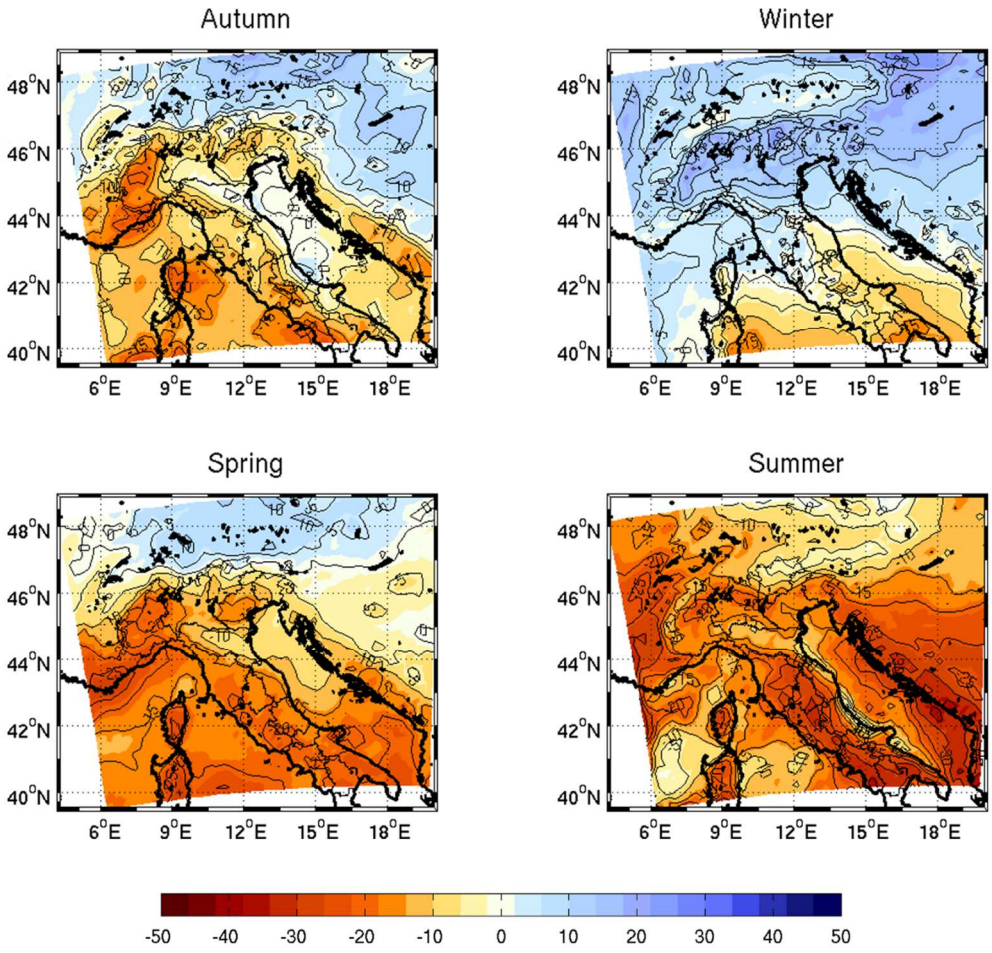

Figure 1.16. Multi-model ensemble mean seasonal precipitation (pr) change (2061-2090 minus 1961-1990). Units are %.

Mean precipitation change (pr, figure. 1.16) presents relevant seasonal and spatial patterns oscillations. Autumn season shows moderate drying signal mainly on western Italy peaking over northwest and Campania region (≈ -30%). Padana valley and Adriatic coast resulted characterized by a close to zero signal while western Italy shows general higher negative signal. In autumn and especially in winter, precipitation change signal over the Peninsula presents a dipolar pattern with an increase in the northern regions (up to 25%) and a decrease in the southern ones (10-15%). Moreover, differently from what resulted in autumn, winter signal shows east-west gradient across the Appennines of central Italy. In the future climate we expect an increase in low-level westerly winds, which tends to produce more precipitation in the upwind (western) side of the Appennines (Coppola and Giorgi 2010). Spring season

shows from moderate to high (-10 up to -30%) negative precipitation change signal over Italy. Interestingly, spring pattern largely resemble those presented in autumn season but shifted toward higher negative signal. A latitudinal and slight longitudinal gradient is indeed resulted. In summer, whole domain results affected by drying signal, though different spatial pattern exists. Lower signal has been found in the Adriatic coast while the higher in correspondence of inner-southern part of domain. Signal varies from -10% to -40%. Discussing precipitation results, it is noteworthy the strong latitudinal gradient affecting autumn and especially winter precipitation signal. From figure 1.16, it is noticeable how expected northward displacement of Atlantic storm-track would be greater in spring and summer and weaker in autumn and winter seasons. Autumn and winter precipitation are generally anti-correlated with NAO phase, where the last decades decreased autumn-winter precipitation resulted from an anomalous lasting NAO positive-phase (Giorgi and Lionello 2008). In fact, oscillation in such large-scale atmospheric mode has been observed to largely affect the entire Mediterranean precipitation regime especially in winter, significantly altering zonal storm track intensity and cyclonic activity. In turn, NAO and the principal north-hemisphere large-scale atmospheric circulation modes, present evident connection and response to Arctic sea-ice extension and its current massive retreat. (Trigo et al. 2002; Seierstad and Bader 2009; Overland and Wang 2010). Concerning Mediterranean region and Italy, different authors project different NAO future responses. A reduction of mid-latitude storminess and winter (especially in march) coherent with a negative NAO phase was found by Seierstad and Bader (2009) for the end 21st century. More specifically for Mediterranean basin, Grassi et al. (2013) highlighted dynamical mechanisms connecting Arctic sea-ice loss with negative Arctic Oscillation (AO), closely related to NAO, leading to wetter winter season. Conversely Giorgi and Lionello (2008) suggest a projected shift toward NAO positive phase and a related decrease of precipitation over central and southern Italy also in autumn and winter seasons. At this regard, Giorgi and Coppola (2007), detected in north Italy latitude a sort of borderline between drier (southward) and positive (northward) signal identifying this particular pattern as “European Climate change Oscillation”. Concerning spring and summer precipitation change signal, resulting severe negative signal accord to an increase of anticyclonic condition expected over the Mediterranean basin (Gao and Giorgi 2008; Giorgi and Lionello 2008). The central and southern part of the basin especially in summer would be under the influence of the dry descending branch of the Hadley cell. As hypothesized for the mid-latitude Atlantic storm track, also the Hadley is expected

undergoing to higher latitude expansion (Planton et al. 2012; Xoplaki et al. 2012) extending sub-tropical arid conditions over the greater part of Mediterranean region. . Lu et al. (2007) analyzing markers of Hadley cell edges, found a robust weakening and poleward expansion in simulations of the 21st century climate. The baroclinic instability of Mediterranean latitude would be suppressed by an increase of stability in subtropical latitudes, allowing thermally-drive cell to reach higher extratropical latitudes.

Extreme precipitation

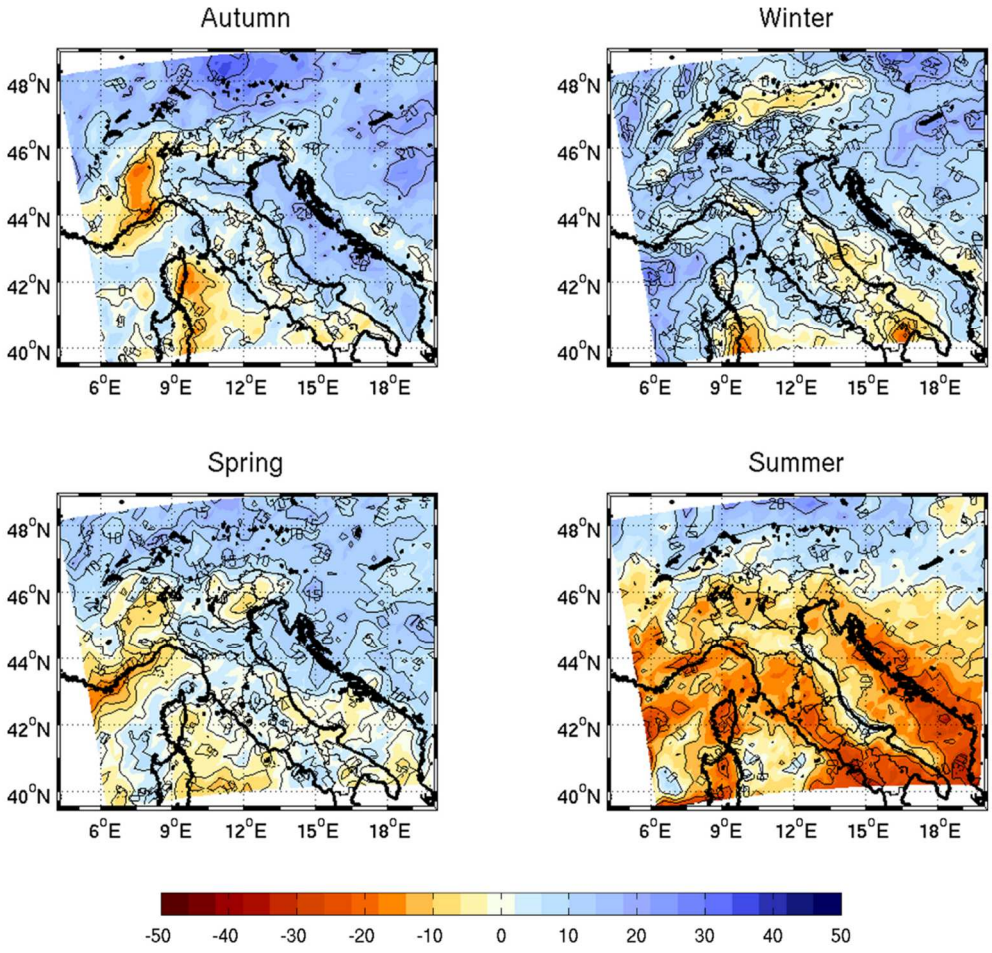

Figure 1.17. Multi-model ensemble seasonal precipitation 99th percentile (pr99P) change (2061-2090 minus 1961-1990). Units are %.

As stated for temperatures, also for precipitation is essential to assess expected changes over impact-relevant events. The right tail of daily cumulated precipitation distribution (99th percentile of the seasonal precipitation distribution, hereafter pr99P) identifies these particularly high precipitation events. This kind of precipitation events have deep impacts on exposed infrastructures with serious socio-economic repercussions. Given the climatic context of Mediterranean basin, particular severe precipitation events can make up the large portion of the total precipitation (Hertig et al. 2014). Also for precipitation, a skewed change signal resulted, with high-percentile precipitation varying differently from mean events (figure 1.17). Spatial patterns of changes roughly resemble those seen for mean precipitation though scattered spatial heterogeneity and weaker seasonal oscillation resulted. What is noteworthy is a shift toward wetter signal compared to the mean. In the greatest part of domain and in all the seasons (especially autumn and spring transition seasons) we assist either to an important reduction of the negative anomalies and to larger positive change signal (i.e. northern part of domain). In autumn and spring seasons, we note null or slight positive anomaly also in the south of domain, regions where mean precipitation was resulted strongly decrease. Autumn and winter are expected the most affected by increasing in intensity of extreme precipitation events. 99th percentile change signal shows peaks of +30% over the northernmost part of domain. Even though on a general increase of autumn and winter extreme events, some localized negative signal resulted. Is the case of north side of Alps (in winter) and northwest Italy (in autumn) that shows drying signal in both mean and extreme precipitation. Changes resulted for Alpine region are in good agreement with a recent studies (Rajczak et al. 2013; Gobiet et al. 2014) that have assessed projected changes in Alpine precipitation in larger detail. Focusing on summer season, the most drought-prone season, over western part of Italy and western side of Dynaric Alps a relevant decrease of -20% is resulted. Concerning high-percentile signal, it is interesting to note how also in summer are present positive signal. At this regard, Alps act as borderline between negative (southward) and positive (northward) changes. The entire Alpine region resulted interested by increase in summer precipitation 99th percentile signal up to 20%.

Assessment of changes in magnitude and frequency of heavy and extreme precipitation events and more in general of hydrological cycle changes represent one of the most challenging aspect for climate change science. The interpretation of linkages between changes in the large-scale atmospheric modes (Trigo et al. 2002; Trigo 2006; Toreti et al. 2010; Xoplaki et al. 2012), and local precipitation evolution remain still uncertain. Moreover,

specifically for changes in extreme precipitation a relevant role is played by the interaction between thermodynamic (i.e. Clausius-Clapeyron low) end dynamic processes (Palmer 2013; Allen & Ingram 2002; Allan & Soden 2008) coupled to the relevant role played by complex morphological conditions.

1.2.3 Inter-seasonal variability change

Temperature

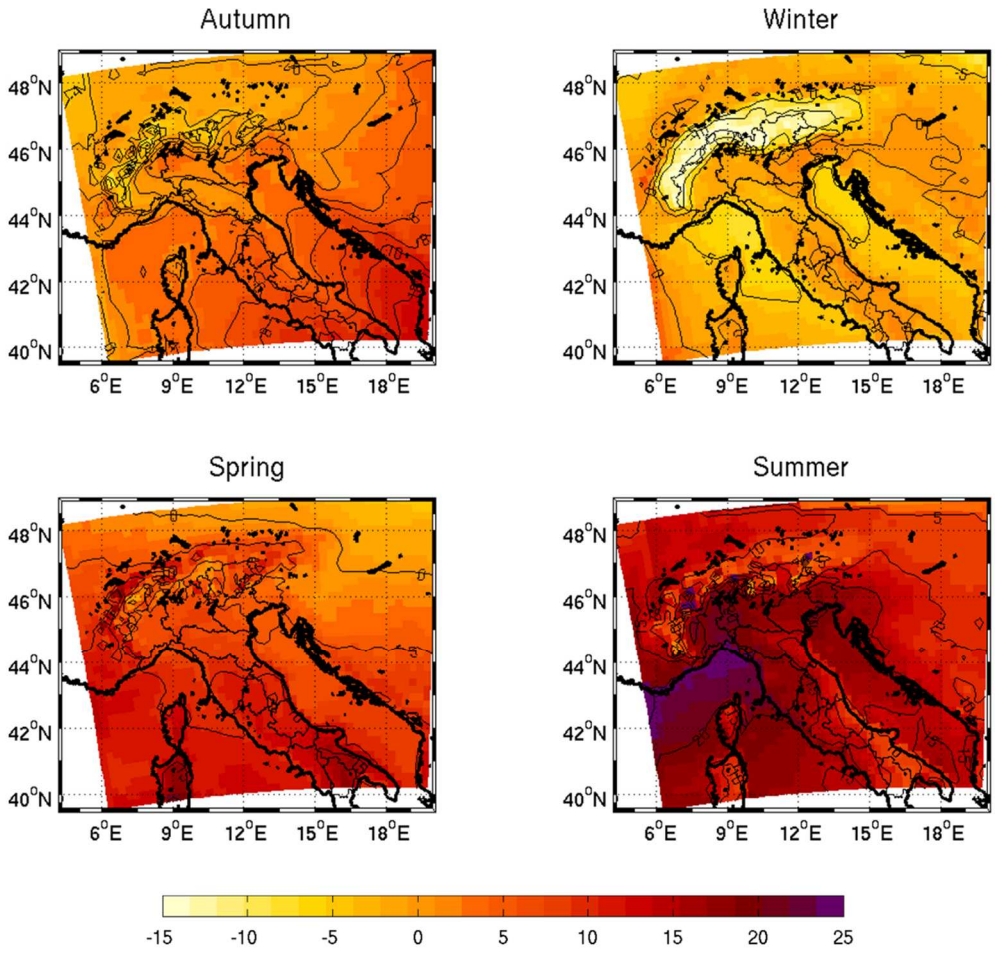

Figure 1.18. Multi-model ensemble seasonal temperature inter-annual variability change (2061-2090 minus 1961-1990). Values are expressed as percentage of the reference period (1961-1990).

One of the metric for assessing future asymmetry of temperature changes, namely a higher signal affecting extreme values respect to the mean is represented by inter-annual variability. Inter-annual variability indicates the oscillation of climate conditions year by year. It could be idealized as the dispersion of variable values around a time series linear interpolation or the stretching of related Probability Density Function (PDF). As expected, change signal (here shown in percentage [%] of standard deviation change between the two time segments) of seasonal inter-annual variability roughly follows mean temperature changes, though with substantial distinctions. Summer season characterized by the highest mean change signal shows also highest change signal in inter-seasonal variability up to 25% (over northern

Tirrenian Sea). The greater signal of the warm seasons (spring and summer) could be attributed, at least partially, to an enhancement of soil moisture-temperature feedbacks (Coppola and Giorgi 2010) exacerbating heatwaves magnitude. For what concerns spatial pattern, autumn and spring seasons show a slight latitudinal gradient with a small negative signal over northernmost area and a positive one (up to + 15%) in the southernmost area. Winter season signal stands out over the Alps in winter. This reduction over Alps is connected to the relative significant cold-temperature warming (see figures. 1.10, 1.12 and 1.13). Again, we underline the relevant effect of the reduction in snow cover, and resulting reduce effectiveness of the snow-albedo feedback mechanism (Giorgi and Lionello 2008). Greater warming of cold (tas05P, figure 1.10) and extreme-cold days (tmin05P, figure 1.13) compared with those affecting mean temperature, leads a decreasing variance of future daily temperature. Not subjected to such cold-temperature warming, the rest of study area does not show relevant changes over winter inter-seasonal variability.

Precipitation

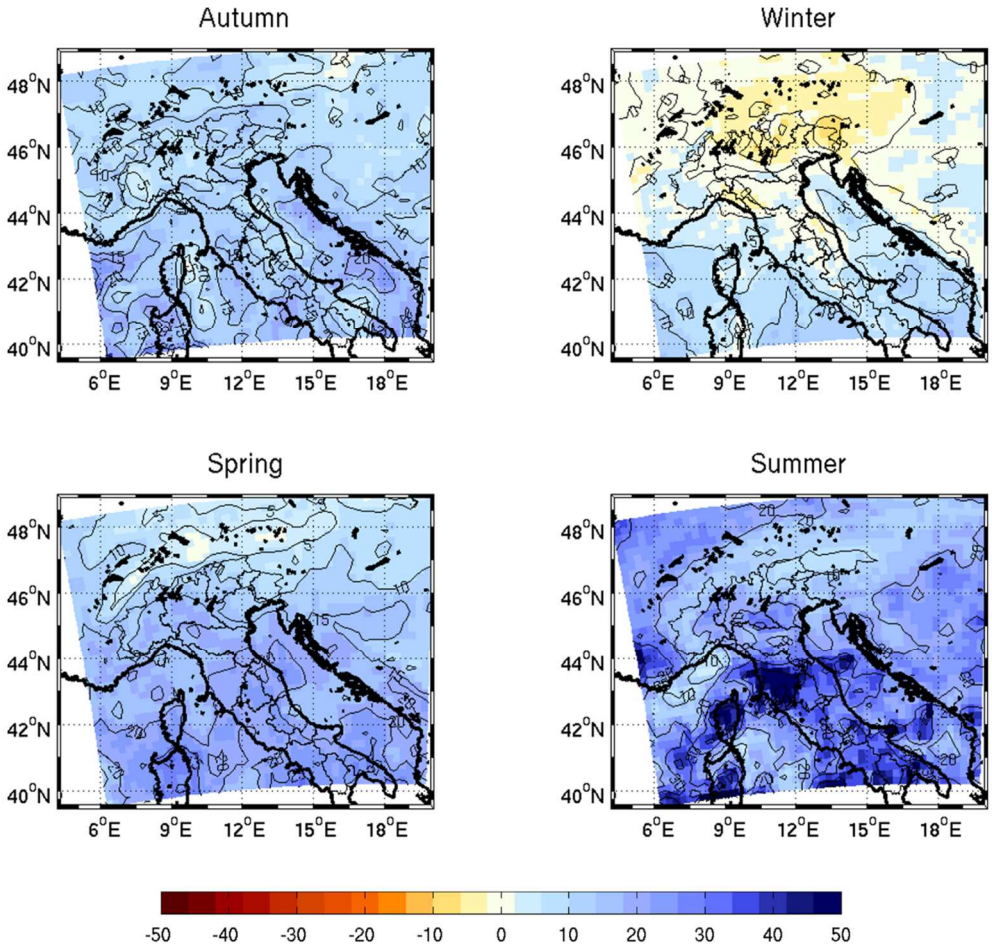

Figure 1.19. Multi-model ensemble seasonal precipitation Coefficient of Variance (COV) change (2061-2090 minus 1961-1990). Values are expressed as percentage of the reference period (1961-1990).

Another relevant aspect of future precipitation is represented by the seasonal inter-annual variability, reflecting an year by year oscillation of precipitation (Fatichi et al. 2012). Future change over inter-seasonal oscillation of the precipitation is inferred by the change signal affecting the Coefficient of Variance (COV, standard deviation normalized by mean value) (Coppola and Giorgi 2010). Figure 1.19 reports a general increase of inter-annual variability over all domain and all the seasons excluding winter. As for temperature, precipitation inter-seasonal variability signal results substantially related with the mean value changes. Autumn and spring inter-seasonal variability signal shows an increase over all domain (up to + 30%). Summer season shows an intense inter-annual variability increase. In fact, the severe decrease in mean daily cumulated precipitation (figure 1.16) does not match an equivalent-

magnitude change over extreme precipitation (figure 1.17). This leads to a larger future precipitation variance. Increase that appears consistent with the expected intensification of hydrological cycle under warmer conditions (Giorgi and Lionello 2008). Longer recharge time to get local saturation conditions would be required coupled to a higher intensity precipitation events. Winter season inter-annual variability shows a characteristic change signal. Compared to the other seasons, smaller changes have been resulted all over the domain. Slight increase (decrease) signal and on central-southern (northern) domain was obtained. According to what inferred from mean changes winter season will be characterized by wetter condition over Alpine and northernmost domain areas. Finally, it is likely that during summer the increase in temperature and precipitation variability are coupled to each other, as clear sky (rainy conditions) are associated with higher (lower) insolation and higher (lower) temperature.

1.2.4 Mapping inter-model agreement on future climate projections

Agreement over statistical significance of temperature change

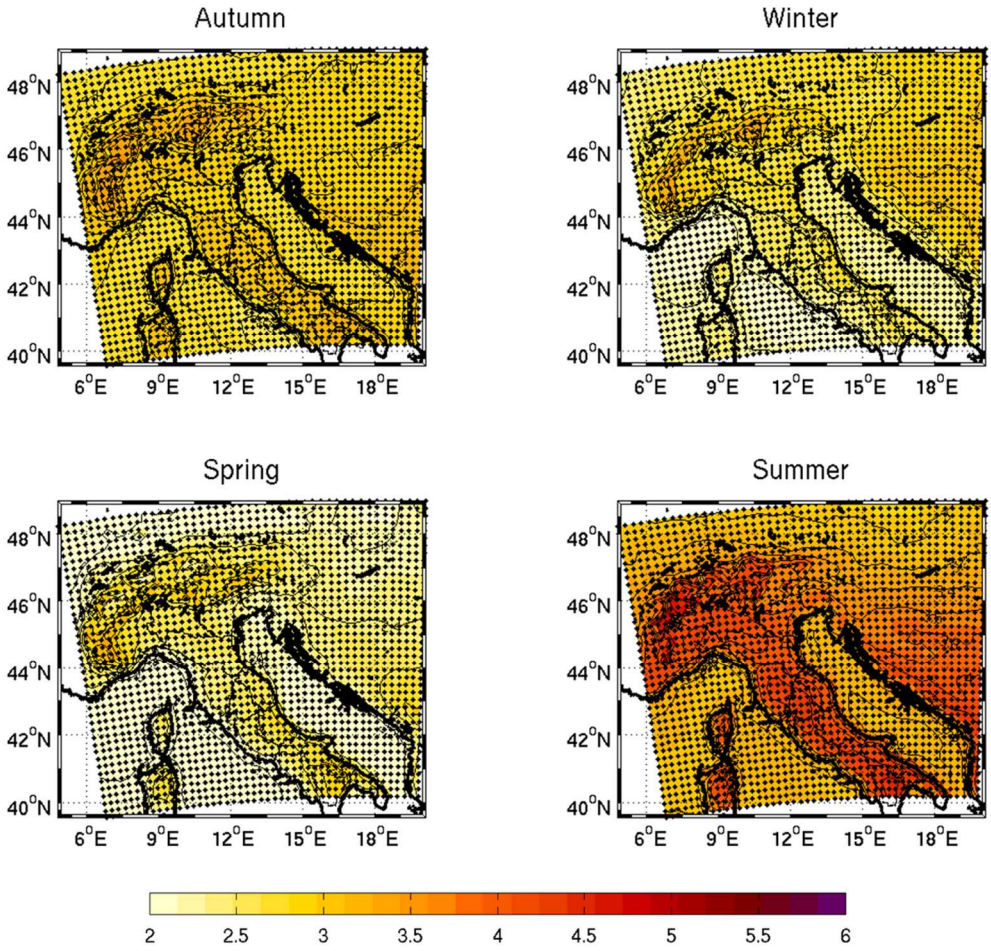

Figure 1.20. Two-layered maps representing signal and inter-model agreement over statistical significance of climate change signal.
Dotes denote areas characterized by the 100% of the models agreement on the mean temperature change statistical significance (t-test).

Figure 1.20 shows results for the metric proposed by Tebaldi et al. (2011), that maps inter-model agreement on the significance of temperature change. This double-layer representation (signal + level of significance agreement) allows allocating signal robustness or uncertainty. Black squares are present when the totality RCMs agreed over significant (t-test) change over a specific grid point. Results show that the mean temperature signal is significant for all RCMs in each grid point in all the four seasons.

Agreement over sign of precipitation change

For what concerns precipitation, higher inter-annual variability noise, makes detection of a clear change signal more complex. (Hawkins and Sutton 2009; Tebaldi et al. 2011). This intrinsic characteristic of precipitation variable makes more difficult to detect robust signal emerging from the internal variability noise (Deser et al. 2012). This particular condition could potentially bring to misleading conclusions. Indeed, especially for precipitation, level of agreement among ensemble members deserve considerable importance. To dial with inter-model agreement over precipitation projection, two different metrics have been employed. Both metrics were performed according to two different agreement-level threshold (66 and 100% of models agreement). Moreover, to provide comprehensive results the two metrics have been applied over both seasonal and annual basis signal. Figure 1.21 indicates grid nodes where the majority (>= 66% at least 4 out 6 RCMs) of ensemble members agrees on change sign. On annual basis (*a* panel), majority of models agree on the drying signal not only over southern Italy but also over the northwest sector. Consistent inter-model agreement has also resulted over the moderate wetter signal of the northernmost (north of Alps) part. As expected in the correspondence of transitional change sign we did not get consistent agreement (less than 4 RCMs out 6). In this transition latitudinal band, signal was characterized by very low values, (either positive or negative) such that change-sign can vary model by model (e.g. central Adriatic Sea). In general, low and uncertain change has been found over sea grid points, where models physical parameterization differences could play a relevant role. Also on a seasonal basis, central-northern Adriatic coast is characterized by a low change signal coupled to a lack models agreement, mainly in autumn. Lack of models agreement has also found in correspondence of the latitudinal sign-transition zone (roughly 43.5 °N) in winter. Spring and summer seasons are characterized by larger agreement. In general, to uncertain sign change areas correspond a low change signal (± 5%) indicating low signal robustness. As previously stated, on annual basis, the Alpine region latitude marks a neutral-sign border where northward a positive and southward a negative signal resulted.

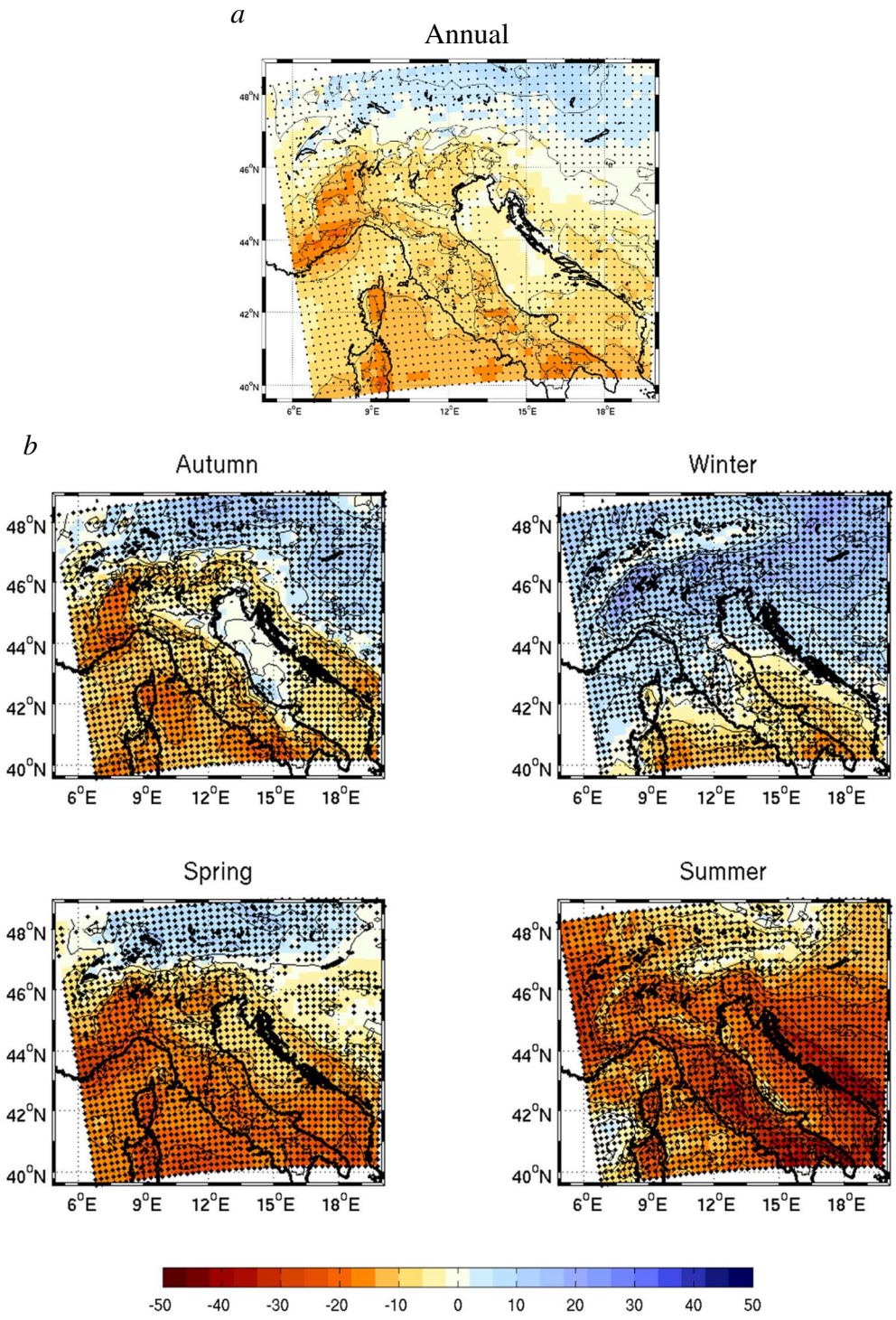

Figure 1.21. Two-layered maps representing signal and inter-model agreement over sign of climate change signal. Dotes denote areas where at least 66% of the models agreed on the mean annual (a) and mean seasonal (b) precipitation change sign.

Agreement over statistical significance of precipitation change

Figure 1.22 reports results concerning inter-model agreement over the statistical significance of precipitation change signal. Areas where the majority (>= 66%, 4 out 6 models, circles) and totality (100% or 6 out 6 models, filled circles) are underlined. Different response of the two metrics are evident. This emphasizes the importance of assessing not only sign but also significance agreement of change. In figure 1.22, spatial patterns resemble sign-agreement distribution (figure 1.21), but empty spaces (grid-nodes where less than 4 out 6 models agreed over significant change) are wider. Significance agreement (majority or totality of models), is mainly located in correspondence of moderate signal, at least ± 10%. As expected, total agreement only over relevant signal (± 20%) has resulted. Absence of significance agreement means negligible signal, where at least, 3 out 6 models produced future changes within inter-annual variability boundary. As seen for annual basis, seasonally, inter-model significance agreement characterizes areas where a relevant change signal magnitude resulted. It is worth underline significance agreement of wetter condition in almost the whole areas placed north of 45 °N, mainly in winter. The same for the severe summer and spring drying over Italy land-points. This double metric analysis assigns higher confidence on a wetter-winter (north of 46 °N) and the dryer-summer (almost the entire Italy) future conditions.

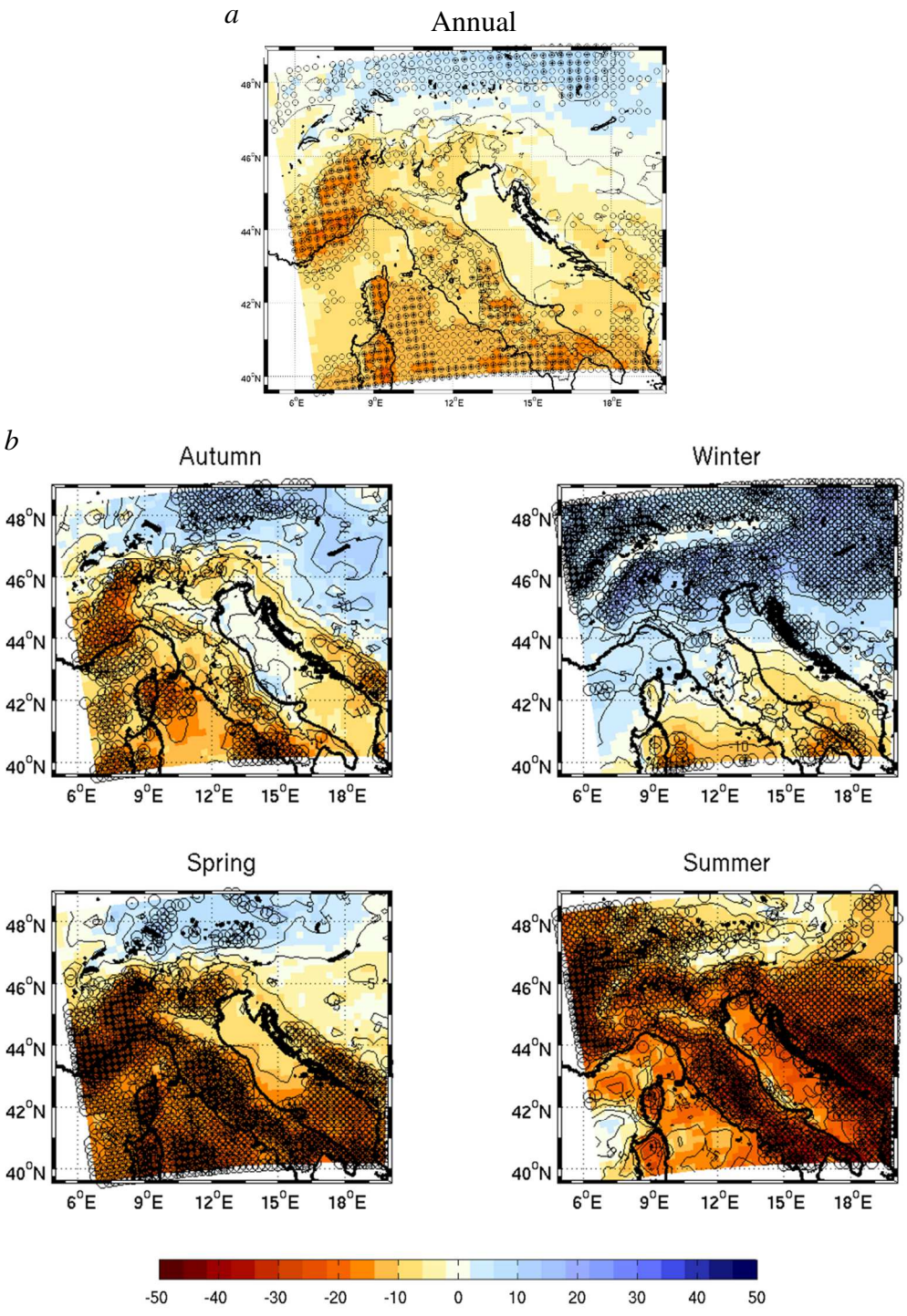

Figure 1.22. Two-layered maps representing change signal and inter-model agreement over statistical significance of climate change signal.
Circles denote areas where at least 66% of the models agreed on statistical significance of the mean annual (a) and mean seasonal (b) precipitation changes.
Filled circles denote areas where 100% of the models agreed on statistical significance of the mean annual (a) and mean seasonal (b) precipitation changes.

1.3 Conclusions and summary

This study provided for a comprehensive assessment of multi-model ensemble projections referred to the end-21st century. The study area investigated roughly cover Italian peninsula and climate variable considered are daily mean, minimum, maximum temperature and daily cumulated precipitation. Simulations are provided by a six-multi model ensemble run in the context of European project ENSEMBLES. Analysis have been conducted over climate change signal affecting mean values and tails of distribution as well. Climate change signal was derived as the difference of a statistic characterizing a future (2061-2090) and a past reference period (1961-1990). Moreover, seasonal inter-annual variability affecting mean temperature and mean cumulated precipitation has been assessed. Adopting a multi-model ensemble approach the robustness and uncertainties of reported climate projection has been assessed through two metrics evaluating the level of inter-model agreement over sign and significance of climate change signal resulted. To provide a basic idea of the performance of climate models employed, three statistical metrics were initially performed to evaluate the capability of each ensemble member to reproduce recent past observed temperature and precipitation annual cycle over representative stations.

Regarding temperature, distribution and magnitude of the mean, minimum and maximum temperatures projected changes agreed with the principal studies conducted for Mediterranean, Italy and Alpine region (Giorgi et al. 2004; Lionello et al. 2006; Giorgi and Lionello 2008; Coppola and Giorgi 2010; Hertig et al. 2010; Efthymiadis et al. 2011; Gobiet et al. 2014). Temperatures are expected to particularly increase in summer on the mean values but even more over distribution tails. Generally, in winter, a minor increase of temperature resulted. Specifically for winter season, signal standed out over Alpine region where the lack of albedo-effect provokes severe warming of cold and very cold temperature values.

Precipitation results showed relevant seasonal and latitudinal varying signal in response of changes in large-scale circulations and atmospheric moisture holding capacity. The latitudinal gradient is particular evident during winter season where a dipolar anomaly pattern resulted. Only over north Italy wetter winters up to ~ 20% are expected , in response of the increased Atlantic storm track activity (Giorgi et al. 2004; Giorgi and Coppola 2007). Conversely, a precipitation decrease projected over southern Italy. In winter season precipitation changes, show a transition signal over central Italy. Summer season showed a

widespread relevant decrease with a peak down to -30% over central and south Italy. To lesser extent, also spring season has resulted affected by drier conditions down to -20% over the entire domain. However, the relevance of such springtime precipitation decrease should not be underestimated. Several studies underline as springtime soil moisture and temperature can trigger soil-atmosphere feedbacks, potentially exacerbating drought conditions during following summer season (Seneviratne et al. 2006; Fischer et al. 2007; Seneviratne et al. 2010; Heinrich and Gobiet 2012). Follows a summary of the results obtained in this first chapter.

1.3.1 Temperature

- **Climate models evaluation:** multi-model ensemble well performed on the reproduction of reference period temperature. For the representative Marche region coast and hill stations, monthly mean bias (negative) does not exceed 1 °C. Over mountain sector, simulations underestimated observed vales of about 2 °C in all seasons except for summer season.
- **Climate change signal:** Mean summer temperature resulted the most affected season by larger and spatially homogeneous temperature increase up to + 5 °C over its 95th percentile. Spatial patterns indicated Alps as the most affected area by increase in low temperature (5th percentile) during winter season up to + 5 °C.

  Minimum temperature: summer season (and winter only for Alps) is the season showing higher expected change (+ 4.5 °C). It is interesting to note how signal affecting the mean value of the variable is different from that affecting left tail of distribution (5th percentile, cold extreme). Change signal up to +5.5-6.0 °C characterized the entire alpine region during autumn and winter seasons and to lesser extent spring season.

  Maximum temperature: homogeneous change signal over Italy land points between +4 to 5 °C in summer season (up to 5.5 °C for the 95th percentile). Signal presents similar spatial pattern and magnitude of the mean temperature.

  Change signal related to the inter-seasonal variability roughly follows mean value changes. Summer season resulted the season with the larger increase in future inter-seasonal oscillation (up to 25%). Least increase resulted in winter, where over the northern Italy is expected a negative signal (~ -10%).

- **Inter-model agreement:** multi-models ensemble members showed total statistical significance agreement over the aforementioned mean temperature changes.

1.3.2 Precipitation

- **Climate models evaluation:** Multi-model ensemble well reproduce precipitation annual cycle over coast and hill stations with negligible bias. A decrease of model performances was resulted over complex-terrain station with an underestimation of observed mean precipitation in autumn months (≈ 3 mm).
- **Climate change signal:** mean seasonal precipitation showed a general decrease in summer down to -30% over central and southern Italian peninsula while a dipolar latitudinal signal pattern resulted in winter (positive north 45°N and negative south of 42°N). Extreme precipitation events are expected increasing in all the season except for summer season, following fine-scale pattern in response of mountain systems and coastline morphology forcing. For such events, high resolution simulations would be necessary in order to better reproduce for example orography induced convective precipitation.

  Stronger precipitation inter-annual variability is expected, especially in summer season (up to 50%). Latitudinal winter inter-seasonal variability gradient is resulted with a slight negative signal over Alps that progressively fade into positive signal over the south of Italy.
- **Inter-model agreement:** Good inter-model agreement over significant wetter conditions over northern areas (mainly in winter) and over the widespread and severe summer drying signal characterizing the entire study area land points. Conversely, especially in autumn and winter seasons, the signal over central part of Italian peninsula resulted uncertain without consistent inter-model agreement.

Bibliography

Allan RP, Soden BJ (2008) Atmospheric warming and the amplification of precipitation extremes. Science (New York, NY) 321:1481–4. doi: 10.1126/science.1160787

Allen MR, Ingram WJ (2002) Constraints on future changes in climate and the hydrologic cycle. Nature 419:224–232. doi: 10.1038/nature01092

Beniston M, Stephenson DB, Christensen OB, Ferro C a T, Frei C, Goyette S, Halsnaes K, Holt T, Jylhä K, Koffi B, Palutikof J, Schöll R, Semmler T, Woth K (2007) Future extreme events in European climate: An exploration of regional climate model projections. Climatic Change 81:71–95. doi: 10.1007/s10584-006-9226-z

Bucchignani E, Montesarchio M, Zollo AL, Mercogliano P (2015) High-resolution climate simulations with COSMO-CLM over Italy: performance evaluation and climate projections for the 21st century. International Journal of Climatology. doi: 10.1002/joc.4379

Christensen J, Kjellström E, Giorgi F, Lenderink G, Rummukainen M (2010) Weight assignment in regional climate models. Climate Research 44:179–194. doi: 10.3354/cr00916

Ciais P, Reichstein M, Viovy N, Granier a, Ogée J, Allard V, Aubinet M, Buchmann N, Bernhofer C, Carrara a, Chevallier F, De Noblet N, Friend a D, Friedlingstein P, Grünwald T, Heinesch B, Keronen P, Knohl a, Krinner G, Loustau D, Manca G, Matteucci G, Miglietta F, Ourcival JM, Papale D, Pilegaard K, Rambal S, Seufert G, Soussana JF, Sanz MJ, Schulze ED, Vesala T, Valentini R (2005) Europe-wide reduction in primary productivity caused by the heat and drought in 2003. Nature 437:529–533. doi: 10.1038/nature03972

Collins M, Booth BBB, Bhaskaran B, Harris GR, Murphy JM, Sexton DMH, Webb MJ (2011) Climate model errors, feedbacks and forcings: a comparison of perturbed physics and multi-model ensembles. Climate Dynamics 36:1737–1766. doi: 10.1007/s00382-010-0808-0

Coppola E, Giorgi F (2010) An assessment of temperature and precipitation change projections over Italy from recent global and regional climate model simulations. International Journal of Climatology 32:11–32. doi: 10.1002/joc

Deser C, Phillips A, Bourdette V, Teng H (2012) Uncertainty in climate change projections:

The role of internal variability. Climate Dynamics 38:527–546. doi: 10.1007/s00382-010-0977-x

Efthymiadis D, Goodess CM, Jones PD (2011) Trends in Mediterranean gridded temperature extremes and large-scale circulation influences. Natural Hazards and Earth System Science 11:2199–2214. doi: 10.5194/nhess-11-2199-2011

Fatichi S, Ivanov VY, Caporali E (2012) Investigating interannual variability of precipitation at the global scale: Is there a connection with seasonality? Journal of Climate 25:5512–5523. doi: 10.1175/JCLI-D-11-00356.1

Fischer EM, Seneviratne SI, Vidale PL, Lüthi D, Schär C (2007) Soil moisture-atmosphere interactions during the 2003 European summer heat wave. Journal of Climate 20:5081–5099. doi: 10.1175/JCLI4288.1

Gao X, Giorgi F (2008) Increased aridity in the Mediterranean region under greenhouse gas forcing estimated from high resolution simulations with a regional climate model. Global and Planetary Change 62:195–209. doi: 10.1016/j.gloplacha.2008.02.002

Giorgi F, Bi X, Pal J (2004) Mean, interannual variability and trends in a regional climate change experiment over Europe. II: Climate change scenarios (2071-2100). Climate Dynamics 23:839–858. doi: 10.1007/s00382-004-0467-0

Giorgi F, Coppola E (2007) European climate-change oscillation (ECO). Geophysical Research Letters 34:1–6. doi: 10.1029/2007GL031223

Giorgi F, Hurrell JW, Marinucci MR, Beniston M (1997) Elevation dependency of the surface climate change signal: A model study. Journal of Climate 10:288–296. doi: 10.1175/1520-0442(1997)010<0288:EDOTSC>2.0.CO;2

Giorgi F, Lionello P (2008) Climate change projections for the Mediterranean region. Global and Planetary Change 63:90–104. doi: 10.1016/j.gloplacha.2007.09.005

Gobiet A, Kotlarski S, Beniston M, Heinrich G, Rajczak J, Stoffel M (2014) 21st century climate change in the European Alps-A review. Science of the Total Environment 493:1138–1151. doi: 10.1016/j.scitotenv.2013.07.050

Goubanova K, Li L (2007) Extremes in temperature and precipitation around the Mediterranean basin in an ensemble of future climate scenario simulations. Global and Planetary Change 57:27–42. doi: 10.1016/j.gloplacha.2006.11.012

Grassi B, Redaelli G, Visconti G (2013) Arctic sea ice reduction and extreme climate events over the mediterranean region. Journal of Climate 26:10101–10110. doi: 10.1175/JCLI-D-12-00697.1

Hall A (2004) The role of surface albedo feedback in climate. Journal of Climate 17:1550–1568. doi: 10.1175/1520-0442(2004)017<1550:TROSAF>2.0.CO;2

Hawkins E, Sutton R (2009) The potential to narrow uncertainty in regional climate predictions. Bulletin of the American Meteorological Society 90:1095–1107. doi: 10.1175/2009BAMS2607.1

Heinrich G, Gobiet A (2012) The future of dry and wet spells in Europe: A comprehensive study based on the ENSEMBLES regional climate models. International Journal of Climatology 32:1951–1970. doi: 10.1002/joc.2421

Hertig E, Seubert S, Jacobeit J (2010) Temperature extremes in the Mediterranean area: Trends in the past and assessments for the future. Natural Hazards and Earth System Science 10:2039–2050. doi: 10.5194/nhess-10-2039-2010

Hertig E, Seubert S, Paxian a, Vogt G, Paeth H, Jacobeit J (2014) Statistical modelling of extreme precipitation indices for the Mediterranean area under future climate change. International Journal of Climatology 34:1132–1156. doi: 10.1002/joc.3751

Jordà G, Gomis D, Alvarez-Fanjul E, Somot S (2012) Atmospheric contribution to Mediterranean and nearby Atlantic sea level variability under different climate change scenarios. Global and Planetary Change 80-81:198–214. doi: 10.1016/j.gloplacha.2011.10.013

Knutti R, Furrer R, Tebaldi C, Cermak J, Meehl G a. (2010) Challenges in Combining Projections from Multiple Climate Models. Journal of Climate 23:2739–2758. doi: 10.1175/2009JCLI3361.1

Kotlarski S, Bosshard T, Lüthi D, Pall P, Schär C (2012) Elevation gradients of European climate change in the regional climate model COSMO-CLM. Climatic Change 112:189–215. doi: 10.1007/s10584-011-0195-5

Lionello P, Malanotte-Rizzoli P, Boscolo R (2006) Mediterranean climate variability. Elsevier

Lu J, Vecchi G a, Reichler T (2007) Expansion of the Headley cell under global warming. Geophysical Research Letters 34:L06805. doi: 10.1029/2006GL028443

Nakicenovic N, Swart R (2000) Special Report on Emissions Scenarios.

Neelin, J. D. (2010) Climate change and climate modeling. Cambridge University Press.

Overland JE, Wang M (2010) Large-scale atmospheric circulation changes are associated with the recent loss of Arctic sea ice. Tellus, Series A: Dynamic Meteorology and Oceanography 62:1–9. doi: 10.1111/j.1600-0870.2009.00421.x

Palmer TN (2013) Climate extremes and the role of dynamics. Proceedings of the National Academy of Sciences of the United States of America 110:5281–2. doi: 10.1073/pnas.1303295110

Palmer TN, Alessandri a., Andersen U, Cantelaube P, Davey M, Délécluse P, Déqué M, Díez E, Doblas-Reyes FJ, Feddersen H, Graham R, Gualdi S, Guérémy JF, Hagedorn R, Hoshen M, Keenlyside N, Latif M, Lazar a., Maisonnave E, Marletto V, Morse a. P, Orfila B, Rogel P, Terres JM, Thomson MC (2004) Development of a European multimodel ensemble system for seasonal-to-interannual prediction (DEMETER). Bulletin of the American Meteorological Society 85:853–872. doi: 10.1175/BAMS-85-6-853

Planton S, Lionello P, Artale V, Aznar R, Carrillo A, Colin J, Congedi L, Dubois C, Elizalde A, Gualdi S, Hertig E, Jacobeit J, JordÃ G, Li L, Mariotti A, Piani C, Ruti P, Sanchez-Gomez E, Sannino G, Sevault F, Somot S, Tsimplis M (2012) The Climate of the Mediterranean Region in Future Climate Projections.

Rajczak J, Pall P, Schär C (2013) Projections of extreme precipitation events in regional climate simulations for Europe and the Alpine Region. Journal of Geophysical Research: Atmospheres 118:3610–3626. doi: 10.1002/jgrd.502972013

Schär C, Vidale PL, Lüthi D, Frei C, Häberli C, Liniger M a, Appenzeller C (2004) The role of increasing temperature variability in European summer heatwaves. Nature 427:332–336. doi: 10.1038/nature02300

Scherrer SC, Ceppi P, Croci-Maspoli M, Appenzeller C (2012) Snow-albedo feedback and Swiss spring temperature trends. Theoretical and Applied Climatology 110:509–516. doi: 10.1007/s00704-012-0712-0

Seierstad I a., Bader J (2009) Impact of a projected future Arctic Sea Ice reduction on extratropical storminess and the NAO. Climate Dynamics 33:937–943. doi: 10.1007/s00382-008-0463-x

Seneviratne SI, Corti T, Davin EL, Hirschi M, Jaeger EB, Lehner I, Orlowsky B, Teuling AJ (2010) Investigating soil moisture-climate interactions in a changing climate: A review. Earth-Science Reviews 99:125–161. doi: 10.1016/j.earscirev.2010.02.004

Seneviratne SI, Lüthi D, Litschi M, Schär C (2006) Land-atmosphere coupling and climate change in Europe. Nature 443:205–209. doi: 10.1038/nature05095

Solomon, S. D, Qin M, Manning Z, Chen M, Marquis KB, Averyt MT, Miller HL, Solomon S, Qin D, Manning M, Chen Z, Marquis M, Averyt KB, Tignor M, Miller HL (2007)

Summary for Policymakers. In: Climate Change 2007: The Physical Science Basis. Contribution of Working Group I to the Fourth Assessment Report of the Intergovernmental Panel on Climate Change. D Qin M Manning Z Chen M Marquis K Averyt M Tignor and HL Miller New York Cambridge University Press pp Geneva:996. doi: 10.1038/446727a

Tebaldi C, Arblaster JM, Knutti R (2011) Mapping model agreement on future climate projections. Geophysical Research Letters 38:1–5. doi: 10.1029/2011GL049863

Tebaldi C, Knutti R (2007) The use of the multi-model ensemble in probabilistic climate projections. Philosophical transactions Series A, Mathematical, physical, and engineering sciences 365:2053–75. doi: 10.1098/rsta.2007.2076

Tolika K, Maheras P, Tegoulias I (2009) Extreme temperatures in Greece during 2007: Could this be a "return to the future"? Geophysical Research Letters 36:1–5. doi: 10.1029/2009GL038538

Toreti a., Xoplaki E, Maraun D, Kuglitsch FG, Wanner H, Luterbacher J (2010) Characterisation of extreme winter precipitation in mediterranean coastal sites and associated anomalous atmospheric circulation patterns. Natural Hazards and Earth System Science 10:1037–1050. doi: 10.5194/nhess-10-1037-2010

Trigo RM (2006) Relations between variability in the Mediterranean region and Mid-latitude variability. The Mediterranean Climate: an overview of the main characteristics and issues 179–226. doi: 10.1016/S1571-9197(06)80006-6

Trigo RM, Osborn TJ, Corte-real JM (2002) The North Atlantic Oscillation influence on Europe: climate impacts and associated physical mechanisms. Climate Research 20:9–17. doi: 10.3354/cr020009

van der Lindend P, Mitchell JFB (2009) Climate change and its impacts: Summary of research and results from the ENSEMBLES project.

Vautard R, Gobiet A, Jacob D, Belda M, Colette A, Déqué M, Fernández J, García-Díez M, Goergen K, Güttler I, Halenka T, Karacostas T, Katragkou E, Keuler K, Kotlarski S, Mayer S, Meijgaard E, Nikulin G, Patarčić M, Scinocca J, Sobolowski S, Suklitsch M, Teichmann C, Warrach-Sagi K, Wulfmeyer V, Yiou P (2013) The simulation of European heat waves from an ensemble of regional climate models within the EURO-CORDEX project. Climate Dynamics 41:2555–2575. doi: 10.1007/s00382-013-1714-z

Xoplaki E, Trigo RM, García-Herrera R, Barriopedro D, D'Andrea F, Fischer EM, Gimeno L, Gouveia C, Hernández E, Kuglitsch FG, Mariotti A, Nieto R, Pinto JG, Pozo-

Vázquez D, Saaroni H, Toreti A, Trigo IF, Vicente-Serrano SM, Yiou P, Ziv B (2012) Large-scale atmospheric circulation driving extreme climate events in the mediterranean and its related impacts. In: The Climate of the Mediterranean Region. pp 347–417

Wilks, D. S. (2011). Statistical methods in the atmospheric sciences (Vol. 100). Academic press.

2. Bias correction of ENSEMBLES climate projections

2.1 Datasets and methodology

2.1.1 Observational datasets and study Area

Observed datasets are provided by the 10th version of the European daily high resolution gridded data set EOBS (Haylock et al. 2008). This dataset provides land-only daily high-resolution gridded dataset for precipitation, minimum, maximum and mean surface temperature, and sea-level pressure from 1950 to 2013 covering the entire European continent. Here, we make use of daily mean surface temperature and daily-cumulated precipitation from 1971 to 2000 over an area roughly covering Italian peninsula with a 25 km horizontal resolution (figure 2.1).

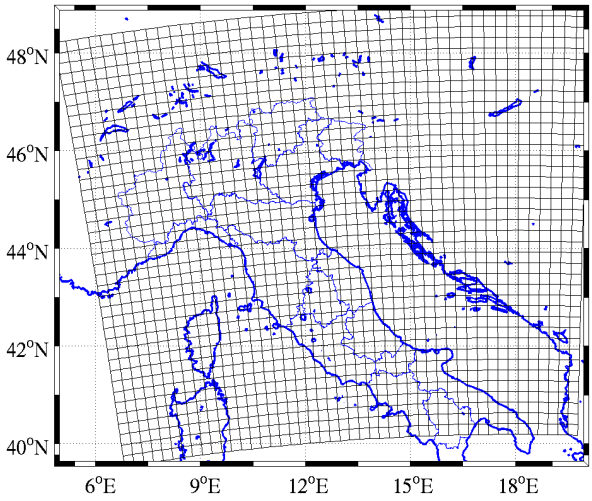

Figure 2.1. Study area geographical domain. Observed and simulated datasets are provided at each grid-node.

Interpolated data sets provides spatial-homogeneous estimates of climate variables at locations far away from observational stations, allowing local climatological analysis over data-sparse regions. Other benefit, regards their employment in the validation of regional climate models outputs, in the context of climate change studies. A very popular approach consists on the direct comparison of the simulations and the interpolated observations since indicative of processes at the same spatial scale. By construction, models have generally expected to better represent area averaged processes rather than at point-scale. Therefore, the best estimate average of the grid square observation is often regarded as most appropriate observational basis for climate models validation and bias-correction phases. Finally, the absence of spatial resolution mismatch between observation and simulations prevent interpolation procedure that could represent a high computing sources demanding step. On the other hand, quality of gridded data sets largely depends on the spatial density of stations within each grid cell being subjected to interpolation. Remote-mountainous areas with a low observational stations spatial density, general provide lower quality data, since the interpolation operated over greater distances with highly diversified morphological

conditions. Even for extreme events, that generally has station-scale nature, an area-averaged representation could soften this pick values especially for convective intense precipitation.

2.1.2 Climate simulations

Climate simulations employed in this section are the same of the previous section (chapter-1) and are summarized in table 2.1.

Institute	RCM	Driving GCM	Resolution	Period	SRES	Variable
DMI	HIRHAM5	ECHAM5-r3	25 km	1971-2090	A1B	tas; pr
KNMI	RACMO2.1	ECHAM5-r3	25 km	1971-2090	A1B	tas; pr
MPI	REMO5.7	ECHAM5-r3	25 km	1971-2090	A1B	tas; pr
SMHI	RCA3.0	ECHAM5-r3	25 km	1971-2090	A1B	tas; pr
CNRM	Aladin	ARPEGE_RM5.1	25 km	1971-2090	A1B	tas; pr
ICTP	RegCM3	ECHAM5-r3	25 km	1971-2090	A1B	tas; pr

Table 2.1. List of climate models employed

This section relies on the climate simulations provided by an ensemble of six regional climate models run in the context of European project ENSEMBLES (van der Lindend and Mitchell 2009). As reported in table 2.1, the six regional climate models are driven by the same global climate model (ECHAM5-r3) but the Aladin model, driven by the global climate model ARPEGE. The characteristics of the driving global climate represent crucial factor for the regional climate model behavior. Boundary conditions and general dynamics interpretation have provided by the driving global model and processes misrepresentation in the large-scale could be directly inherited (if not amplified) in the regional climate models. Therefore, the large spectrum of future climate uncertainties would be better addressed considering regional models driven by a as wider as possible number of global models.

For each climate model have been extracted two runs, one referred to the historical period (1971-2000) and one for a future time segment (2061-2090) for both daily mean surface temperature and daily cumulated precipitation. The emission boundary conditions of climate simulations are provided by the intermediate IPCC A1B emission scenario (Nakicenovic and Swart 2000). It allows assessing the response of climate system to an atmospheric

greenhouse gasses concentration resulting from an intermediate emission scenario. The emission scenario is derived as a function of a certain evolution of political socio-economic and ecological parameters determining precise chemical composition of the atmosphere. All the climate models employed have been interpolated on a common regular grid with horizontal resolution of 25 km. Originally, all the climate models had a same-resolution grid, but a sub-set adopted a rotated instead a regular grid. For this reason, an interpolation over a regular common grid have been necessary. Once interpolated, on a common grid the two time segments have been arithmetically averaged grid-node by grid-node to obtain the multi-model ensemble simulations. Then, the two temporal segments have been employed to compute seasonal climate change signal.

Finally, each ensemble member's reference and future runs, have been subjected to a statistical bias correction and a bias-corrected multi-model ensemble has been performed to compute a bias-corrected climate change signal.

2.1.3 Methodology: Quantile Mapping bias correction – theory and application

Temperature and precipitation reference and future runs of each ensemble member has been post-processed using an empirical statistical quantile mapping method (Deque 2007; Themeßl et al. 2011a). In principle, statistical bias correction methodologies act on model outputs so the statistical properties of the corrected data match those of observation (Haerter et al. 2011). Quantile mapping bias correction technique consists on a correction function built on the relationship between the statistical distribution of the observed and simulated variable over a common period (preferably >= 30 years accounting for natural climate inter-annual variability). Empirical quantile mapping approach was first propose by Panofsky and Brier (1968) and applied in several study aiming to bias correct and to downscale climate model simulations in the context of hydrological applications (Boé et al. 2007; Deque 2007; Themeßl et al. 2011a). The concept behind the quantile-mapping bias correction technique is to derive a correction function from the mismatch of the statistical distribution of observed and simulated time series at each specific quantile. Then, the correction function is applied to the physical simulated values, representing the mathematical operation that have to be performed on each simulated quantile to obtain the corresponding observed quantile (Gennaretti et al. 2015). More in details, a scaling factor is derived by the difference (for temperature) or ratio (for precipitation) of each observed and simulated statistical

distribution quantile. The scaling factor is then linearly interpolated to the query points corresponding to the physical values of the simulated time series. Resulting correction function is applied to the simulated values with an addition (temperature) or a multiplication (precipitation) of the physical values of the reference and future period simulations. The term "physical values" indicates that the correction function is applied to the individual physical simulated value instead to the statistic that this value represents within the time series (e.g. 95th percentile). The difference of applying correction function to the physical value instead to the statistical role played by that individual value within the considered time series is easy to understand through this example: imagine correcting a simulated temperature of 13 °C of July 16 1983 within the time series 1979-2002. Comparing this simulated value to the same day observed temperature the bias is of -1 °C (observed value = 14 °C). To correct the simulated value we have to add 1 °C to get the observed value of 14 °C. If now, we have to correct the same-day simulated temperature but within a different-length time series (1979-2010), this bias should be corrected, by definition, with same correction factor of +1 °C (physical coherence). Applying the correction factor to the statistic assumed by the simulated value within the considered time series. According to this latter principle, the same temperature value in two different-length time series will represent a different statistic (e.g. 13 °C would represent the 95th percentile in the first and 98th percentile in the second). Consequently, the same value (affected by the same bias) will be differently corrected in the two time series and this is not physically coherent.

According to the physical approach, the correction function calibrated along a common time segment between simulation and observation, and applied to the reference and future period simulations. By construction, correction of the reference period will produce a simulated time series having a statistical distribution equal to the observed distribution. In this way, the correction is able to correct bias related to the physical simulated values and variability as well. Considering the correction of the future time segment, it would require an extrapolation of the correction values in the case that the future period contains values not present in the reference simulation used for calibrating the correction function. For this reason, we constantly extrapolated correction function values at the lowest and highest quantiles of the calibration period. For example, if the last quantile of temperature in the present climate simulation is corrected by 1.8 °C all the superior values in the climate scenario will be corrected with the same correction factor (Boé et al. 2007).

Quantile mapping application can affect the original climate change signal. The effect of quantile mapping application has been investigated in several other studies (Hagemann et al. 2011; Themeßl et al. 2011a; Dosio et al. 2012; Casati et al. 2013; Gobiet et al. 2015) and will in deep investigated in the next section. Haerter et al. (2011), in the case of a bias correction involving normal-distributed climate variable, found that quantile mapping stretched the original climate change signal equivalent to the ratio of the observed and simulated standard deviations (σ_{obs} / σ_{sim}). For example bias correction could affects climate change signal in the case of low precipitation or temperature are differently corrected as high amounts (due to different model bias in the reference and future period) or if the distribution between low and high values changes in a future climate (Hagemann et al. 2011).

However, it is important to note that quantile mapping correction relies on the assumption of time-invariant error and does not correct the temporal auto-correlation properties of the series (Deque 2007). Quantile mapping intends that relationships between observation and simulation will be preserved even in the future. If model errors is caused by physical processes misrepresentation (e.g. overestimation of high summer temperature due to a poor soil-atmosphere feedback representation), it is plausible that this kind of inability will be kept even in the representation of the future climate. Therefore, physical inconsistencies seem to play a major role on determining climate model bias (Seneviratne et al. 2006; Boberg and Christensen 2012) compared, for instance, to the changes in greenhouse gasses concentration that determine climate change signal magnitude. It is expected that the misrepresentation of physical process characterizing present climate will be misrepresented also in the future climate, with similar bias in correspondence of similar conditions (Casati et al. 2013). On the other hand, quantile mapping cannot correct bias associated with new physical mechanisms not observed in the past-present climate (Casati et al. 2013). Finally, Maraun (2012), using a set of the same regional climate models employed in this section over Europe, found that biases in general are stable, such that bias correction on average improves scenarios for climate impact studies.

In figure 2.2, principal methodological steps of the bias correction technique are reported. The first two panels show the two numerical grids providing observations and simulations. For exemplificative reason the procedure for only one regional climate model, one season (Autumn), one variable (temperature) and one grid cell time series has been shown (red dots, figure 2.2 – panels *a* and *b*). The two grids have the same horizontal resolution of 25 km. The panel *c* reports the quantile-quantile plot, built on the match of ranked reference period

(1971-2000) temperature observation and simulation. Quantile-quantile plot consists on the comparison of the two ranked data sets providing the different mismatch (error or bias) magnitude along the entire statistical distribution. Moreover, the variance mismatch between observation and simulation is indicated by the slope over the diagonal x = y. The area between the x = y diagonal and quantile-quantile line also defines the correction function applied to the simulation. Panel *d* represents the value of the correction function at each simulated quantile and consists on the values that must be added (temperature) or multiplied (precipitation) to obtain the corresponding observed quantile. This correction function has been interpolated to the query points represented by the physical values of the simulated time series (panel *e*) to obtain the bias corrected time series (panel *f*). Panel *g* reports the observed time series to quantify the improvement of the corrected simulation versus the original one. Means and standard deviations are reported to facilitate the evaluation. Actually, the resulted perfect correspondence between corrected and observed time series is not surprising, since the correction function has built over the same time segment (calibration period 1971-2000).

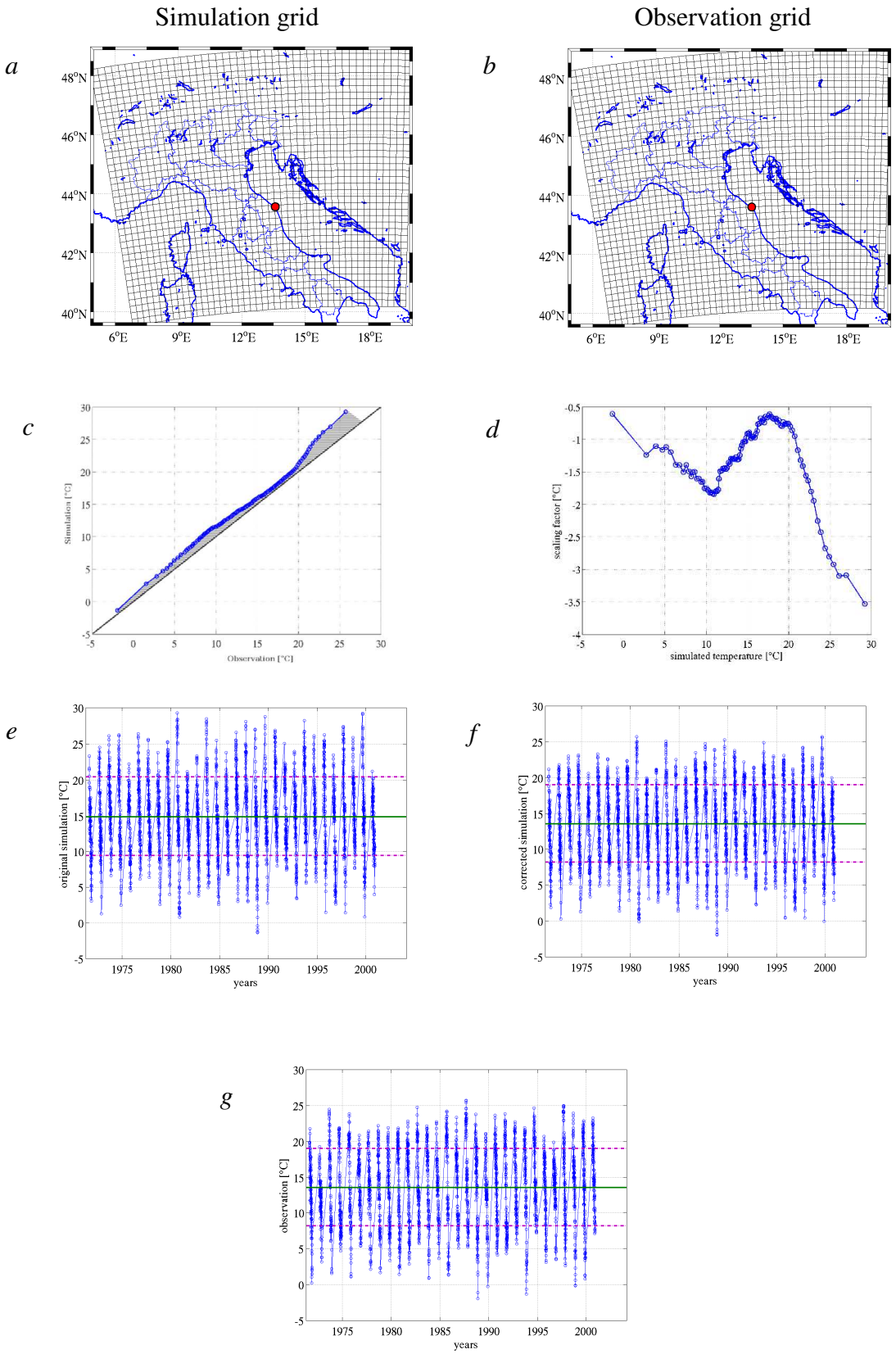

Figure 2.2. Quantile mapping methodological steps. Panels a and b display numerical grids providing simulated and observed time series. Datasets used in this figure belong to two exemplificative grid nodes indicated with red dots. Panel c reports the observation vs. simulation quantile-quantile plot. Quantile-specific correction function is reported in panel d. Panels e, f and g report respectively original simulation, bias-corrected simulation and observation. In panels e f and g green and purple lines indicate relative mean and standard deviation.

2.2 Results - effect of bias correction on the climate change signal

2.2.1 Temperature

In figure 2.3, top-down on the left column, observation (1971-2000), reference period simulation (1971-2000), end-21st century simulation (2061-2090) and related climate change signal for the mean summer (June-July-August) temperature original ensemble simulation have reported. The right column follows the same structure but reporting bias corrected ensemble results. Comparing reference period simulation and observation, ensemble mean simulation well reproduced observed temperature climatology. Moderate bias (≈ 1 °C) are, not surprising, localized in correspondence of Alps. Reproduction of atmospheric dynamics over such complex orography still represents a well-known limit even in the newest generation of regional climate models. In the bias corrected runs, it is noteworthy how bias is successfully removed. For the future period, original and corrected simulations present a consistent increase of temperature (≈ 4-5 °C) reported in the lower-end panels. The focus of this section is devoted to assess discrepancies between the original and bias corrected climate change signal. In fact, this is the most relevant aspect for climate impact studies since directly relying on climate model results to assess the response, of different systems, to the changes in climate conditions. In the lower panels of figure 2.3, direct comparison between original and bias-corrected climate change signal has reported. Bias correction produces a dampening of the signal, over coastal and plain areas of about 0.8 °C. In Alpine and Apennine areas signal is mainly conserved, highlighting a signal elevation-dependency introduced by the statistical adjustment. This dampening of summer temperature signal also resulted in other studies (Themeßl et al. 2011a; Dosio et al. 2012; Boberg and Christensen 2012) concerning Mediterranean basin. In these studies, has been found an intensity-dependence of the climate model errors. Especially in Mediterranean basin and southeast Europe, climate simulations have often demonstrated a warm-summer temperature overestimation as a function of the observed temperature. Even the magnitude of signal reduction is close to what observed in Christensen et al. (2008), which following a different statistical approach, obtained bias correction of 0.8 °C in the whole Mediterranean sub-region. From a model physics point of view, the inflated warming signal, has mainly expected from a misrepresentation of the

complex feedback between soil (especially in prolonged drought condition) and atmosphere (Seneviratne et al. 2006).

Figure 2.4, reports original and bias corrected ensemble simulations of the summer temperature 95th percentile. Through a comparison with observation (upper panels) original ensemble simulation, well reproduce the observed temperature with a moderate overestimation (positive bias) over the eastern part of study area. Slight underestimation of ≈ 1 °C, over the Apennines chain. Bias are successfully removed in the bias corrected simulation run. As seen for the mean seasonal value, change signal of coastal and plain areas in reduced from ≈ 4 to ≈ 3 °C by the bias correction application. Conversely, in the mountainous and most southern areas, the corrected signal resulted amplified, especially in the Alpine region, where the signal is scattered strengthen from 4-4.5 °C up to 6 °C. However, results from the 95th percentile have to be considered with greater caution than those referred to the mean value. The right part of distribution has by definition considered the "noisy" portion of statistical distribution of climate variables and subjected to higher distortion. Even for what concerns the statistical correction, the tails of distribution represent a more complex exercise. For the future period, the correction function involves values that have to be extrapolated (with a constant function) for correcting values outside the calibration (1971-2000) period range. In the context of high percentile analysis uncertainties pertain also to the gridded observational datasets. EOBS data are the result of an interpolation of gauge stations within the same grid cell. Areas with complex terrain characterized by lower stations density provide in general a data of lower quality especially over high percentiles. Therefore, correction function could result in such orographic contexts poor, affecting the bias correction effect over the high-percentile climate change signal.

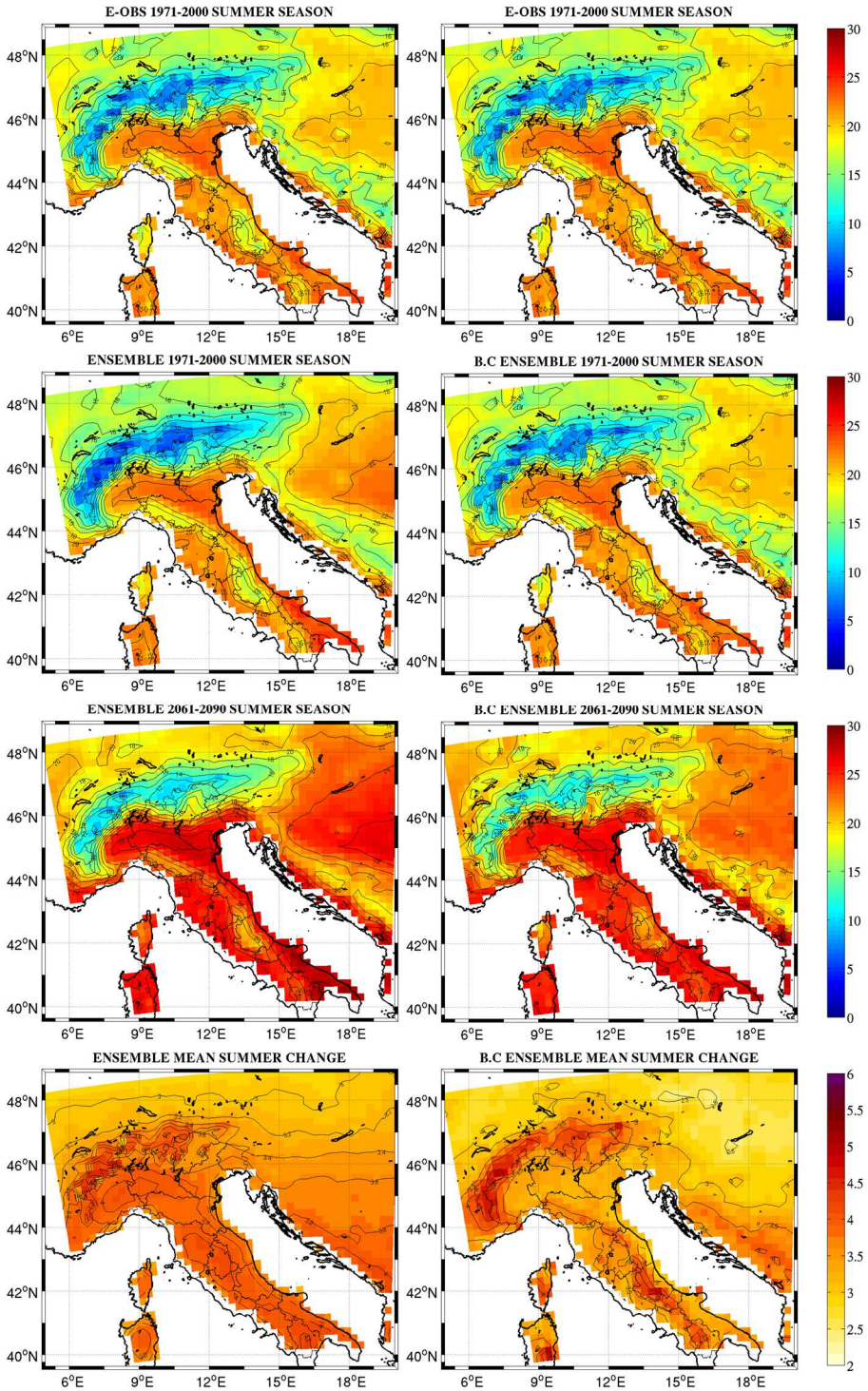

Figure 2.3. Summer mean surface temperature simulated by the original multi-model ensemble (left column) and bias-corrected (B.C.) runs (right column). From top to bottom: observed E-OBS reference period climatology (1971-2000), multi-model ensemble mean for the reference period (1971-2000); multi-model ensemble mean for the future period (2061-2090); multi-model ensemble mean climate change signal (2061-2090 minus 1971-2000). Units are C°.

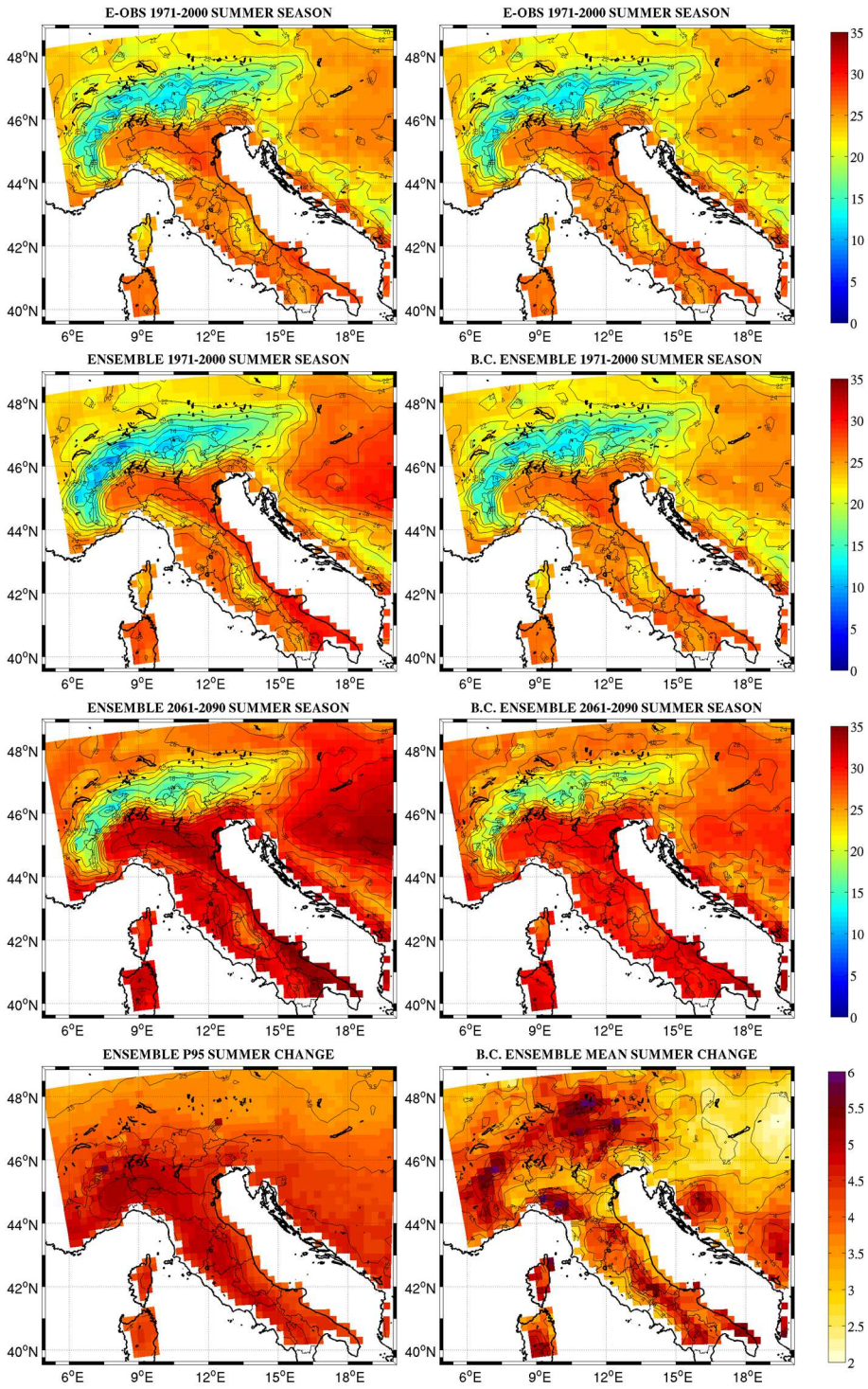

Figure 2.4. Same as figure 2.3 but for the seasonal 95th percentile.

Figure 2.5 shows mean winter (December-January-February) temperature observation, reference and future ensemble simulations, together with the climate change signal. As in the previous figures on the left column original simulations and on the right column bias-corrected ensemble simulations are reported. Original ensemble simulation well reproduced the observation but an underestimation over Tirrenian coast and alpine region is resulted. Bias has successfully removed in the corrected runs. Original climate change signal ranging from 2.5 to 3 °C is slightly dampened over coastal and plain areas within Italian peninsula, in general less than 0.5 °C. Over European continental areas signal is slightly strengthen of about 0.3 – 0.5 °C. The patterns of bias correction effect on the change signal resemble those seen in summer season. The dampening of the winter season signal is of minor magnitude, probably related to the minor signal affecting winter temperature. For the 95th percentile of winter season temperature (figure 2.6) climate model ensemble shows a cold bias over Alps removed in the bias corrected simulation. Here, bias correction effect over the climate change signal consists on a scattered strengthen of the signal of about 1 °C over the majority of study area. Specifically considering Italian peninsula, some similarities could be found on the spatial pattern characterizing effect of bias correction over mean summer signal (dampening) and winter 95th percentile signal (strengthen).

Commenting obtained results, alteration of the temperature signal is currently debated, since knowledge about the influence over climate change signal is still limited. The effect of the quantile mapping bias correction over the climate change signal has been analytically described in Gobiet et al. 2015. Gobiet and colleagues argue how the quantile mapping effect over the change signal derive by the correction of the intensity-dependence of model error and such modification should be therefore considered as an improvement of the signal quality. It is important to keep in mind that all the considerations over the effect of quantile mapping on the climate change signal rely on the assumption of the time-invariant model error characteristic. Another relevant aspect of the results in figure 2.3 is the introduction of an elevation-dependency of signal. This would be consistent with the consideration of Giorgi et al. 1997 and Kotlarski et al. 2012 where an elevation dependency of current and projected climate change signal has been demonstrated. However, considering the quantile mapping "statistical nature" namely that does not act on the physics of climate models makes this hypothesis remote. According to the above cited intensity dependency, model errors would

be deduced a minor correction magnitude in mountainous areas, where model grid point simulate lower temperature values. However, this aspect deserve further analysis.

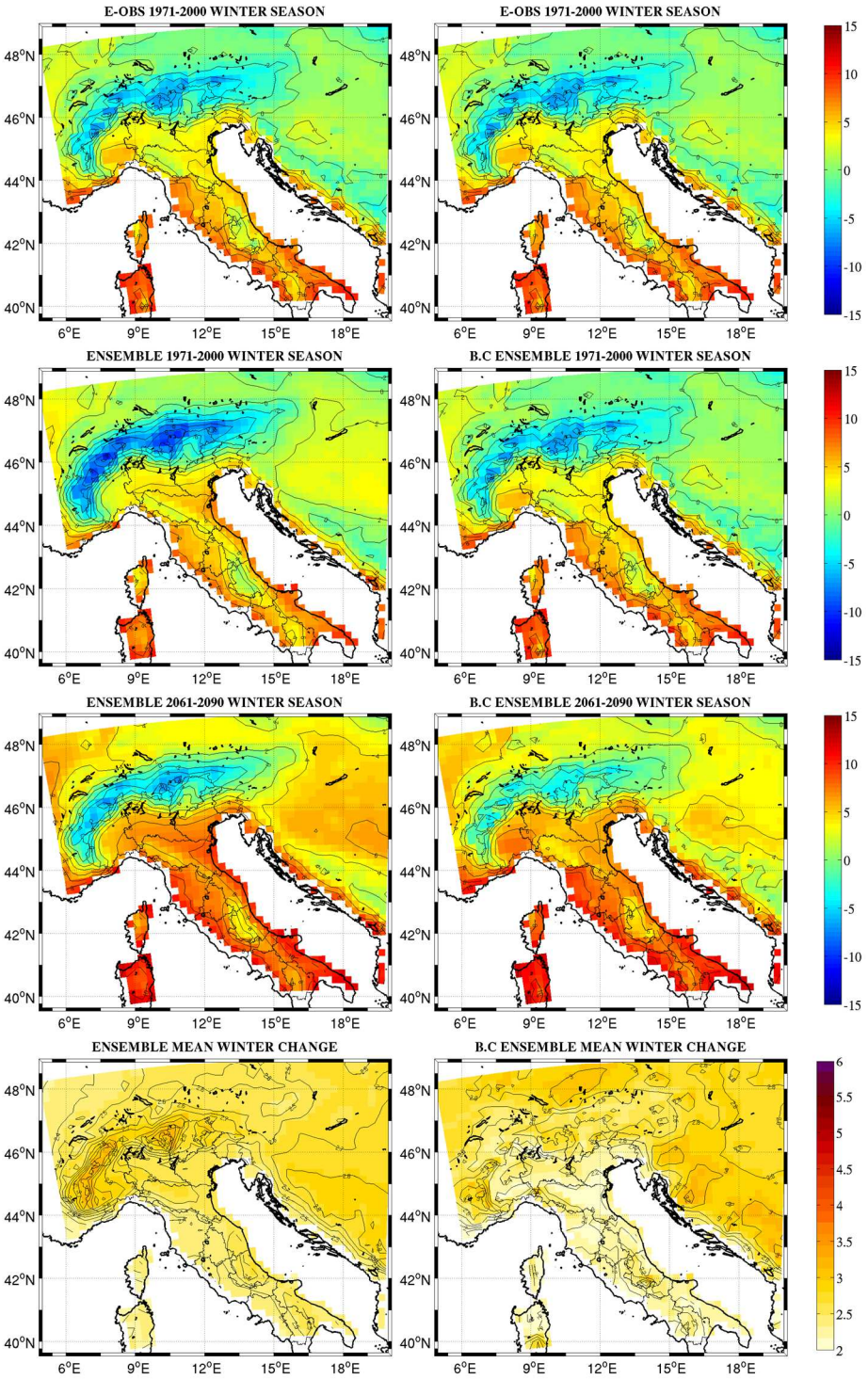

Figure 2.5. Same as figure 2.3 but for mean winter season temperature

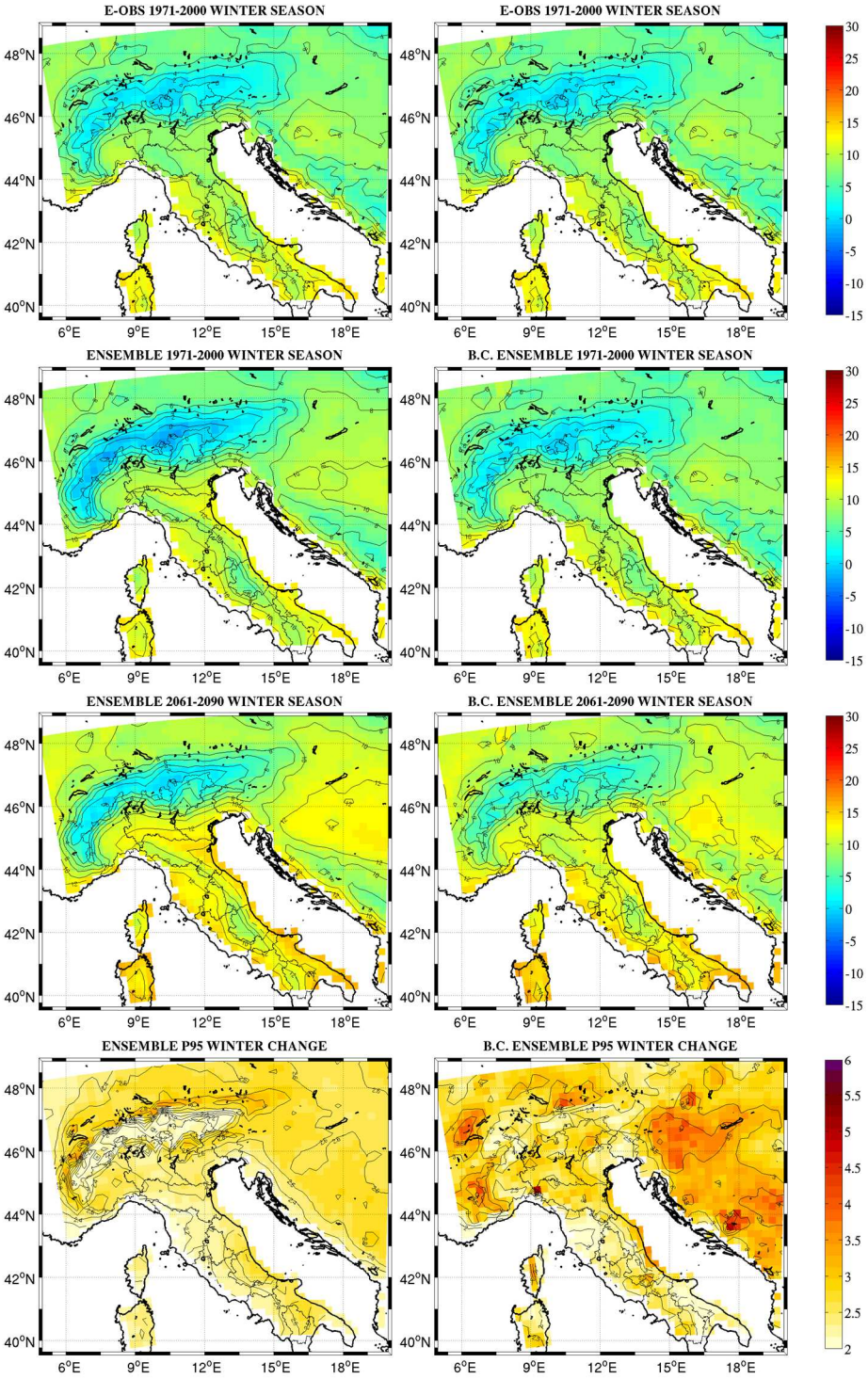

Figure 2.6. Same as figure 2.5 but for the seasonal 95th percentile.

2.2.2 Precipitation

In figure 2.7, results for summer precipitation are displayed. Original multi-model ensemble noticeably overestimates precipitation over western Alps and northern part of Italian peninsula. Observation shows how higher precipitation characterizing Alps central and eastern sectors. Simulation resulted not able to accurately reproduce precipitation distribution spatial pattern over Alps complex orography. It is noteworthy how bias are shaped by a clear model orography misrepresentation. Spatial pattern of precipitation bias was somehow expected especially for summer precipitation, mainly generated by convective phenomena. Detection of such occurrences would require very high climate model horizontal and vertical resolution able to catch complex uplift motion of air masses in function of the orography. Original simulation indeed homogenously distribute precipitation in the entire Alps chain. In the bias corrected reference period simulation, bias are successfully removed and the spatial pattern of higher precipitation are properly represented. This effect on the simulation does not affect climate change signal. Indeed, a general preservation of the severe negative signal (down to -30 %) covering most of the domain has resulted. Latitudinal gradient such as the main magnitude of the signal is preserved. A slight strengthening of the negative signal over western and the southernmost part of the study is resulted. Similar pattern resulted for the assessment of the 95^{th} percentile of the summer season precipitation (figure 2.8). For the same reason bias spatial pattern resembles that seen for the mean seasonal values and the effect of bias correction on the climate change signal as well. Signal latitudinal gradient is mainly conserved after bias correction; noteworthy is the slight strengthening of the negative signal affecting the southernmost areas.

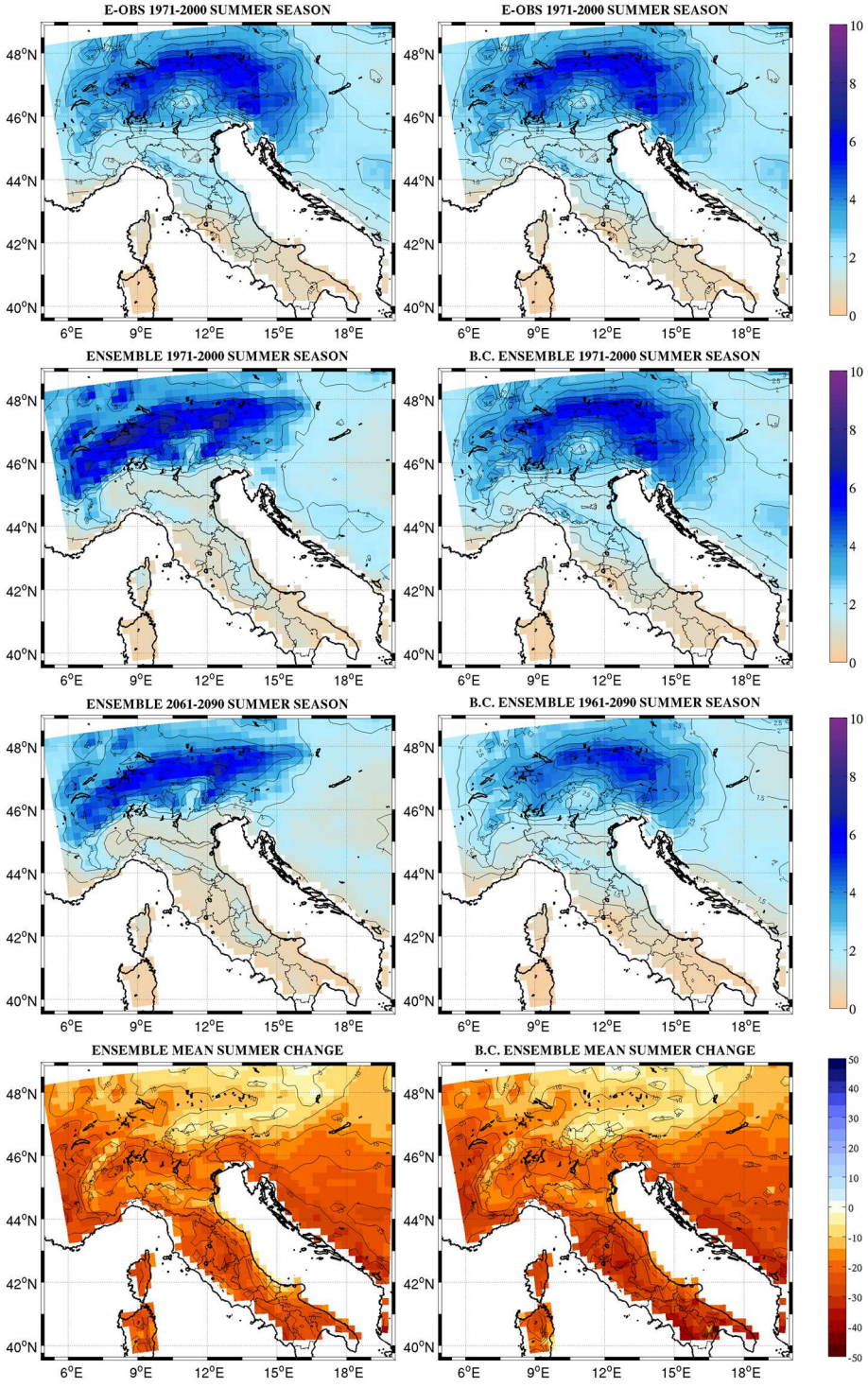

Figure 2.7. Summer mean daily cumulated precipitation simulated by the original multi-model ensemble (left column) and bias-corrected (B.C.) runs (right column). From top to bottom: observed E-OBS reference period climatology (1971-2000), multi-model ensemble mean for the reference period (1971-2000); multi-model ensemble mean for the future period (2061-2090); multi-model ensemble mean climate change signal (2061-2090 minus 1971-2000). Units are mm except for two bottom panels expressed in percentage [%].

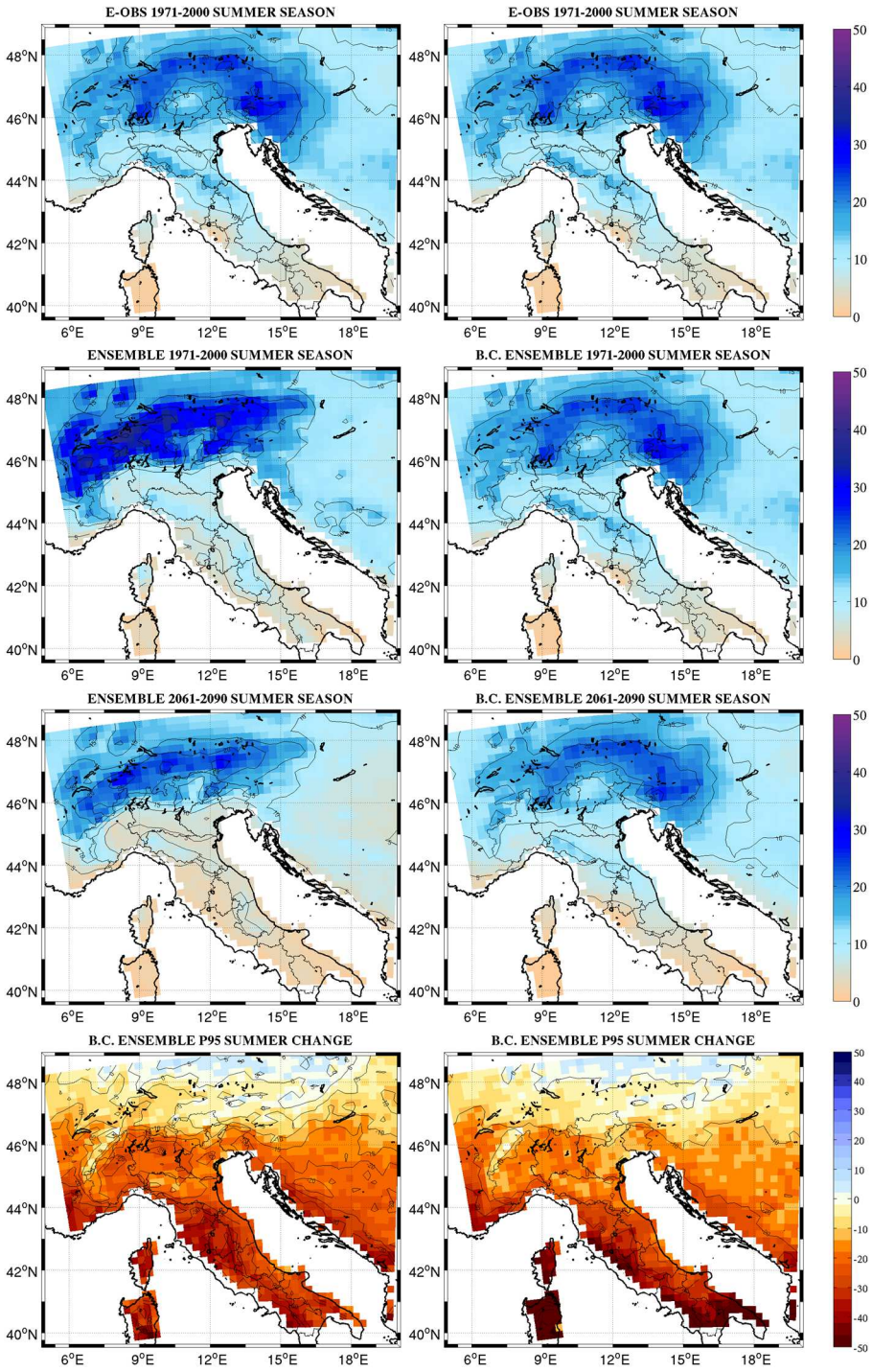

Figure 2.8. As for figure 2.7 but for seasonal 95th percentile.

Figures 2.9 and 2.10 report respectively mean and 95th percentile of winter daily-cumulated precipitation. It is interesting to note very large wet bias (overestimation) of winter precipitation performed by the original multi-model ensemble. Western side of the

major mountain chains shows greatest bias value up to ≈ + 4 mm/day representing a percentage around 70%. Again, major bias have found over complex-orography terrain. Moreover, bias spatial pattern depicts an apparent overestimation of zonal storm track flow affecting the mountain western upwind side producing wetter condition than observed. These relevant biases are removed in the corrected simulation run providing a correct spatial pattern distribution of winter mean precipitation. Related climate change signal resulted not affected by the bias correction. Strong latitudinal gradient (positive signal in the north and negative in the south) and the general magnitude of the changes are preserved. In figure 2.10 are reported results for the 95th percentile of winter precipitation. Original simulation shows similar pattern of precipitation overestimation resulted for the mean value. The bias are again spatially centered on mountain territories, but mainly in the southern side of Alps. This effect could result from the misrepresentation of orography air-uplift producing intense precipitation during meridional low-level wind regime. Also for the 95th percentile, bias correction application does not alter the original climate change signal spatial pattern and magnitude. Differently from temperature, not direct relation between the observed value and corresponding simulation biases has been identified; as resulted in Christensen et al. (2008).

Precipitation variable represents a challenging signal detection and bias correction exercise. For what concerns the former, derivation of a clear and statistical significant signal has complicated by the low signal to noise ratio given by the precipitation intrinsic inter-annual variability. In addition, also bias correction represents a challenging exercise, given the asymmetry (no negative values) in empirical cumulative distribution of the variable. In addition to the adjustment of the statistical properties of precipitation events, even the frequency of the dry-wet days have to be treated. Given the well-known “drizzle effect” (too much days with very low precipitation events e.g. <= 0.1 mm/day instead of dry conditions), which could distort precipitation distribution, a preventive an RCM-specific precipitation threshold should be introduced before to define the correction function; as proposed by Teutschbein and Seibert 2012.

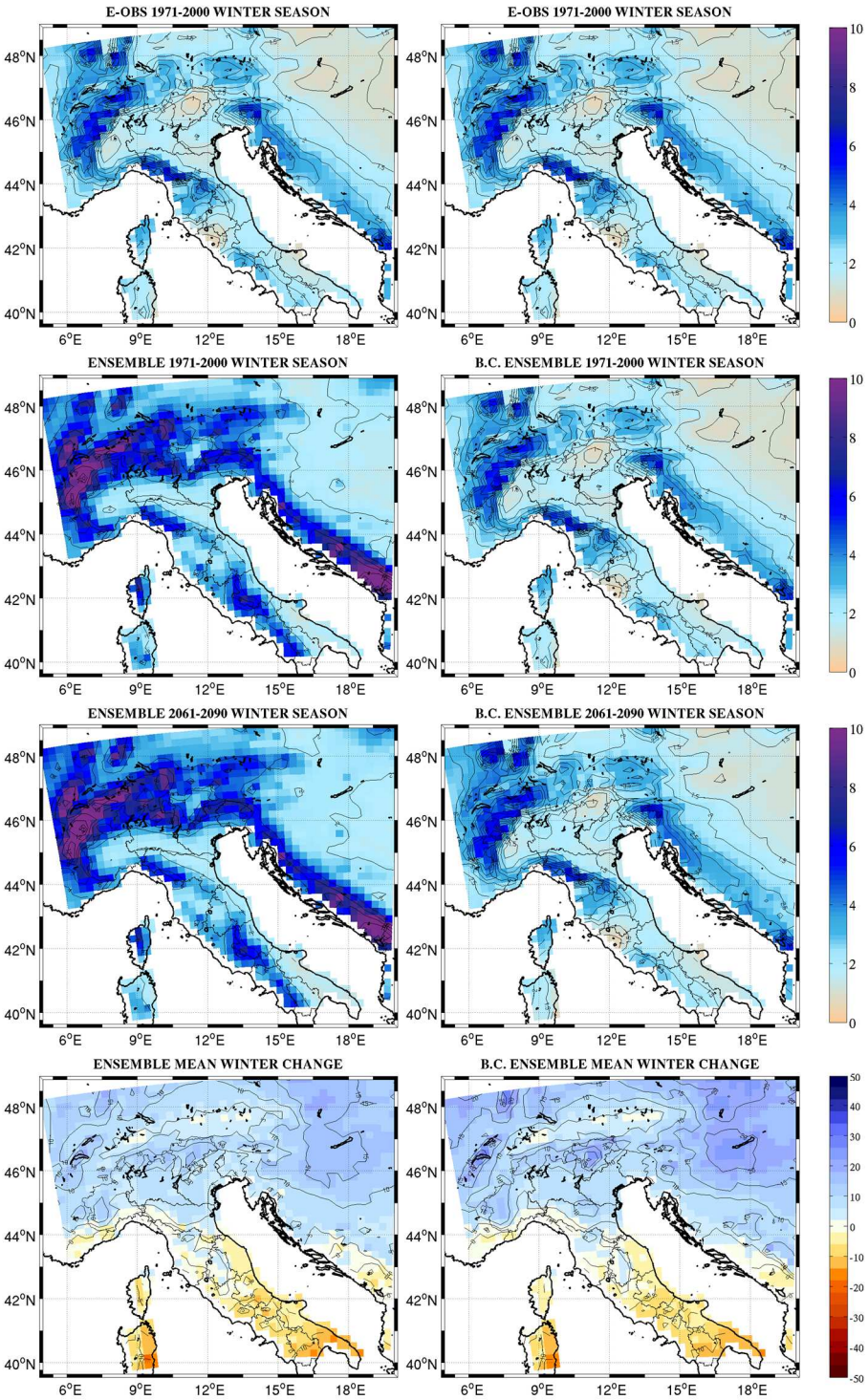

Figure 2.9. As for figure 2.7 but for winter season.

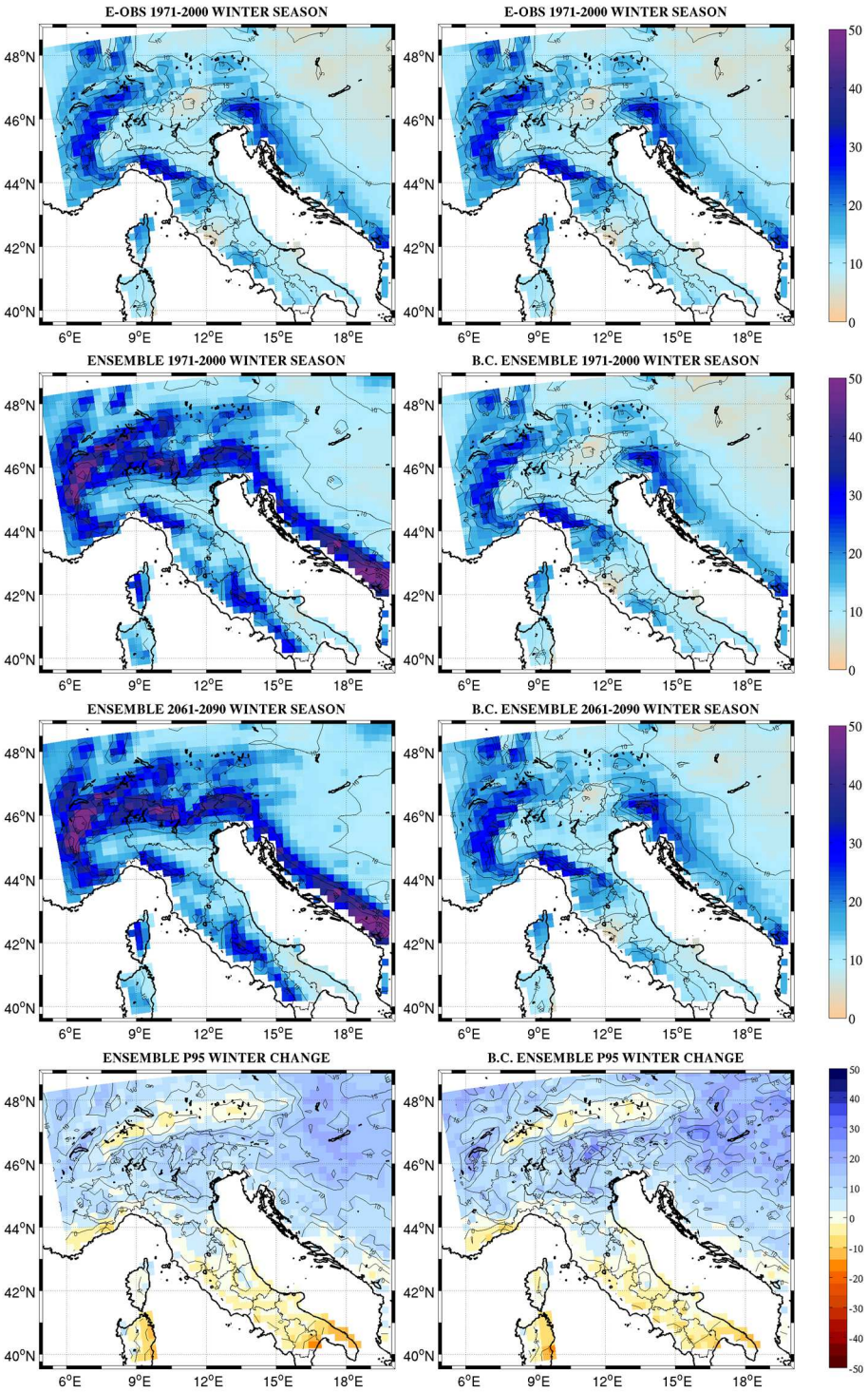

Figure 2.10. As in figure 2.9 but for the seasonal 95th percentile.

2.3 Conclusions and final remarks

In this section a statistical bias correction technique (empirical quantile mapping) was applied to a set of high-resolution climate change simulations over a domain roughly cover Italian peninsula. Impact of bias correction on the climate change signal referred to the ending part of 21st century for temperature and precipitation (mean and 95th percentile values) was analyzed. Connected with the previous first chapter, here particular attention was devoted to the analysis of discrepancies between original and bias-corrected ensemble mean climate change signal. Results would be discerned according to the different effect of statistical bias correction over temperature and precipitation signals. For temperature, bias corrected results showed a general reduction of the temperature signal compared to the original multi-model ensemble simulations (≈ 0.8 °C in summer and ≈ 0.5 in winter). This was detected only over plain and coastal areas differently by mountainous territories where the signal is preserved or locally increased. As impact models response are heavily dependent over mean and especially extreme events the analysis has repeated for the 95th percentile of the seasonal temperature distribution. The signal related the right tail of temperature distribution is higher than for the mean value. However, the effect of bias correction in both cases introduced a signal elevation-dependency since reduction of the signal only in plain and coastal areas resulted. Differently from the mean, over the 95th percentile the signal is in same case scattered strengthened especially in summer over mountainous areas. About precipitation we observed that bias correction do not alter the general magnitude of the climate change signal nor the spatial pattern. What is to underline is the relevant winter precipitation overestimation operated by the original multi-model ensemble simulation and how this bias was successfully removed by the bias correction application. This fact is not surprising since the correction function is built over the same thirty-year time slice and, by construction, the simulated distribution is mapped into the observed. At the end of the 21st century, the ensemble of simulation showed an enlargement of area characterized by positive 95th percentile signal indicating an increase of heavy-precipitation intensity. Bias correction does not alter severe-precipitation change signal. Only a slight strengthen of the negative signal over southernmost part of study area is resulted. It must be taken into account that bias correction techniques, not only empirical but also parametric methods (Piani et al. 2009; Piani et al. 2010), assume that the correction function remains constant between present and future climate. This assumption relies on the fact that bias does not depend by the forcing

level (e.g. atmospheric CO_2 concentration) but by the individual systematic distortion of the regional climate model and relative driving global climate model. Bias would be indeed considered constant or at least generated by the same misconception in the reference and future period as well. Repercussions of these concepts are considered in the next chapter where the bias correction effects are assessed also over a recent-past time segment not used in the calibration of the correction function. This give us a basic idea of the capability of quantile mapping of correcting a future time segment. Main outcome and motivation of this section is to develop a bias-corrected datasets (joined to an implicit performance evaluation) of a multi-model ensemble runs for climate impact model community, still not existing for Italian peninsula. Hagemann et al. (2011) highlights that in some world's region, the impact of the bias correction on the climate change signal may be larger than the signal itself, thereby identifying another level of uncertainty comparable in magnitude to the choice of climate model. Our results are not assignable to this latter statement. For the temperature the effect of bias correction is resulted connected to an intensity-dependency of model error found in several studies (Christensen et al. 2008; Themeßl et al. 2011a; Boberg and Christensen 2012). Following the analytical demonstration in Gobiet et al. (2015), quantile mapping is able to limit this dependency improving the quality of climate change signal. For precipitation, bias correction does not affect spatial pattern and magnitude of summer and winter climate change signal. Nevertheless, knowledge of the effect of bias correction effect on the climate change signal is still in their infancy. For this reason was chosen to provide both original and corrected climate change signal.

Bibliography

Boberg F, Christensen JH (2012) Overestimation of Mediterranean summer temperature projections due to model deficiencies. Nature Climate Change 2:433–436. doi: 10.1038/nclimate1454

Boé J, Terray L, Habets F, Martin E (2007) Statistical and dynamical downscaling of the Seine basin climate for hydro-meteorological studies. International Journal of Climatology 1655:1643–1655. doi: 10.1002/joc

Casati B, Yagouti A, Chaumont D (2013) Regional climate projections of extreme heat events in nine pilot Canadian communities for public health planning. Journal of Applied Meteorology and Climatology 52:2669–2698. doi: 10.1175/JAMC-D-12-0341.1

Christensen JH, Boberg F, Christensen OB, Lucas-Picher P (2008) On the need for bias correction of regional climate change projections of temperature and precipitation. Geophysical Research Letters 35:L20709. doi: 10.1029/2008GL035694

Deque M (2007) Frequency of precipitation and temperature extremes over France in an anthropogenic scenario: Model results and statistical correction according to observed values. Global and Planetary Change 57:16–26. doi: 10.1016/j.gloplacha.2006.11.030

Dosio a., Paruolo P, Rojas R (2012) Bias correction of the ENSEMBLES high resolution climate change projections for use by impact models: Analysis of the climate change signal. Journal of Geophysical Research: Atmospheres 117:1–24. doi: 10.1029/2012JD017968

Gennaretti F, Sangelantoni L, Grenier P (2015) Toward daily climate scenarios for Canadian Arctic coastal zones with more realistic temperature-precipitation interdependence. Journal of Geophysical Research: Atmospheres 120, doi: 10.1002/2015JD023890

Giorgi F, Hurrell JW, Marinucci MR, Beniston M (1997) Elevation dependency of the surface climate change signal: A model study. Journal of Climate 10:288–296. doi: 10.1175/1520-0442(1997)010<0288:EDOTSC>2.0.CO;2

Gobiet a., Suklitsch M, Heinrich G (2015) The effect of empirical-statistical correction of intensity-dependent model errors on the climate change signal. Hydrology and Earth System Sciences Discussions 12:5671–5701. doi: 10.5194/hessd-12-5671-2015

Haerter JO, Hagemann S, Moseley C, Piani C (2011) Climate model bias correction and the

role of timescales. Hydrology and Earth System Sciences 15:1065–1079. doi: 10.5194/hess-15-1065-2011

Hagemann S, Chen C, Haerter JO, Heinke J, Gerten D, Piani C (2011) Impact of a Statistical Bias Correction on the Projected Hydrological Changes Obtained from Three GCMs and Two Hydrology Models. Journal of Hydrometeorology 12:556–578. doi: 10.1175/2011JHM1336.1

Haylock MR, Hofstra N, Klein Tank a. MG, Klok EJ, Jones PD, New M (2008) A European daily high-resolution gridded data set of surface temperature and precipitation for 1950-2006. Journal of Geophysical Research: Atmospheres. doi: 10.1029/2008JD010201

Kotlarski S, Bosshard T, Lüthi D, Pall P, Schär C (2012) Elevation gradients of European climate change in the regional climate model COSMO-CLM. Climatic Change 112:189–215. doi: 10.1007/s10584-011-0195-5

Maraun D (2012) Nonstationarities of regional climate model biases in European seasonal mean temperature and precipitation sums. Geophysical Research Letters 39:1–5. doi: 10.1029/2012GL051210

Nakicenovic N, Swart R (2000) Special Report on Emissions Scenarios.

Panofsky, H. A., and G. W. Brier, 1968: Some Applications of Statistics to Meteorology. The Pennsylvania State University Press, 224 pp.

Piani C, Haerter JO, Coppola E (2009) Statistical bias correction for daily precipitation in regional climate models over Europe. Theoretical and Applied Climatology 99:187–192. doi: 10.1007/s00704-009-0134-9

Piani C, Weedon GP, Best M, Gomes SM, Viterbo P, Hagemann S, Haerter JO (2010) Statistical bias correction of global simulated daily precipitation and temperature for the application of hydrological models. Journal of Hydrology 395:199–215. doi: 10.1016/j.jhydrol.2010.10.024

Seneviratne SI, Lüthi D, Litschi M, Schär C (2006) Land-atmosphere coupling and climate change in Europe. Nature 443:205–209. doi: 10.1038/nature05095

Teutschbein C, Seibert J (2012) Bias correction of regional climate model simulations for hydrological climate-change impact studies: Review and evaluation of different methods. Journal of Hydrology 456-457:12–29. doi: 10.1016/j.jhydrol.2012.05.052

Themeßl MJ, Gobiet A, Heinrich G (2011) Empirical-statistical downscaling and error correction of regional climate models and its impact on the climate change signal. Climatic Change 112:449–468. doi: 10.1007/s10584-011-0224-4

van der Lindend P, Mitchell JFB (2009) Climate change and its impacts: Summary of research and results from the ENSEMBLES project.

3. Local climate scenario and the effect of bias correction on station-scale climate change signal

3.1 Datasets and methodology

3.1.1 Observational datasets

In this chapter, 21 temperature and 9 precipitation Marche region observational stations were considered as geographical reference for extracting climate simulations. Observational datasets are provided by Marche region "Centro Funzionale della Protezione Civile". Within this set, a subset of 8 stations has been chosen as representative (table 3.1). This subset provides on the one hand adequate temporal homogeneous datasets during the period 1970-2010, on the other hand a geographical distribution allowing to properly represent the two principal climatic sectors of Marche region. 4 stations are located along the coast or in valleys not far from the sea. The other 4 stations, are located at least 40 km far from the coast and represent a hill or high-hill/mountain elevation. However, only Camerino station could be considered as representative for mountain climate being the only station slightly over the limit of 600 m a.s.l., which, at this latitude, marks the border elevation between hill and mountain. In the context of climate scenario definition, observational datasets act as:

- Reference basis for validating original climate model simulations over a reference period (1971-2000).
- Reference basis to calibrate the correction function built from the quantile-quantile disagreement between observed and simulated datasets (1971-2000).
- Evaluation basis for bias-corrected simulations testing improvements when correction is applied over a period not used in the calibration phase (2001-2010).

Climatic sector	Stations	Altitude (m)	Latitude (N)	Longitude (E)	Variable
Coast-valley	Ancona	6	43°36'35"	13°27'13"	tas/pr
	Jesi	96	43°31'27"	13°14'48"	tas/pr
	Pesaro	11	43°54'45"	12°54'38"	tas/pr
	Senigallia	6	43°42'58"	13°12'31"	pr
Hill-mountain	Amandola	478	42°58'41"	12°21'16"	pr
	AscoliPiceno	136	42°51'30"	13°35'43"	tas/pr
	Camerino	670	43°80′25″	13°40′80″	tas
	Urbino	451	43°43'30"	12°38'08"	tas/pr

Table 3.1. Reference stations providing homogeneous time series 1971-2010 used as basis for climate simulations statistical correction. Amandola and Senigallia provided only for precipitation time series and Camerino only temperature.

3.1.2 Climate model simulations

To define future local climate scenario, a three high-resolution multi-model ensemble was employed. Climate models have been established for Europe geographical domain within the World Climate Research Program Regional Downscaling Experiment (EURO-CORDEX) initiative (Jacob et al. 2013). From the entire set of 11 regional climate models run in the context of EURO-CORDEX project, a subset of 4 models was considered covering time segment 1971-2090. With a dedicated function, climate simulations were extracted from the nearest grid-point to the observational stations as reported in figure 3.1.

Compared to the climate simulations run in the ENSEMBLES projects (van der Lindend and Mitchell 2009), two relevant developments regarding higher horizontal resolution and new radiative forcing boundary conditions are introduced. Concerning horizontal resolution, EURO-CORDEX simulations here considered shared a resolution of 12.5 km instead of 25 km characterizing ENSEMBLES climate simulations. At least in principle, higher resolution allows a better interpretation of local climatology dynamics. For instance, soil-atmosphere interaction and mutual feedbacks, local orography convective processes and cloud composition would be better represented on a finer resolution grid. However, not systematically higher resolution means better climate model simulations (Bellprat et al. 2013; Jacob et al. 2013; Jacob and Preuschmann 2014; Kotlarski et al. 2014; Smith et al. 2014; Maraun et al. 2015) since sub-grid processes parameterization and global model driving fields quality remain essential. The radiative forcing boundary conditions represent the second novelty of CORDEX project. In this experiment, future simulation segments consider the new Representative Pathway Concentration RCP4.5 and RCP8.5. Differently from SRES scenarios, (Nakicenovic and Swart 2000) RCPs do not specify socio-economic scenario, but assumes pathways to different target radiative forcing at the end of 21st century (Moss et al. 2010; Thomson et al. 2011; Riahi et al. 2011; Jacob et al. 2013). The RCP4.5 and RCP8.5 consider an increase of radiative forcing of 4.5 W/m^2 and 8.5 W/m^2 by the end of 21st century relative to the pre-industrial conditions. Representative Concentration Pathway 4.5 is a scenario of long-term, global emission of greenhouse gases, short live species, land-use-land-cover according to policies for achieving goal of limiting emissions and consequential radiative forcing which stabilizes radiative forcing (+4.5 W/m^2) by the 2100 (Thomson et al. 2011). Representative Concentration Pathway 8.5 assumes high demographical and economic growth, coupled to modest technological change and energy intensity improvements and absence of decisive mitigation policies. These assumptions lead

to an increase of radiative forcing of 8.5 W/m^2 relative to the pre-industrial conditions (Riahi et al. 2011). Follows a resuming table with regional climate models providing climate simulations.

Institute	RCM	Driving GCM	Resolution (km)	Period	RCP	Variable
SMHI	RCA4	EC-EARTH	12.5 km	1971-2090	4.5/8.5	tas; pr
KNMI	RACMO22E	EC-EARTH	12.5 km	1971-2090	4.5/8.5	tas, pr
CLMcom	CCLM4	CM5	12.5 km	1971-2090	4.5/8.5	tas
DMI	HIRAM5	EC-EARTH	12.5 km	1971-2090	4.5/8.5	pr

Table 3.2. Regional climate models employed in the local experiment.

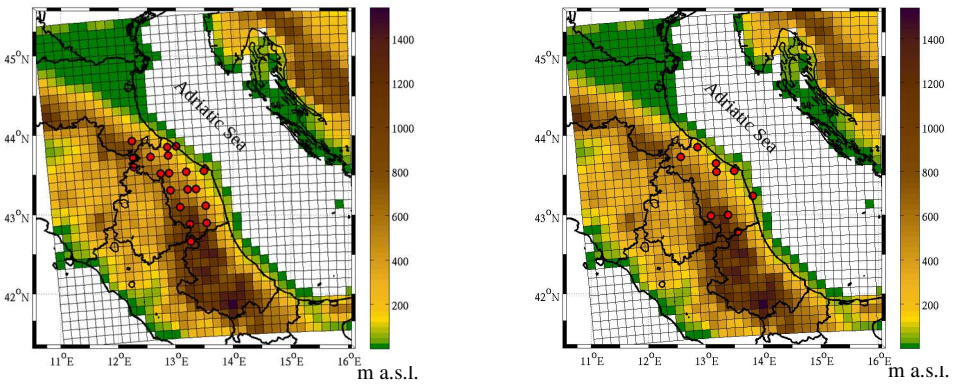

Figure 3.1. Geographical distribution of temperature (left) and precipitation (right) grid nodes providing simulations. They represent the nearest grid points to the observational stations. Model grid is overlaid to the orography of a representative climate model (RCA4). (For temperature, in two cases, two observational weather stations are so close that fall within the same grid-cell).

3.1.3 Methodology: Bias correction and downscaling of climate simulations

It is well known that climate model outputs cannot be directly used as inputs in impact models without some previous post-processing, aimed to reduce systematic errors (Wood et al. 2004; Boé et al. 2007; Mpelasoka and Chiew 2009; Maraun et al. 2010; Hagemann et al. 2011; Themeßl et al. 2011b; Themeßl et al. 2011a; Dosio et al. 2012; Ehret et al. 2012; Gudmundsson et al. 2012; Thrasher et al. 2012; Hoffmann and Rath 2012; Maraun 2013; Maurer and Pierce 2014; Smith et al. 2014). Bias correction are techniques identified to reduce model errors making climate model outputs suitable as input in impacts modeling.

In local climate change studies, where simulated and observed time series spatial-scale mismatch exists, bias correction in addition to error reduction is expected to downscale climate simulations to station scale. In such context, two main sources determine discrepancies between simulated and observed values: systematic climate model error given by the physical processes misrepresentation and representativeness error, rising from the spatial scale mismatch between observed and simulated datasets. To remedy to the double source of model error, post-processing technique here chosen, consists on an empirical statistical bias correction defined as quantile mapping (Deque 2007; Themeßl et al. 2011a). Amongst several bias correction methodologies quantile mapping has been demonstrated to successfully reduce discrepancies between observed and simulated climatic datasets (Themeßl et al. 2011b; Teutschbein and Seibert 2012). The basic idea of quantile mapping is to describe the discrepancies between the simulated and observed distribution at specific quantile during a common, at least thirty-year, and reference (or calibration) time segment. Then is derived a correction function that could be though as the arithmetic operation that must be performed on each simulated quantile to obtain the corresponding observed value (Gennaretti et al. 2015). The correction function was applied to all daily physical values of the reference and future simulations. Here the key-concept is matching each point-scale observed dataset statistical distribution to the distribution of simulation belonging to the nearest grid point. In this approach, an area-averaged simulation is corrected with the statistical intensity characterizing a point-scale observation. This particular configuration allows combining climate simulations error reduction and the increase of spatial resolution (downscaling).

Technically, the statistical adjustment procedure could be discerned in: (i) correction function calibration, (ii) evaluation and (iii) application to a future climate simulation. The first phase consists on deriving a correction function from the discrepancies between

simulation and observation at specific quantile over a common period (1971-2000). Moreover it is possible to inspect how biases are differently distributed along the statistical distribution of simulated variables. I fact it is expected that different statistics will be affected by different biases. Moreover, biases will differently affect the different models and the different stations characterized by different morphology and climate. This phase, gives us a basic idea on the models capability of representing a point-scale climatology. Once derived, the correction function is applied over this same time segment obtaining the reference period (1971-2000) bias-corrected simulations.

Evaluation phase consists on applying the correction function over a block of data (2001-2010) not used in the derivation of the correction function (1971-2000). This phase allows inferring the plausibility of correcting a future time segment not involved in the definition of the correction function. Finally, the correction function derived in the calibration segment, is applied to a future simulation for performing the bias-corrected climate change signal. For correcting values present in the future simulation and not in the calibration (outside the calibration range), a constant extrapolation at the lowest and highest quantiles of the calibration range was used. Bias correction function is built up on daily (monthly or seasonal basis) observed and simulated time series. As for the original simulations a multi-model ensemble (arithmetic average of all the simulation used) has been performed with the bias-corrected simulations. Finally, the two (original and bias corrected) ensembles have been employed to define a station-wise climate change signal.

In figure 3.2 quantile mapping calibration main methodological steps are shown. Panels *a* and *b* report spatial distribution of grid nodes providing simulated datasets (*a*) and the corresponding observational stations (*b*). Quantile-quantile plot of a representative (Ancona station) simulation matched with the corresponding observed time series is shown in panel *c*. Quantile-quantile plot consists on the comparison of the two ranked data sets providing the different mismatch (error or bias) magnitude along the entire statistical distribution. Moreover, the variance mismatch between observation and simulation is indicated by the slope over the diagonal x = y. The area between the x = y axes and quantile-quantile plot line also defines the correction function that will be applied to the simulation. Panel *d* represents the value of the correction function at each simulated quantile. This correction function has been interpolated to the query points represented by the physical values of the daily simulated time series (panel *e*) obtaining bias-corrected time series (panel *f*). Panel *g* reports the observed time series to quantify the improvement of the corrected simulation versus the

original one. Means and standard deviations (respectively green and purple lines) are reported to facilitate the evaluation. Actually, the resulting roughly perfect correspondence between corrected and observed time series is not surprising, since the correction function has been built over the same time segment (calibration period 1971-2000).

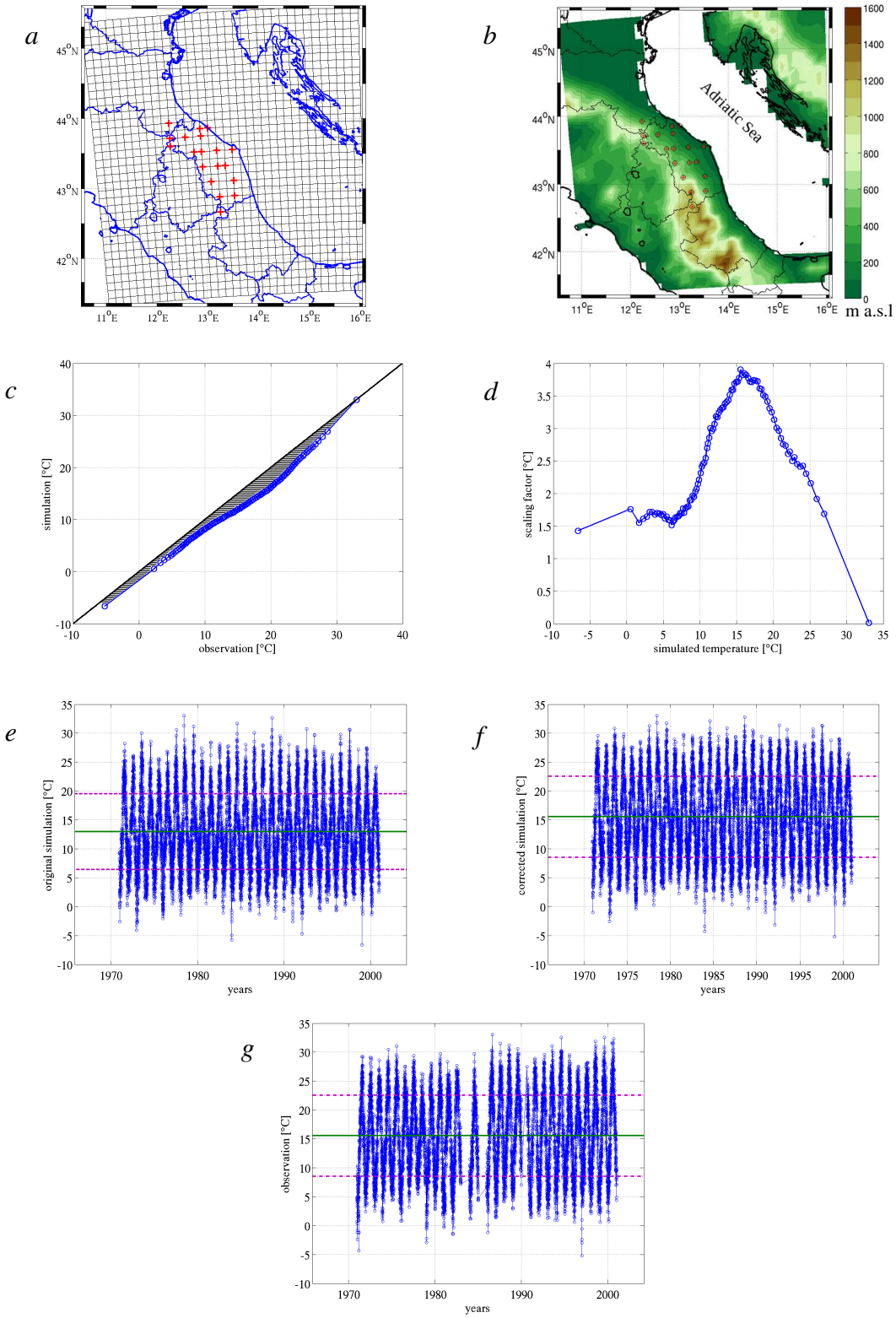

Figure 3.2. Correction function calibrations methodological steps. Red crosses in panel a indicate grid nodes providing climate simulations (for temperature). Panel b geographical distribution of weather stations providing temperature observed time series. Panel c reports the observation vs. simulation quantile-quantile plot for the representative station of Ancona. Quantile-specific correction function is reported in panel d. Panels e, f and g report respectively original simulation, bias-corrected simulation and observation. In panels e f and g green and purple lines indicated relative mean and standard deviation of respectively raw simulation, bias-corrected simulation and observation.

3.1.4 Methodology: Climate change signal

With *original* and *bias-corrected* simulations, a station-wise climate change signal was performed according to the following methodologies:

Climate change signal annual cycle

Consists on assessment of projected monthly means changes over the reference Marche region stations. Daily simulations are aggregated on monthly basis for the reference and future periods. Then the monthly mean values characterizing reference segment are subtracted to the monthly means characterizing future segment.

$$Temperature_{Monthly_{ccs}} = \overline{scen(\imath)} - \overline{ref(\imath)}$$
$$with\ i = 1 : 12$$

$$Precipitation_{Monthly_{ccs}} \left[\frac{\overline{(scen(\imath)} - \overline{ref(\imath))}}{\overline{ref(\imath)}} \right] * 100$$
$$with\ i = 1 : 12$$

Statistical significance of the monthly mean change signal has been tested through Wilcoxon rank-sum test (Wilks, 2011). For this analysis, the correction function is month-specific, namely singularly calibrated over single month pertaining to calibration time segment (1971-2000). Representative results for temperature and precipitation RCP8.5 and ending 21st century scenario (2061:2090 – 1971:2000) will be reported.

Climate change signal distribution

To not limit our considerations over climate change signal and effect of the statistical adjustment over mean values, assessment of climate change signal affecting the entire statistical distribution (original and bias-corrected simulations) has been provided. Here, both original and bias-corrected climate variables have been quantile-ranked and the climate change signal was computed quantile by quantile.

$$Temperature_{Distribution_{ccs}} = scen(P) - ref(P)$$

$$with\ P = quantiles\ (1{:}\,99)$$

$$Precipitation_{Distribution_{ccs}} = \left[\frac{\left(scen(P) - ref(P)\right)}{ref(P)}\right] * 100$$

$$with\ P = quantiles\ (1{:}\,99)$$

It allows analyzing different signal magnitude over the different statistics (low, middle, high percentiles) and the effect of the bias correction as well. Results are reported for two different time horizon (middle and end 21st century) according to two emission boundary conditions (RCP 4.5 and RCP 8.5). Correction function is seasonally calibrated for temperature and over the entire calibration segment for precipitation. For this latter variable, only rainy days have been considered.

Response of local hydrologic cycle to global warming

One of the major concerns of climate change outcomes refer to alteration of the hydrologic cycle given the increase in moisture holding capacity of a warmer atmosphere. To provide a comprehensive characterization of expected changes in precipitation a station-wise Hydro-climatic intensity index (Giorgi et al. 2011) was computed. This index integrates mean annual precipitation intensity with mean annual dry spell length, considering the response of the two metric deeply interconnected to global warming. It aims to investigate a hypothetic acceleration of the hydrologic cycle in a warmer atmosphere. The trend assessed regards the period 1971-2100. As the previous analysis, the index was computed with both original and bias-corrected precipitation simulations.

$$HY_{INT} = \overline{INT(y_i)} * \overline{DSL(y_i)};\ where\ y\ indicates\ i^{th}\ year\ from\ 1971\ to\ 2100$$

$\overline{INT}$ = mean annual precipitation intensity during rainy days.

$\overline{DSL}$ = mean annual dry-spell-length.

3.2 Results and discussions

As previously stated in the 3.1.1 section, results here reported refer to stations belonging to the 8 representative stations (of coast/valley and hill/mountain sectors). Besides Marche region climatic features representativeness, these stations provide time series appropriately long to evaluate statistical correction over a time segment not used in the calibration.

3.2.1 Quantile mapping bias correction

Before directly analyze results, some previous considerations could be helpful for an accurate comprehension of temperature and precipitation correction functions calibration (sections: 3.2.1.1 and 3.2.1.3). The quantile-quantile plot on the left panels describe the capability of models to reproduce observed variable distribution during the calibration period (1971 - 2000). Through this kind of representation, it is possible to infer magnitude of discrepancies between simulated and observed values over the entire statistical spectrum. It is indeed possible assessing climate models capability on reproducing mean values, extremes and variance of the observed local climatology. Variance biases are identified by the slope of the quantile-quantile curve over the diagonal (x = y) line. The higher the slope of the simulation-observation matching curve, the higher is the underestimation of the observed variability. Finally, a perfect correspondence between simulation-observation curve and diagonal (x = y) line represent a perfect simulation of observed local climatology. In the assessment of results, it is important to take in account that simulations provide an area-averaged (12.5 km^2) climatic data validated against observed data representative for a point-scale station climatology. Repercussion of spatial-scale mismatch may be particularly relevant for the reproduction of distribution-tails events. Indeed, strong atmosphere and soil-moisture interactions and other physical feedbacks play key role on determining temperature and precipitation extremes. These processes, in some cases, are still not completely understood or properly parameterized and consequently misrepresented even in the newest generation of regional climate models (Christensen et al. 2008; Kotlarski et al. 2014). Even adopting very high resolution, models cannot identifying micro-scale processes occurring between soil, vegetation and atmosphere that characterize climate particularly in mountain areas. Moreover, in a local context a relevant role could be played by the representativeness error occurring when an area-averaged simulation attempts to reproduce point-scale

climatology. This latter error sources has to be regarded not as an intrinsic model error but determined from the gap between grid box and point scale.

3.2.1.1 Correction function calibration – Temperature

In figure 3.3 is reported calibration of the quantile mapping correction for Ancona, representative station for coastal area climatology. Given the small number of ensemble members used in the local experiment, calibration results for all the three models have analyzed. In fact, adopting an arithmetic-averaged ensemble approach, results from the individual members may greatly affect the overall ensemble simulation. Concerning the coastal representative station, the best simulation has provided by CCLM4 model with an annual mean temperature of 13.9 °C against an observed of 15.5 °C. A moderate underestimation ≈ 2.5 °C affects the left tail of distribution, representing low winter values. Original simulation well reproduced right part of distribution, namely high summer temperature, with a negative bias ≈ 0.5 °C. Observed variance is only slightly overestimated (less than 2 °C). The other two models in general underestimate observed temperature. RACMO22E model presents negative bias of ≈ 3.5 and ≈ 4.5 °C respectively over mean and 95th percentile temperature. The variance resulted slightly underestimated. RCA4 model performs negative bias of ≈ 2.5 °C over the mean temperature. This latter model, noticeable better reproduced distribution tails (warm and cold extremes) than the central part of distribution. Right panels in figure 3.3 shows bias corrected simulations. We can note that bias correction leads to a roughly perfect simulation of the past reference period over the entire distribution for all the models. These results are not surprising since by construction statistical correction maps simulated empirical cumulative distribution such it is equal to the observed one. This is true when the correction function is applied to the block of data employed to calibrate correction function. In figure 3.4, the same bias correction exercise has reported but for another station, located in the hill-mountain band of Marche region. This station represents different morphological and climate conditions. Distance from the sea and the altitude (631 meters a.s.l) determines different climate features compared to the previous case. In this context, it is interesting to assess the capability of climate models of reproducing climatology over morphological complex terrain. In such heterogeneous morphology, representativeness error could play a major role in determining simulation bias than in valley-coastal area. Looking at models response, it is noticeable a general temperature underestimation, greater than in the previous representative station. CCLM and RCA4

models show similar mean bias ≈ 3 °C. Over 95th percentile are respectively of 2.6 °C and 1.3 °C. To underline is that CCLM model outperforms RCA4 model on observed temperature variability reproduction. RACMO22 model resulted poorly able to reproduce mean and 95th percentile observed temperature value with a negative bias to ≈ 5 °C resulted. A common deficiency of models regards the misrepresentation of the cold extremes on which a considerable underestimation (negative bias) resulted (up to -6 °C). This outlines potential repercussions of spatial mismatch over complex territories. Biases are successfully removed in the right panels of the figure, where the bias corrected simulations have shown. Again, results have to be considered as the direct effect of building and applying correction function over the same time segment.

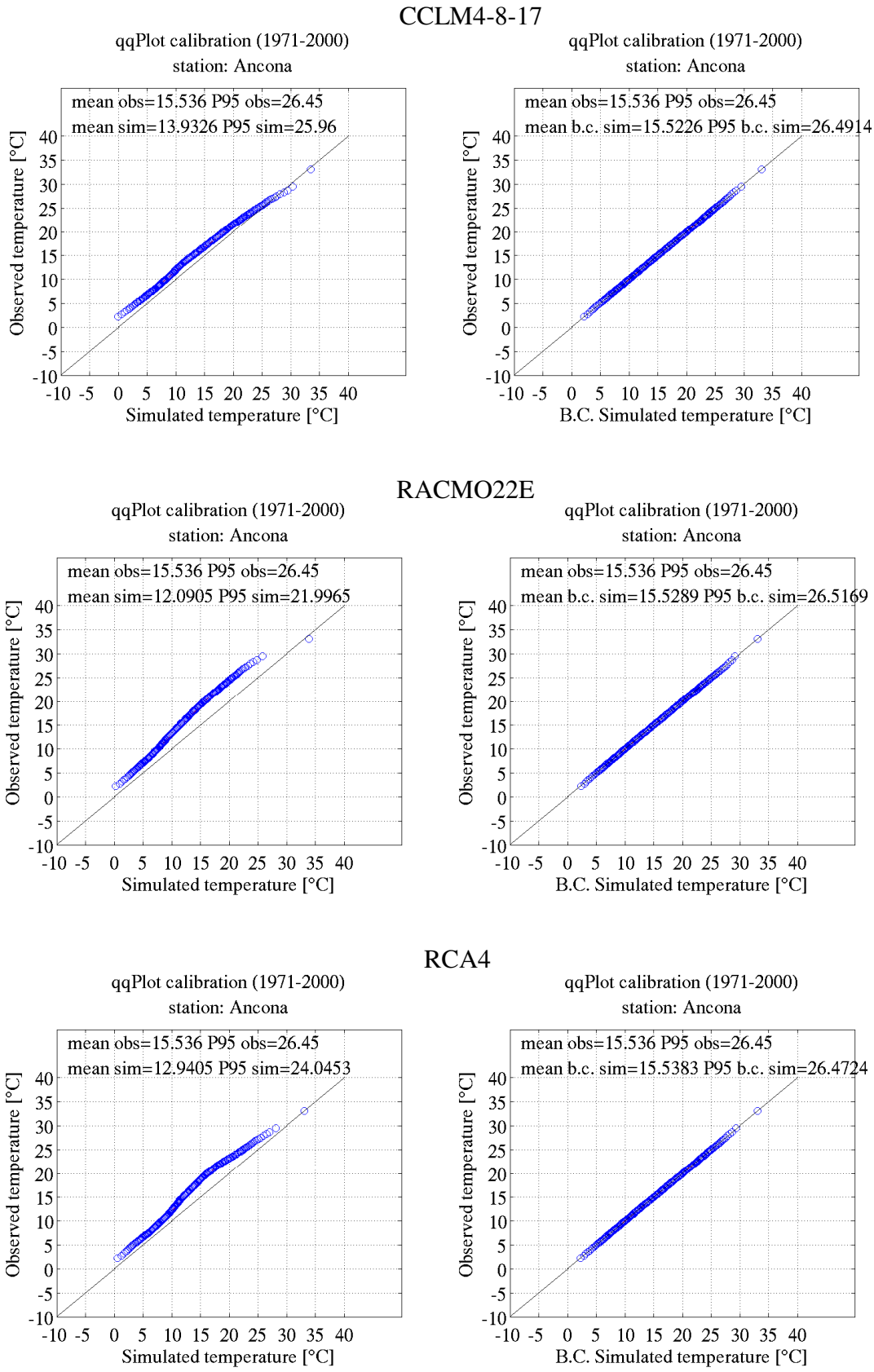

Figure 3.3. Bias correction calibration for the three regional climate models. Simulations refer to Ancona station, representative for coastal area of Marche region. On the left panels quantile-quantile plot of the original simulations and observations. On the right panels, quantile-quantile plot of the bias-corrected simulations joined with the observations. During calibration phase the correction is derived and applied over the same time segment (1971 - 2010).

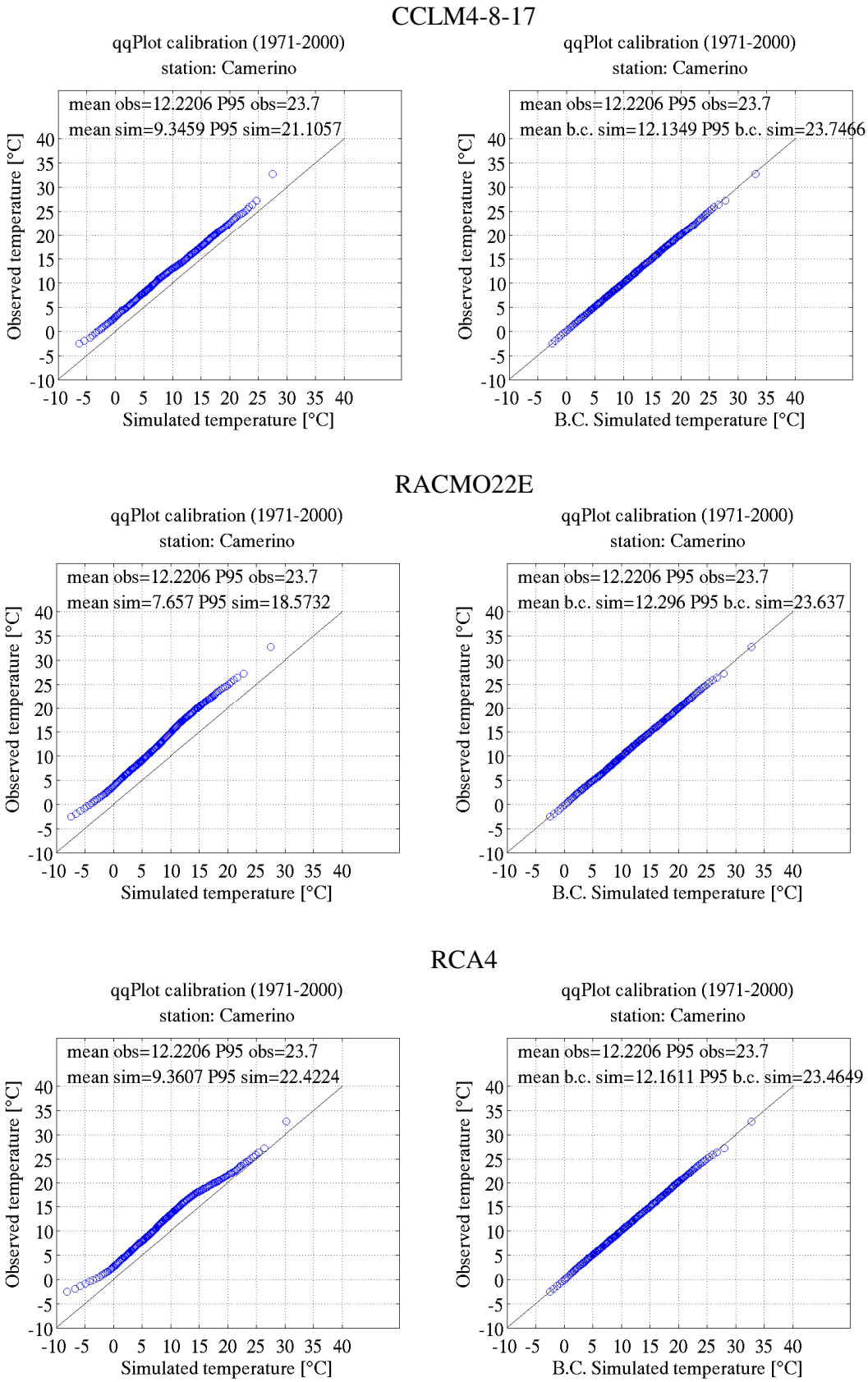

Figure 3.4. Same as figure 3.3 but for mountain area representative station of Camerino (631 meters above sea level).

3.2.1.2 Correction function evaluation – Temperature

Figures 3.5 and 3.6 report results for the evaluation phase of bias correction technique. This phase wants to address focal question about the capability of bias correction of correcting a simulated time series not used in the calibration of correction function. Through the evaluation phase, we get a basic idea of the plausibility of correcting future simulation. Indeed, the effect of the quantile mapping will be evaluated over a 10-year period did not used in the calibration of the correction function. Ten-year period could result short for properly encompassing intrinsic natural climate variability but it represents longest common period between observations and simulations. Moreover, calibrating correction function in time segment shorter than thirty years could imply even greater drawbacks. Figure 3.5 reports the effect of bias correction over temperature simulation 2001-2010 period for Ancona station. The correction function, as in the previous section, was calibrated over the period 1971-2000. As expected, bias distribution over the statistical spectrum resembles those seen over the 1971-2000 period. Also in this time segment, CCLM4 model well performs on reproducing observed temperature climatology. For this model, the bias for the mean and 95th percentile, are respectively of 2.5 °C and 1.5 °C. Also in this case high temperature resulted better reproduced than the mean value. The bias corrected simulations present a reduction of bias with a residual bias of 0.9 °C over mean and 1.1 °C over 95th percentile. KNMI-RACMO22E model is affected by considerable negative bias over mean and 95th percentile temperature, respectively of 3.8 °C and 5.6 °C. In the bias corrected run we note a strong reduction of bias especially over the mean value (from 3.8 °C to 0.3 °C). Left and right tails of distribution, even if reduced, are still affected by bias (from 5.6 °C to 1.2 °C at the 95th percentile). Bias correction well performs even in the third ensemble member SMHI-RC4 with original bias on mean and 95th percentile bias of ≈ 3 °C and ≈ 3.5 °C are respectively significantly reduced to 0.4 °C and ≈ 1 °C.

In figure 3.6 evaluation phase results for Camerino station have reported. This latter station representative of the inland mountainous regional band presents different climate condition compared to the coastal area. In this area, mitigating see effect is poor given the block effect provided by the eastern part of Appenines ridge. As seen in the calibration phase climate models over complex orography terrains, worsen their capability on reproducing observed climatology. It is now interesting to assess the effect of bias correction starting from higher original-simulation bias.

All the three ensemble members underestimate temperature over the entire distribution, particularly over the left tail, representing cold winter extremes.

As expected, CCLM4 model degrades its performance compared to the coastal station, with negative bias of ≈ 3.5 °C and ≈ 4 °C respectively for mean and 95th percentile. Over the left tail of distribution, the bias resulted even higher, ≈ 5 °C. It is noteworthy the reduction of negative biases in the corrected simulation, from 3.5 °C to 0.7 °C. Even out of the calibration-temporal range biases are reduced over all the statistical distribution, improving simulation over both central part and tails of distribution. This quantile mapping property is particularly relevant for impact research (such hydrology or agriculture) that relies on a proper representation of future extreme events. Bias correction reduces negative original simulation bias affecting the 95th percentile from ≈ 4 °C to ≈ 1.2 °C.

RACMO22 model roughly confirms severe bias resulted for coastal station. KNMI institute model simulates mean temperature value with an underestimation of ≈ 4.5 °C and ≈ 6.5 °C for what concerns the 95th value. Again, bias correction, regardless the original simulation bias magnitude, corrects climate simulation. After quantile mapping, simulation shows no bias over mean temperature and residual underestimation over the 95th percentile, ≈ 1.5 °C. Similar are the results for SMHI RC4 model. Quantile mapping cancels mean negative bias (originally of ≈ 3 °C) and improves both tails of distribution where 95th percentile bias of ≈ 2.5 °C is dampened to ≈ 1.2 °C.

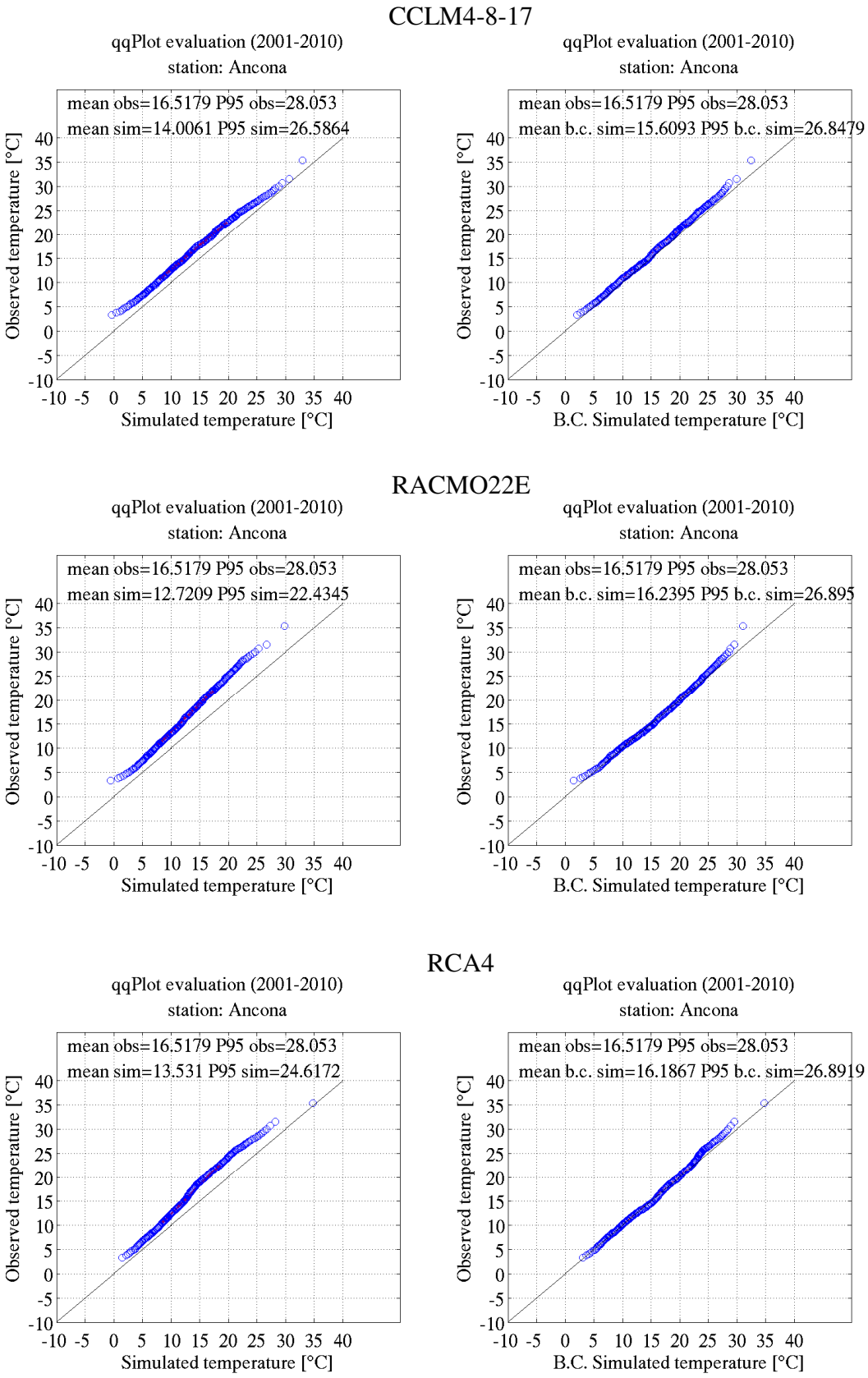

Figure 3.5. Same as figure 3.3 but for the bias correction evaluation: in this phase, the correction is derived over the 1971-2000 time segment and applied to 2001-2010 time segment.

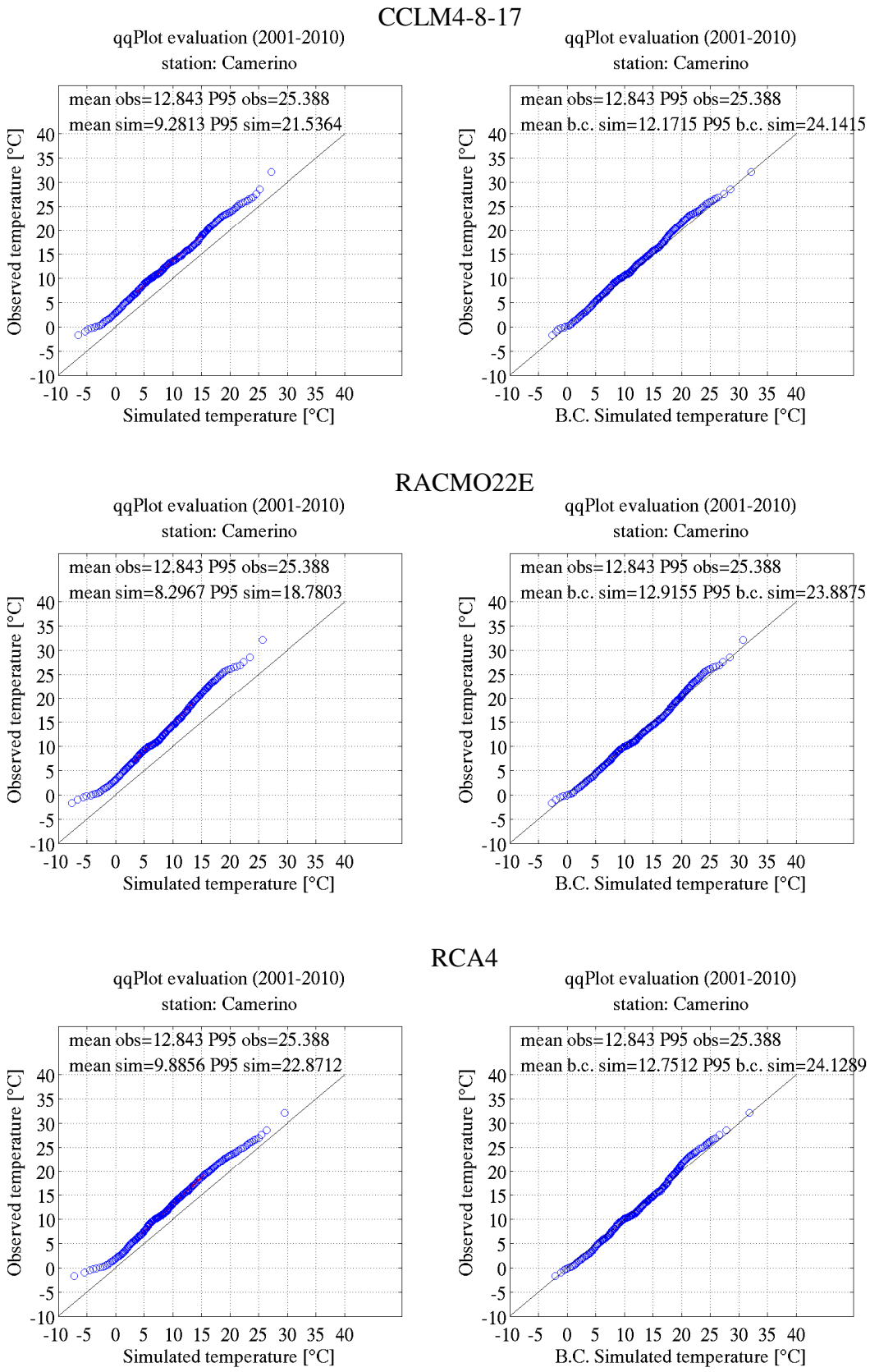

Figure 3.6. Same as figure 3.5 but for Camerino station.

Analyzing calibration and evaluation phase together, we note general underestimation of simulated temperature over both coastal and mountainous representative stations. As expected, mountainous station presents major biases compared to those affecting coastal station. More in detail, negative biases affect left tail of temperature distribution representing cold winter extreme, underestimating observation up to ≈ 5 °C over mountainous station. In addition to the intrinsic climate model error, discrepancies could be observation-simulation spatial scale mismatch, since physical feedbacks driven by the local morphology can only be roughly captured in area-averaged simulation. Soil-atmosphere interaction feedbacks could play role on the simulation of temperature extremes. For the bias characterizing cold temperature over mountainous station, an improper representation of snow cover and relative albedo-effect could determine the severe underestimation over winter cold temperature observed in all the models.

Quantile mapping for all the three models and over the two representative stations successfully reduced bias. For the calibration phase, by construction, simulation statistical distribution mapped into the observed given roughly perfect results. Residual discrepancies belong, once again by construction, to the linear interpolation involving values located between two neighboring quantiles. More important are results of evaluation phase. Here, bias affecting both mean and 95^{th} percentile values are considerably diminished. In general, residual bias are less than the 1 °C for the mean value and slightly higher for the right tail of distribution (up to 1.5 °C). It is interesting noting that the capability of quantile mapping of reducing bias is not dependent (not proportional) to the original simulation bias magnitude well performing on coastal and mountain station as well. An example is the statistical correction of Camerino station provided by RACMO22E model (figure 3.6, central panels). The original simulation resulted affected by the highest bias was equally corrected and brought to values not far from those observed. The correction function effect is particularly palpable over the sever bias of left tail of distribution resulting the most biased part of distribution.

Results point out usability of quantile mapping in the context of a station-wise approach where relevant spatial scale mismatch exists. In this configuration, quantile mapping couple error reduction and downscaling effect, accounting also for the representativeness error. Finally, as easily predictable, at local scale model outputs cannot be directly used as input of climate impact models since affected by relevant biases. Errors of such magnitude could be

directly inherited and amplified in the impact-modelling phase leading to important distortions in the results over the specific field.

3.2.1.3 Correction function calibration – Precipitation

As for temperature, bias correction calibration and evaluation results are reported for two representative stations. One for valley-coast and one for hill-mountain regional sector. Figure 3.7 shows bias correction calibration phase for the three climate models employed for Pesaro station, representative for coastal Marche region area. In the left column, quantile-quantile plots with the observed and original simulated precipitation matched over the reference period 1971-2000 are displayed. Same as left column but for the bias-corrected simulations in the right column panels. The DMI-HIRAM_5 model outperforms the other two climate models, well reproducing distribution of reference precipitation climatology. It could be noted a constant underestimation of precipitation roughly proportional with statistical distribution of the variable. In any case, for this climate model bias resulted low, with no bias for the mean precipitation value and an underestimation of 95th precipitation percentile of 1.1 mm ≈ 10% is resulted. Bias correction applied over the same calibration block of data by construction leads to a roughly perfect simulated precipitation distribution. The other two climate models, RACMO22E and RCA4, show similar behavior, well reproducing the mean precipitation values and underestimating high-precipitation intensity events of roughly 1.5 mm (less than 10%). Bias corrected precipitation roughly perfectly reproduce observations except for percentiles >=99th where residual biases resulted.

In figure 3.8, bias correction calibration for Urbino station is shown. As expected in more complex morphology station larger bias resulted. The bias as the same negative sign (underestimation) of the coastal area representative station but the magnitude resulted amplified. The best performing model is RACMO22E, which results in the central panels of the figure 3.8 are displayed. -0.2 mm and -3 mm are biases resulted respectively for the mean and 95th percentile of the reference period daily-cumulated precipitation. Very high biases resulted for the RCA4 climate model reported in the bottom panels of figure 3.8. The original simulation underestimates of ≈ 1 mm the mean precipitation value representing a percentage of roughly 50%. The negative bias is kept constant over the 95th percentile where an observed value of 14.4 mm is simulated equal to 7.8 mm. The Intermediate performance belongs to the DMI HIRAM_5 climate model with bias of ≈ 0.8 mm and ≈ 5.5 mm respectively for mean and 95th percentile. Again, by construction, biases are successfully removed also in

more biased original simulation. In the next section, will be interesting to inspect if quantile mapping will be able to remove such relevant bias, even applied over a block of data not used to calibrate of the correction function.

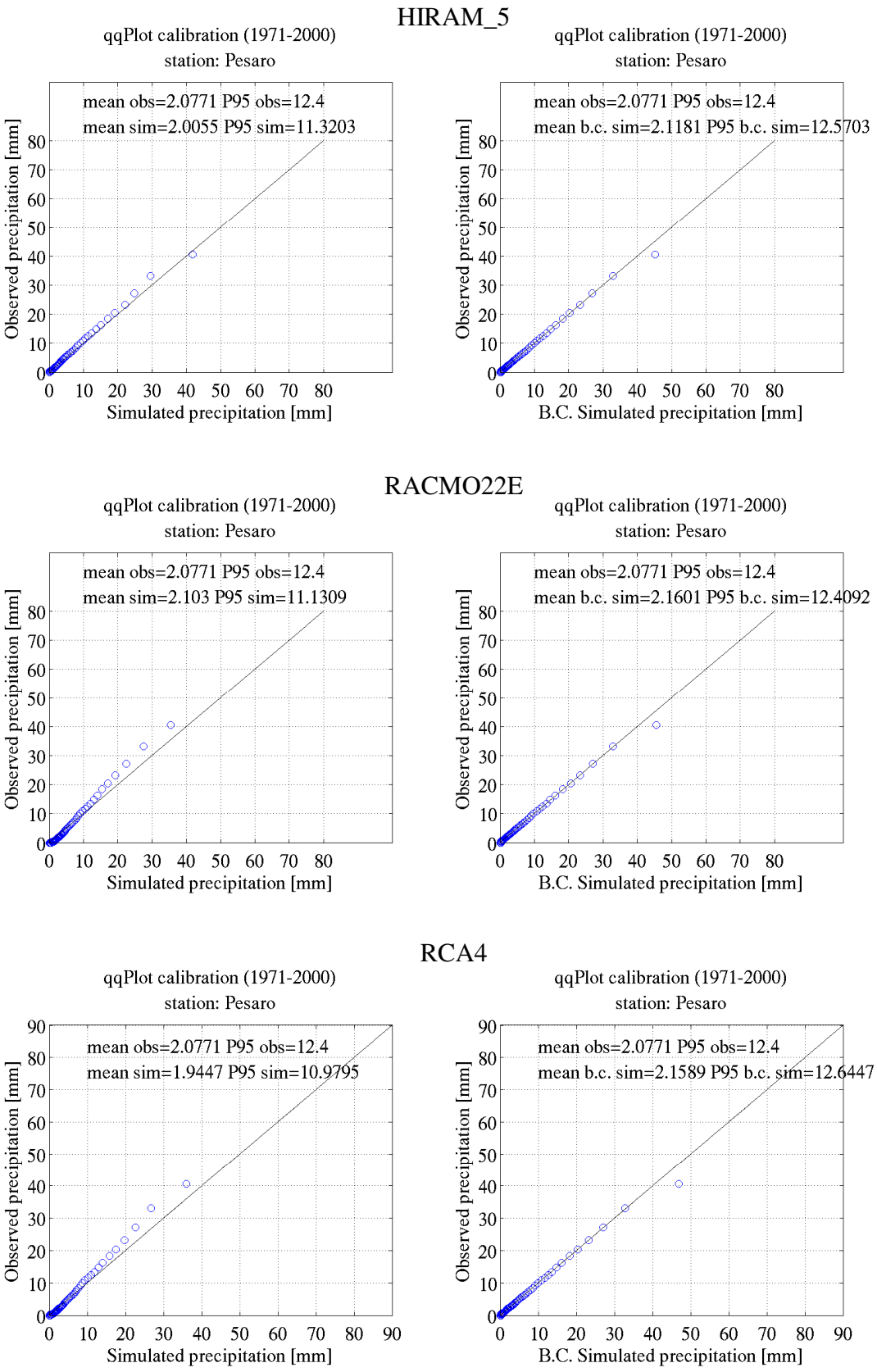

Figure 3.7. Bias correction calibration phase for precipitation; here reported coast representative station of Pesaro.

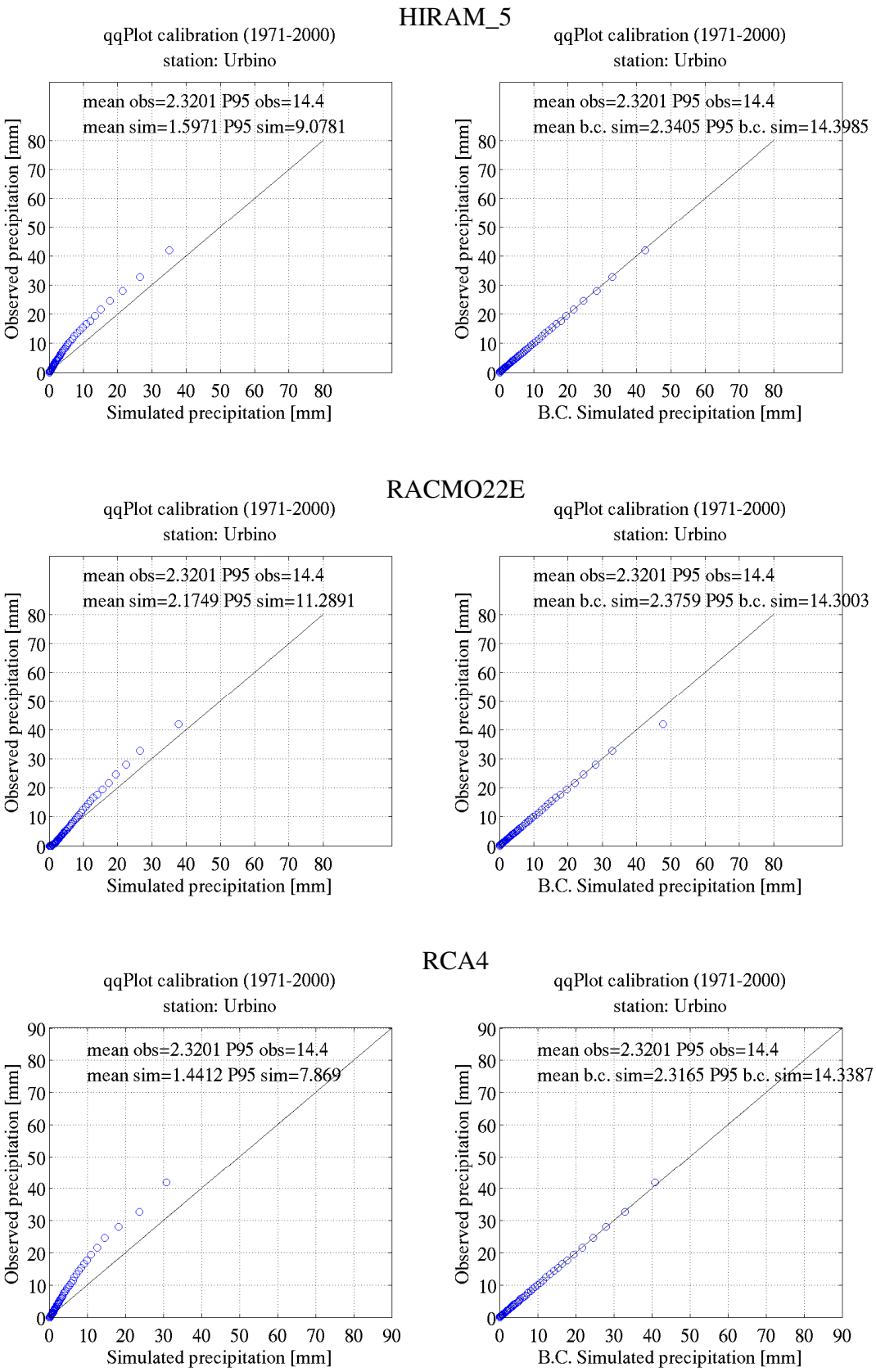

Figure 3.8. As for figure 3.7 but for hill representative station of Urbino. Noteworthy is higher negative bias affecting original climate model simulations in more complex orography. In particular, RCA4 model shows a negative bias over the 95th percentile of roughly 50%.

3.2.1.4 Correction function evaluation – Precipitation

Figure 3.9 reports bias correction evaluation for precipitation over representative coastal area station of Pesaro. As for temperature, the correction function has derived over the period 1917-2000 and applied over a 2001-2010 simulation block of data. In the left column original and in the right column bias-corrected simulations are shown. Simulation performed by DMI-HIRAM_5 model are reported in the upper panels. According to what seen in the reference period this model well reproduce precipitation statistical distribution, even over the tail representing severe-precipitation events. Quantile mapping application reduces the negative bias over mean value from 0.2 mm to 0.1 mm and over 95th percentile from ≈ 1.7 mm to 0.7 mm. A slight over correction results for the RACMO22E model over the 95th percentile (figure 3.8 central panel – right column). This model was able to almost perfectly reproduce observed precipitation climatology (with a negative bias of 0.4 mm affecting the 95th percentile). Statistical correction has an inflation effect, adding a positive bias over the 95th percentile even if less than 1 mm. The same effect has been observed for the SMHI - RCA4 model where a slight underestimation of the 95th percentile ≈ 0.4 mm is over corrected into an overestimation of ≈ 1.1 mm. However, it represents negligible drawback comparing the inflation to the absolute value of 14 mm (corresponding to the 95th percentile of the precipitation statistical distribution).

Over the other representative station, bias correction application has been demonstrated crucial for reducing simulation errors. As shown for the calibration phase simulated precipitation of Urbino station resulted heavily biased, especially for HIRAM_5 and RCA4 models. Even calibrated and applied over different blocks of data quantile mapping well performs on correcting mean and extreme values of simulated precipitation. For the HIRAM_5 model, significant biases (0.8 mm and ≈ 5 mm, respectively for mean and 95th percentile representing a percentage bias of roughly 30-40 %) have been successfully removed. Residual bias does not exceed 0.5 mm (95th percentile). In front of very well performing simulation (RACMO22E) quantile mapping reproduces again a slight inflation of the correction. The bias over the mean are completely removed but the 95th percentile is over corrected where a negative bias of 1.5 mm becomes a positive bias of the same magnitude. Quantile mapping has been demonstrated to be crucial on reducing high bias characterizing the simulation from RCA4 model. Similar to the HIRAM_5 both precipitation mean and 95th percentile resulted heavily underestimated. Again, residual bias of the bias-corrected simulation stays ≈ 1 mm (only for the 95th percentile).

Precipitation results, displayed different models performance in function of the morphologic/climate context. All the three models showed same sign of error but the magnitude resulted highly diversified model by model. Climate models used, have reproduced the precipitation climatology of coastal station in satisfactory manner. Over more complex orography, represented by Urbino station, two of the three models showed not negligible bias up to 40%. This underlines how working on a local scale the performance of the model depends on the particular condition of the station's characteristics. However, even in front of high bias, quantile mapping has demonstrated able to drastically reduce climate simulation errors showing high efficiency over both central and right part of precipitation distribution. A little drawback consists on the over correction of the 95^{th} percentile in front of roughly bias-free original simulations. This inflation effect has been already noticed by Maraun (2013) when it attempted to downscale simulated grid box area averaged to point-scale values. In this error reduction-downscaling approach quantile mapping rescale simulated time series in an attempt to explain the unexplained point-scale variability. Given that grid-cell simulated variability is frequently underestimated, an inflation of the simulated variability may indeed occur. From our experiment, this is not always true since depending on the station considered. Moreover, in the occurrence of a very small positive bias introduction we observed a drastic improvement of precipitation simulation for both stations. Finally, it is confirmed, especially for hill-mountain station, original simulations cannot be directly used to force climate impact model give negative bias up to $\approx 40\%$ especially over high quantiles.

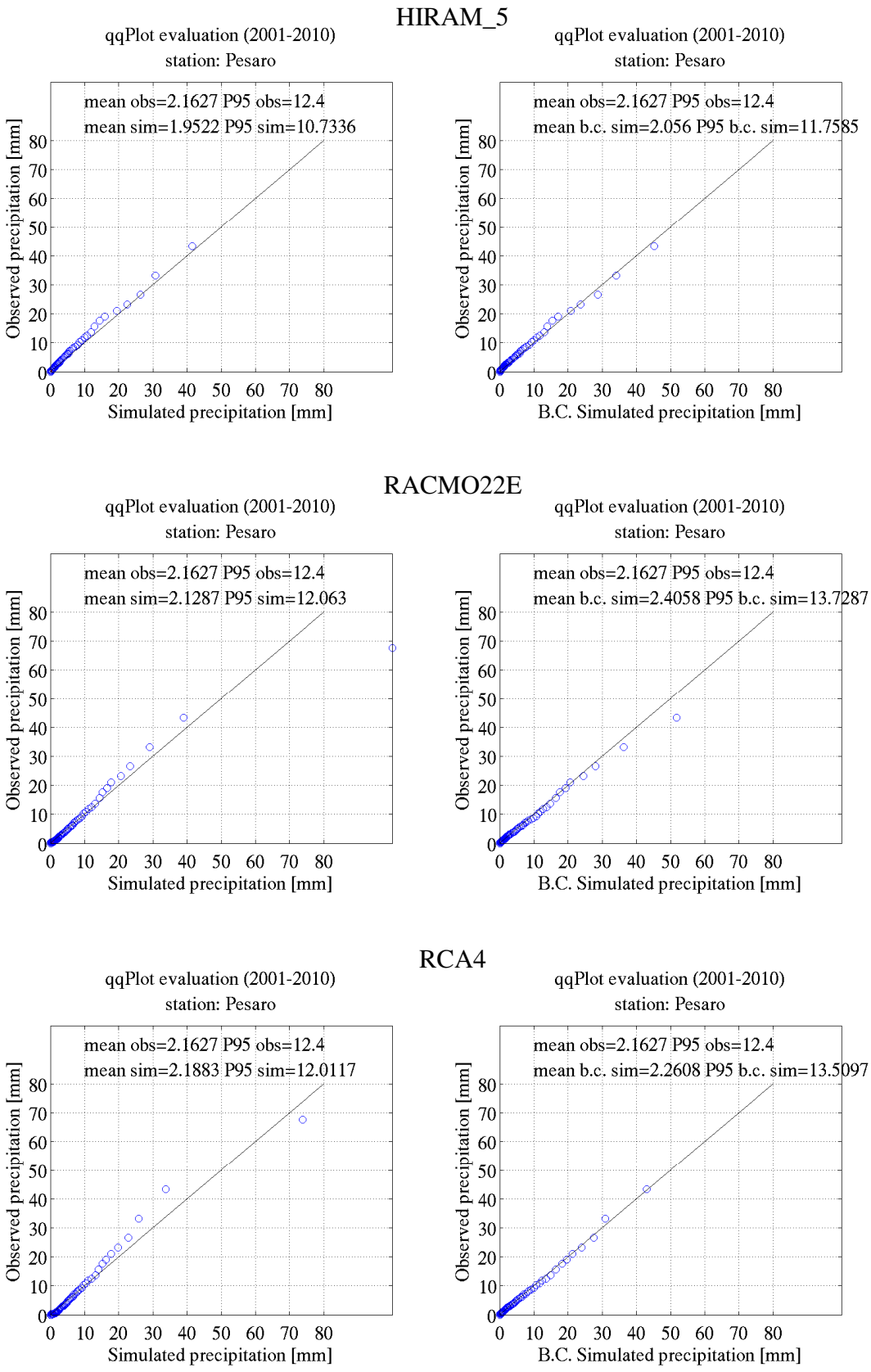

Figure 3.9. Bias correction evaluation for Pesaro station. Improvements are noticeable but even the tendency of overcorrecting high precipitation (see RACMO22E model).

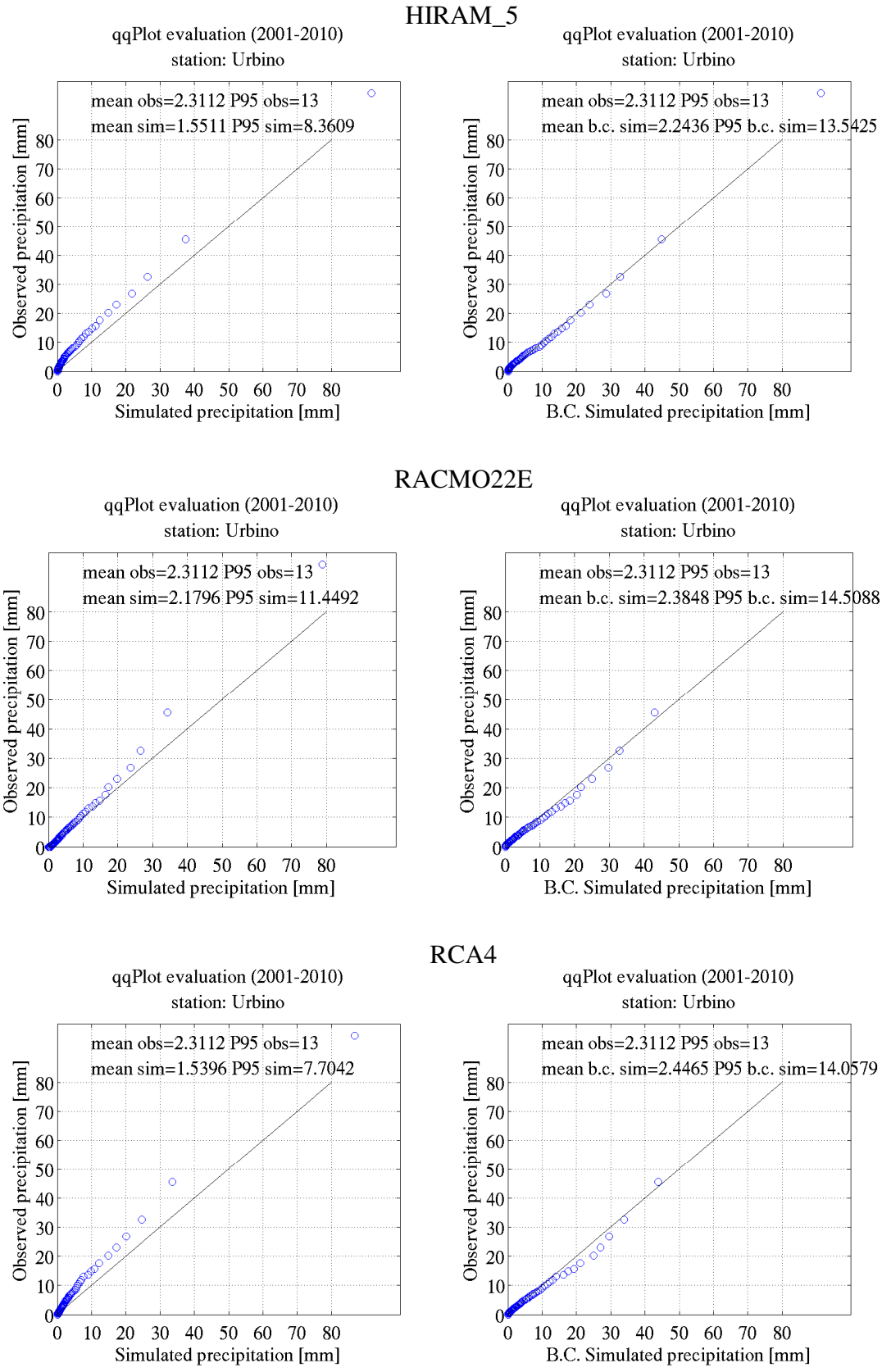

Figure 3.10. As for figure 3.9 but for Urbino station. It could be observed firstly the severe negative bias affecting all models and secondly how biases are considerably reduced after the application of quantile mapping.

3.2.2 Climate change signal and effect of bias correction – Temperature

3.2.2.1 Climate change signal annual cycle

In this section will be assessed annual cycle climate change signal for representative Marche region stations. Moreover, discrepancies between original and bias corrected results will be evaluated. In figures 3.11 and 3.12 climate change signal represents the difference between of future period (2061-2090) and reference period (1971-2000) monthly means. Climate change signal is referred to the emission boundary conditions related to the RCP8.5 scenario. Figure 3.11 reports signal for valley-coastal stations while figure 3.12 refers to the hill-mountain stations. In both figures, left panels show original simulations signal and the right panels the bias-corrected monthly climate change signal.

For the valley-coast stations, original ensemble climate change signal is ≈ 3 °C for all the seasons except for summer season months (mainly July and August) affected by a higher signal ≈ 4 °C. It is noteworthy a higher inter-model spread over intermediate season months (spring and autumn). Higher inter-model spread could be considered as higher uncertainties over related climate change signal. Assessing the multi-model ensemble (black line) bias-corrected results, we note a dampening of the summer month's signal (especially in august) of about 0.5 °C – 0.8 °C. This effect is common to all the three reference coastal stations. Moreover it is noticeable an increase of the November and December months signal over coastal area stations (from 3 to 3.5-4 °C). These effects are consistent with those obtained in the regional experiment (chapter 2). As explained in the previous section quantile mapping would act on the original simulations reducing the intensity-dependence of model error. It involves a reduction effect that would be higher in the future segment given higher simulated values explaining the occurrence of the summer month's signal dampening.

In figure 3.12, the same analysis for other three representative stations located on the hill and mountainous sector of the Marche region is reported. According to what resulted in the regional experiment, the hill stations signal seems not significantly affected by the application of bias correction. Original simulations show a signal with similar annual pattern and similar magnitude of those affecting coastal stations (≈ 3 °C in winter and almost 4 °C in summer) but it is interesting to note that, differently from coast stations, bias correction does not dampen summer season signal. Only slight dampening over Ascoli Piceno is noticeable (August and September months). In fact, this station presents intermediate-climate condition, being located on a valley at an elevation lower than 200 meters above the

sea level (but far away more than 30 km from the seaside). For the three hill-mountain stations multi-model mean climate change signal after correction remains roughly of 3 °C all year long and 3.5-4 °C during summer months.

Furthermore, in the upper part of the 3.11 and 3.12 figures results from the Wilcoxon statistical test are shown. This statistical test aims to assign statistical significance to the monthly mean climate change single. A significant monthly signal is indicated with "1" a monthly signal included in the natural temperature variability range would be indicated with "0".

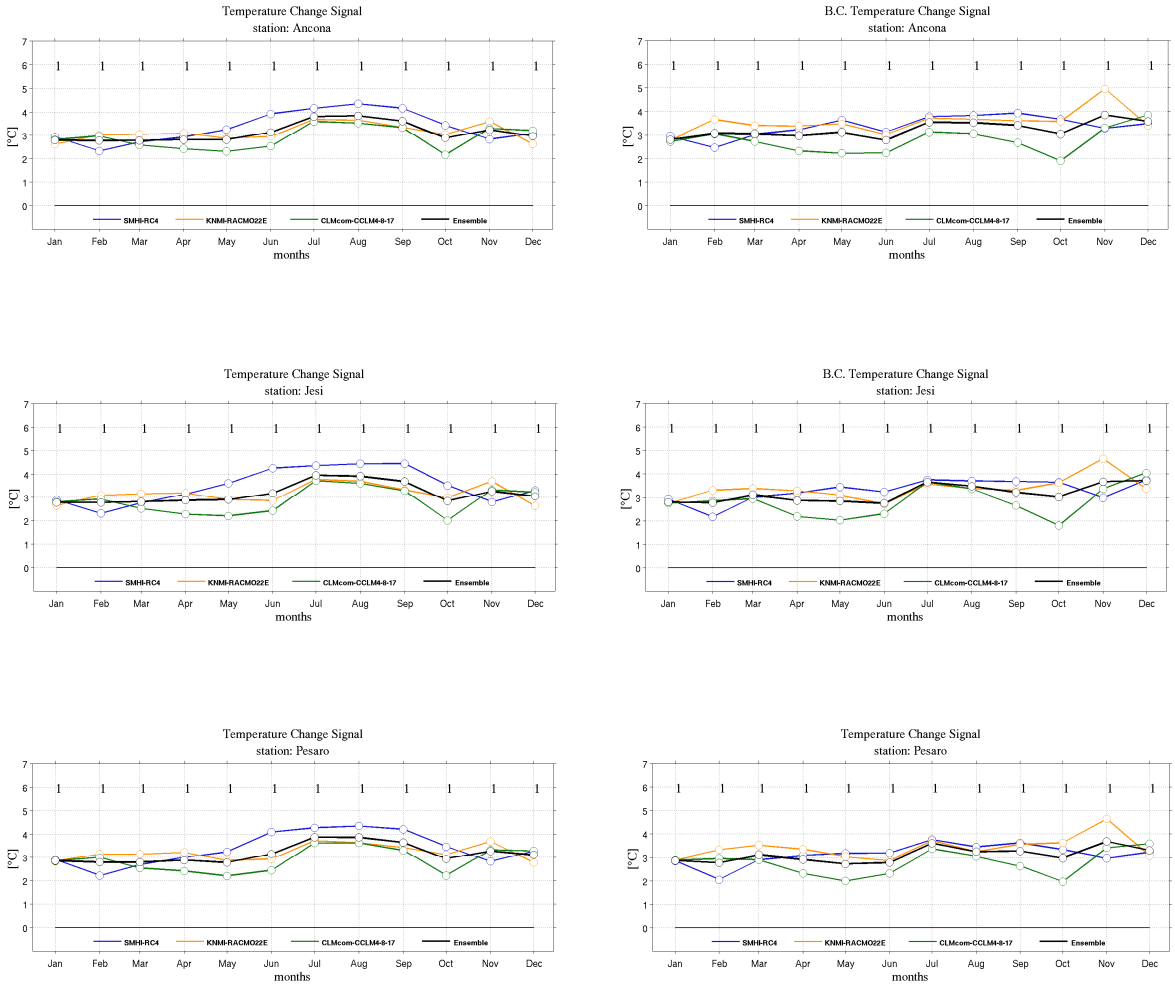

Figure 3.11. Temperature annual cycle climate change signal for valley-coast representative Marche region stations. Colored lines represent the response of individual climate models. Black line the three-model ensemble mean. On the left panels original-simulations change signal and the right panels bias-corrected simulations change signal are shown. Numbers (1 or 0) in the upper part of the plots are the results of Wilcoxon statistical test. It assess changes in the median between ensemble reference and future time segments attributing or not statistically significance to the changes in the temperature distribution. Monthly mean signal has been computed for the long-term time horizon (2061-2090) compared to the reference period 1971-2000. Results are relative to the RCP8.5 boundary conditions.

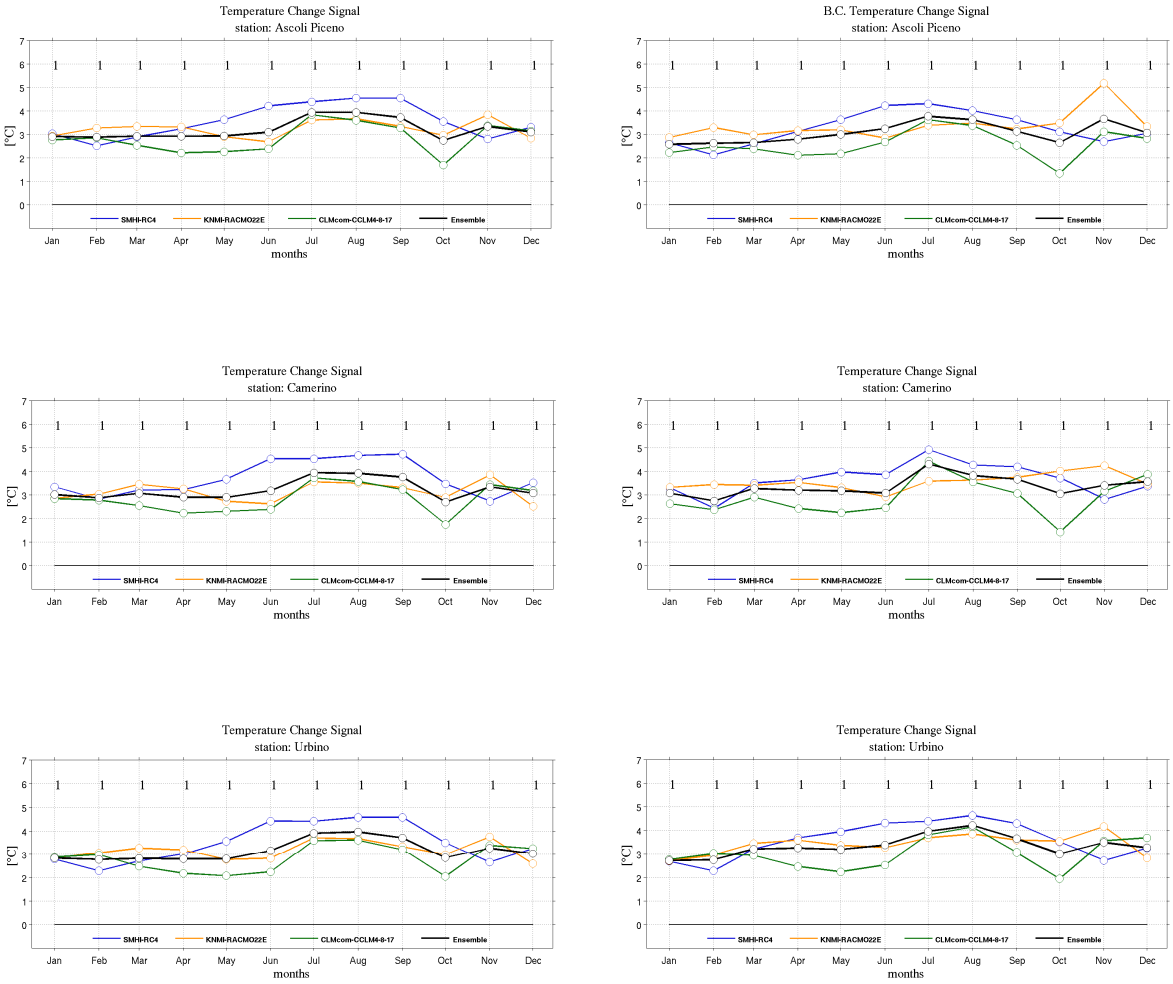

Figure 3.12. Same as 3.11 but for the hill-mountain stations

3.2.2.2 Climate change signal distribution – Temperature

In this section will be assessed the climate change signal affecting the entire temperature distribution with original and bias-corrected ensemble simulations. The signal value reported in the *y*-axes refers to each quantile constituting variable distribution. In figures, 3.13 and 3.14, RCP4.5 mid-term scenario (2021:2050 minus 1971:2000) is shown. The 12 panels that compose each figure want to report results for each of the three representative stations (three for coast and three for hill-mountainous sector) for the two seasons (summer and winter) run with original and bias-corrected ensemble simulations [3 stations * 2 seasons * 2 runs (raw/b.c.)] = 12. In figure 3.13, that reports valley-coast stations results, we can note how in the original simulation summer season shows higher signal (≈ 1.5 °C) especially over the right portion of the distribution. Winter signal is around the 1 °C, slightly higher in the right part of the distribution. Bias correction does not appreciably affects the original ensemble signal but as in the previous analysis, a reduction of the right distribution signal in summer is resulted. For what concerns hill-mountain stations (figure 3.14), a similar seasonal signal and effect of bias correction is obtained. It is interesting noting that the signal of the right part of distribution is not dampened by the bias correction.

The long-term scenario (2061:2090 – 1971:2000) is reported in figures 3.15 and 3.16. Original simulations indicate higher signal in both seasons (2.2-2.5 °C in summer and ≈ 2 °C in winter). Bias correction dampens summer signal only in the highest percentiles signal (≈ 0.5 °C) and strengthen winter higher percentiles signal magnitude with the same magnitude. Remarkably, both effects resulted more noticeable for valley-coast stations.

Mid-term scenario (2021-2050) – RCP4.5

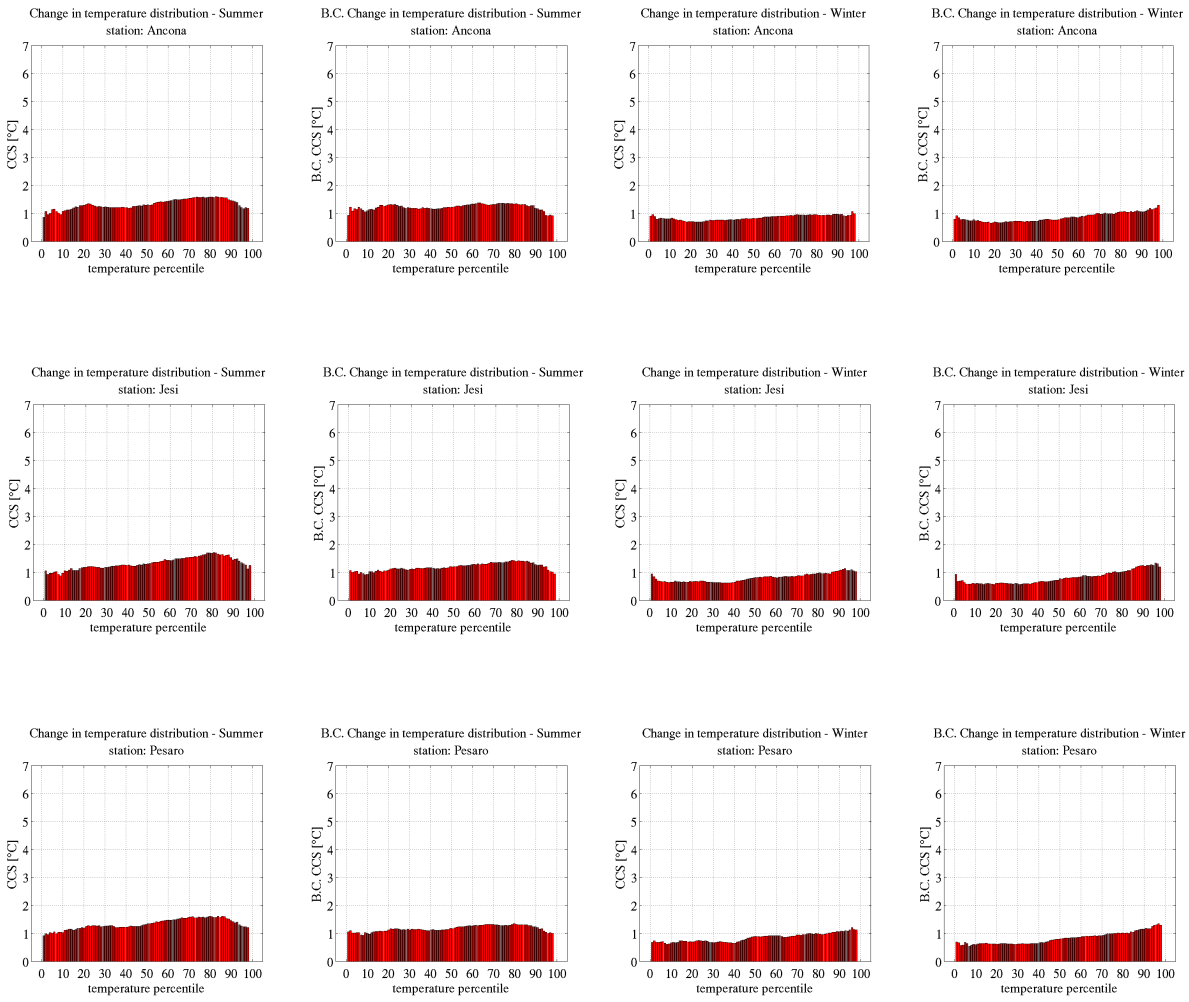

Figure 3.13. Mid-term scenario (2021-2050) for coast-valley stations. Left panels show summer climate change signal and right panel climate change signal for winter season. For each season, original and bias corrected projections are reported. In this experiment, climate model boundary conditions are provided by the RCP (Representative Concentration Pathway) 4.5, representing radiative forcing (+4.5 W m^{-2} relative to pre-industrial conditions) corresponding to an atmospheric greenhouse gas concentration of 650 CO_2 equivalent. The signal value reported in the y axes [°C] is referred to each quantile of the variable distribution (x axes)

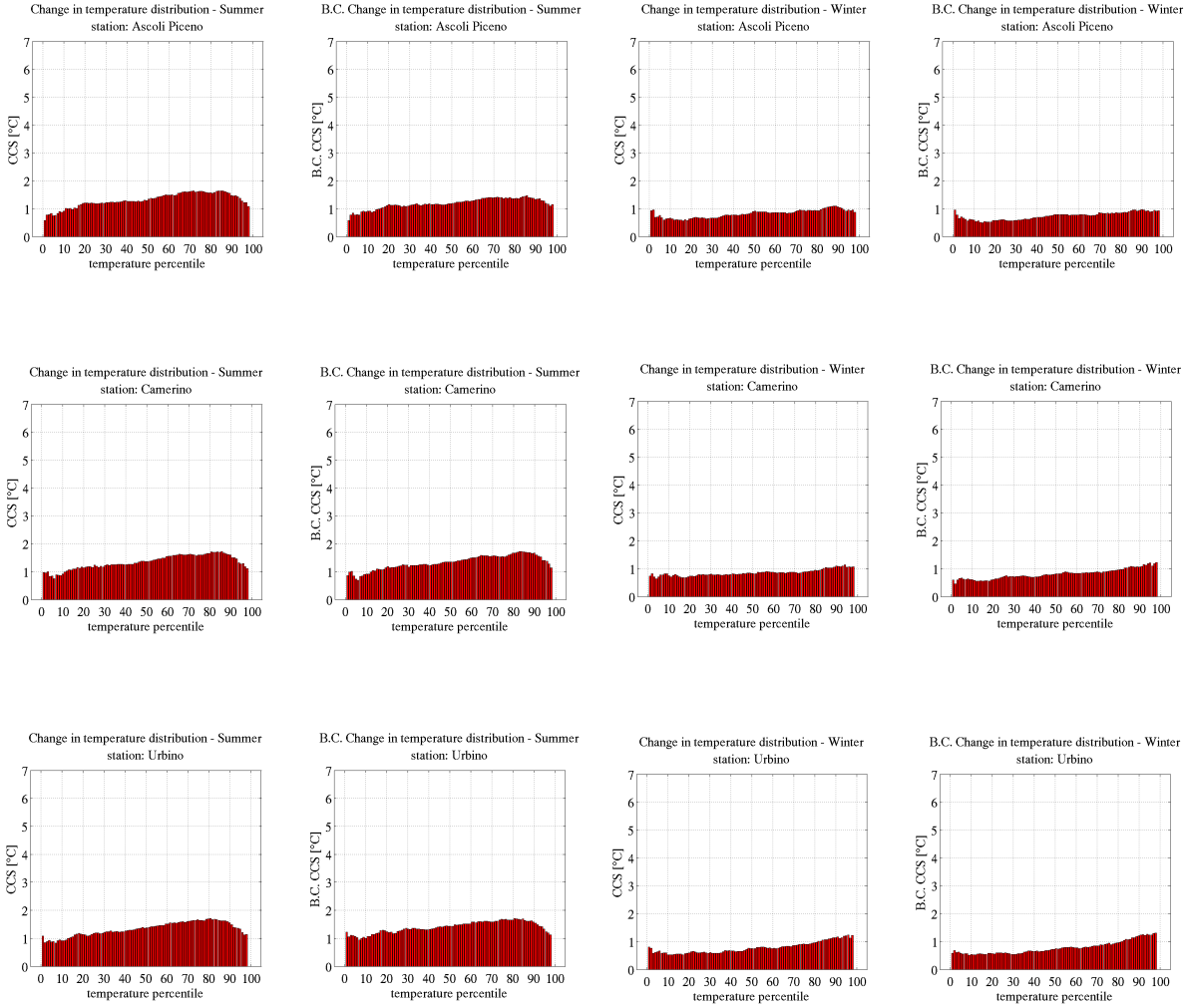

Figure 3.14. Same as figure 3.13 but hill-mountain stations are considered.

Long-term scenario (2061-2090) – RCP4.5

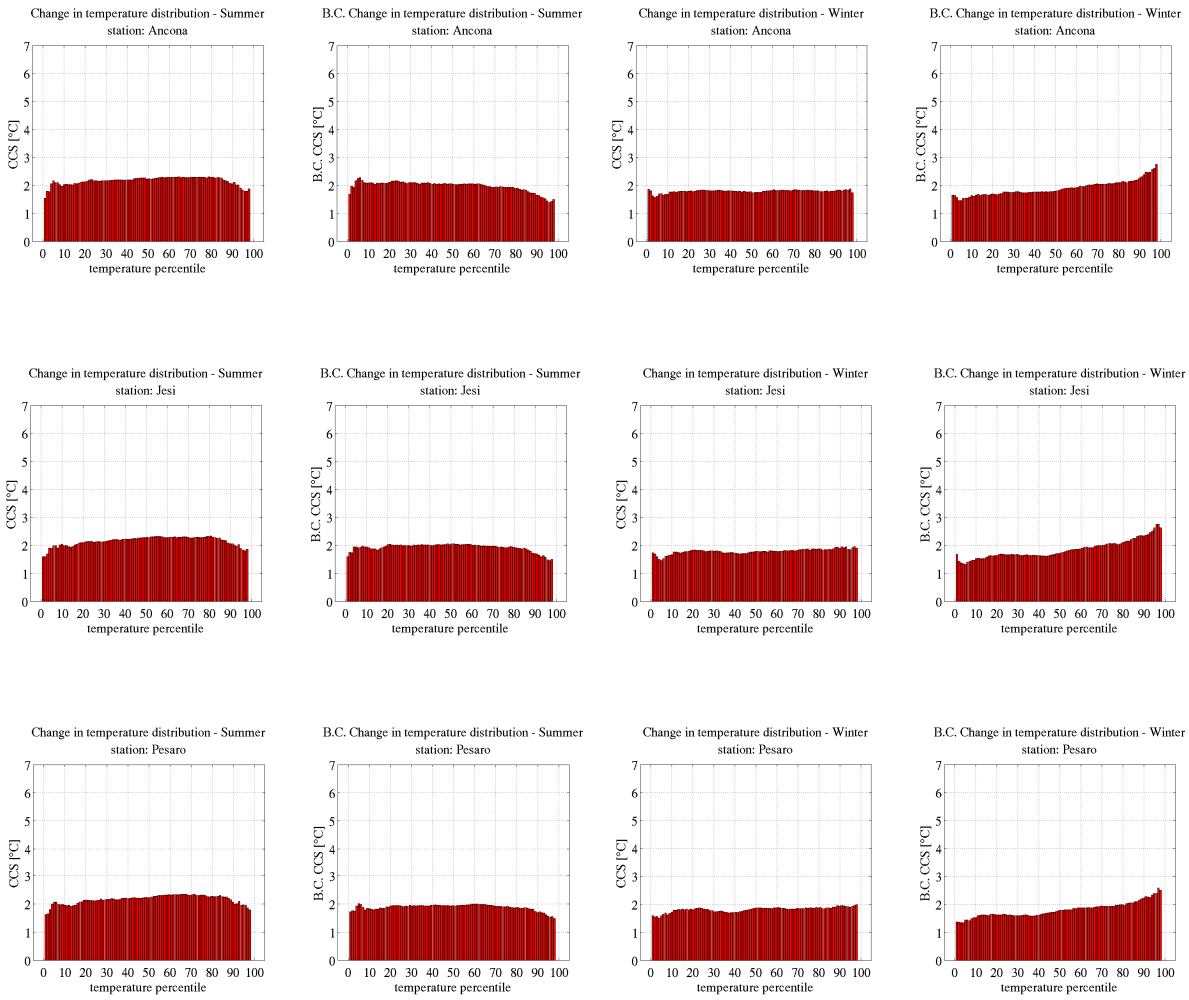

Figure 3.15. Long-term (2061-2090) valley-coast stations temperature climate change signal

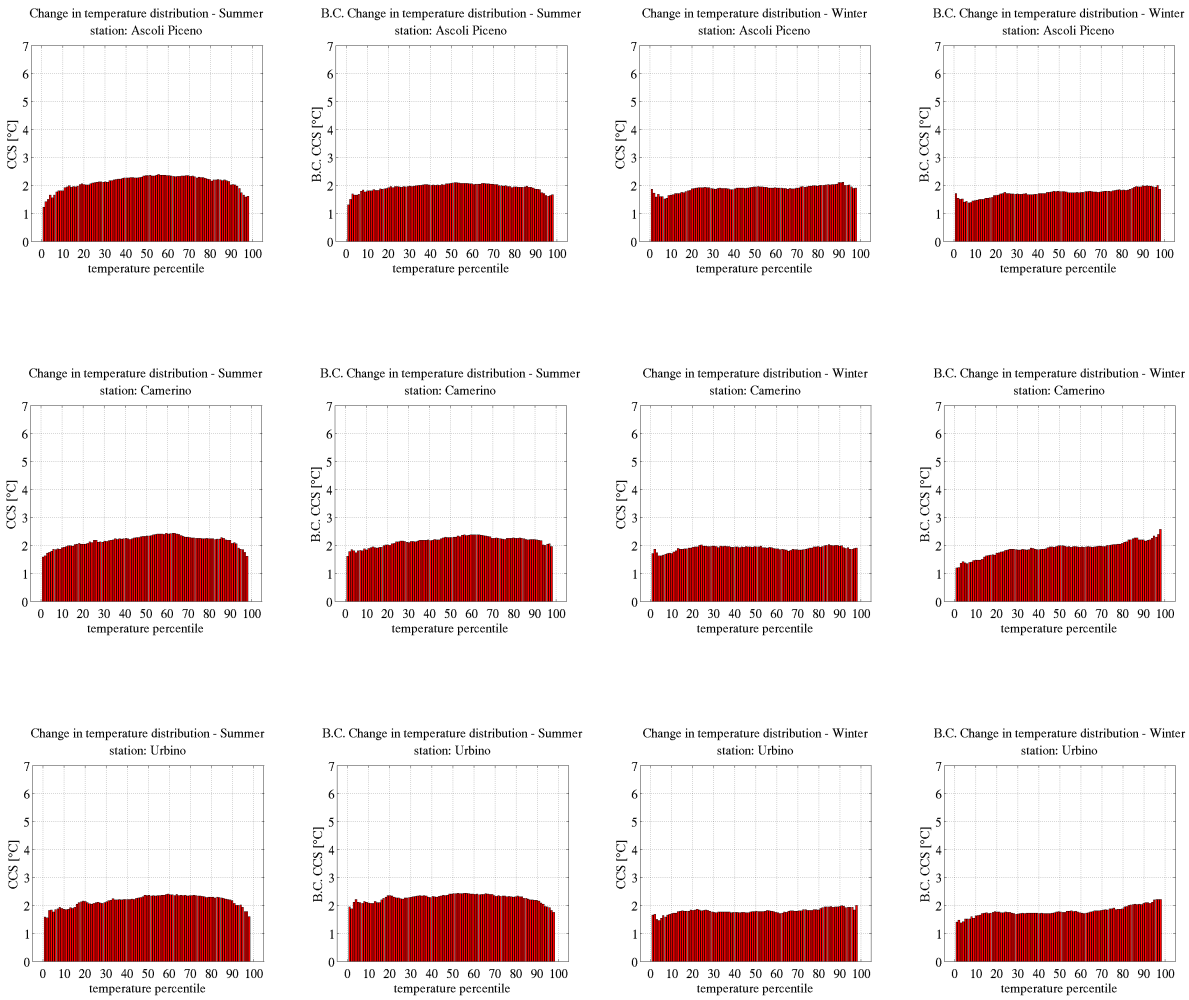

Figure 3.16. As for figure 3.15 but for hill-mountain stations.

Figures 3.17 and 3.18 show results for the mid-term (2021-2050) temperature climate change referred to higher radiative forcing relative to the RCP8.5 (8.5 Wm^{-2} against the previous value of 4.5 Wm^{-2} compared to pre-industrial value) corresponding to a greenhouse gasses concentration of 1370 ppm CO_2 equivalent at the end of this century. The seasonal signal in this case results on average ≈ 0.2 °C higher than relative RCP4.5 radiative forcing. The RCP8.5, considers no mitigations measure undertaken in the next decades with a roughly increase in stabilization of emission rate around 2080's and a roughly linear increase of radiative forcing for all the 21st century (Moss et al. 2010). On the regional context temperature signal remains still sligthly below +2 °C in summer and between 1.2 °C and 1.5 °C during the winter. Coast and hill representative stations resulted substantially equally affected by the positive signal. The effect of the statistical correction over the RCP8.5 runs is similar to what seen in the RCP4.5 experiment. A dampening of the right-tail signal over coast stations in summer (≈ 0.3 °C), coupled to a strenghten of the right-tail-signal in winter mainly (≈ 0.5 °C) over coast stations was resulted.

In figures 3.19 and 3.20, reports RCP8.5 temperature long-term scenario characterizing the thirty-year time slice 2061-2090. Departure of temperature signal compared to the mid-term horizon is massive. Differently from that resulting from RCP4.5 experiment, we observed a doubling of signal in 40 years (time separating mid and long-term scenario time segments). Beyond certain radiative forcing threshold, temperature increase seems to assume not linear behavior as hypothesize in Scheffer et al. (2009) end Mora et al. (2013). Original summer temperature signal exceeds +4 °C, especially over the right part of distribution and the +3 °C during winter season. Original change signal resulted roughly equally distributed over coastal and hill stations. Bias correction effects in the cost stations are different to those affecting hill stations signal. In summer, coherently with previous results, bias correction dampens summer signal over right tail of distribution about 0.8 °C. Over the same stations, in winter, the right tail signal is noticeable strengthen up to 1 °C. Indeed, coast winter signal reaches +4.5-5 °C in correspondence of distribution right tail. In winter season, for both coast-valley and hill-mountain stations, bias correction strengths the quantile-dependence of the signal. It means that the higher the quantile considered the higher is the signal resulted with the signal increased from ≈ 3 °C to ≈ 4.5 °C in the bias-corrected winter signal.

Mid-term scenario (2021-2050) – RCP8.5

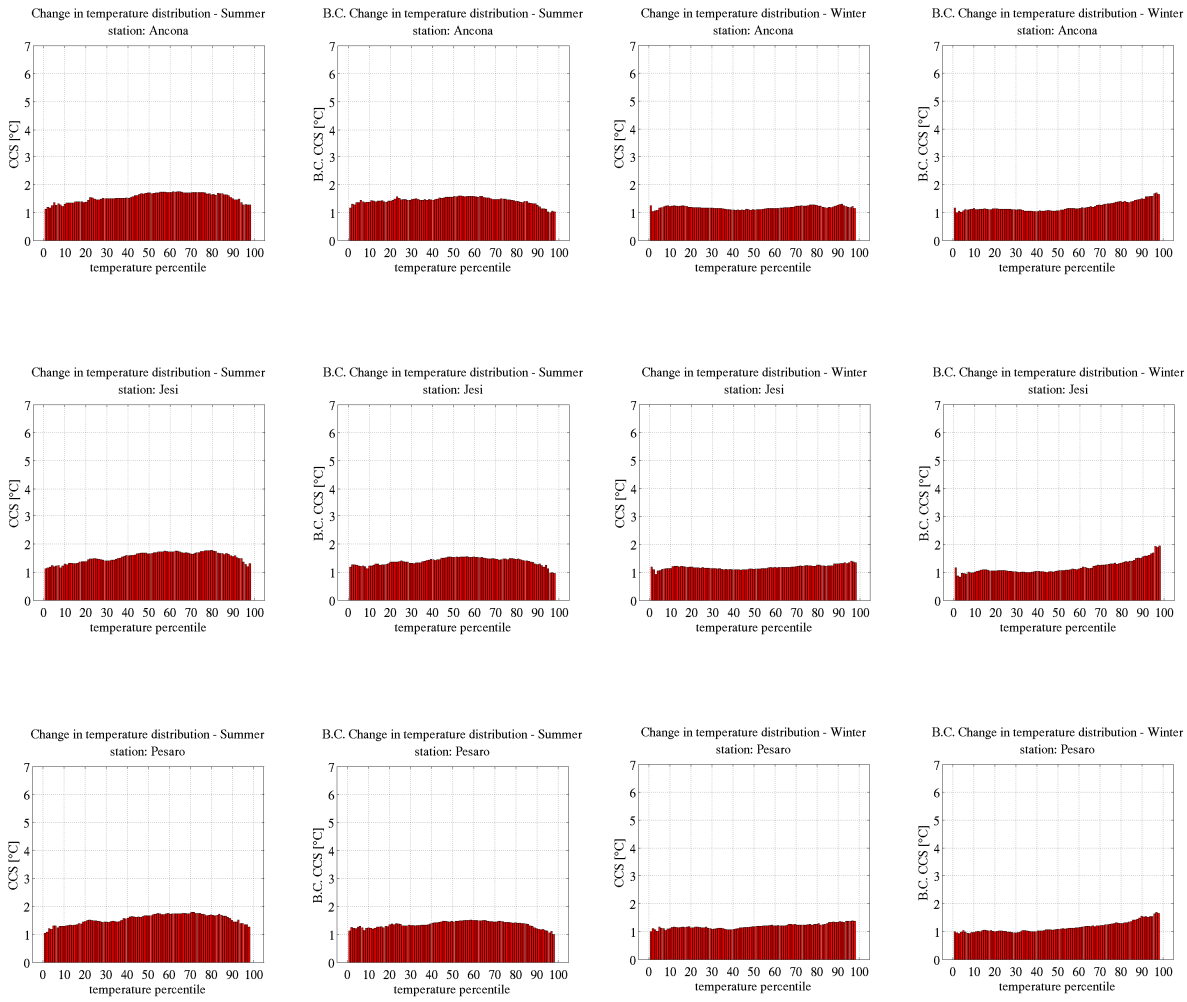

Figure 3.17. Temperature mid-term climate change signal. Here climate model boundary conditions are provided by the RCP (Representative Concentration Pathway) 8.5, representing radiative forcing (+8.5 W m^{-2} relative to pre-industrial conditions) corresponding to an atmospheric greenhouse gas concentration of 1370 CO_2 equivalent at 2100.

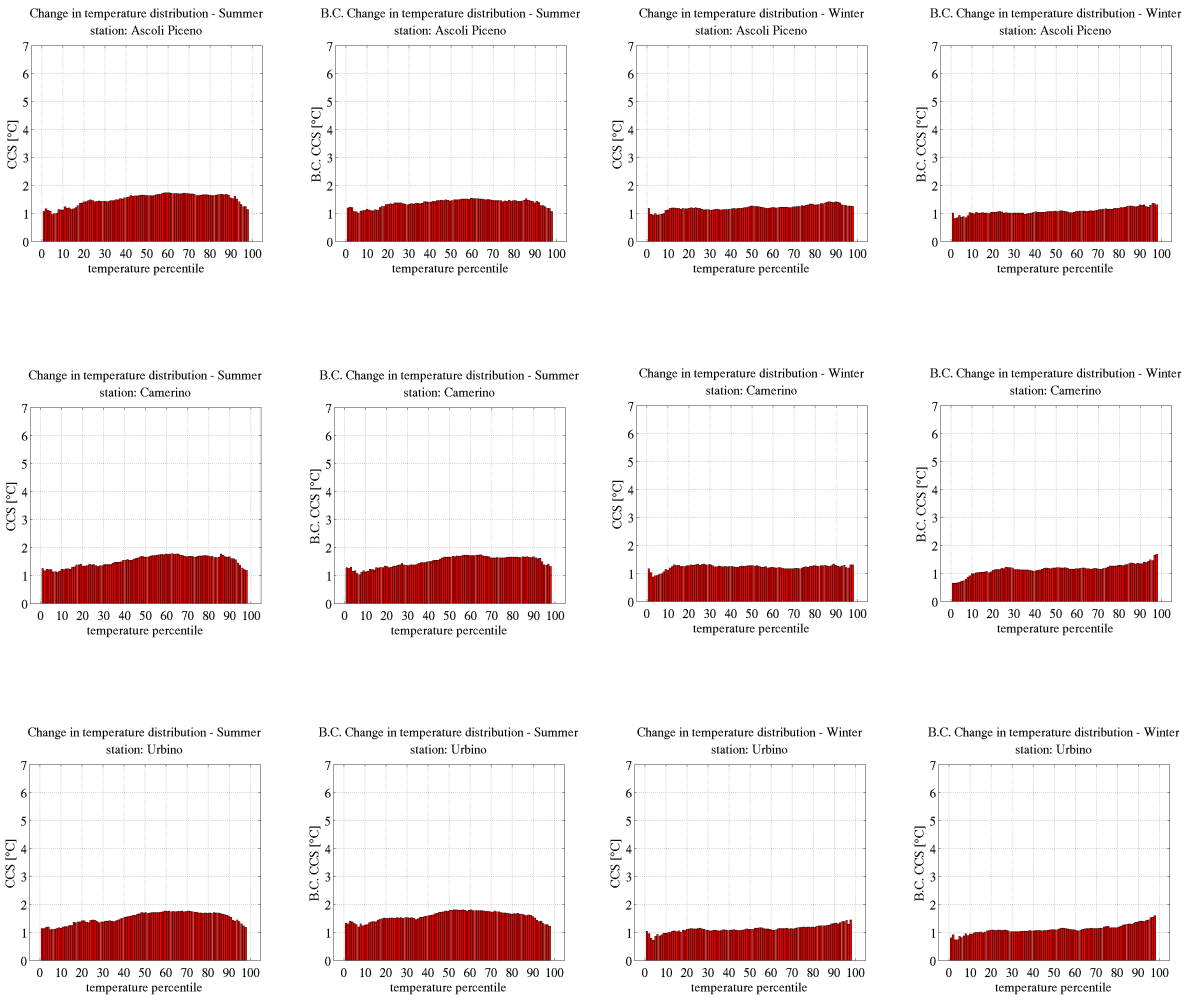

Figure 3.18. As for figure 3.17 but for hill-mountain stations.

Long-term scenario (2061-2090) – RCP8.5

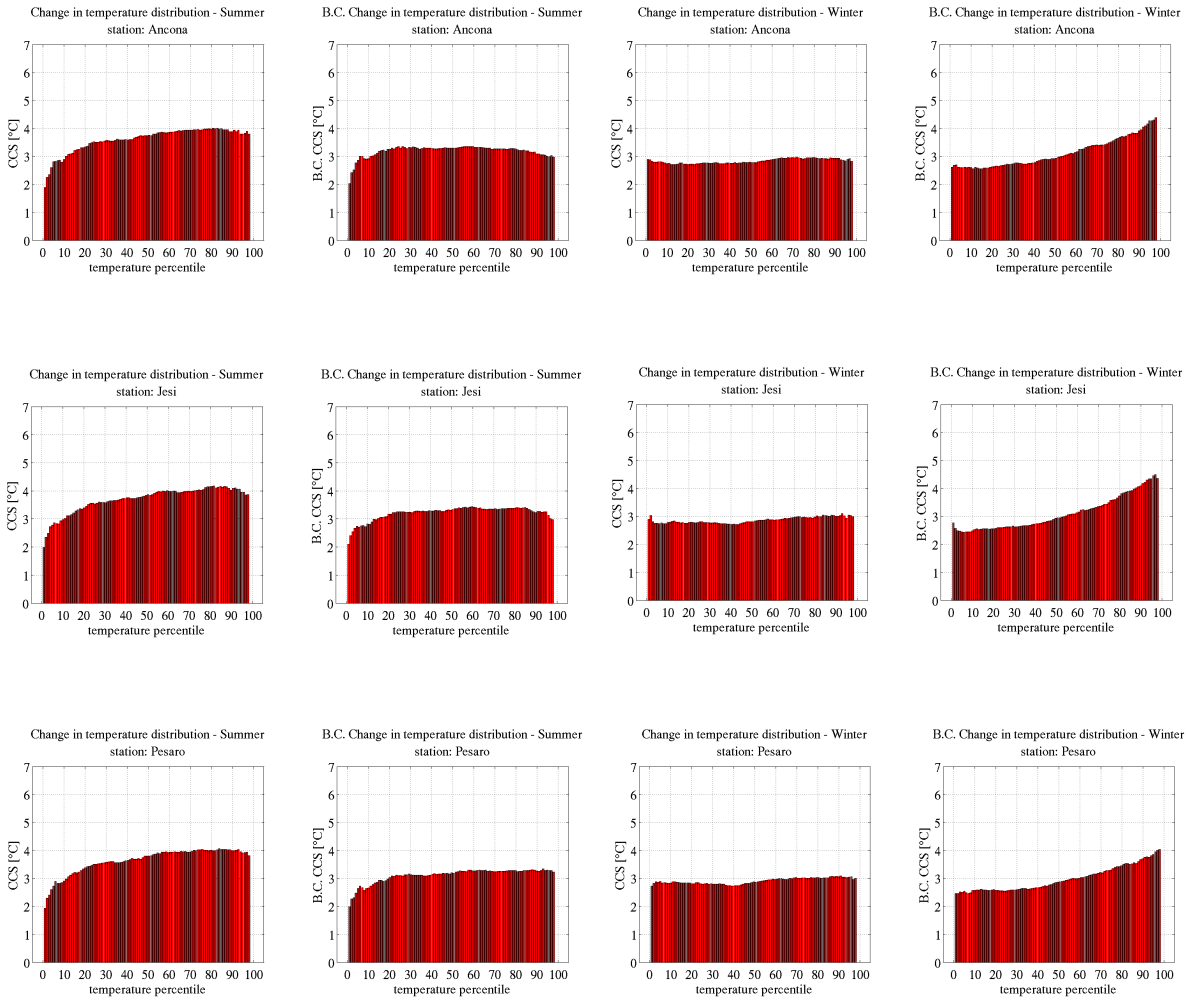

Figure 3.19. Long-term (2061-2090) valley-coast temperature climate change signal.

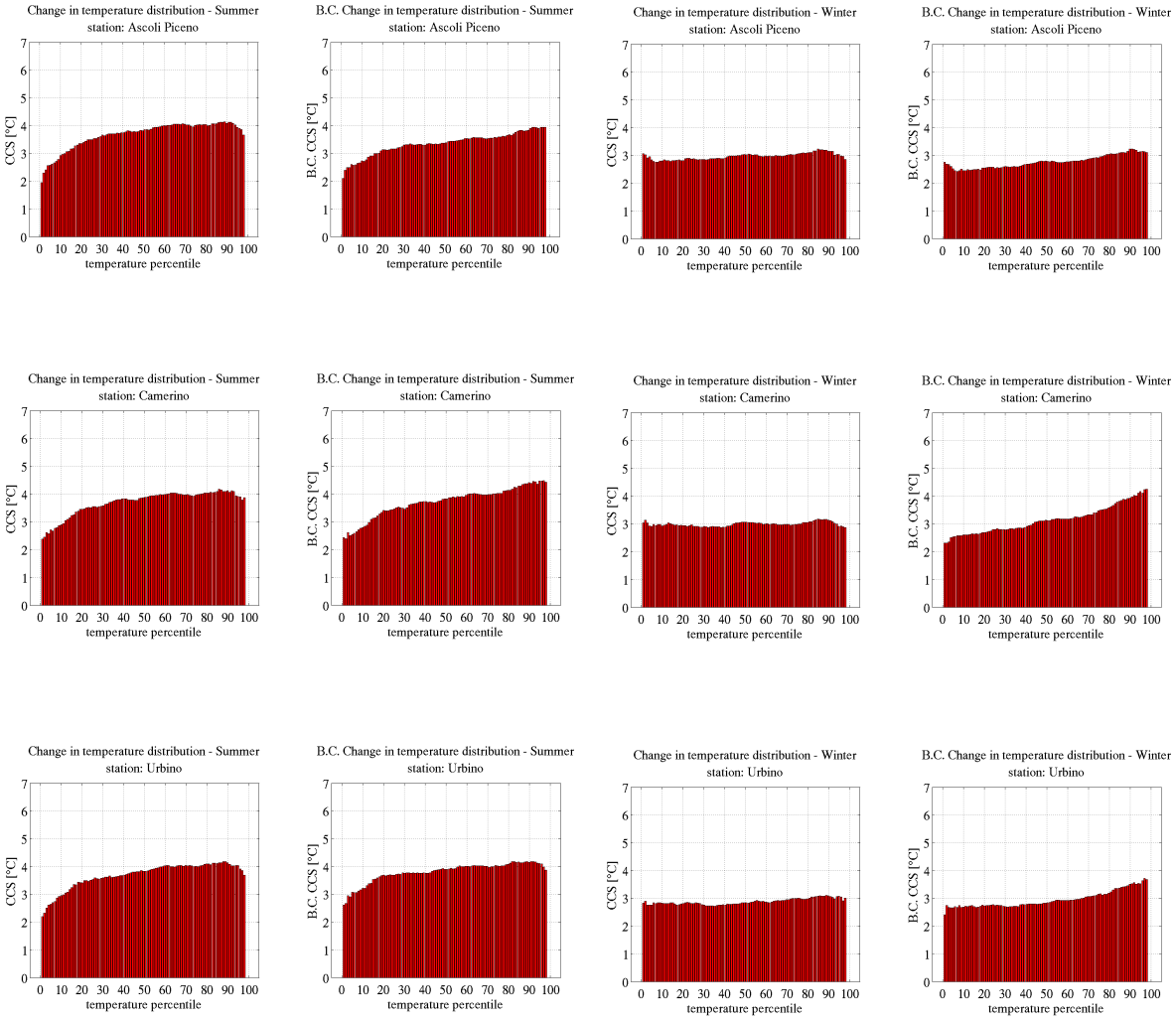

Figure 3.20. As figure 3.19 but for hill-mountain stations.

3.2.2.3 Summary boxplots – Temperature

Figures from 3.21 to 3.26 summarize in one-plot solution all the methodological steps in developing a local temperature scenario referring to each model and each station considered. From the left to the right, boxplots show: observation, original simulation and corrected simulation over the period 1971-2000 (corresponding to the correction function calibration phase). The same sequence for the evaluation period (2001-2010), where the correction function is applied over a block of data not used in the function calibration (2001-2010). Finally, future period (2061-2090) original and bias-corrected simulations are shown (RCP8.5 is considered). The add value of boxplots is allowing comprehensive assessment of the fundamental statistics at one time. Boxplots report 5^{th}, 25^{th}, 50^{th}, 75^{th}, 95^{th} percentiles and outliers of each block of data considered. Furthermore, this approach has been applied for each climate model and station considered. This allows analyzing: performance of original simulations over the observation, bias correction effects and distribution of future time segments.

Results highlight how original simulations generally underestimate observed temperature over both valley-coast and hill-mountain stations. Especially KNMI-RACMO22E model shows severe negative bias in the median (50^{th} percentile of distribution) up to 5 °C over complex-orography stations. Conversely, original simulations fairly reproduced observed temperature variability. Bias-corrected simulations are able to perfectly reproduce observed climatology during calibration period (B.C. SIM 1971-2000). This is not surprising and we have already argued on the plausibility of getting a "perfect simulation" over the calibration period. More significant is to assess the effect of bias correction over validation period (2001-2010). It is noteworthy how quantile mapping effect varies from station by station and model by model. This aspect should be carefully taken in account when a local climate scenario has to be defined. It does not exist a climate model that systematically best performs over all the situations. The most suitable configuration is indeed in function of the particular climatic analysis (e.g. variable, season climate context considered etc.) and must be with care sought between the available solutions. Following these considerations, results for each individual ensemble member has in this phase reported. In general, over the evaluation time segment we obtained a satisfactory improvement of the simulations especially over the median, 25^{th} and 75^{th} percentiles. Simulation improvements are particularly palpable in correspondence of hill-mountain stations for all the models. This evidences quantile mapping capability in adjusting physical values and variance as well. For the tails of distribution (5^{th}

and 95th percentiles) the improvements are evident even not systematic. This suggests to treat extreme values distribution separately by the rest of distribution through specific parametric distributions as Casati et al. (2013) proposed.

Finally, boxplots on the right represent the future time segments (2061-2090) of original and bias corrected simulations. Two interesting aspects resulted: the increase of temperature over the different statistics and how correction effects vary station by stations and model by model. For what concerns the change signal (original and bias corrected), it is inferred through the comparison with the reference period (1971-2000) segment boxplots. It is noteworthy how greater signal affects the 75th and 95th percentiles, in some cases exceeding 5 °C, confirming previous results.

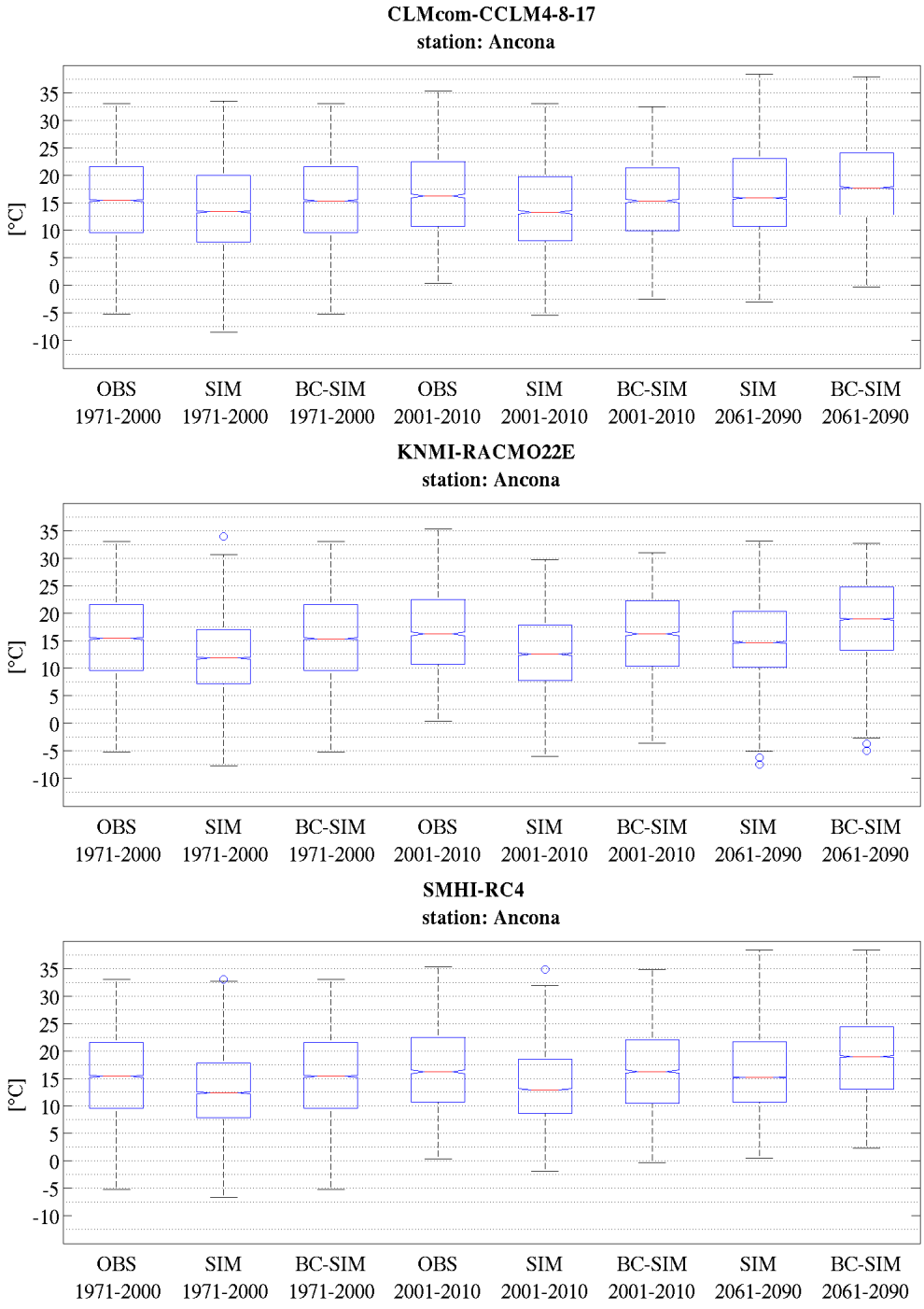

Figures 3.21 to 3.26. From left to right for each panel: calibration phase consisting on observation, original simulation and bias-corrected simulation over 1971-2000. Evaluation phase same as calibration but regarding to the 2001-2010 period. Finally, far future original and bias-corrected simulation (2061-2090). Results has been reported for each climate models employed and for representative Marche region stations (Ancona, Jesi, Pesaro, Ascoli Piceno, Camerino, Urbino).

.

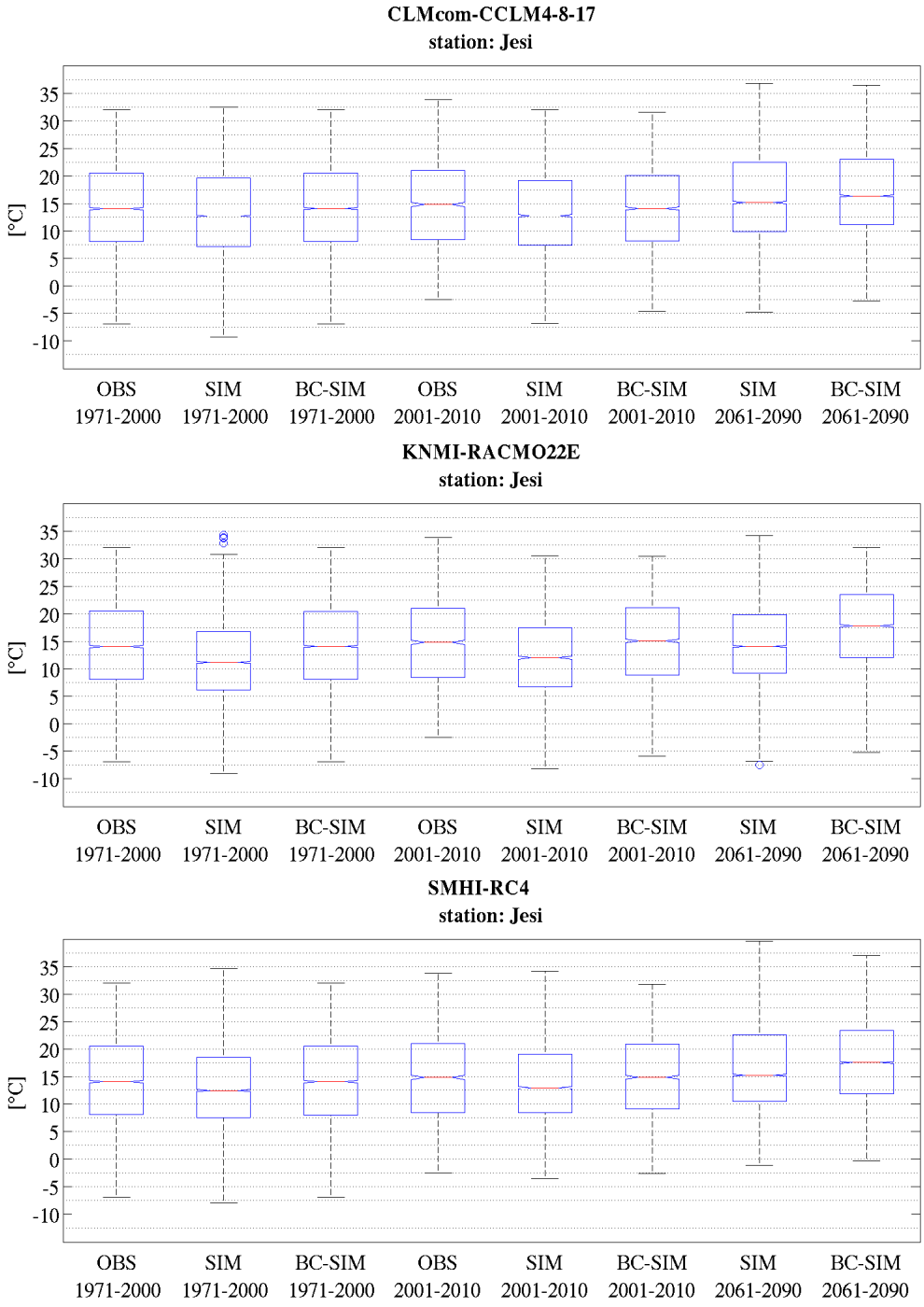

Figure 3.22. Summary boxplots for Jesi station temperature.

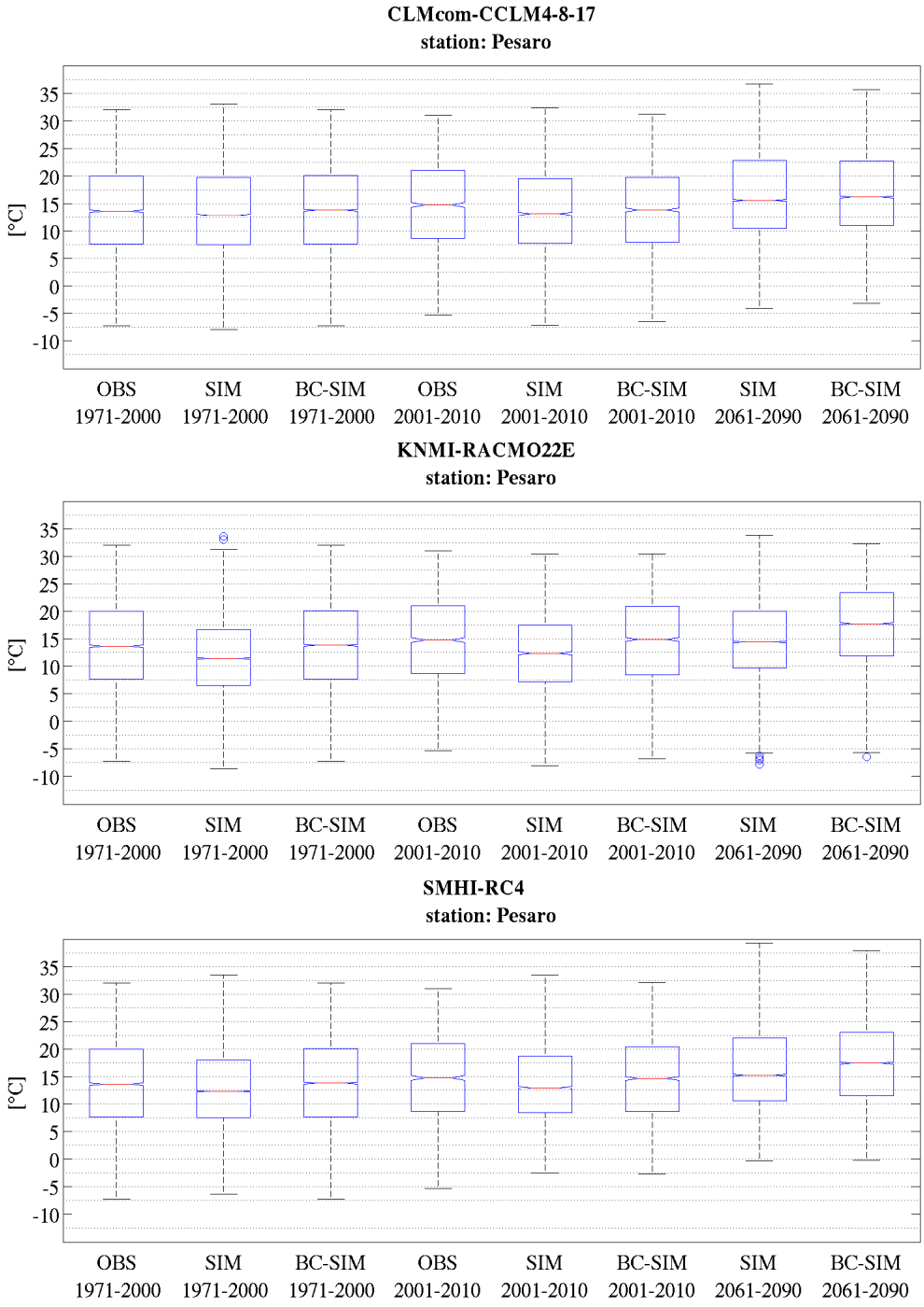

Figure 3.23. Summary boxplots for Pesaro station temperature.

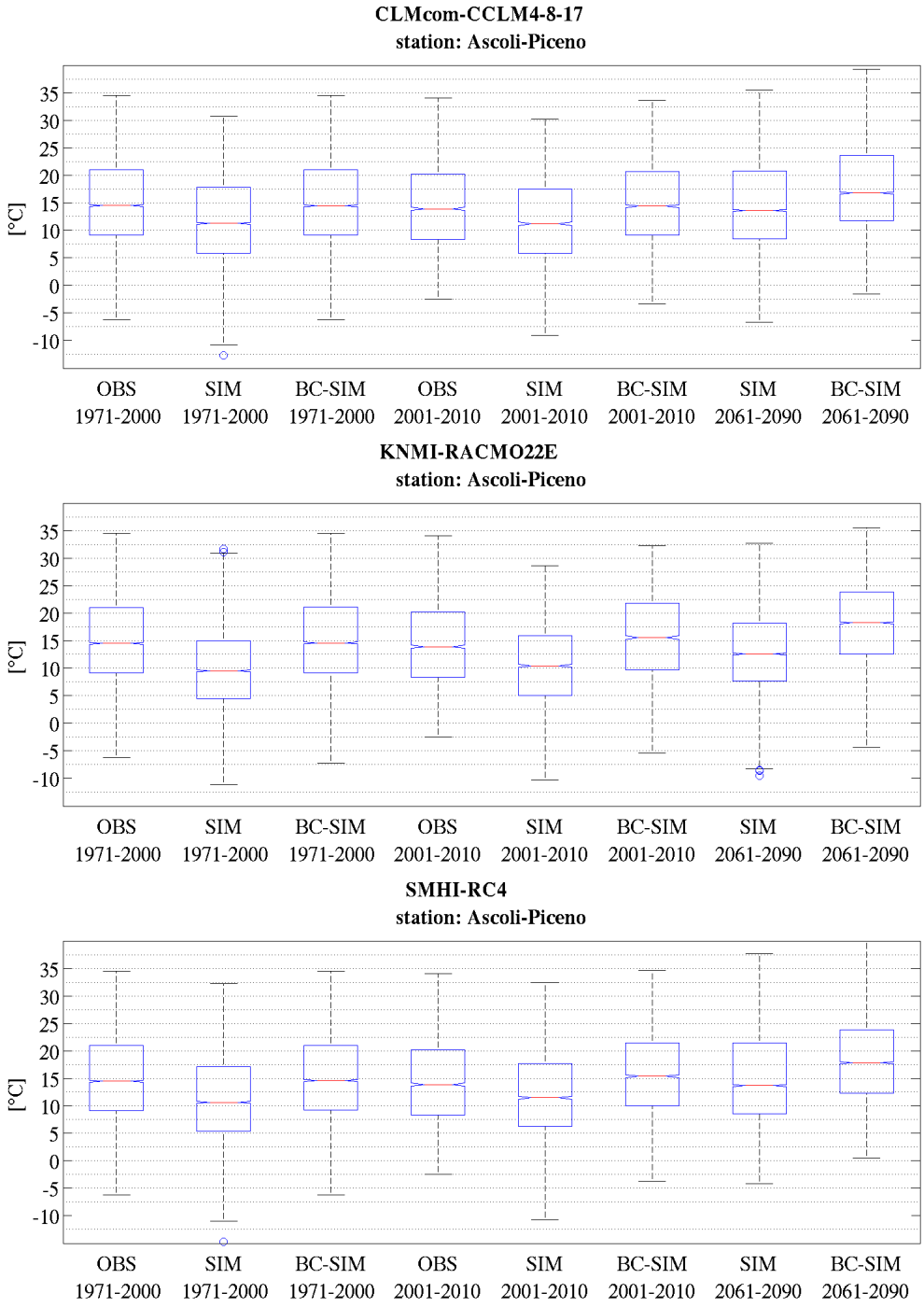

Figure 3.24. Summary boxplots for Ascoli Piceno station temperature.

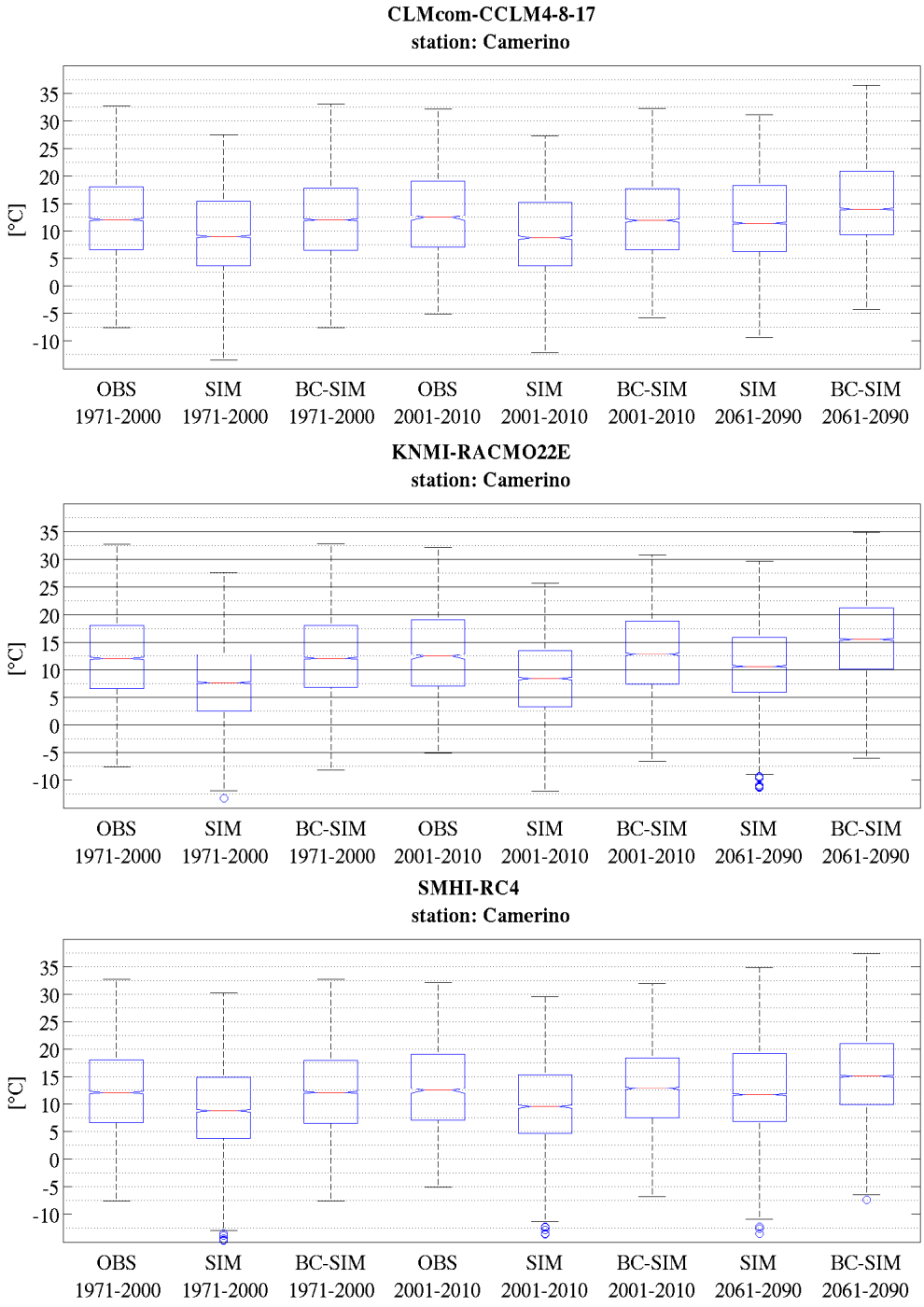

Figure 3.25. Summary boxplots for Camerino station temperature.

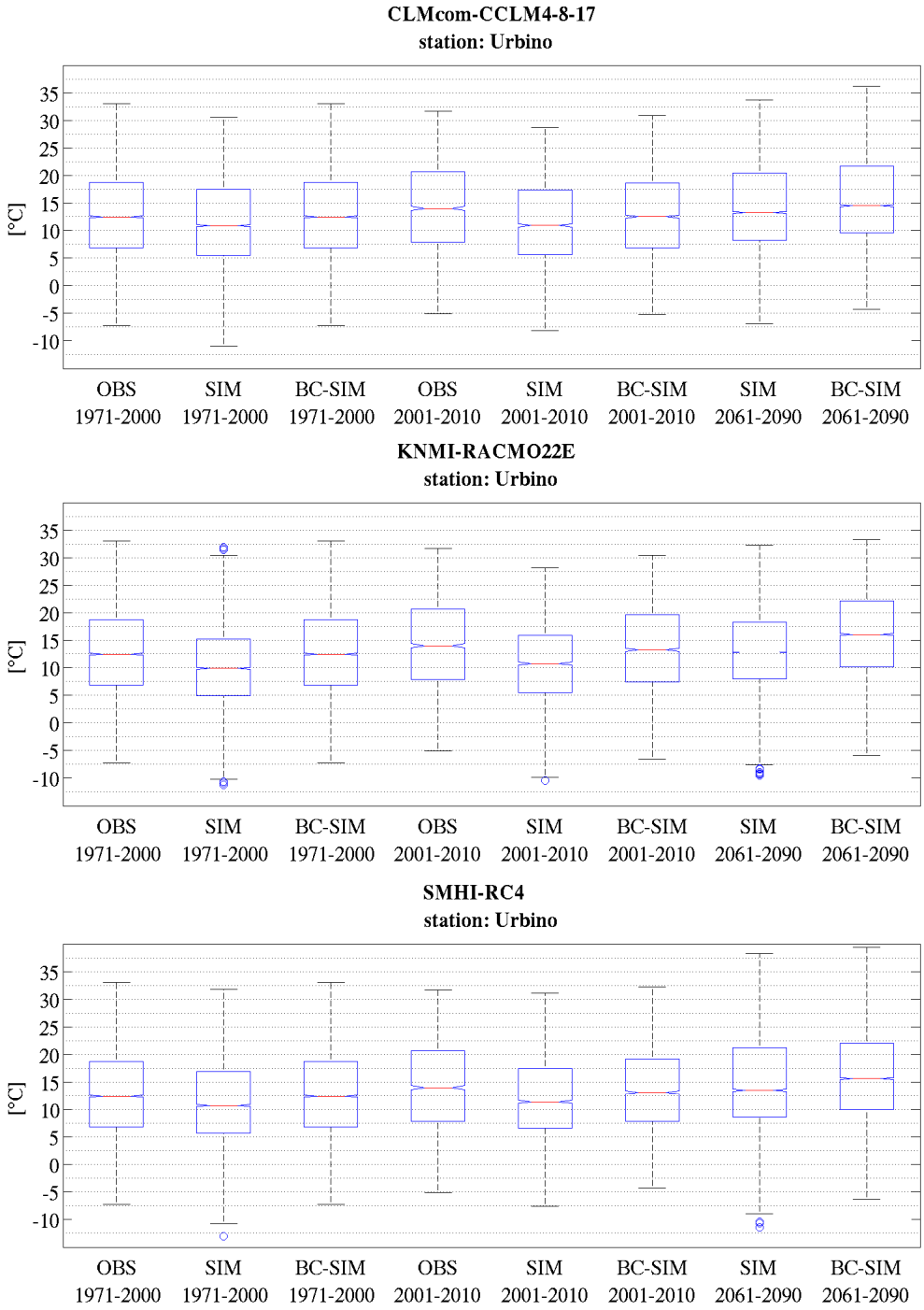

Figure 3.26. Summary boxplots for Urbino station temperature.

3.2.3 Climate change signal and effect of bias correction – Precipitation

3.2.3.1 Climate change signal annual cycle

In figures 3.27 and 3.28 precipitation annual cycle change signal (long-term RCP8.5) for representative Marche region stations is reported. Original simulations on the left and bias-corrected ones on the right panels. Statistical significance of the monthly change signal is expressed through the Wilcoxon test applied to the ensemble mean (upper part of the plots). (1) indicates statistically significant monthly signal, (0) if changes are not statistically significant. Wilcoxon or rank-sum test pertains to the classical nonparametric test for two data sample location (Wilks D.S. 2011). Test aims to assign significance to the possible difference in location with the null-hypothesis that the two data samples (in this case reference and future block of data) have been drawn from the same distribution. Here the concept of location refers to the central tendency or general magnitude of the two blocks of data. Common measure of central tendency is represented by the median.

The annual cycle signal shows a general decrease of precipitation during summer months (down to -30%) and an almost-equal increase during autumn-winter months. The results are similar for both regional climatic sectors, with a slight higher autumn months (especially November) increase over hill-mountain representative stations. Summer months precipitation negative signal substantially agrees with signal resulted in the regional experiment (chapter 2). Differently, for autumn and winter precipitation, newest generation of climate models indicates a local moderate increase of precipitation not previously resulted in the regional experiment. At this regard, it should be underlined, that models here employed present crucial differences compared to those employed in the regional experiment. Different horizontal resolution and radiative forcing boundary conditions make inappropriate a direct comparison of the two experiments. However, changes outlined could be ascribed to the increase of the summer-months sub-tropical high-pressure regime and an increase of winter NAO negative phase leading to drier summer and wetter autumn-winter months. Interestingly, in common to the two experiments there is that statistical correction does not affect original signal in both valley-coast and hill-mountain stations. Besides, we obtained scattered influence of bias correction over the significance of monthly signal. Indeed, significance has preserved in some stations (and months) altered in others. This aspect is relevant and deserves further and specific analysis before making definitive considerations. This is also considering that statistical adjustment of precipitation represents a more

complicated exercise. Especially concerning the well-known underestimation of dry-days by climate models, that would require a preliminary dry-days frequency correction (Boé et al. 2007).

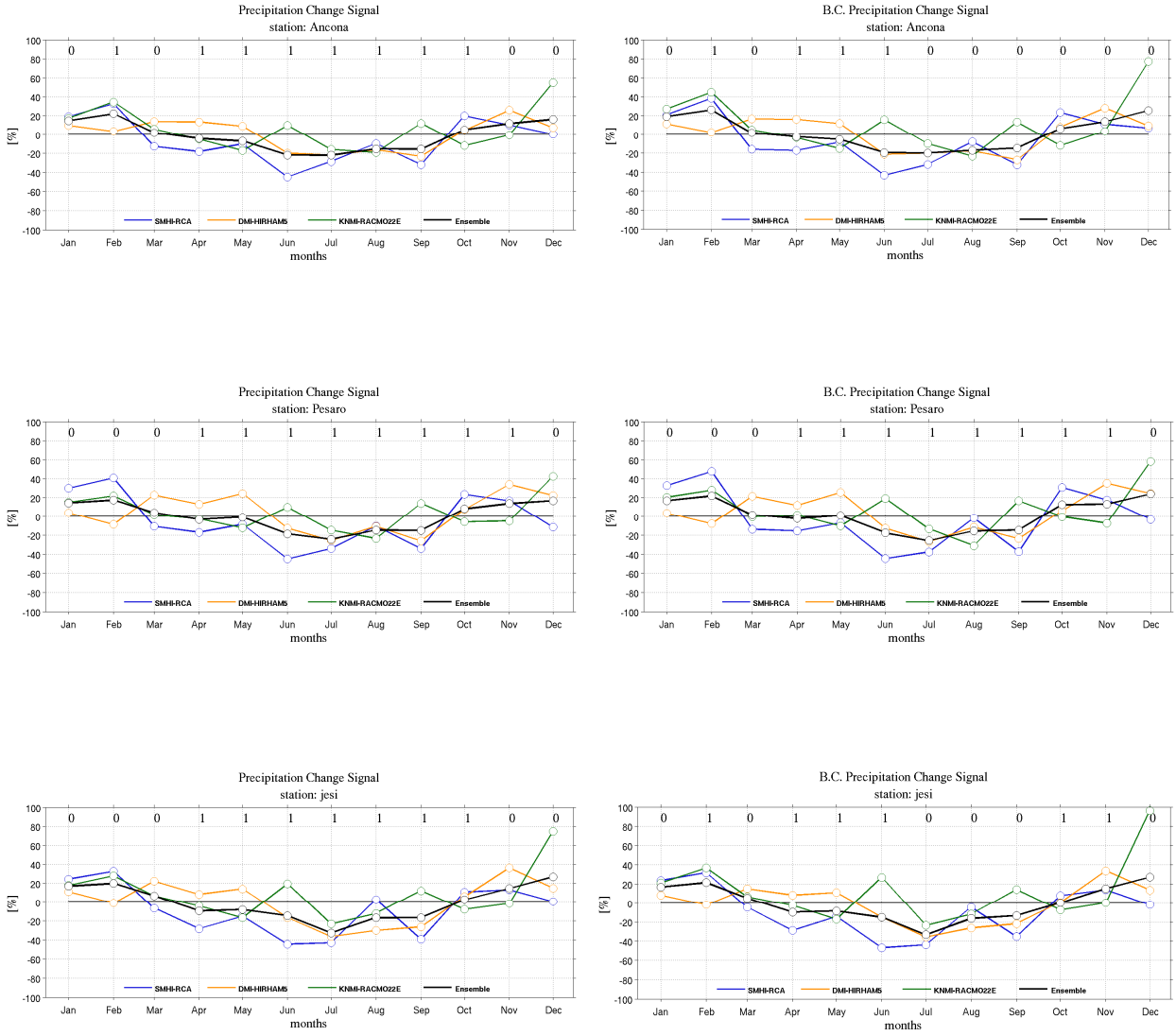

Figure 3.27. Precipitation annual cycle climate change signal for valley-coast representative Marche region stations. Colored lines represent the response of individual climate models. Black line the three-model ensemble mean. On the left panels original-simulations change signal and on the right panels bias-corrected simulations change signal are shown. Numbers (1 or 0) in the upper part of the plots are the results of Wilcoxon statistical test. It assess changes in the median between ensemble reference and future time segments attributing or not statistically significance to the changes in the precipitation distribution. Monthly mean signal has been computed for the long-term time horizon (2061-2090) compared to the reference period 1971-2000. Results are relative to the RCP8.5 boundary conditions.

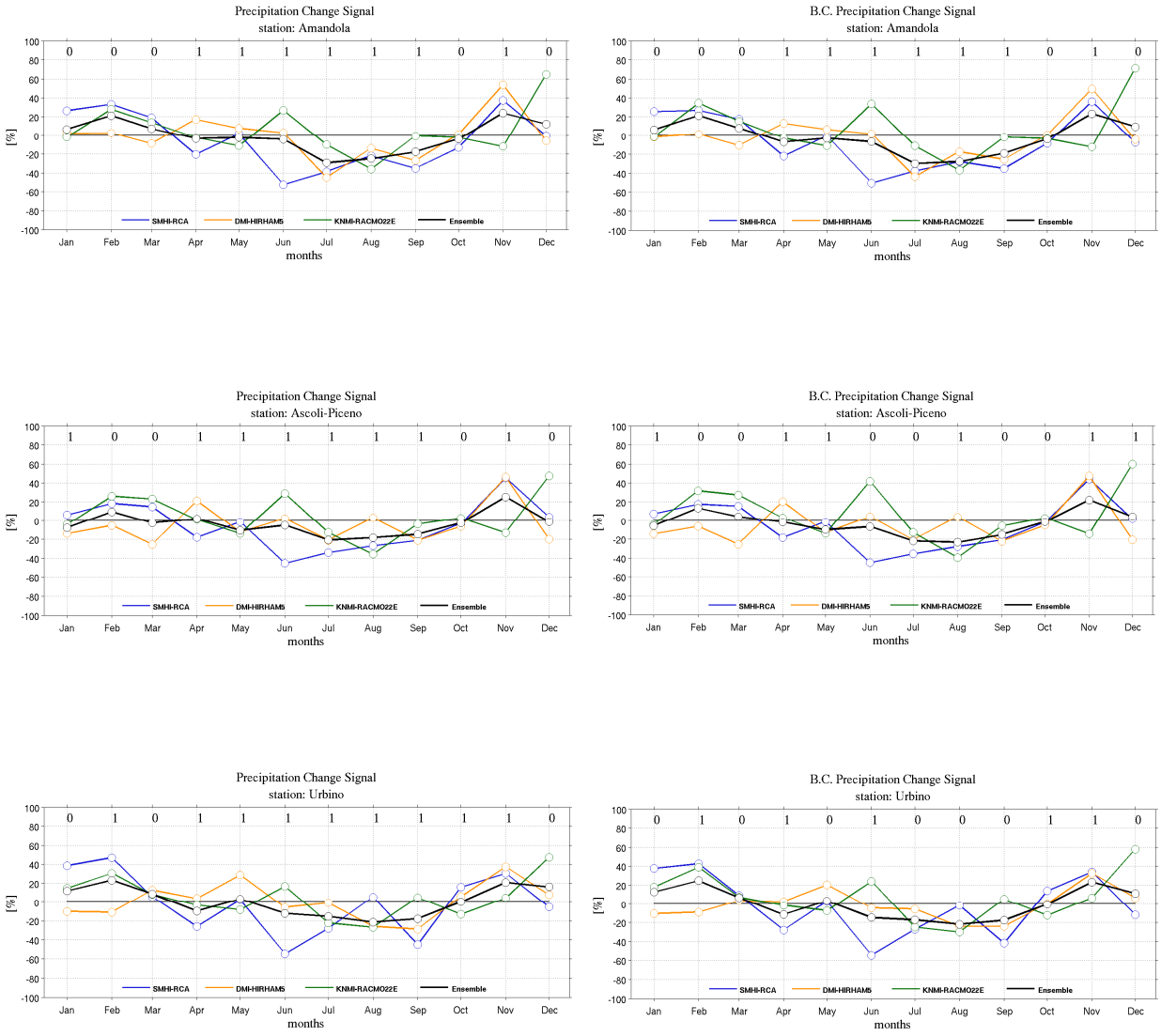

Figure 3.28. Same as figure 3.27 but for hill-mountain stations.

3.2.3.2 Climate change signal statistical distribution – Precipitation

According to the evidence that changes affect differently mean and extreme values, signal related to the entire statistical distribution is in this section assessed. Expected local precipitation response refers to radiative forcing boundary conditions imposed by RCP4.5 and RCP8.5. Signal was derived from the comparison of the two entire blocks of data (reference and future) distribution considering only rainy days. As the previous analysis, results belong to a three-model ensemble run over six representative stations. Distribution signal is computed in percentage, allowing signal to be independent from physical precipitation value considered. In this way, relative changes affecting different statistics are comparable. Conversely, computing signal in the physical value (mm), future oscillation would be intensity-dependent with higher signal over higher quantiles and hiding changes over middle and lower quantiles. Here the focuses is devoted to assess the expected changes over rainy days with precipitation >= 0.3 mm/day and the effect of the statistical bias correction. This methodology has been chosen to investigate changes in precipitation character (not in frequency of rainy days). Moreover, it prevents the risk of inconsistencies correction function inconsistencies over very low quantiles given the observed "drizzle effect" of models (Teutschbein and Seibert 2012). Figures 3.29 and 3.32 report changes in precipitation distribution for the mid-term and long-term scenario according to RCP4.5 boundary conditions. In this regard, we can note only slight signal over the entire statistical distribution without systematic signal behavior along the statistical distribution and over the different representative stations. Precipitation signal is in general enclosed between ± 5% (figures 3.29 and 3.30). Considering a mitigation-undertaken scenario, the period 2021-2050 precipitation does not show evident changes compared to the reference period 1971-2000. Bias correction does not affect the noisy signal resulted. However, it is noticeable how in the correction of right-tail quantile value some instabilities could result. This probably represents an aftermath of the multiplicative approach of the precipitation correction (e.g. bottom-right panel of figure 3.29). The bias corrected signal remains within the range of ± 5% in all the stations considered. Extending temporal horizon (signal relative to 2061-2090 period, figures 3.31 and 3.32), wet days signal shows again noisy characteristics. Signal rarely exceeds 5% of increase in precipitation intensity. Positive signal exceeds 5% only over left part of distribution representing slight precipitation events. Such low signal does not allow to properly evaluating bias correction effect over the original climate change signal.

Mid-term scenario (2021-2050) – RCP4.5

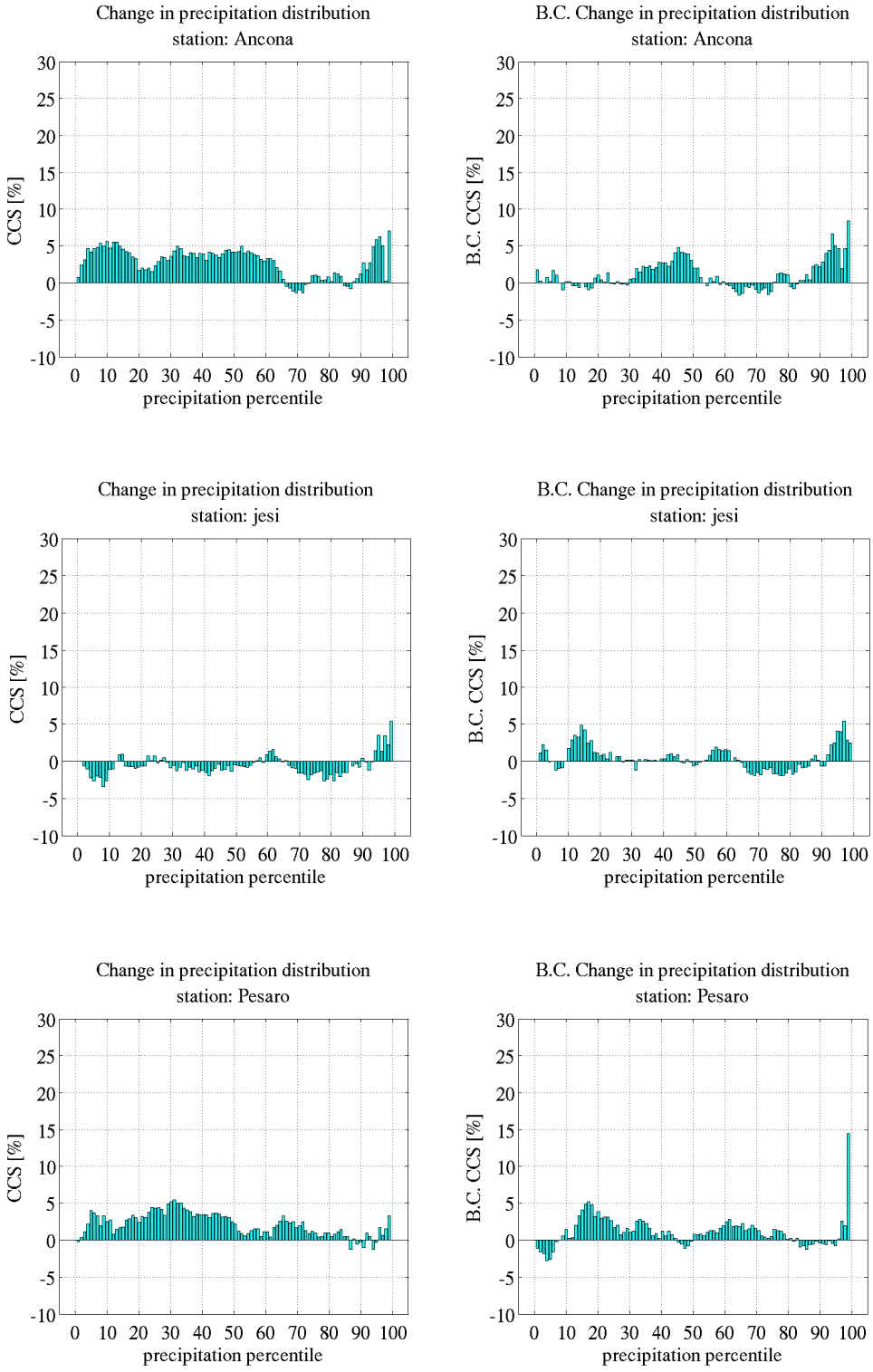

Figure 3.29. Valley-coast stations distribution climate change signal. On the left panels original results and on the right panels the bias-corrected simulations are reported. Mid-term scenario - RCP4.5.

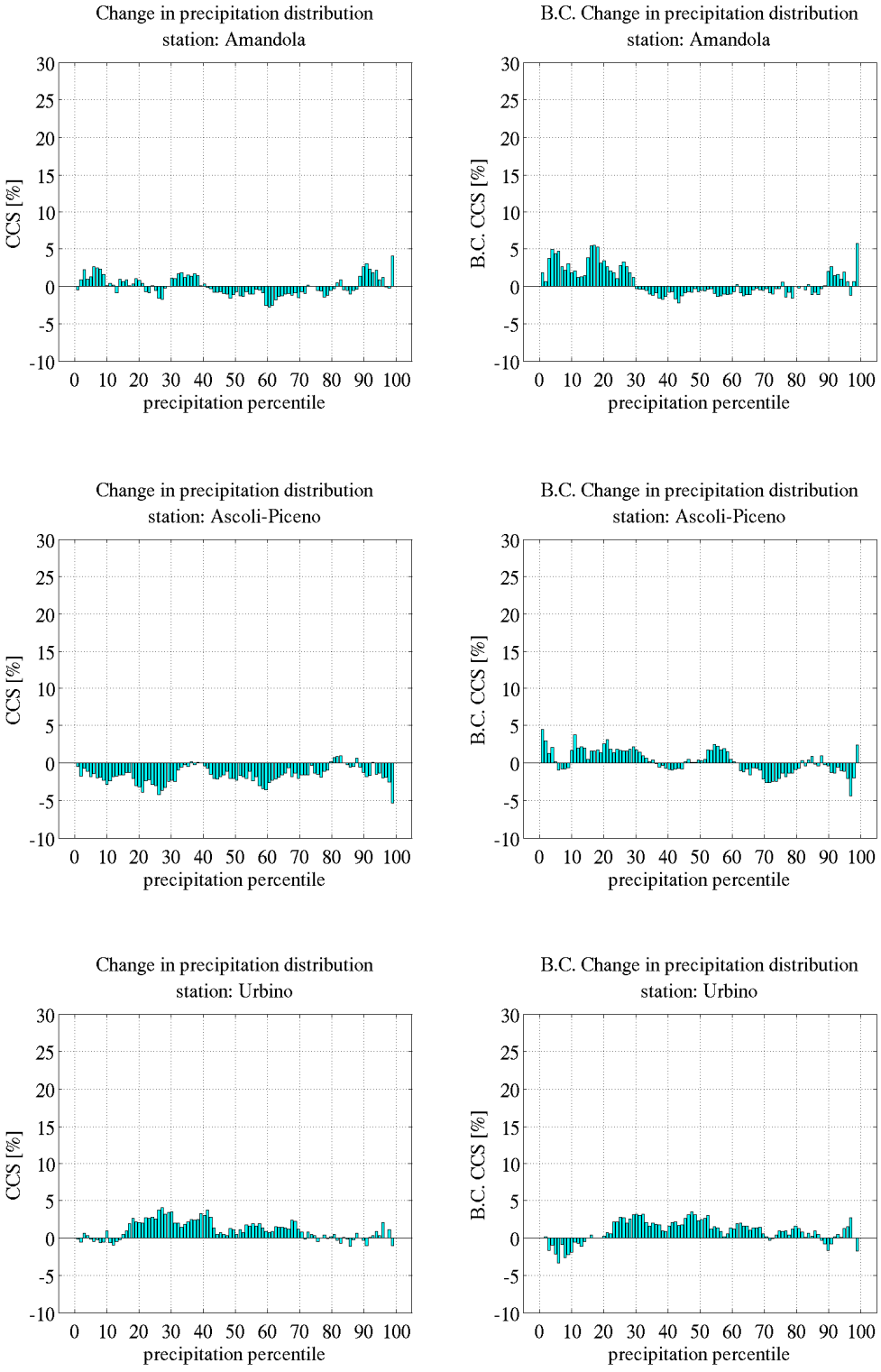

Figure 3.30. As in figure 3.29 but for hill-mountain stations.

Long-term scenario (2061-2090) – RCP4.5

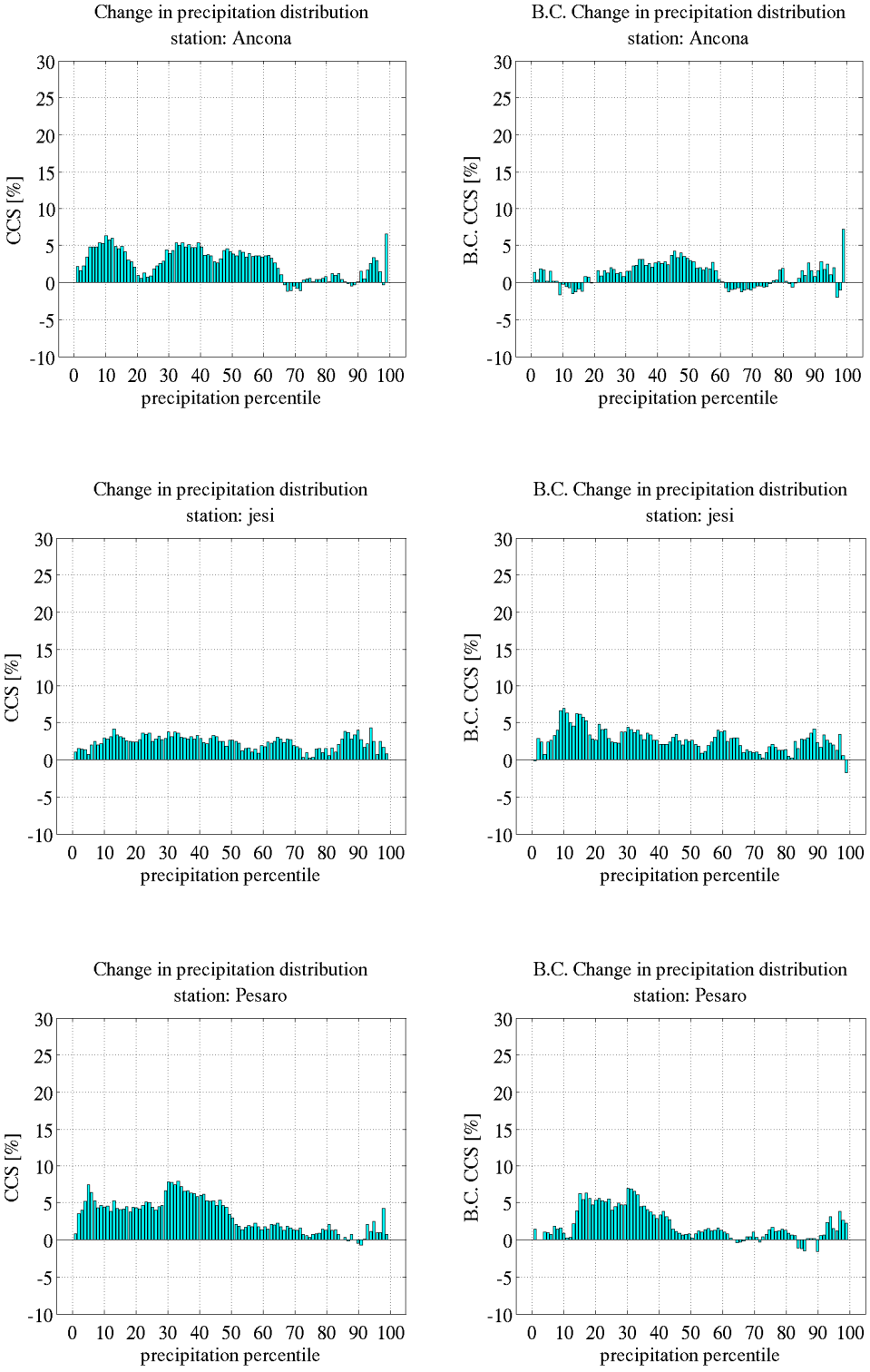

Figure 3.31. Valley-coast stations distribution climate change signal. On the left panels original results and on the right panels the bias-corrected simulations are reported. Long-term scenario - RCP4.5.

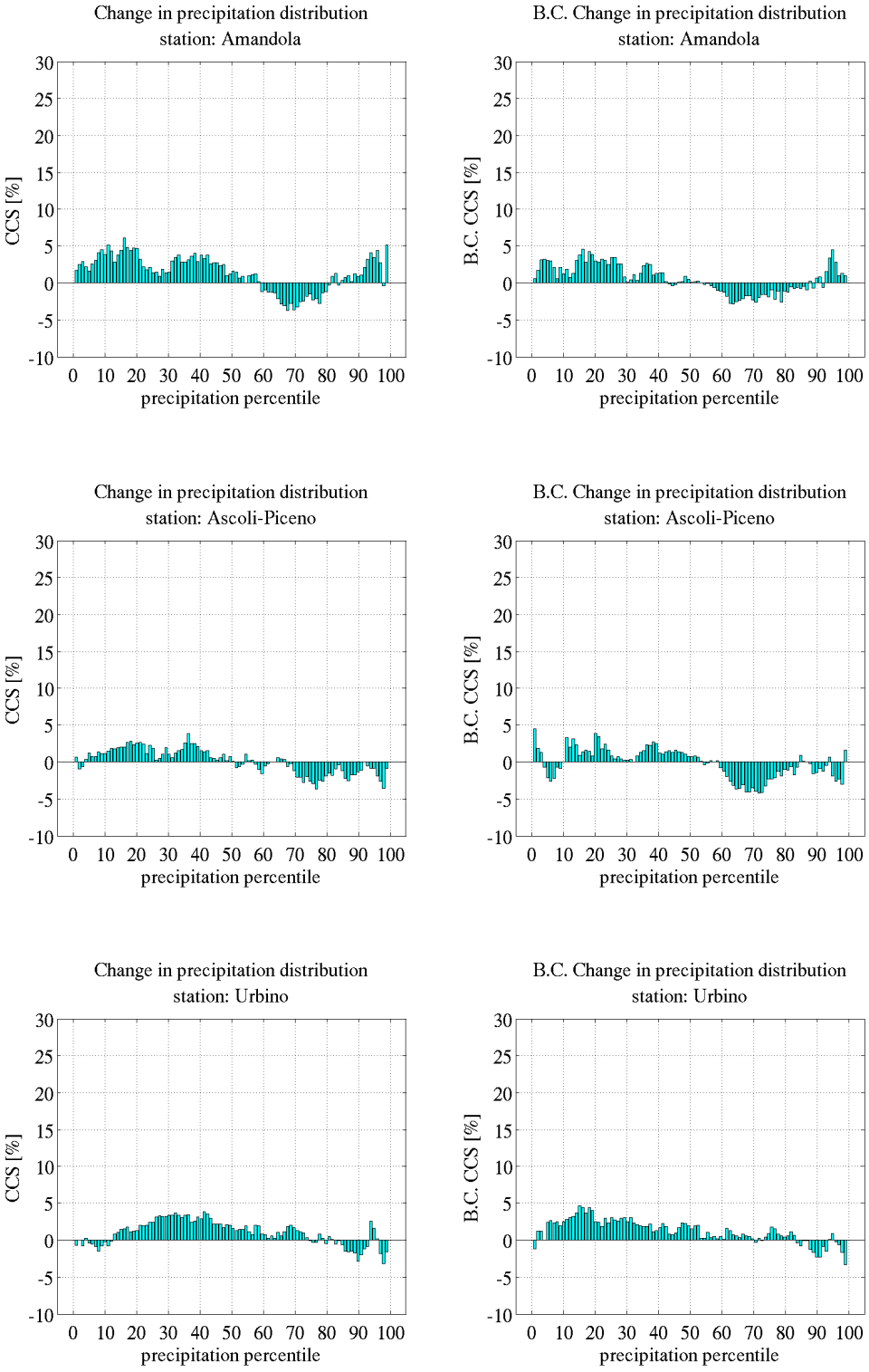

Figure 3.32. As in figure 3.31 but for hill-mountain representative stations.

It is now interesting assessing local precipitation response considering the *"business as usual"* emission scenario (Riahi et al. 2011) displayed in figures from 3.33 to 3.36. This scenario considers higher radiative forcing (+8.5 $W \cdot m^{-2}$ compared to the pre-industrial period) as consequence of increasing emission level until 2080's. For the mid-term scenario (2021-2050) original simulations indicate a slight increase of precipitation, during rainy days, over Marche region stations. The signal does not show clear patterns over specific part of distribution. Precipitation increase is generally below 10%. As in the previous experiments, bias correction does not affect magnitude and distribution of climate change signal.

For the long-term scenario (2061-2090), precipitation signal shows clearer distribution pattern. The central part of distribution, representing mean precipitation values, shows only slight increase approximately 5% - 8% and major increase focused on the right tails (10-15%). Moreover, we can note a regional latitudinal gradient with the two southernmost stations (Amandola and Ascoli Piceno) characterized by the smallest variation <+5% for Amandola and a small negative signal (≈ -3%) for Ascoli Piceno. Coherently with the previous results, bias correction application does not alter signal distribution and magnitude. Quantile mapping only moderate affects the left noisy part of signal distribution. This is the distribution part representing light precipitation events. Over such small precipitation amount correction function inconsistencies could be expected (Teutschbein and Seibert 2012).

A lot on the expected precipitation changes has been told. At Mediterranean basin scale, a relevant summer decrease (down to -30%) and a strong latitudinal pattern in winter are expected (see chapter 1). Moreover, particular attention on changing in extremes considered varying differently from the mean in the last decades is arisen (Frei and Schär 2001; Trenberth et al. 2003; Pal et al. 2004; Emori 2005; Trenberth and Shea 2005; Gao et al. 2006; Vrac et al. 2007; Allan and Soden 2007; Lenderink and Meijgaard 2008; Allan and Soden 2008; Liu et al. 2009; Lenderink and van Meijgaard 2010a; Toreti et al. 2010; Andrews et al. 2010; Reale and Lionello 2013; Hertig et al. 2014; Krichak et al. 2014). However, relating intense events changes to the mean changes is by no means trivial; it is difficult to establish a direct relationship, in any statistically meaningful manner, between isolated events and long-term trends (Frei and Schär 2001). At this regard, scientific literature suggests an exacerbation of dry-spell length coupled to intense-precipitation increase in the 21st century warmer atmosphere (Pall et al. 2007; Lenderink and van Meijgaard 2010a; Lenderink and

van Meijgaard 2010b). This is in accordance to Clausius-Clapeyron low, which derives relation between the increase of air masses temperature and related increase in moisture holding capacity. In a warmer atmosphere, if changes in the ambient flows have little impacts on moisture convergence, precipitation rate modification are indeed expected. Magnitude of atmospheric moisture exponentially growth with temperature, approximately 6.5% K^{-1} for high-percentile and approximately 3.4% K^{-1} for the mean precipitation (Pall et al. 2007). These theoretical values have to be tested on the different regional and local conditions. Synoptic circulation patterns, local physiography and soil cover could deeply alter local response. Indeed, increase in extreme precipitation of 6.5% K^{-1} indicated by Pall et al. (2007) for the mid-latitude seems to exceed the end-21st century local response shown in figures 3.35 and 3.36. Increase of precipitation right tail is roughly enclosed between 10-15%, coupled to an increase in temperature of roughly 3.5°C – 4 °C (figures 3.19 and 3.20). Finally, to underline is that only considering RCP8.5 long-term horizon precipitation scenario provides clear signal distribution-pattern signal, where larger increase over the right tail (≈ 15%) resulted in all stations considered. While temperature scenario resulted characterized by coherent temporal and distribution patterns, precipitation signal characterization more problematic. Also for what concerns the statistical correction, precipitation requires more complex approach than for temperature. Hence, these preliminary considerations should be followed by further analysis devoted to assign statistical weights to resulting change signal and to the effect of the bias correction.

Mid-term scenario (2021-2050) – RCP8.5

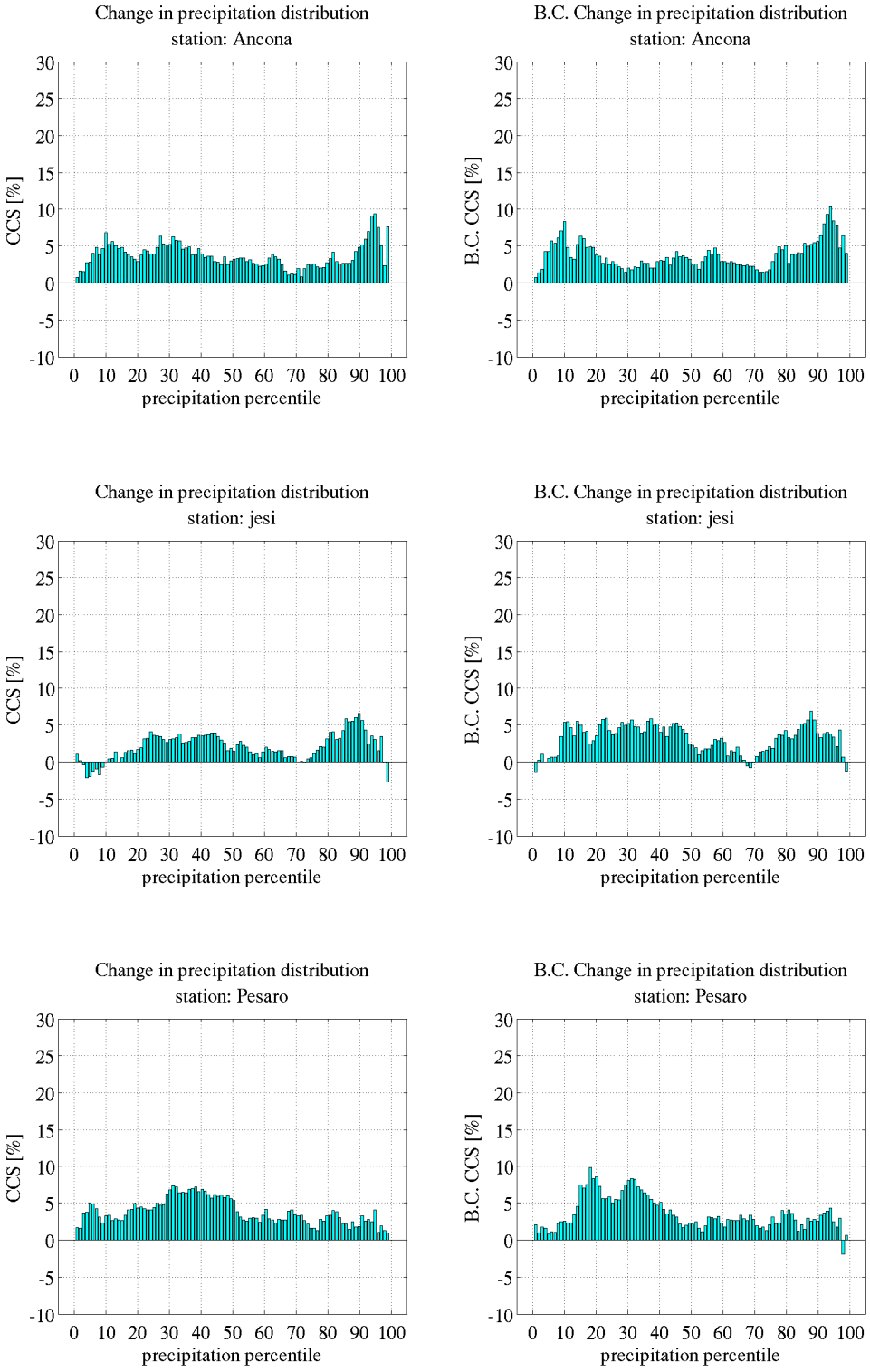

Figure 3.33. Valley-coast stations distribution climate change signal. On the left panels original results and on the right the bias-corrected simulations are used. Mid-term scenario - RCP8.5.

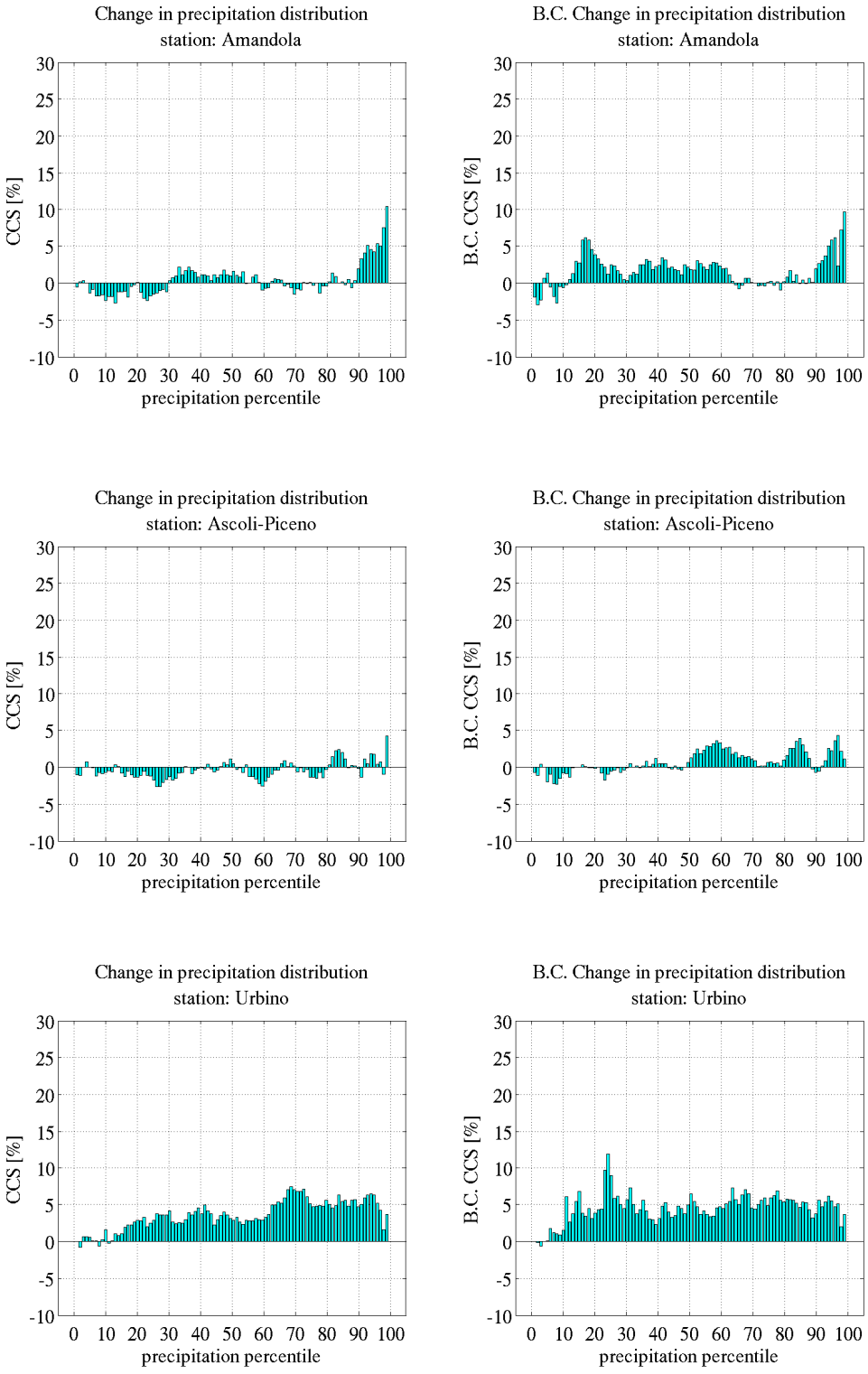

Figure 3.34. As figure in 3.33 but for hill-mountain stations.

Long-term scenario (2061-2090) – RCP8.5

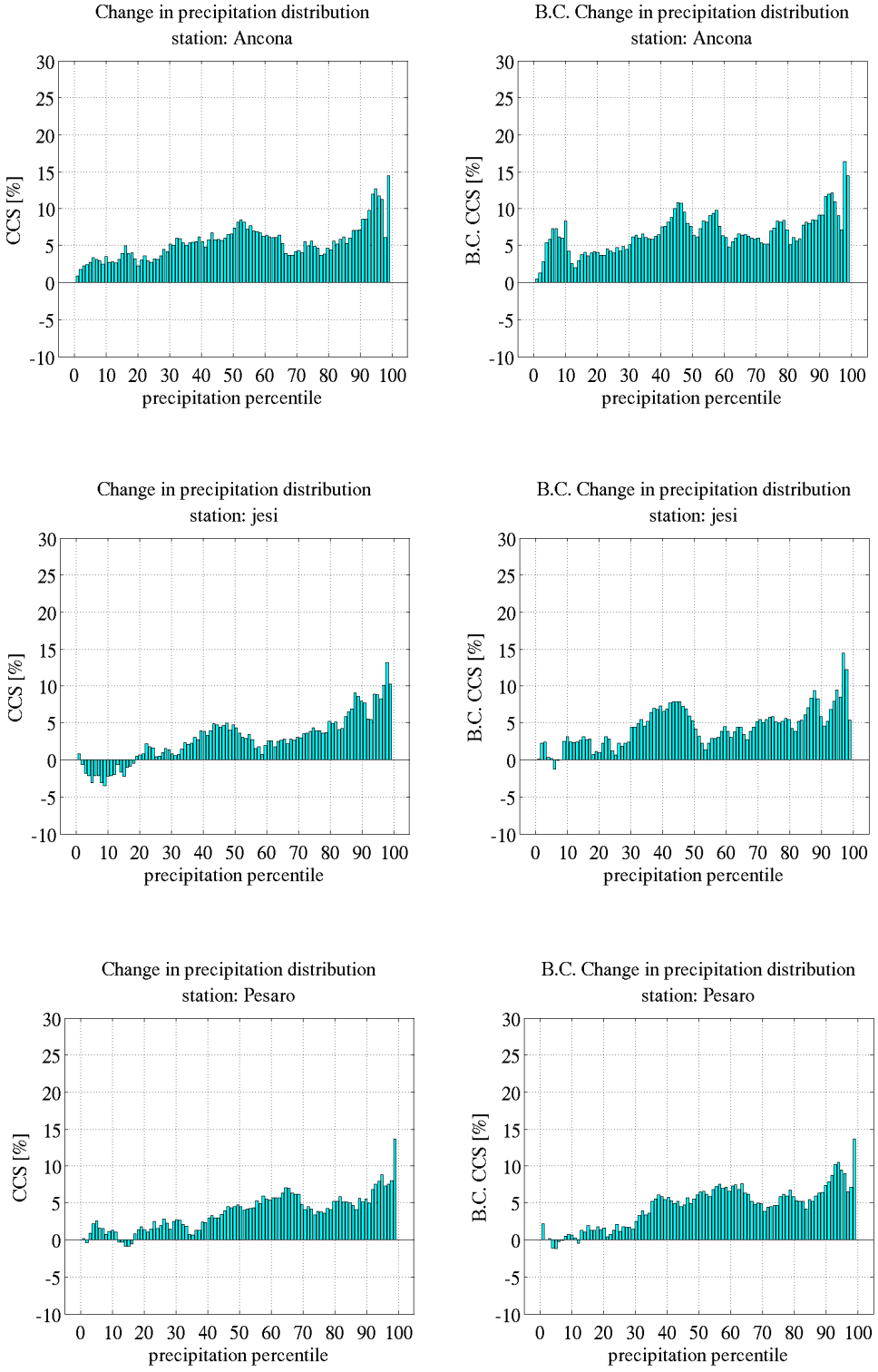

Figure 3.35. Valley-coast stations distribution climate change signal. On the left panels original results and on the right the bias-corrected simulations are used. Long-term scenario - RCP8.5

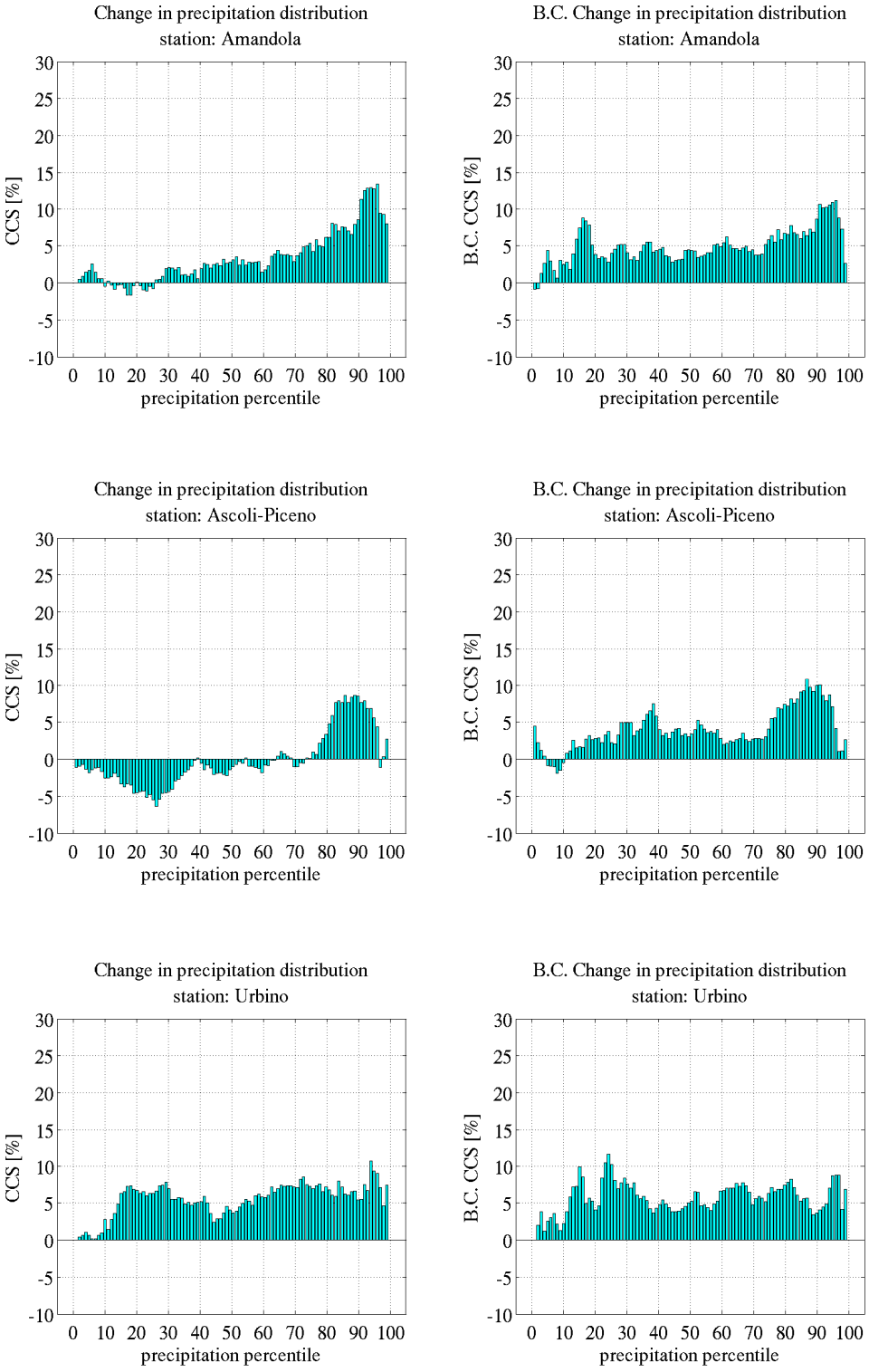

Figure 3.36. As in figure 3.35 but for hill-mountain representative stations.

3.2.3.3 Summary boxplots - Precipitation

Figures from 3.37 to 3.42, report summarizing boxplots for precipitation local climate scenario experiment. Through this kind of representation, it is possible to inspect, within a single plot, performance of original simulations, effect of bias correction (calibration and evaluation phases) and climate change signal for the 2061-2090 period (RCP8.5). Boxplots are built considering only rainy days (>= 1 mm/day) of each block of data, for each regional climate model used and each representative station considered.

The first two boxplots on the left of each panel assess the capability of original climate model simulations to reproduce the observed precipitation climatology over the period 1971-2000. Boxplots provide 5^{th}, 25^{th}, 50^{th}, 75^{th}, 95^{th} percentile and outliers (values beyond 95^{th} percentile) of the daily precipitation amount of the considered block of data. Going through figures, it is noticeable an underestimation of simulated precipitation in almost all the stations affecting all climate models employed over reference period 1971-2000. As seen in the temperature boxplots assessment KNMI-RACMO22E model is the most affected by negative bias up to more than 10 mm for the 95^{th} percentile, corresponding to a relative percentage bias of 35-45%. These biases are mostly affecting plain-coast stations. However it is evident a generalized underestimation of local precipitation performed by all the climate models. Over the calibration period bias correction lead to a perfect simulation of the same-period precipitation. This effect is not surprising since the correction function is built and applied over the same period. More interesting is to assess the capability of bias correction to reduce the simulation error over the 2001-2010 period since not used in the correction function calibration. Satisfactory results were obtained for what concerns correction of hill-mountain stations precipitation especially over 95^{th} percentile and outliers. A drawback of bias correction is a moderate overcorrection over coastal stations. For what concerns future precipitation change signal according to the previous analysis, increase mainly focused on the 95^{th} percentile of distribution resulted ($\approx$ 5 mm). KNMI-RACMO22E is the climate model showing a higher precipitation change signal in all the stations and Ascoli Piceno is the only station showing a reduction of precipitation 95^{th} percentile (indicated by the 2/3 of models).

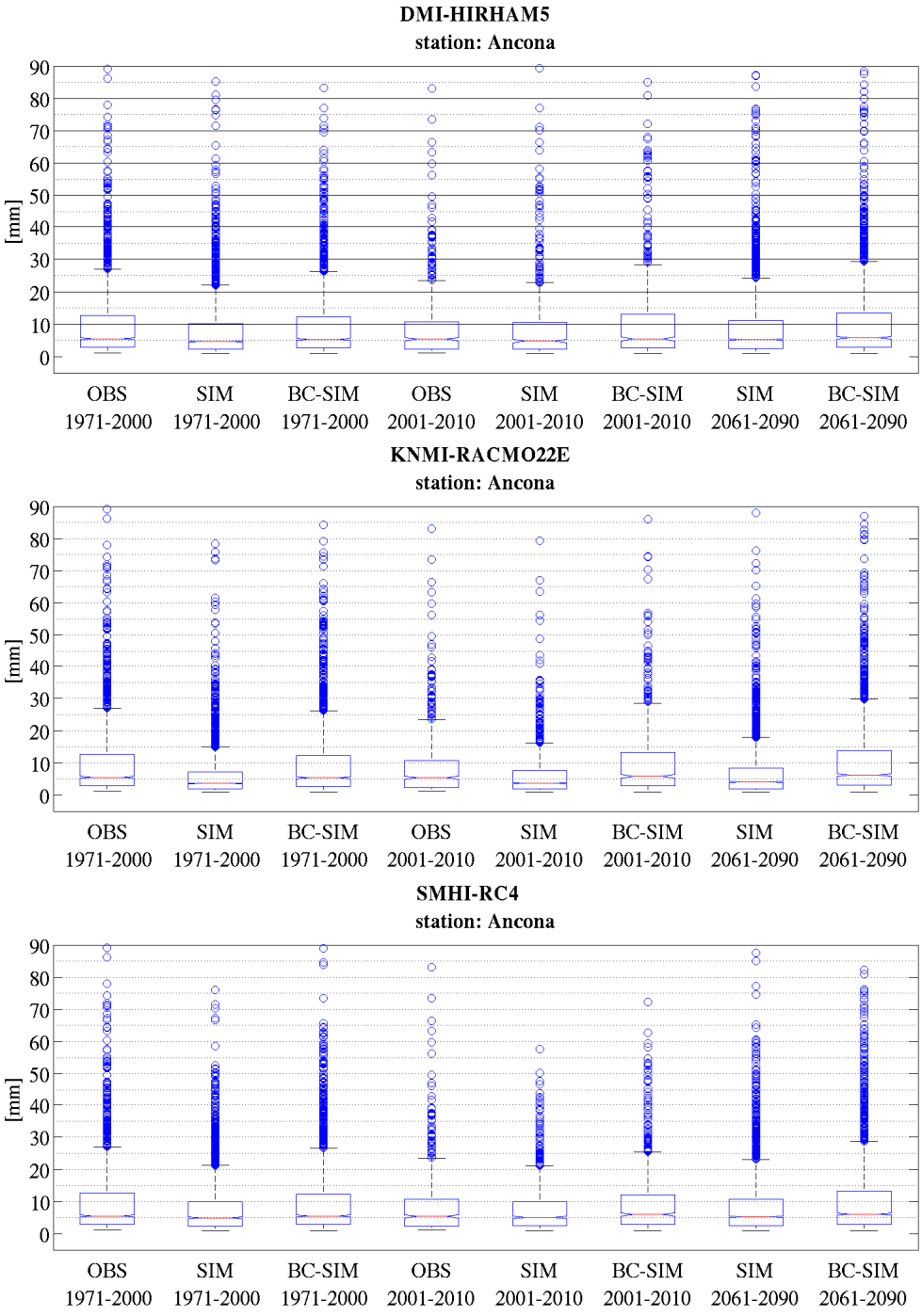

Figures 3.37 – 3.42. From left to right for each panel: calibration phase consisting on observation, original simulation and bias-corrected simulation over 1971-2000. Evaluation phase same as calibration but regarding to the 2001-2010 period. Right-end boxplots report, far future original and bias-corrected simulation (2061-2090). Results has been reported for each climate models employed and for 6 representative Marche region stations (Ancona, Pesaro, Senigallia, Amandola, Ascoli Piceno, Urbino).

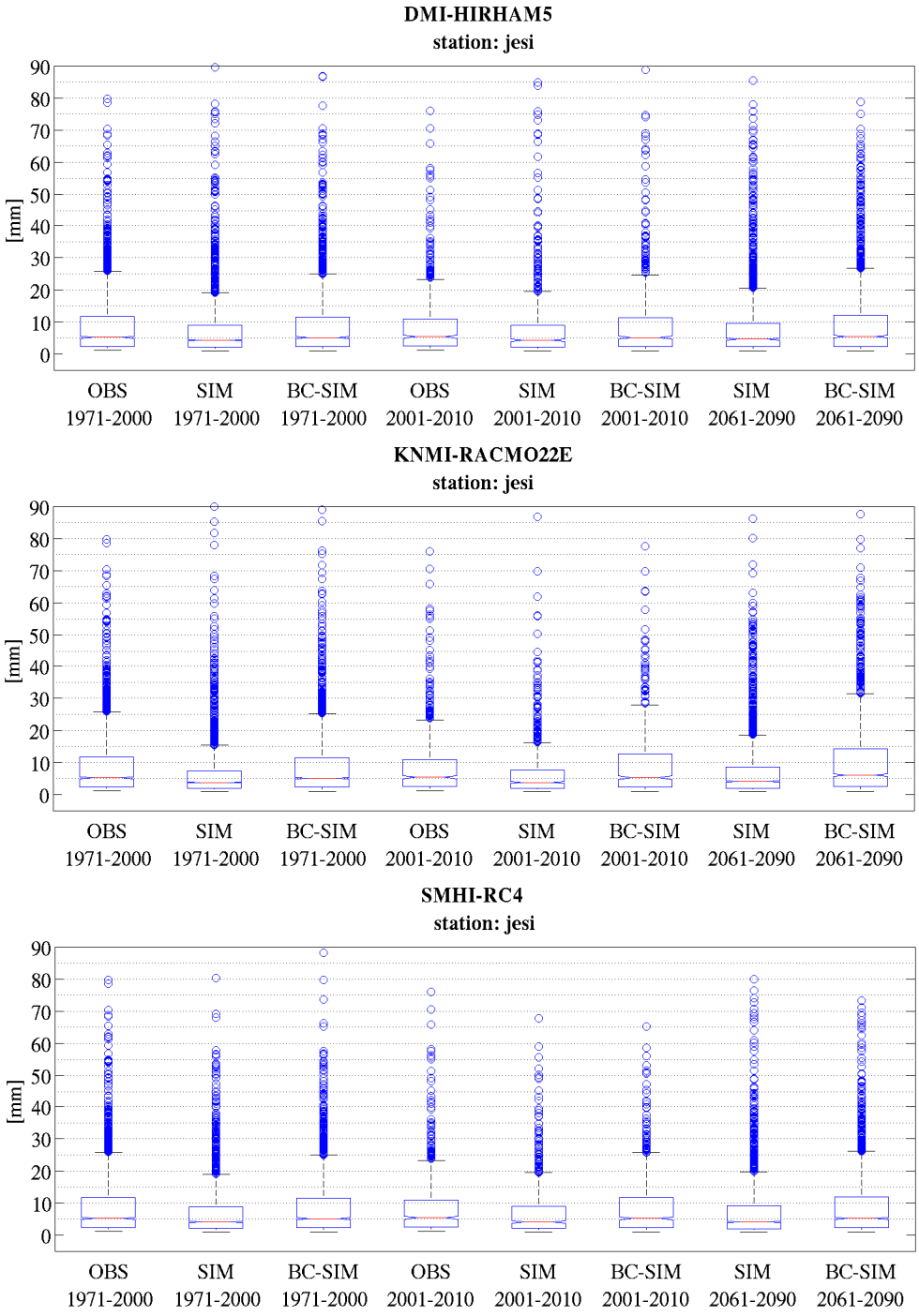

Figure 3.38. Boxplots for Jesi station precipitation.

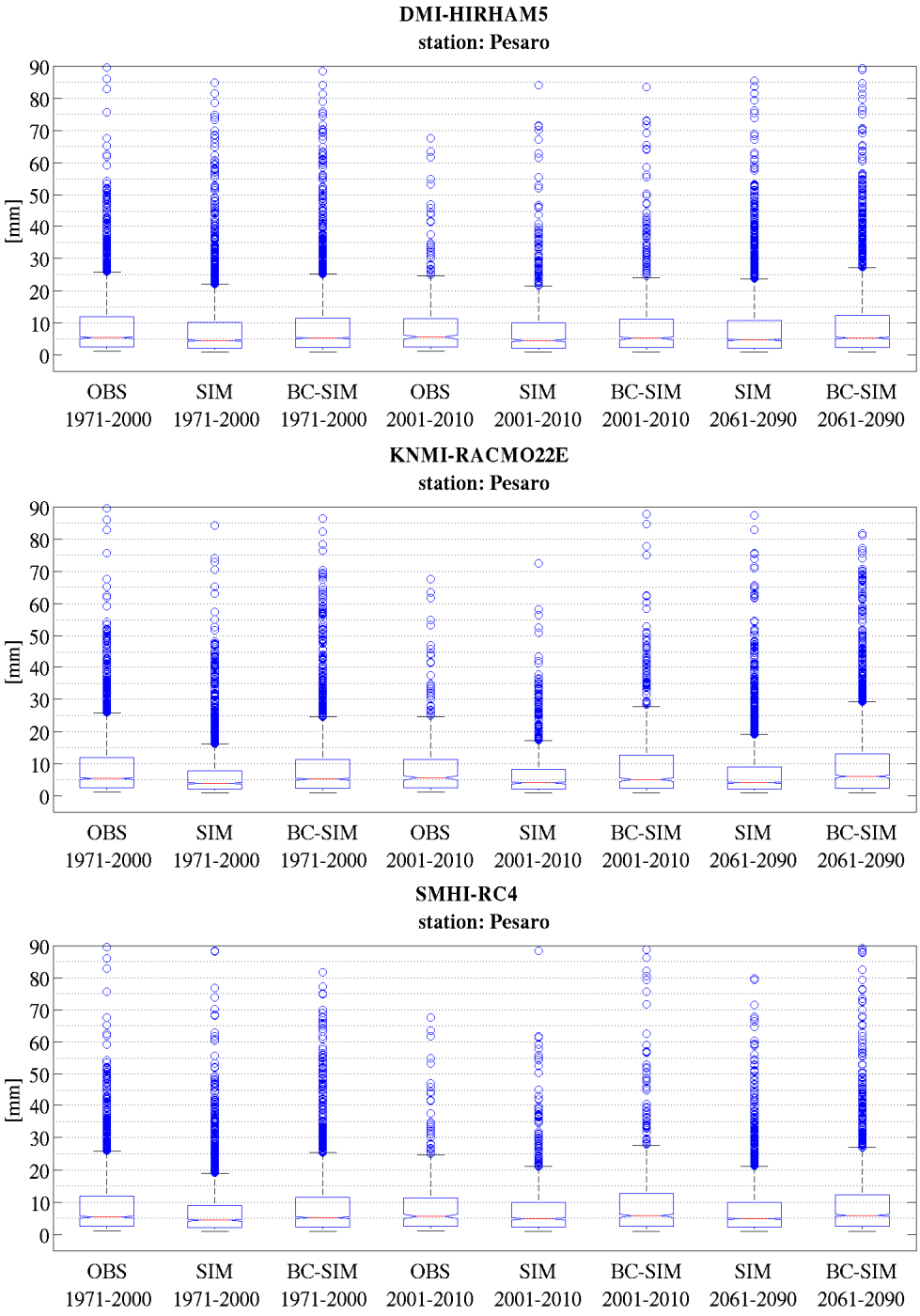

Figure 3.39. Boxplots for Pesaro station precipitation.

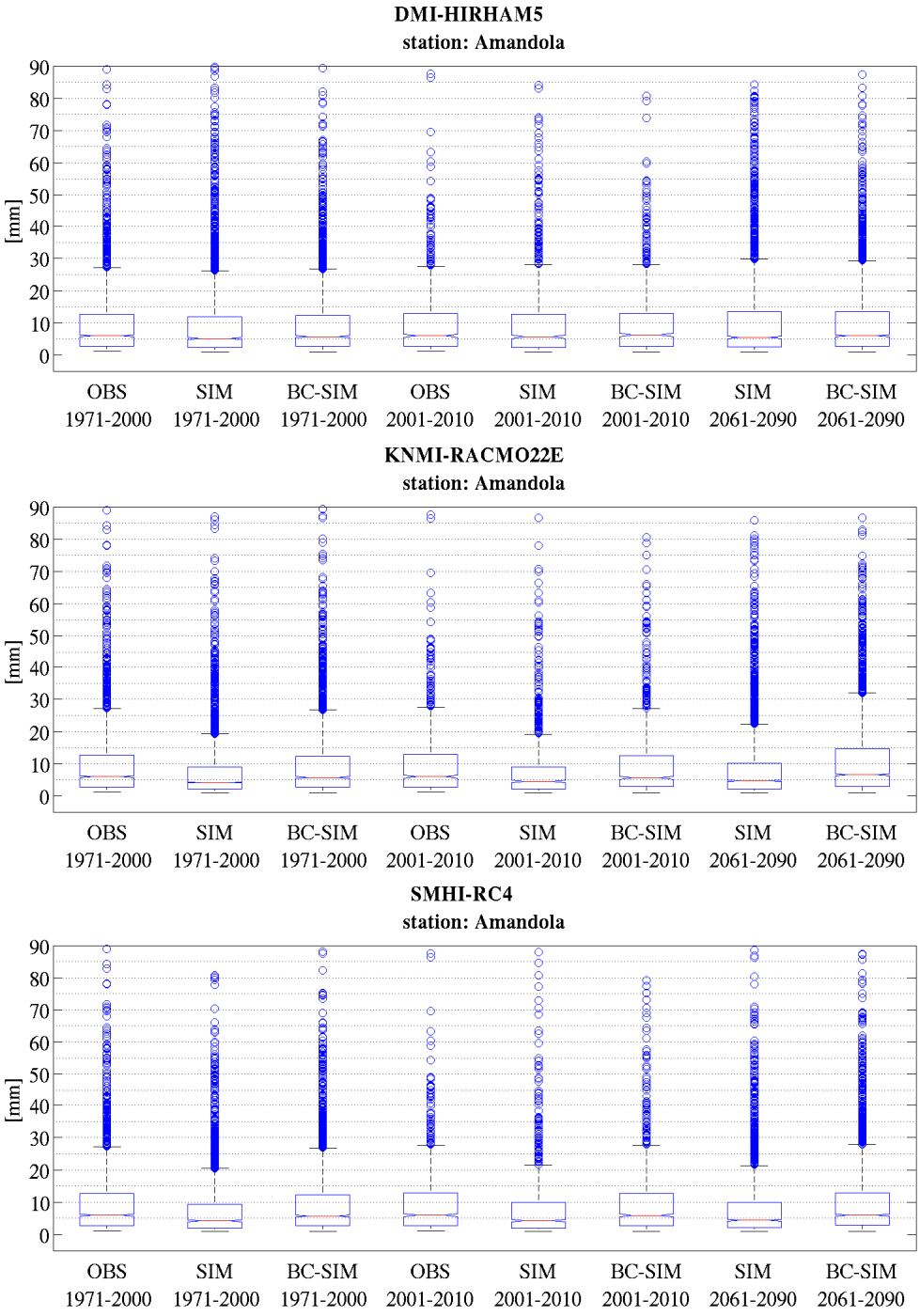

Figure 3.40. Boxplots for Amandola station precipitation.

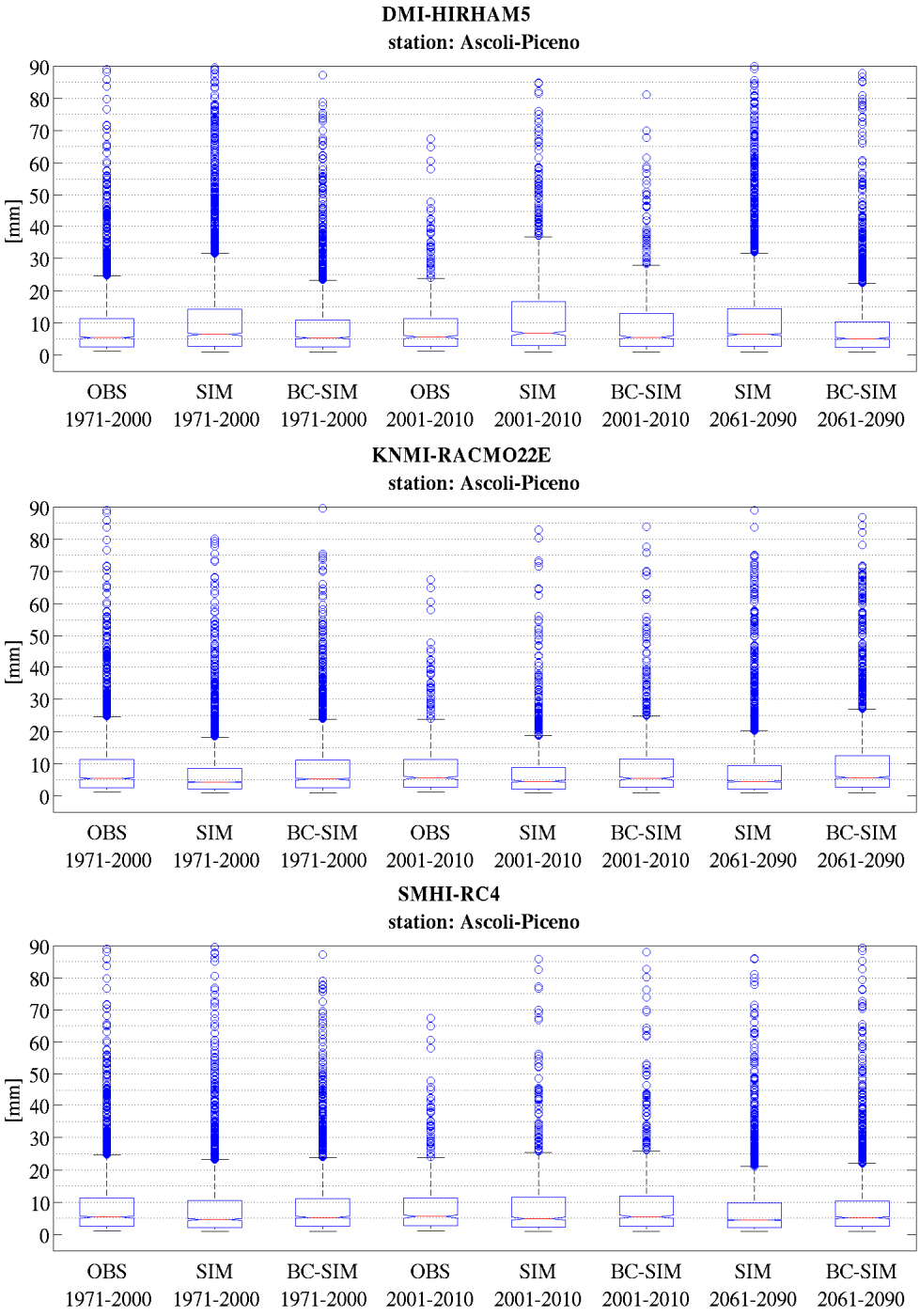

Figure 3.41. Boxplots for Ascoli Piceno station precipitation.

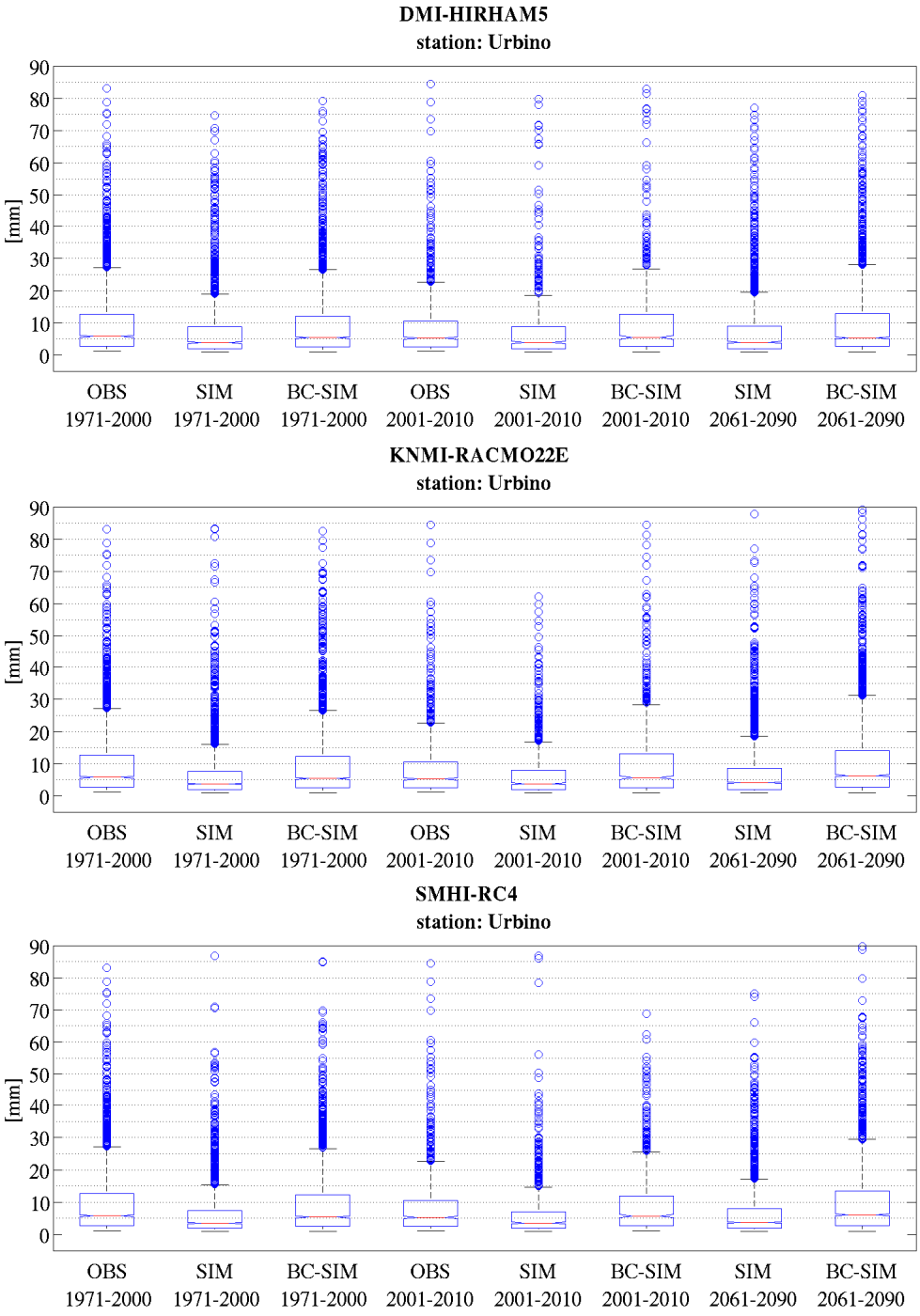

Figure 3.42. Boxplots for Urbino station precipitation.

3.2.4 Changes of the hydrologic cycle in a warmer atmosphere: Hydro-climatic Intensity Index (HY-INT)

To complete precipitation analysis, figures 3.43-3.47 show results from the Hydro-climatic Intensity Index (HY-INT) following Giorgi et al. (2011). Differently from previous assessments, the temporal evolution (1971-2100) of mean annual values of the index is reported. Annual mean trends were derived in comparison to the reference period 1971-2000. Given the similarity obtained in trends intensity involving all the reference stations, only results of 4 representative Marche region stations are in this section reported. Two of those for valley-coastal and other two for hill-mountain sector. As in the previous analysis, HY-INT index has been computed using original and bias-corrected three-multi model ensemble climate simulations. Each figure from 3.43 to 3.46 reports three columns. Hence was considered useful to investigate, besides the index (right column), individual response of the two metrics constituting HY-INT index. In the upper-row panels original simulations and in the lower-row panels bias-corrected simulations are presented. RCP8.5 radiative boundary conditions are considered. For the two metrics (mean annual precipitation intensity during rainy days (INT) and mean annual dry-spell-length (DSL)) and the index (HY-INT) trends statistical significance has been inferred through Mann-Kendall statistical test (Wilks D.S., 2011). In left-column panels linear trend for the INT metric are reported. It shows temporal evolution of mean precipitation intensity during rainy days. For all the stations considered, positive statistical significant trends resulted. Assessing the bias corrected simulation results we can note that the statistical significance of trends is not affected. Effects over the absolute value (mm/day) of metrics did not alter the statistical significance. Recalling the underestimation of simulated precipitation resulted in the previous phase, higher bias-corrected precipitation intensity is coherent with a positive correction produced by the quantile mapping. Moreover, bias-corrected time series present higher inter-annual variance especially for the coastal stations. Following the temporal structure of trends, we can note a trend getting stepper after roughly 2020's.

In the central-column panels dry-spell-length metric (DSL) trends are reported. For all the stations studied statistical significant positive trends resulted. Relatively longer "recharge time" (longer dry periods) would be need for moisture to replenish a warmer atmosphere to local saturation condition. In accordance with the Clausius-Clapeyron relationship that implies an increase of atmospheric moisture holding capacity of approximately 7% $(°C)^{-1}$ of warming. The intensity of the trends is coherent distributed over coast and hill representative

stations. Also for DSL metric, bias corrected simulations show no alteration of the statistical significance of resulting trends. On the right-column panels, HY-INT index trends are reported, normalized over the reference period 1971-2000. Directly depending on the increasing of the two factors, significant increasing trends resulted in all stations. Statistical intensity of trends (p-values) resulted homogeneous over coast and hill stations. Ancona station stands out with a stepper interpolating regression line indicating relative higher acceleration of local hydrologic cycle. Aggregated results could be seen as measure of the acceleration of local hydrologic cycle to global warming connected. However, it is important to keep in mind that this index does not intend to represent a hydro-climatic extreme index, such droughts or floods. Especially it does not intended to capture any short-term events (Giorgi et al. 2011). Rather, it is a measure of strength of hydrologic cycle as reflected by precipitation intensity and length of dry periods (Giorgi et al. 2011) in a warmer atmosphere.

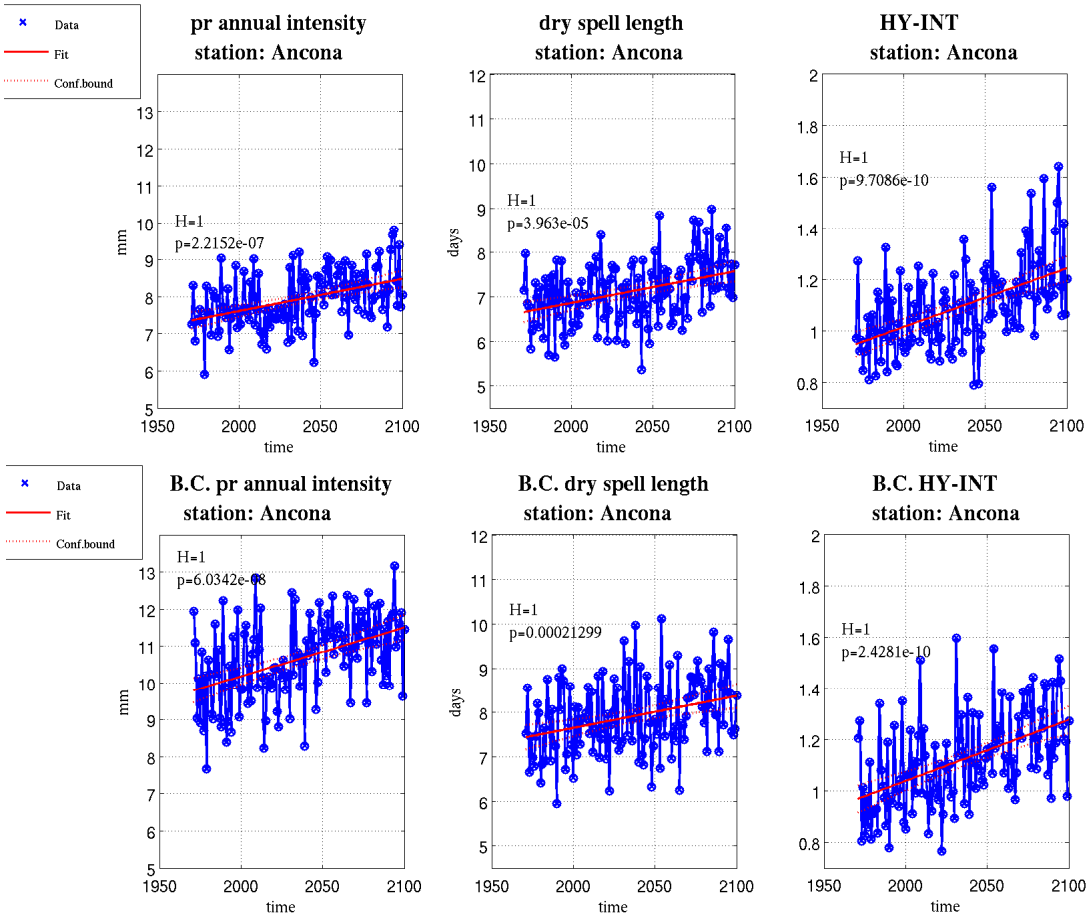

Figures 3.43:3.46. Original simulations (upper) and bias corrected simulations (lower) for mean annual precipitation intensity (left), mean annual dry spell length (central) and normalized hydro-climatic intensity index (right) panel. Trends are performed over the reference period 1971-2000. H value tests for the statistical significance of resulting trends. p value identifies intensity (slope) of derived trend. Red line represents mean annual values linear regression. Here are reported results belonging to 4 representative Marche region stations (Ancona, Pesaro, Amandola, Urbino).

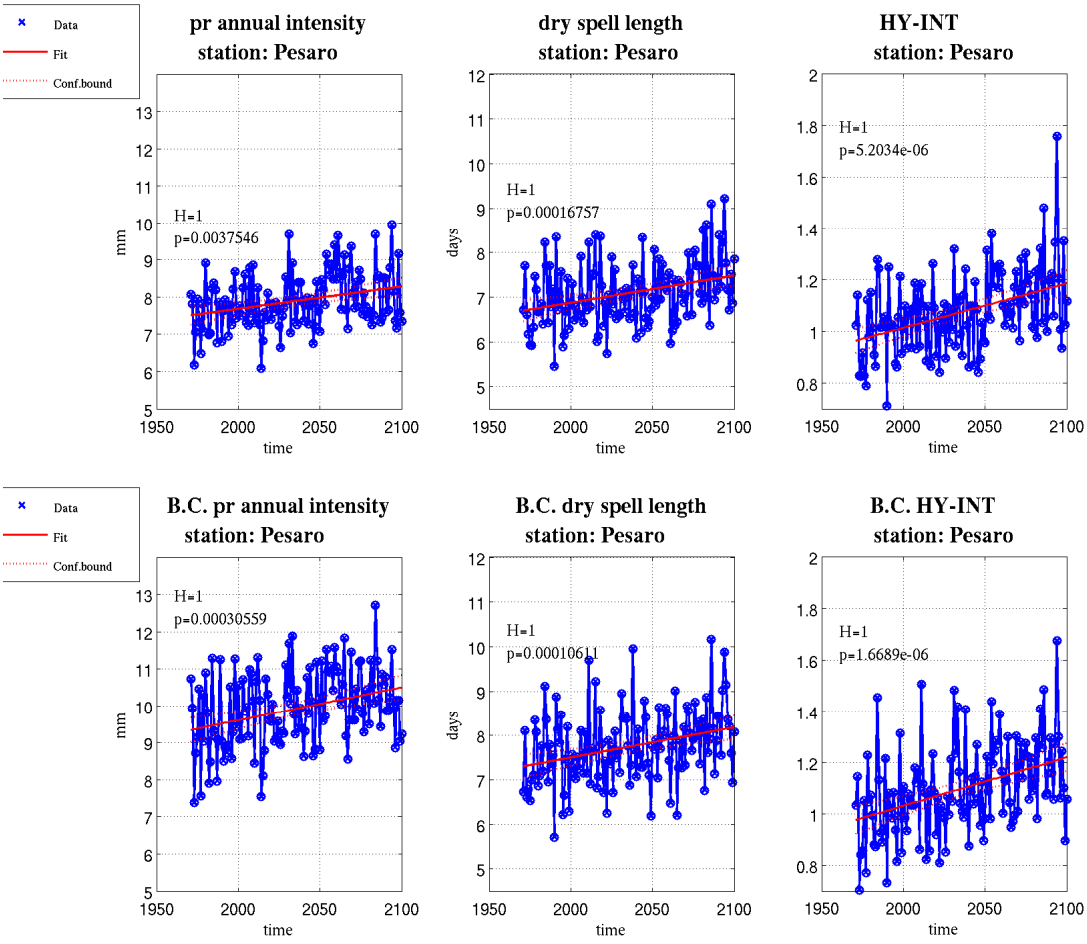

Figure 3.44. Hydro-climatic intensity index with original (upper row) and bias-corrected simulation (bottom row) for Pesaro station.

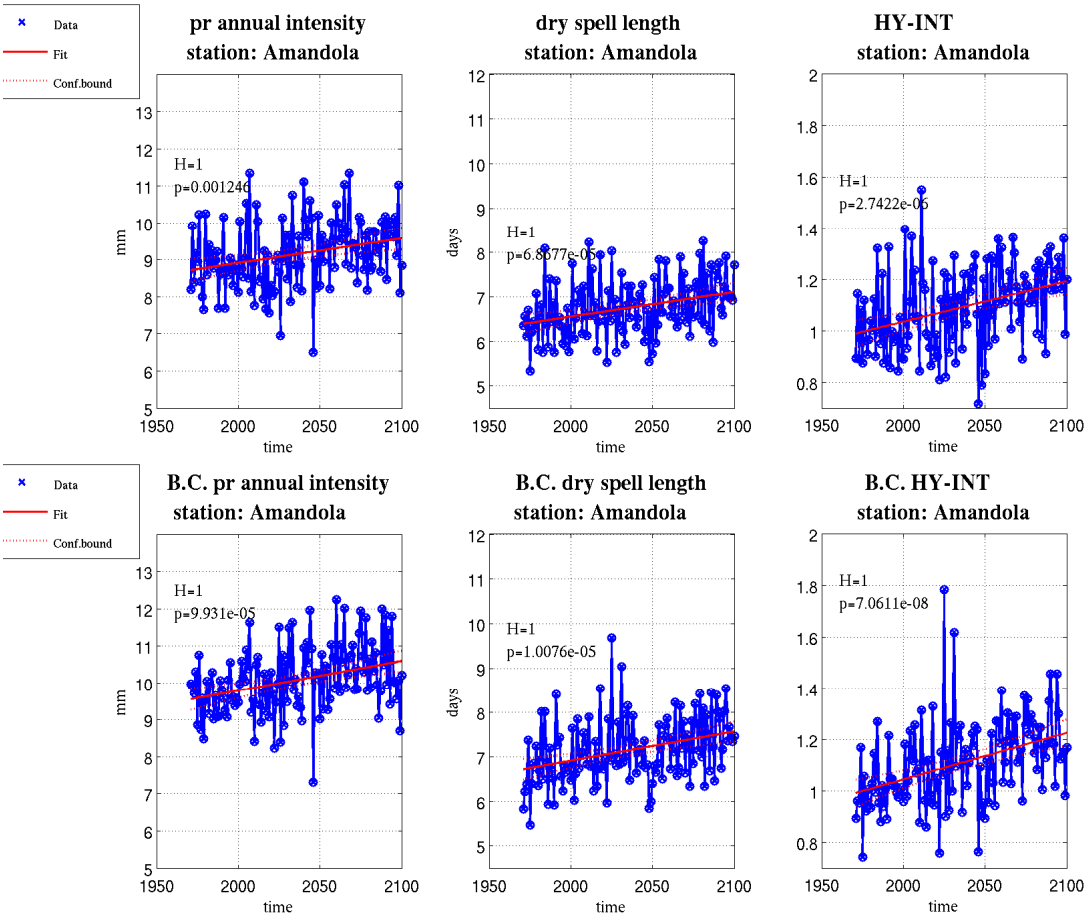

Figure 3.45. Hydro-climatic intensity index with original (upper row) and bias-corrected simulation (bottom row) for Amandola station.

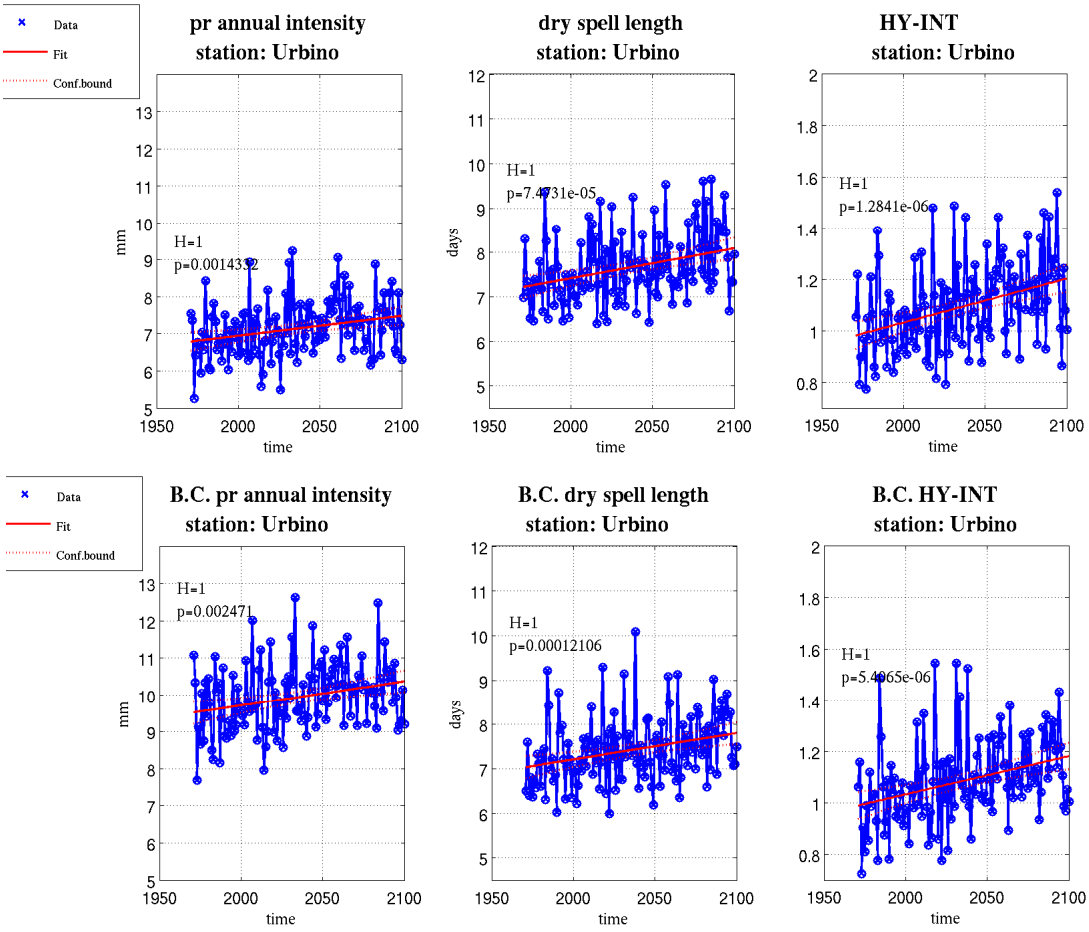

Figure 3.46. Hydro-climatic intensity index with original (upper row) and bias-corrected simulation (bottom row) for Urbino station.

3.3 Conclusions and summary

This third chapter wanted to bridge the gap between the resolution of climate models and local scale. In fact is local the spatial scale at witch climate impacts act and have to be characterized. This holds strategical importance, addressing all-level society needs of benefiting of future climate information strictly spatially referenced. This kind of information would in this way promptly usable to assess vulnerability and impacts resulting by combination of expected changes in climate dynamics and local-scale exposure.

A three-multi model ensemble of very high resolution has been employed to define future local climate conditions (temperature and precipitation). Climate simulations are extracted in correspondence of Marche region representative stations. Climate simulations were statistically adjusted employing station-scale observed datasets provided by the regional Civil Protection weather stations network. Results from the correction function calibration and evaluation phases have been reported for each model employed over representative stations. Raw and bias-corrected simulations are successively employed to compute station-wise climate change signal. Annual-cycle, and the distribution climate change signal have been in depth investigated. Moreover, focus of this section was devoted to study the effect of the statistical adjustment on climate change signal, assessing the results before and after bias correction.

Specific analysis were conducted to test expected changes in the hydrologic cycle in a warmer atmosphere. This assessment was carried out computing (with original and bias-corrected climate model simulations) a hydro-climatic intensity index. This index joins metrics of mean precipitation intensity (during rainy days) and dry spell length 21st century trends.

Results concerning temporal distribution of the signal (annual cycle) highlighted summer season as the most affected season by warmer and drier future conditions (up to +4.5 °C for temperature and -20% for precipitation) at the end of 21st century (RCP8.5). Concerning the precipitation signal, autumn and winter seasons signal showed a moderate increase of precipitation intensity (up to 20%). Concerning the statistical characterization of the signal, right tail of statistical distribution resulted affected by higher signal for both temperature and precipitation. In addition, a significant acceleration of hydrological cycle was resulted consisting on higher precipitation intensity during rainy days and longer dry spell length resulted in all the stations considered.

The effect of bias correction over the climate change signal accords with the results of the regional experiment. The summer signal is reduced of about 0.5-0.8 °C only over coast-valley representative stations. Over hill-mountain stations, summer temperature signal was not altered by the statistical correction. These results are supported by outcomes of several studies asserting an intensity-dependence of climate models error. (Christensen et al., 2008; Themeßl et al., 2012; Boberg and Christensen, 2012). Simulating higher temperature, the coast-valley areas future summer temperature would be subjected to a major correction than the corresponding reference segment. This is not true over hill-mountain stations where simulated temperature values are smaller. Here, the signal was confirmed even after the correction since. This explains the reduction of summer climate change signal focused in areas characterized by high summer temperature (valley and coast). Furthermore, a consistent increase of the signal affecting the right tail of temperature distribution was observed during winter season over both coast-valley and hill-mountain stations. Bias correction did not affect precipitation annual cycle signal nor the distribution signal. Influences were observed over the statistical significance of monthly-mean changes and this fact deserves further analysis. Finally, even adopting different climate models with different boundary conditions and different observation resolution the effect of bias correction over temperature and precipitation signal resulted analogous in both regional and local experiment.

Follows summary results of each methodological section:

3.3.1 Quantile mapping bias correction – Calibration phase

Temperature

Original climate model simulations generally underestimate (up to 4 °C) local observed temperature especially over complex physiography terrain. The bias-corrected simulation perfectly reproduce observed statistical distribution. In the calibration phase this effect was expected since the correction function is built over the same thirty-year time slice.

Precipitation

Original climate model simulations well reproduce observed precipitation distribution over plain-coast representative stations. Original simulations perform sensibly worse on complex terrains. In this regard, it has been highlighted impossibility of using original climate model outputs as input in impacts modeling without previous statistical adjustment.

Bias-corrected precipitation perfectly reproduced observations. Also in this case, this is not surprising since the correction function is derived and applied over the same block of data.

3.3.2 Quantile mapping bias correction – Evaluation phase

Temperature

Bias correction has demonstrated able to correct temperature distribution (physical values and their variance) also over time segment not used in the calibration of the correction function. In the context of climate change studies, results of the evaluation phase are of particular importance since giving us a basic idea on the plausibility of applying bias correction over a future temporal segment. Residual errors remain over the extreme values represented by tails of distribution.

Precipitation

Simulated precipitation errors and variance resulted adjusted after the application of quantile mapping bias correction. Even residual errors are still present, quantile mapping improves the reproduction of observed precipitation especially the high-quantile precipitation events.

3.3.3 Climate change signal annual cycle

Temperature

In all the stations considered, summer months temperature resulted the most affected by warmer conditions (+3 °C / + 4 °C) compared to 1971-2000 period. Bias correction affects mean climate change signal reducing summer signal over coast station (≈ 0.6 °C) and strengthening winter signal on the same stations (≈ 0.5 °C). Signal of the hill-mountain stations resulted not affected by the bias correction. Radiative forcing boundary conditions relative to the RCP8.5 are here considered.

Precipitation

Precipitation monthly mean climate change signal showed characteristic seasonal pattern. Summer months showed a decrease of roughly 20% and an equal-magnitude increase over autumn and winter months. Climate change signal resulted not affected by the bias correction

application. These considerations refer to radiative forcing boundary conditions relative to the RCP8.5.

3.3.4 Climate change signal distribution

Temperature - Mid-term scenario (2021-2050) – RCP4.5

In all the stations considered changes in temperature are ≈ 1.5 °C in summer and ≈ 0.8 °C in winter. Bias correction dampens summer signal to (from 1.5 to 1.2 °C) and strengths original winter signal ≈ 1 °C to 1.2 °C (in the coast stations) affecting the right tail of distribution.

Temperature - Long-term scenario (2061-2090) – RCP4.5

Signal resulted ≈ 2.0 - 2.5 °C in summer. In winter, signal is below the + 2 °C in all the stations assessed. Bias correction dampens summer signal over the right tail of distribution (≈ 0.5 °C) and considerably strengthens right tail signal (from 2 °C to 2.8 °C) in winter only over coast stations.

Temperature - Mid-term scenario (2021-2050) – RCP8.5

Increase ≈ 1.8 °C in summer. In winter, the signal is roughly of + 1.2 °C. The bias correction affects the signal with the same magnitude of the corresponding RCP4.5 scenario.

Temperature - Long-term scenario (2061-2090) – RCP8.5

Increases range from 3 °C up to 4 °C, slightly higher over hill-mountain sector. In winter signal is ≈ 3 °C over both valley-coast and hill-mountain stations. Bias correction dampens summer signal of ≈ 0.8 °C over the right part of distribution in the coast stations and strengths the winter signal (≈ 1 °C) over the right part of distribution over both coast and hill stations up to 1 °C.

Precipitation - Mid-term scenario (2021-2050) – RCP4.5

Precipitation change signal stays within the range ± 5%. The distribution of signal resulted noisy and not affecting particular statistic. The same would be stated for the bias-corrected runs.

Precipitation - Long-term scenario (2061-2090) – RCP4.5

Slight increase of precipitation (5-7%) equally distributed over coast and hill stations. Noisy effects of bias correction over the signal resulted.

Precipitation - Mid-term scenario (2021-2050) – RCP8.5

Increase up to 10% focused on the right tail of distribution. Precipitation increase resulted equally affecting coast and hill stations. Bias correction, does not relevantly influence magnitude and distribution of precipitation change signal.

Precipitation - Long-term scenario (2061-2090) – RCP8.5

Precipitation increase up to 15% focused over the right distribution quantiles. The left and central part of distribution showed minor signal (2-10%). The two southernmost stations (Amandola and Ascoli Piceno) showed slight negative signal over left end central part of distribution.

3.3.5 Local hydrologic cycle response to warmer atmosphere

The response of the hydrologic cycle to a warmer atmosphere has been assessed through the computation of the Hydro-climatic Intensity index (HY-INT). This index studies metrics of mean annual precipitation intensity and mean annual dry spell length future trends, considering the response of the two metrics deeply interconnected to global warming (Giorgi et al. 2011). For all the stations considered in this study, a statistically significant increase of HY-INT was obtained (statistical significance inferred through Mann-Kendall statistical test). A stepper trend after 2020-2030 resulted over both coast and hill stations.

The trend of two metrics of mean annual precipitation intensity during rainy days (INT) and mean annual dry spell length (DSL) resulted statistically significant increasing. Trends affecting the two metrics are usually of similar magnitude.

Bibliography

Allan RP, Soden BJ (2008) Atmospheric warming and the amplification of precipitation extremes. Science 321:1481–4. doi: 10.1126/science.1160787

Allan RP, Soden BJ (2007) Large discrepancy between observed and simulated precipitation trends in the ascending and descending branches of the tropical circulation. Geophysical Research Letters 34:L18705. doi: 10.1029/2007GL031460

Andrews T, Forster PM, Boucher O, Bellouin N, Jones A (2010) Precipitation, radiative forcing and global temperature change. Geophysical Research Letters 37:L14701. doi: 10.1029/2010GL043991

Bellprat O, Kotlarski S, Lüthi D, Schär C (2013) Physical constraints for temperature biases in climate models. Geophysical Research Letters 40:4042–4047. doi: 10.1002/grl.50737

Boé J, Terray L, Habets F, Martin E (2007) Statistical and dynamical downscaling of the Seine basin climate for hydro-meteorological studies. International Journal of Climatology 1655:1643–1655. doi: 10.1002/joc

Casati B, Yagouti A, Chaumont D (2013) Regional climate projections of extreme heat events in nine pilot Canadian communities for public health planning. Journal of Applied Meteorology and Climatology 52:2669–2698. doi: 10.1175/JAMC-D-12-0341.1

Christensen JH, Boberg F, Christensen OB, Lucas-Picher P (2008) On the need for bias correction of regional climate change projections of temperature and precipitation. Geophysical Research Letters 35:L20709. doi: 10.1029/2008GL035694

Deque M (2007) Frequency of precipitation and temperature extremes over France in an anthropogenic scenario: Model results and statistical correction according to observed values. Global and Planetary Change 57:16–26. doi: 10.1016/j.gloplacha.2006.11.030

Dosio a., Paruolo P, Rojas R (2012) Bias correction of the ENSEMBLES high resolution climate change projections for use by impact models: Analysis of the climate change signal. Journal of Geophysical Research: Atmospheres 117:1–24. doi: 10.1029/2012JD017968

Ehret U, Zehe E, Wulfmeyer V, Warrach-Sagi K, Liebert J (2012) HESS Opinions “should we apply bias correction to global and regional climate model data?” Hydrology and

Earth System Sciences 16:3391–3404. doi: 10.5194/hess-16-3391-2012

Emori S (2005) Dynamic and thermodynamic changes in mean and extreme precipitation under changed climate. Geophysical Research Letters 32:L17706. doi: 10.1029/2005GL023272

Frei C, Schär C (2001) Detection Probability of Trends in Rare Events: Theory and Application to Heavy Precipitation in the Alpine Region. Journal of Climate 14:1568–1584. doi: 10.1175/1520-0442(2001)014<1568:DPOTIR>2.0.CO;2

Gao X, Pal JS, Giorgi F (2006) Projected changes in mean and extreme precipitation over the Mediterranean region from a high resolution double nested RCM simulation. Geophysical Research Letters 33:2–5. doi: 10.1029/2005GL024954

Gennaretti F, Sangelantoni L, Grenier P (2015) Toward daily climate scenarios for Canadian Arctic coastal zones with more realistic temperature-precipitation interdependence. Journal of Geophysical Research: Atmospheres 120, doi: 10.1002/2015JD023890

Giorgi F, Im E-S, Coppola E, Diffenbaugh NS, Gao XJ, Mariotti L, Shi Y (2011) Higher Hydroclimatic Intensity with Global Warming. Journal of Climate 24:5309–5324. doi: 10.1175/2011JCLI3979.1

Gudmundsson L, Bremnes JB, Haugen JE, Engen-Skaugen T (2012) Technical Note: Downscaling RCM precipitation to the station scale using statistical transformations - a comparison of methods. Hydrology and Earth System Sciences 16:3383–3390. doi: 10.5194/hess-16-3383-2012

Hagemann S, Chen C, Haerter JO, Heinke J, Gerten D, Piani C (2011) Impact of a Statistical Bias Correction on the Projected Hydrological Changes Obtained from Three GCMs and Two Hydrology Models. Journal of Hydrometeorology 12:556–578. doi: 10.1175/2011JHM1336.1

Hertig E, Seubert S, Paxian a, Vogt G, Paeth H, Jacobeit J (2014) Statistical modelling of extreme precipitation indices for the Mediterranean area under future climate change. International Journal of Climatology 34:1132–1156. doi: 10.1002/joc.3751

Hoffmann H, Rath T (2012) Meteorologically consistent bias correction of climate time series for agricultural models. Theoretical and Applied Climatology 110:129–141. doi: 10.1007/s00704-012-0618-x

Jacob D, Petersen J, Eggert B, Alias A, Christensen OB, Bouwer LM, Braun A, Colette A, Déqué M, Georgievski G, Georgopoulou E, Gobiet A, Menut L, Nikulin G, Haensler A, Hempelmann N, Jones C, Keuler K, Kovats S, Kröner N, Kotlarski S, Kriegsmann

A, Martin E, Meijgaard E, Moseley C, Pfeifer S, Preuschmann S, Radermacher C, Radtke K, Rechid D, Rounsevell M, Samuelsson P, Somot S, Soussana J-F, Teichmann C, Valentini R, Vautard R, Weber B, Yiou P (2013) EURO-CORDEX: new high-resolution climate change projections for European impact research. Regional Environmental Change 14:563–578. doi: 10.1007/s10113-013-0499-2

Jacob D, Preuschmann S (2014) Climate Change Signals in the EURO-CORDEX Simulations. Geophysical Research Abstracts 16:15434.

Kotlarski S, Keuler K, Christensen OB, Colette a., Déqué M, Gobiet a., Goergen K, Jacob D, Lüthi D, Van Meijgaard E, Nikulin G, Schär C, Teichmann C, Vautard R, Warrach-Sagi K, Wulfmeyer V (2014) Regional climate modeling on European scales: A joint standard evaluation of the EURO-CORDEX RCM ensemble. Geoscientific Model Development 7:1297–1333. doi: 10.5194/gmd-7-1297-2014

Krichak SO, Barkan J, Breitgand JS, Gualdi S, Feldstein SB (2014) The role of the export of tropical moisture into midlatitudes for extreme precipitation events in the Mediterranean region. Theoretical and Applied Climatology 499–515. doi: 10.1007/s00704-014-1244-6

Lenderink G, van Meijgaard E (2010a) Linking increases in hourly precipitation extremes to atmospheric temperature and moisture changes. Environmental Research Letters 5:025208. doi: 10.1088/1748-9326/5/2/025208

Lenderink G, Van meijgaard E (2008) Increase in hourly precipitation extremes beyond expectations from temperature changes. Nature Geoscience 511–514. doi: 10.1038/ngeo262

Lenderink G, van Meijgaard E (2010b) Linking increases in hourly precipitation extremes to atmospheric temperature and moisture changes. Environmental Research Letters 5:025208. doi: 10.1088/1748-9326/5/2/025208

Liu SC, Fu C, Shiu C-J, Chen J-P, Wu F (2009) Temperature dependence of global precipitation extremes. Geophysical Research Letters 36:1–4. doi: 10.1029/2009GL040218

Maraun D (2013) Bias Correction, Quantile Mapping, and Downscaling: Revisiting the Inflation Issue. Journal of Climate 26:2137–2143. doi: 10.1175/JCLI-D-12-00821.1

Maraun D, Wetterhall F, Ireson AM, Chandler RE, Kendon JE, Widmann M, Brienen S, Rust HW, Sauter T, Themeßl M, Venema VKC, Chun KP (2010) Precipitation Downscaling Under Climate Change : Recent Developments To Bridge the Gap

Between Dynamical Models and the End User. Reviews of geophysics 1–34. doi: 10.1029/2009RG000314

Maraun D, Widmann M, Gutierrez JM, Kotlarski S, Chandler RE, Hertig E, Wibig J, Huth R, Wilcke R a I (2015) VALUE: A framework to validate downscaling approaches for climate change studies. Earth's Future 3:1–14. doi: 10.1002/2014EF000259

Maurer EP, Pierce DW (2014) Bias correction can modify climate model simulated precipitation changes without adverse effect on the ensemble mean. Hydrology and Earth System Sciences 18:915–925. doi: 10.5194/hess-18-915-2014

Mora C, Frazier AG, Longman RJ, Dacks RS, Walton MM, Tong EJ, Sanchez JJ, Kaiser LR, Stender YO, Anderson JM, Ambrosino CM, Fernandez-Silva I, Giuseffi LM, Giambelluca TW (2013) The projected timing of climate departure from recent variability. Nature 502:183–7. doi: 10.1038/nature12540

Moss RH, Edmonds J a, Hibbard K a, Manning MR, Rose SK, van Vuuren DP, Carter TR, Emori S, Kainuma M, Kram T, Meehl G a, Mitchell JFB, Nakicenovic N, Riahi K, Smith SJ, Stouffer RJ, Thomson AM, Weyant JP, Wilbanks TJ (2010) The next generation of scenarios for climate change research and assessment. Nature 463:747–56. doi: 10.1038/nature08823

Mpelasoka FS, Chiew FHS (2009) Influence of Rainfall Scenario Construction Methods on Runoff Projections. Journal of Hydrometeorology 10:1168–1183. doi: 10.1175/2009JHM1045.1

Nakicenovic N, Swart R (2000) Special Report on Emissions Scenarios.

Pal JS, Giorgi F, Bi X (2004) Consistency of recent European summer precipitation trends and extremes with future regional climate projections. Geophysical Research Letters 31:20–23. doi: 10.1029/2004GL019836

Pall P, Allen MR, Stone D a. (2007) Testing the Clausius-Clapeyron constraint on changes in extreme precipitation under CO2 warming. Climate Dynamics 28:351–363. doi: 10.1007/s00382-006-0180-2

Reale M, Lionello P (2013) Synoptic climatology of winter intense precipitation events along the Mediterranean coasts. Natural Hazards and Earth System Sciences 13:1707–1722. doi: 10.5194/nhess-13-1707-2013

Riahi K, Rao S, Krey V, Cho C, Chirkov V, Fischer G, Kindermann G, Nakicenovic N, Rafaj P (2011) RCP 8.5 A scenario of comparatively high greenhouse gas emissions. Climatic Change 109:33–57. doi: 10.1007/s10584-011-0149-y

Scheffer M, Bascompte J, Brock W a, Brovkin V, Carpenter SR, Dakos V, Held H, van Nes EH, Rietkerk M, Sugihara G (2009) Early-warning signals for critical transitions. Nature 461:53–59. doi: 10.1038/nature08227

Smith PC, Heinrich G, Suklitsch M, Gobiet A, Stoffel M, Fuhrer J (2014) Station-scale bias correction and uncertainty analysis for the estimation of irrigation water requirements in the Swiss Rhone catchment under climate change. Climatic Change 127:521–534. doi: 10.1007/s10584-014-1263-4

Teutschbein C, Seibert J (2012) Bias correction of regional climate model simulations for hydrological climate-change impact studies: Review and evaluation of different methods. Journal of Hydrology 456-457:12–29. doi: 10.1016/j.jhydrol.2012.05.052

Themeßl MJ, Gobiet A, Heinrich G (2011a) Empirical-statistical downscaling and error correction of regional climate models and its impact on the climate change signal. Climatic Change 112:449–468. doi: 10.1007/s10584-011-0224-4

Themeßl MJ, Gobiet A, Leuprecht A (2011b) Empirical-statistical downscaling and error correction of daily precipitation from regional climate models. International Journal of Climatology 1544:1530–1544. doi: 10.1002/joc.2168

Thomson AM, Calvin K V., Smith SJ, Kyle GP, Volke A, Patel P, Delgado-Arias S, Bond-Lamberty B, Wise M a., Clarke LE, Edmonds J a. (2011) RCP4.5: a pathway for stabilization of radiative forcing by 2100. Climatic Change 109:77–94. doi: 10.1007/s10584-011-0151-4

Thrasher B, Maurer EP, McKellar C, Duffy PB (2012) Technical Note: Bias correcting climate model simulated daily temperature extremes with quantile mapping. Hydrology and Earth System Sciences 16:3309–3314. doi: 10.5194/hess-16-3309-2012

Toreti a., Xoplaki E, Maraun D, Kuglitsch FG, Wanner H, Luterbacher J (2010) Characterisation of extreme winter precipitation in mediterranean coastal sites and associated anomalous atmospheric circulation patterns. Natural Hazards and Earth System Science 10:1037–1050. doi: 10.5194/nhess-10-1037-2010

Trenberth KE, Dai A, Rasmussen RM, Parsons DB (2003) The Changing Character of Precipitation. Bulletin of the American Meteorological Society 84:1205–1217. doi: 10.1175/BAMS-84-9-1205

Trenberth KE, Shea DJ (2005) Relationships between precipitation and surface temperature. Geophysical Research Letters 32:1-4 doi: 10.1029/2005GL022760

van der Lindend P, Mitchell JFB (2009) Climate change and its impacts: Summary of

research and results from the ENSEMBLES project.

Vrac M, Naveau P, Drobinski P (2007) Nonlinear Processes in Geophysics Modeling pairwise dependencies in precipitation intensities. 789–797

Wilks, D. S. (2011). Statistical methods in the atmospheric sciences (Vol. 100). Academic press.

Wood a. W, Leung LR, Sridhar V, Lettenmaier DP (2004) Hydrologic implications of dynamical and statistical approaches to downscaling climate model outputs. Climatic Change 62:189–216. doi: 10.1023/B:CLIM.0000013685.99609.9e

Conclusions

This study proposed two different spatial scale climate scenarios resulting from two different climate model ensembles. Ending 21st century climate projections were employed to outline future climate conditions considering an area roughly covering Italian peninsula (regional experiment) and representative Marche region stations (local experiment). On a preliminary analysis of climate projections conducted over Italian peninsula, all climate models employed indicated significant warmer climate conditions, coherently with expected trends for the Mediterranean basin highlighted in the scientific literature (Giorgi and Lionello 2008; Giannakopoulos et al. 2009; Planton et al. 2012; Xoplaki et al. 2012). Climate models employed have proven to realistically reproduce recent-past temperature and precipitation climatology. However, as expected, performance of climate models demonstrated to some extent decline when complex-orography contexts are considered. This is particularly true for precipitation, which demonstrated high positive bias over Alps according to several scientific articles (Gleckler et al. 2008; Flato et al. 2013; Kotlarski et al. 2014). Concerning the climate change signal resulted by climate projections, increase of temperature resulted in all seasons. However, summer season outstands with higher warming signal exceeding 4 °C as resulted in Giorgi and Lionello (2008); Coppola and Giorgi (2010) and Planton et al. (2012). Moreover, summer temperature increase is coupled to a significant reduction of precipitation down to -30% in the southern Italy. For winter precipitation, it is important to remark an evident latitudinal gradient, where northern areas resulted affected by positive signal and southern sectors affected by a negative signal, according to Giorgi and Coppola (2007). Temperature and precipitation inter-annual variability is projected increasing, especially in summer. This explains a signal differently affecting mean and distribution tails. In fact, maximum temperature resulted increase more than relative minimum temperature especially in spring and summer as highlighted in Simolo et al. (2010). A particular case is represented by the Alpine region. Here, particular relevant was the cold temperature warming, due to positive feedbacks related to the reduction of snow cover and the resulting absence of albedo-effect (Gobiet et al. 2014).

For reducing systematic errors, affecting climate model numerical simulations, original outputs were post-processed with a statistical-empirical quantile mapping bias correction technique following Deque (2007) and Themeßl et al. (2011). This technique was applied according to two different configurations, defining a regional and local experiment. Given

the lack of scientific literature on the repercussion of a statistical correction over climate change signal, particular attention was paid to the assessment of climate model results before and after the correction. At regional scale was introduced an elevation-dependency of climate change signal not present in the original results. This is probably connected to the correction of the intensity-dependency of climate model resulted in different studies characterizing Mediterranean summer temperature simulations (Christensen et al. 2008; Themeßl et al. 2011; Boberg and Christensen 2012). Therefore, a dampening of roughly 0.5-1 °C of the summer climate change signal was obtained but only over plain and coast areas. At the same, time over the same areas, an increase of the signal affecting the right tail of the winter mean temperature resulted. Precipitation resulted not affected by the application of the bias correction on both annual cycle and distribution signal.

In the local experiment, climate change signal and effect of bias correction, largely confirmed what resulted at regional scale. Summer season is confirmed the most affected season by warmer conditions followed by spring season. In the Marche region stations, according to "business as usual" RCP8.5 radiative scenario, the threshold of +2 °C is projected to be touched by the half of this century (in comparison to the reference period 1971-2000). According to the same scenario, temperature signal is expected doubling by 2061-2090. Concerning precipitation, Marche region summer mean precipitation are projected decrease about 20% at the end of 21st but compensated by an equal increase during autumn and winter months (RCP8.5). Assessing response of hydrologic cycle metrics (mean precipitation intensity and dry-spell-length), significant acceleration of the local hydrological cycle is projected, in agreement with an increased moisture-holding capacity of a warmer atmosphere (even if with a minor rate compared to what indicated in the Clausius-Clapeyron relationship) (Giorgi et al. 2011; Giorgi et al. 2014). After bias correction, summer temperature signal characterizing the end-21st century Marche region coast stations was reduced of roughly 0.5-0.8 °C. At the same time, in the same stations, winter temperature right tail signal was augmented of about 0.8-1 °C. Also in the local experiment precipitation signal resulted not affected by the statistical correction of the original climate simulations. Only scattered effects over statistical significance of monthly climate change signal and over the left tail of distribution were observed.

Doctoral research findings could be resumed as follows:
(i) Two different spatial scale climate scenarios, with two different climate model ensembles, providing both original and bias-corrected climate simulations have been provided for the first time over considered study areas. (ii) The agreement obtained in the regional and local experiments strengths on the one hand the confidence over changes outlined and on the other hand the coherence of the effects of the statistical correction over the original climate change signal. This is of particular interest since different bias correction configuration in the two experiments were adopted. (iii) Given the original climate simulation biases (locally up to 5 °C for temperature and 40% for precipitation), has been confirmed the unfeasibility of directly employing original model outputs as inputs for impact modelling. (Maraun et al. 2010; Kotlarski et al. 2014; Smith et al. 2014). (iv) Local experiment results allow comprehensive investigation on the feasibility of providing local climate information using state of art climate models. (v) Post-processing technique here employed, has been demonstrated to represent essential advancements in regional to local scale climate scenario. Improvements were particularly palpable for temperature variable, where the quantile mapping technique was demonstrated improving projections reliability in particular in high-complex morphological contexts.

Provision of usable and valuable local climate projections represent a tremendous step forward on fostering mitigation adaptation measures. Temporally and spatially framing climate information could promoting also essential cultural and practical aspects, stimulating citizens and policymakers consciousness and perception of current and expected climatic change. If taken seriously, climate scenario represents the basis for take action against expected climate impacts, spending real money, making real changes to infrastructure, society and the environment, affecting people and ecosystems. To deal with this "ethical" consideration and our limited knowledge of regional and local climate change, state-of-the-art climate model projections were voluntarily reported in their original and bias-corrected form.

Finally, besides technical and "cultural" considerations from a practical point of view, this research provides usable climate information in climate impacts research. This climate information properly tailored and contextualized, could serve sector as diverse as agriculture, health and water management and disaster risk reduction. This in accordance with concepts

and principles of climate services (http://www.gfcs-climate.org/, 2009), expected to ensure that every climate-sensitive sector of society is well equipped to access to relevant and usable climate information for better manage risks of climate variability and changes.

Bibliography

Boberg F, Christensen JH (2012) Overestimation of Mediterranean summer temperature projections due to model deficiencies. Nature Climate Change 2:433–436. doi: 10.1038/nclimate1454

Christensen JH, Boberg F, Christensen OB, Lucas-Picher P (2008) On the need for bias correction of regional climate change projections of temperature and precipitation. Geophysical Research Letters 35:L20709. doi: 10.1029/2008GL035694

Coppola E, Giorgi F (2010) An assessment of temperature and precipitation change projections over Italy from recent global and regional climate model simulations. International Journal of Climatology 32:11–32. doi: 10.1002/joc

Deque M (2007) Frequency of precipitation and temperature extremes over France in an anthropogenic scenario: Model results and statistical correction according to observed values. Global and Planetary Change 57:16–26. doi: 10.1016/j.gloplacha.2006.11.030

Flato G, Marotzke J, Abiodun B, Braconnot P, Chou SC, Collins W, Cox P, Driouech F, Emori S, Eyring V, Forest C, Gleckler P, Guilyardi E, Jakob C, Kattsov V, Reason C, Rummukainen M (2013) Evaluation of Climate Models. Climate Change 2013: The Physical Science Basis Contribution of Working Group I to the Fifth Assessment Report of the Intergovernmental Panel on Climate Change 741–866. doi: 10.1017/CBO9781107415324

Giannakopoulos C, Le Sager P, Bindi M, Moriondo M, Kostopoulou E, Goodess CM (2009) Climatic changes and associated impacts in the Mediterranean resulting from a 2 °C global warming. Global and Planetary Change 68:209–224. doi: 10.1016/j.gloplacha.2009.06.001

Giorgi F, Coppola E (2007) European climate-change oscillation (ECO). Geophysical Research Letters 34:1–6. doi: 10.1029/2007GL031223

Giorgi F, Coppola E, Raffaele F, Diro GT, Fuentes-Franco R, Giuliani G, Mamgain A, Llopart MP, Mariotti L, Torma C (2014) Changes in extremes and hydroclimatic regimes in the CREMA ensemble projections. Climatic Change 125:39–51. doi: 10.1007/s10584-014-1117-0

Giorgi F, Im E-S, Coppola E, Diffenbaugh NS, Gao XJ, Mariotti L, Shi Y (2011) Higher Hydroclimatic Intensity with Global Warming. Journal of Climate 24:5309–5324. doi:

10.1175/2011JCLI3979.1

Giorgi F, Lionello P (2008) Climate change projections for the Mediterranean region. Global and Planetary Change 63:90–104. doi: 10.1016/j.gloplacha.2007.09.005

Gleckler PJ, Taylor KE, Doutriaux C (2008) Performance metrics for climate models. Journal of Geophysical Research 113:D06104. doi: 10.1029/2007JD008972

Gobiet A, Kotlarski S, Beniston M, Heinrich G, Rajczak J, Stoffel M (2014) 21st century climate change in the European Alps-A review. Science of the Total Environment 493:1138–1151. doi: 10.1016/j.scitotenv.2013.07.050

Kotlarski S, Keuler K, Christensen OB, Colette a., Déqué M, Gobiet a., Goergen K, Jacob D, Lüthi D, Van Meijgaard E, Nikulin G, Schär C, Teichmann C, Vautard R, Warrach-Sagi K, Wulfmeyer V (2014) Regional climate modeling on European scales: A joint standard evaluation of the EURO-CORDEX RCM ensemble. Geoscientific Model Development 7:1297–1333. doi: 10.5194/gmd-7-1297-2014

Maraun D, Wetterhall F, Ireson AM, Chandler RE, Kendon JE, Widmann M, Brienen S, Rust HW, Sauter T, Themeßl M, Venema VKC, Chun KP (2010) Precipitation Downscaling Under Climate Change : Recent Developments To Bridge the Gap Between Dynamical Models and the End User. Reviews of geophysics 1–34. doi: 10.1029/2009RG000314

Planton S, Lionello P, Artale V, Aznar R, Carrillo A, Colin J, Congedi L, Dubois C, Elizalde A, Gualdi S, Hertig E, Jacobeit J, JordÃ G, Li L, Mariotti A, Piani C, Ruti P, Sanchez-Gomez E, Sannino G, Sevault F, Somot S, Tsimplis M (2012) The Climate of the Mediterranean Region in Future Climate Projections.

Simolo C, Brunetti M, Maugeri M, Nanni T, Speranza A (2010) Understanding climate change–induced variations in daily temperature distributions over Italy. Journal of Geophysical Research 115:D22110. doi: 10.1029/2010JD014088

Smith PC, Heinrich G, Suklitsch M, Gobiet A, Stoffel M, Fuhrer J (2014) Station-scale bias correction and uncertainty analysis for the estimation of irrigation water requirements in the Swiss Rhone catchment under climate change. Climatic Change 127:521–534. doi: 10.1007/s10584-014-1263-4

Themeßl MJ, Gobiet A, Leuprecht A (2011) Empirical-statistical downscaling and error correction of daily precipitation from regional climate models. International Journal of Climatology 1544:1530–1544. doi: 10.1002/joc.2168

Xoplaki E, Trigo RM, García-Herrera R, Barriopedro D, D'Andrea F, Fischer EM, Gimeno

L, Gouveia C, Hernández E, Kuglitsch FG, Mariotti A, Nieto R, Pinto JG, Pozo-Vázquez D, Saaroni H, Toreti A, Trigo IF, Vicente-Serrano SM, Yiou P, Ziv B (2012) Large-scale atmospheric circulation driving extreme climate events in the mediterranean and its related impacts. In: The Climate of the Mediterranean Region. pp 347–417

Acknowledgments

I would like to thank:

Prof. Aniello Russo for having given me the possibility of pursuing my research: my dream.

Dr. Alessandro Coluccelli for all I have learnt and for always being close to me as a friend and not as a simple colleague.

Prof. Fausto Marincioni for supporting and endure me in all these years and for all the stimulating and motivating discussions.

Prof. Antonio Dell'Anno for always being enlightening.

Prof. Patrick Grenier for letting me understand what make research at the highest level means, in its widest meaning.

Thanks to all the D-lab.

Last but not the least: the greatest goes to you B.B.